Vol. 62 April, 1958 No. 4

THE JOURNAL OF PHYSICAL CHEMISTRY

(Registered in U. S. Patent Office)

CONTENTS

Kurt H. Stern: Electrode Potentials in Fused Systems. IV. A Thermodynamic and Kinetic Study of the AgCl–NaCl System 385
Jack Schubert, Arthur Lindenbaum and William Westfall: Ion-exchange Separation of Beryllium by Elution with Salicylate Analogs 390
Eli S. Freeman and Benjamin Carroll: The Application of Thermoanalytical Techniques to Reaction Kinetics: The Thermogravimetric Evaluation of the Kinetics of the Decomposition of Calcium Oxalate Monohydrate 394
G. C. Sinke and D. R. Stull: Heats of Combustion of Some Organic Compounds Containing Chlorine 397
H. L. Frisch: The Time Lag in Diffusion. II 401
D. K. Anderson, J. R. Hall and A. L. Babb: Mutual Diffusion in Non-ideal Binary Liquid Mixtures 404
Charles R. Boston and G. Pedro Smith: Visible and Ultraviolet Absorption Spectra of Nickel Chloride Dissolved in Fused LiCl–KCl Mixtures 409
Sherman W. Rabideau: Kinetics of Oxidation-Reduction Reactions of Plutonium. The Reaction between Plutonium (VI) and Vanadium(III) in Perchlorate Solutions 414
F. R. Duke and M. L. Iverson: Complex Ions in Fused Salts 417
James P. Coughlin: Heats of Formation and Hydration of Anhydrous Aluminum Chloride 419
J. E. Walther and H. G. Drickamer: Thermal Diffusion in Dense Gases 421
Robert A. Spurr and H. Franklin Byers: The Intensity of the S–H Stretching Fundamental; Dimerization of Mercaptans 425
S. Aronoff: Perchloric Acid Titrations of Porphyrins in Nitrobenzene 428
G. M. Hebert, H. F. McDuffie and C. H. Secoy: The Densities of Heavy Water Liquid and Saturated Vapor at Elevated Temperatures 431
Laurence E. Wilson and N. W. Gregory: Vapor–Solid Equilibria in the Iron–Chlorine System 433
Bert H. Clampitt and Dale E. German: Heats of Vaporization of Molecules at Liquid–Vapor Interfaces 438
Robert G. Charles and M. Arlene Pawlikowski: Comparative Heat Stabilities of Some Metal Acetylacetonate Chelates 440
Charles R. Bertsch, W. Conard Fernelius and B. P. Block: A Thermodynamic Study of Some Complexes of Metal Ions with Polyamines 444
B. J. Steel and R. H. Stokes: A Hittorf Transference Number Apparatus Employing Conductimetric Analysis of the Solutions 450
Karl A. Sense and Richard W. Stone: Vapor Pressures and Molecular Composition of Vapors of the Sodium Fluoride-Beryllium Fluoride System 453
A. J. Rosenberg and C. S. Martel, Jr.: Thermal Transpiration of Gases at Low Pressures 457
Arthur Veis and Jerome Cohen: The Role of Cross-linkages in the Solubilization of Insoluble Collagen 459
Daniel Cubicciotti, F. J. Keneshea, Jr., and C. M. Kelley: The Vapor Pressures of $BiCl_3$ over Liquid Bi–$BiCl_2$ Solutions 463
Michio Kondo and Masaji Kubo: The Magnetic Susceptibility of Copper(II) Acetate in Various Solvents 468
R. C. Robbins and R. D. Cadle: Kinetics of the Reaction between Gaseous Ammonia and Sulfuric Acid Droplets in an Aerosol 469
L. Leibowitz, M. J. D. Low and H. Austin Taylor: The Adsorption of Hydrogen on Nickel–Kieselguhr 471
F. E. Massoth and W. E. Hensel, Jr.: Kinetics of the Reaction between Sodium Fluoride and Uranium Hexafluoride. I. Sodium Fluoride Powder 479
Kōzō Shinoda and J. H. Hildebrand: Liquid–Liquid Solubility of Pentaerythritol Tetraperfluorobutyrate with Chloroform, Carbon Tetrachloride and Octamethylcyclotetrasiloxane 481
J. D. Graybeal and C. D. Cornwell: Nuclear Quadrupole Spectra of the Chloroacetonitriles 483
Richard F. Porter and Richard C. Schoonmaker: Gaseous Species in the NaOH–KOH System 486

Notes

A. C. Zettlemoyer, J. J. Chessick and C. M. Hollabaugh: Estimations of the Surface Polarity of Solids from Heat of Wetting Measurements 489
Milton D. Scheer: The Molecular Weight and Vapor Pressure of Gaseous Boron Suboxide 490
H. T. Hookway and B. Selton: The Stability of Organic Sulfonic Acids in Dilute Aqueous Hydrogen Peroxide 493
B. B. Fisher and W. G. McMillan: The Sublimation Pressure of Krypton below 80°K 494
Alexander Meller and John E. Bright: The Rate of Reactions as a Function of Time 495
Jean M. Stokes and R. H. Stokes: The Conductances of Some Electrolytes in Aqueous Sucrose and Mannitol Solutions at 25° 497
E. G. King and A. U. Christensen, Jr.: Low Temperature Heat Capacity, Entropy at 298.15°K., and High Temperature Heat Content of Mo_5Si 499
Louis Watts Clark: The Effect of Quinoline and its Derivatives on Malonic Acid 500
P. Ausloos and J. Paulson: Reactions of Methyl Radicals with Water on Quartz and Pyrex Surfaces 501

THE JOURNAL OF PHYSICAL CHEMISTRY

(Registered in U. S. Patent Office)

Published monthly by the American Chemical Society at 20th and Northampton Sts., Easton, Pa.

Second-class mail privileges authorized at Easton, Pa.

The *Journal of Physical Chemistry* is devoted to the publication of selected symposia in the broad field of physical chemistry and to other contributed papers.

Manuscripts originating in the British Isles, Europe and Africa should be sent to F. C. Tompkins, The Faraday Society, 6 Gray's Inn Square, London W. C. 1, England.

Manuscripts originating elsewhere should be sent to W. Albert Noyes, Jr., Department of Chemistry, University of Rochester, Rochester 20, N. Y.

Correspondence regarding accepted copy, proofs and reprints should be directed to Assistant Editor, Allen D. Bliss, Department of Chemistry, Simmons College, 300 The Fenway, Boston 15, Mass.

Business Office: Alden H. Emery, Executive Secretary, American Chemical Society, 1155 Sixteenth St., N. W., Washington 6, D. C.

Advertising Office: Reinhold Publishing Corporation, 430 Park Avenue, New York 22, N. Y.

Articles must be submitted in duplicate, typed and double spaced. They should have at the beginning a brief Abstract, in no case exceeding 300 words. Original drawings should accompany the manuscript. Lettering at the sides of graphs (black on white or blue) may be pencilled in and will be typeset. Figures and tables should be held to a minimum consistent with adequate presentation of information. Photographs will not be printed on glossy paper except by special arrangement. All footnotes and references to the literature should be numbered consecutively and placed in the manuscript at the proper places. Initials of authors referred to in citations should be given. Nomenclature should conform to that used in *Chemical Abstracts*, mathematical characters marked for italic, Greek letters carefully made or annotated, and subscripts and superscripts clearly shown. Articles should be written as briefly as possible consistent with clarity and should avoid historical background unnecessary for specialists.

Notes describe fragmentary or incomplete studies but do not otherwise differ fundamentally from articles and are subjected to the same editorial appraisals as are articles. In their preparation particular attention should be paid to brevity and conciseness. Material included in Notes must be definitive and may not be republished subsequently.

Communications to the Editor are designed to afford prompt preliminary publication of observations or discoveries whose value to science is so great that immediate publication is imperative. The appearance of related work from other laboratories is in itself not considered sufficient justification for the publication of a Communication, which must in addition meet special requirements of timeliness and significance. Their total length may in no case exceed 500 words or their equivalent. They differ from Articles and Notes in that their subject matter may be republished.

Symposium papers should be sent in all cases to Secretaries of Divisions sponsoring the symposium, who will be responsible for their transmittal to the Editor. The Secretary of the Division by agreement with the Editor will specify a time after which symposium papers cannot be accepted. The Editor reserves the right to refuse to publish symposium articles, for valid scientific reasons. Each symposium paper may not exceed four printed pages (about sixteen double spaced typewritten pages) in length except by prior arrangement with the Editor.

Remittances and orders for subscriptions and for single copies, notices of changes of address and new professional connections, and claims for missing numbers should be sent to the American Chemical Society, 1155 Sixteenth St., N. W., Washington 6, D. C. Changes of address for the *Journal of Physical Chemistry* must be received on or before the 30th of the preceding month.

Claims for missing numbers will not be allowed (1) if received more than sixty days from date of issue (because of delivery hazards, no claims can be honored from subscribers in Central Europe, Asia, or Pacific Islands other than Hawaii), (2) if loss was due to failure of notice of change of address to be received before the date specified in the preceding paragraph, or (3) if the reason for the claim is "missing from files."

Subscription Rates (1958): members of American Chemical Society, $8.00 for 1 year; to non-members, $16.00 for 1 year. Postage free to countries in the Pan American Union; Canada, $0.40; all other countries, $1.20. Single copies, current volume, $1.35; foreign postage, $0.15; Canadian postage $0.05. Back volumes (Vol. 56-59), $15.00 per volume; (starting with Vol. 60) $18.00 per volume; foreign postage $1.20, Canadian, $0.40; $1.75 per issue, foreign postage $0.15, Canadian postage $0.05.

The American Chemical Society and the Editors of the *Journal of Physical Chemistry* assume no responsibility for the statements and opinions advanced by contributors to This Journal.

Charles R. Bertsch, B. P. Block and W. Conard Fernelius: The Coördination of Copper(II) with 1,3-Diamino-2-propanol ... 503
Robert W. Bayer and Edward J. O'Reilly, Jr.: Out-of-Plane Hydrogen Vibrations in Some Highly Substituted Naphthalenes ... 504
Sigmund Schuldiner and James P. Hoare: Effect of pH on the Catalytic Activity of Hydrogen-producing Reactions on α- and β-Palladium–Hydrogen Cathodes ... 504
Donald E. Campbell, Herbert M Clark and Walter H. Bauer: The Extraction of Ferric Chloride by Isopropyl Ether. II. A Conductometric Study of the Ether Layer ... 506
Martin H. Kaufman and Alan L. Woodman: Geometric Considerations of Tetrazole Derivatives from Dipole Moment Data ... 508
R. A. Horne: Alcoholic Ferric Perchlorate Solutions ... 509
I. S. Yaffe and R. D. Cadle: The Kinetic Behavior of Submicron Size, Polydispersed Sodium Chloride and Titanium Dioxide Aerosols ... 510
K. J. Miller: Some Physical Properties of the System 2-Ethoxyethanol–Butyl Acetate ... 512

THE JOURNAL OF
PHYSICAL CHEMISTRY

(Registered in U. S. Patent Office) (© Copyright, 1958, by the American Chemical Society)

VOLUME 62 APRIL 22, 1958 NUMBER 4

ELECTRODE POTENTIALS IN FUSED SYSTEMS. IV. A THERMODYNAMIC AND KINETIC STUDY OF THE AgCl–NaCl SYSTEM[1]

BY KURT H. STERN

Department of Chemistry, University of Arkansas, Fayetteville, Arkansas

Received May 29, 1957

The cell Ag/AgCl, NaCl/Cl_2 has been studied over the complete concentration range from pure AgCl to pure NaCl between 750 and 900°. For solutions very dilute in AgCl, silver reacts spontaneously with NaCl. The thermodynamic functions of the binary solution are given and compared with the corresponding bromide system. It is likely that galvanic cells do not yield thermodynamic data in the dilute region. The reaction Ag + NaCl → AgCl + Na has been studied in open and closed systems, and with 270-day Ag^{110m} tracer. Rates of reaction have been measured at several temperatures between 850 and 1080. The reaction is driven by the distillation of sodium.

Introduction

In paper II of this series[2] the cell Ag/AgCl, KCl/Cl_2 was shown to behave reversibly from 0.05 mole fraction of AgCl up to the pure salt. It was shown that the free energy of dilution of AgCl by KCl is linear with concentration down to the lower value and then drops sharply toward minus infinity, *i.e.*, thermodynamic functions cannot be obtained for systems which behave irreversibly.

In agreement with the results obtained by Hildebrand and Salstrom[3] for the AgBr–KBr system, the ΔF of dilution in the AgCl–KCl system also deviates negatively from ideality. Since the sign of the deviation is determined by the dilution of silver ion by the alkali metal cation, the anion only affecting its magnitude, it seemed of interest to extend our work to the AgCl–NaCl system. For the corresponding AgBr–NaBr system Hildebrand and Salstrom already found a positive deviation.

Our concern here is primarily with solutions dilute in silver. The free energy of dilution of the AgCl–KCl system exhibits an abrupt break to a more negative slope near 0.05 mole fraction AgCl. For solutions more dilute than this, silver was found to react spontaneously with KCl to form AgCl and metallic potassium. If the same phenomenon should occur in the AgCl–NaCl system it would lead to a reversal of the slope of the free energy function–mole fraction plot. As our results show this is the case. Consequently, we also examined the kinetics of the reaction between silver and NaCl. To our knowledge the kinetics of reactions between metals and molten salts have not previously been reported though of course many such reactions are known and have been used for preparative purposes. This field is also of interest in connection with high temperature corrosion.[4] The mechanism of many of these reactions is complex, however, and it is difficult even to isolate and identify the products. The reaction reported here is simple and may, on the basis of previous evidence,[2] be hypothesized as Ag + NaCl → AgCl + Na.

The reaction was studied both in open and "closed" systems, using conventional gravimetric methods of analysis, and in an open system by a radiochemical method. "Closed" means in sealed Vycor capsules.

Experimental Part

Galvanic Cell.—The measurements on the galvanic cell Ag/AgCl, NaCl/Cl_2 were made by the same procedure that was used previously on the cell Ag/AgCl, KCl/Cl_2. The sodium chloride was of C.P. grade.

Open System Kinetics.—A 25 × 200 mm. Vycor test-tube was preheated to the desired temperature in a well insulated

(1) This research was supported by the United States Air Force through the Office of Scientific Research of the Air Research and Development Command under Contract AF 18(600)-960. Reproduction in whole or in part is permitted for any purpose of the United States Government. Presented at the 131st meeting of the American Chemical Society, Miami, Fla., April 7–14, 1957.

(2) K. H. Stern, THIS JOURNAL, **60**, 679 (1956).

(3) (a) E. J. Salstrom and J. H. Hildebrand, *J. Am. Chem. Soc.*, **52**, 4650 (1930); (b) E. J. Salstrom, *ibid.*, **53**, 1794 (1931); (c) **53**, 3385 (1931); (d) **54**, 4252 (1932); (e) J. H. Hildebrand and E. J. Salstrom, *ibid.*, **54**, 4257 (1932).

(4) *Cf.* D. M. Mathews and R. F. Kruh, *Ind. Eng. Chem.*, **49**, 55 (1957).

furnace, approximately 40 g. of NaCl added, the system again brought to temperature equilibrium and from 6 to 8 g. of silver added, the metal being variously in the form of sheet, buttons, or wire, uniformly of 99.99% purity (on the initial addition of silver to the melt, flashes of light were emitted, evidence of the initially rapid evolution of sodium vapor). In all the runs the metal was submerged well below the surface of the melt to prevent contact with atmospheric O_2. The melt was constantly stirred by a hollow, motor-driven 9 mm. Vycor tube to minimize concentration gradients. Stirring speed was approximately 250 r.p.m. Samples were withdrawn periodically with a Vycor tube for analysis. Temperature fluctuations were held to ±5°. Since the reaction is very slow and relatively temperature insensitive these are probably rather unimportant. The temperature was measured with a chromel-alumel thermocouple placed in a nickel protection tube. The hot junction was kept near the bottom of the melt. The furnace was well insulated and temperature gradients at the reaction site were negligible.

Closed System Kinetics.—15.00 g. of NaCl and 3.00 g. of Ag were weighed into a Vycor capsule made from 15 mm. tubing and sealed in under vacuum ($\sim 10^{-3}$ mm.). In each run from five to ten such capsules were placed in a furnace preheated to the desired temperature. At intervals they were withdrawn for analysis. Because of the expansion of alkali halides on solidification the vials usually cracked on cooling. The large pieces of glass on the outside of the vial were removed. The layers of glass next to the melt were too firmly attached to it to allow simple removal. This layer contained crystalline SiO_2 as well as metallic Si, produced through the reduction of SiO_2 by sodium vapor formed in the reaction $Ag + NaCl \rightarrow AgCl + Na$.

(The reduction of SiO_2 by the alkali metals, according to the equation $SiO_2 + 4Na \rightarrow 2Na_2O + Si$, is a standard method for the preparation of metallic silicon. That the reaction goes under the conditions of the above experiment was verified by sealing ~ 0.1 g. of Na into a Vycor capsule under vacuum. After 24 hours at 800° the entire inside of the capsule was coated with a layer of black graphitic Si.)

The melt was crushed, the large unreacted pieces of silver removed and weighed, the melt was weighed, dissolved in NH_4OH and the filtrate analyzed gravimetrically for silver by the sulfide method. The remaining solid containing Si, SiO_2 and tiny bits of metallic Ag was treated with HNO_3 to dissolve the silver. In this way a material balance could be run for silver. In most cases agreement was very good.

Silver concentration in both open and closed systems was calculated on the basis of (NaCl + AgCl) weight only.

Vacuum Experiment.—To determine whether small quantities of H_2O or O_2 were responsible for the reaction several grams of NaCl was heated slowly to about 850° in an apparatus similar to the one described under "Open System" except that the test-tube was enclosed in a vacuum system. The salt was dehydrated by heating under continuous pumping, silver added, and the pumping continued for 36 hours. Analysis of the cooled melt showed the presence of AgCl.

Radiochemical Method.—Since the gravimetric analysis for silver is not very satisfactory for small amounts and since the initial course of the reaction is of interest, an "open system" run was made using 270 day Ag^{110m} as a tracer. Seven g. of the silver described above and 1 g. of Reagent Grade AgCl (used as standard) were irradiated 30 days in the X-10 reactor at Oak Ridge at a flux of about 5×10^{11} neutrons/cm.^{2}-sec. to produce 270 day Ag^{110m}.

The samples were counted by the integral-bias method on a scintillation spectrometer fitted with a 1.5 × 1 inch NaI-(Tl) crystal, the discrimination level being set so that only γ-rays above 360 kev. were counted. In this way, the corrections for self-absorption and self-scattering in the source (100 mg./cm.^{2} on the average) were made negligible. Moreover, counting was carried out at two levels of discrimination in order to confirm that such corrections actually are negligible under these conditions. Background inside of a 4-inch thick lead shield was about 50 c./m. Duplicate samples were prepared and counted (twice each) to assure reproducibility, for at least 5 minutes. In all cases, the accuracy and reproducibility checked to within ±2%, when counting was done on the same day to avoid correction for radioactive decay and to minimize variations in electric gain of the scintillation counter. In order to calibrate the specific activity (counts/min. per mg.) of the samples in terms of mole-fraction of silver present, samples of the irradiated AgCl were weighed and counted along with the samples from the kinetic run. This calibration was evaluated to be 1.3×10^9 counts/min. per mg. = 1 mole Ag.

This silver (specific activity $\sim 2 \times 10^4$ dis./sec. per mg.) was then used in a kinetic run at 857° as described under "open system" above. Samples of the melt were withdrawn at intervals for analysis. Since less than 50 mg. was sufficient for the detection of activity, many more samples (25 in all) could be taken than was possible by the conventional method. Moreover, since the method is very sensitive, kinetics for very short times could be obtained. Thus the first sample, taken 2 minutes after immersion of the silver in the melt, showed an activity of three times background, whereas the gravimetric technique restricted analysis to samples taken after 25 hours.

Results

The Cell Ag/AgCl, NaCl/Cl_2.—The temperature variation of the cell Ag/AgCl, NaCl/Cl_2 for various mole fractions of AgCl is shown in Table I. The mole fraction of AgCl is defined as

$$N_{AgCl} = \frac{n_{AgCl}}{n_{AgCl} + n_{NaCl}}$$

and the n's represent the number of moles of the component in question.

TABLE I

ELECTRODE POTENTIALS OF THE CELL Ag/AgCl, NaCl/Cl_2

N_{AgCl}	t(°C.)	E(v.)	$dE/dT \times 10$
0.5260	741	0.8693	−1.88
	788	.8603	
	806	.8572	
	856	.8483	
	896	.8399	
.3331	766	.8947	−1.40
	812	.8867	
	871	.8779	
	918	.8736	
.2530	812	.9101	−1.49
	839	.9068	
	911	.8955	
	949	.8889	
.1233	817	.9780	−0.648
	865	.9752	
	913	.9718	
.0891	813	1.0246	+0.308
	866	1.0329	
	926	1.0280	
.0775	844	1.0185	0.459
	895	1.0514	
	938	1.0530	

Several sets of data are now available for the cell Ag/AgCl/Cl_2. Because the potential of this cell, E^0, is involved in all subsequent calculations a comparison is of interest. The earliest reliable measurement was made by Salstrom,[5] who worked in the temperature range 460–600°. The results recently reported by the author[2] are within 2 mv. of Salstrom's data. While the current work was in progress I learned of similar work being done by a group at the Oak Ridge National Laboratory.[6] Their measurements were carried to 800°. They are in substantial agreement with the studies cited above and show that dE/dt is linear over the

(5) E. J. Salstrom, *J. Am. Chem. Soc.*, **55**, 2426 (1933).

(6) M. B. Panish, R. F. Newton, W. R. Grimes, F. F. Blankenship; Dr. Panish has very kindly sent me the data in advance of publication.

entire range of temperature. E^0 values also have been computed from heat capacity data.[7] While the agreement is close between these and the experimental values at the lower temperatures, the slope is sufficiently less so that the computed E^0 is about 20 mv. higher at 900° than the straight-line extrapolations of the experimental data. The experimental values probably are more reliable.

The curves, linear over the temperature range studied, are qualitatively similar to those for the AgCl–KCl system. One difference, however, is noticeable. For solutions below 0.1 N_{AgCl} the sign of dE/dT becomes positive. Since this quantity corresponds to the entropy of formation of AgCl in a medium of the indicated composition, it follows that the entropy term is favorable to the formation of AgCl in dilute NaCl, but not in KCl.

Open System Kinetics.—The dependence of silver concentrations on time for four temperatures is shown in Fig. 1. No correction has been made for the change of NaCl/Ag ratio resulting from the withdrawal of sample. The data for the radiochemical measurement are plotted in Fig. 2. Since the samples required for analysis were less than 50 mg., the NaCl/Ag ratio remained nearly constant during the entire run. This difference accounts for the divergence of the two 860° runs. The agreement with the data resulting from chemical analysis is quite good for the first 300 hours. The problem of determining the order of the reaction is quite difficult and will be treated in the Discussion. Several conclusions may be drawn.

1. Silver at concentrations near 10^{-5} mole fraction is found in the melt after only two minutes. This may be atomic or ionic silver. The radiochemical method does not distinguish.

2. Over the range of time and concentration for which both chemical and radiochemical methods were used the concentration of silver found by both methods is nearly the same. Thus, at least after 20 hours, the silver in the melt is predominantly ionic.

3. The rate of reaction clearly increases with temperature.

Closed System Kinetics.—The kinetic data for the closed system runs are shown in Fig. 3. This set of runs was made to see whether (1) the presence of oxygen is necessary for the reaction to occur, and (2) preventing the distillation of sodium from the system prevents the reaction from occurring. This had been postulated previously.[2,8]

The answer to question (1) is clearly negative, as is shown also by the experiment done under vacuum. The experiment does not provide a completely unambiguous answer to question (2), but is good evidence for the hypothesis. The reaction rate is definitely less in the sealed capsules than in the open tubes but the reaction of sodium with the SiO_2 of the container walls means that the system is not really closed in the thermodynamic sense. However, the reaction of SiO_2 is good evidence that the reaction is driven by the distillation of sodium. The distillation of sodium into the walls of the sealed capsules would be slower than its distillation into the open atmosphere. It follows that the reaction would not go in a closed container of an inert material, but such a substance is difficult to

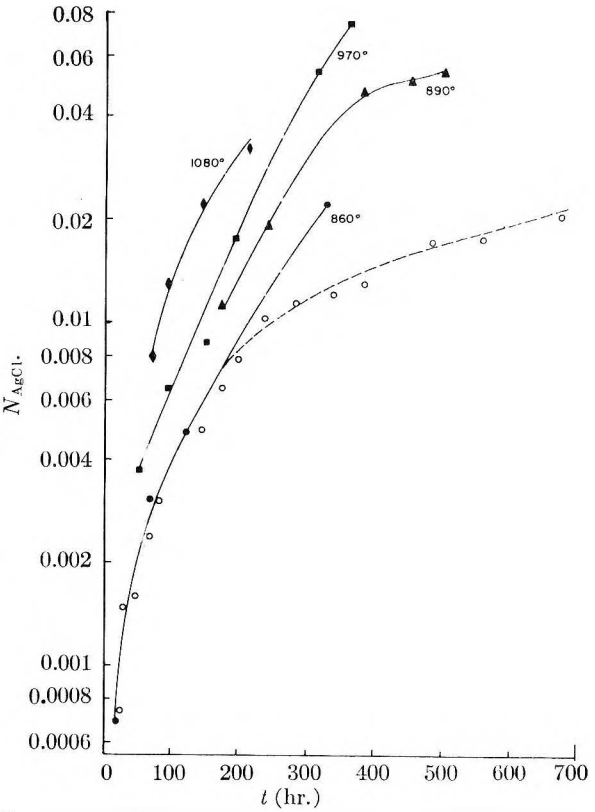

Fig. 1.—Kinetic data for the reaction Ag + NaCl → AgCl + Na: open system; —○—, radiochemical data.

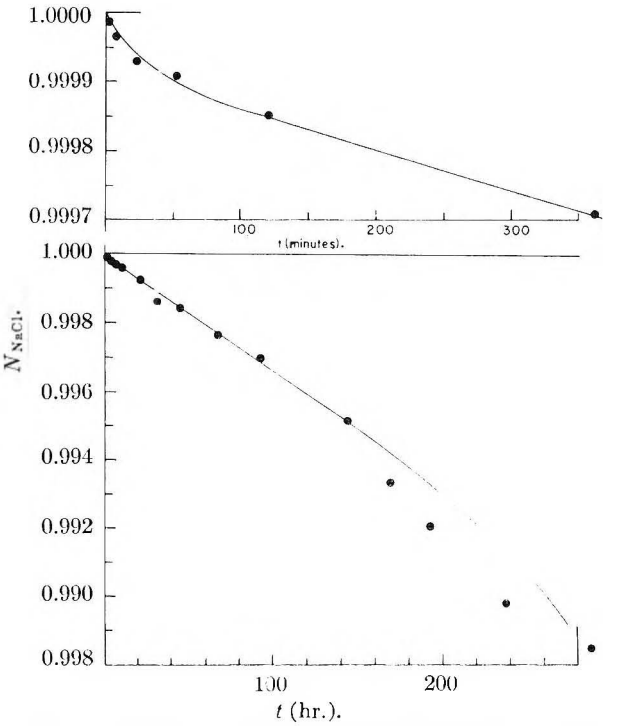

Fig. 2.—Change of NaCl concentration from radiochemical data in reaction NaCl + Ag^{110m} → $Ag^{110m}Cl$ + Na: upper curve shows the initial rate, lower curve the first 300 hours; t = 857°.

(7) W. H. Hamer, M. S. Malmberg and B. Rubin, *J. Electrochem. Soc.*, **103**, 8 (1956).

(8) K. H. Stern, THIS JOURNAL, **60**, 1443 (1956).

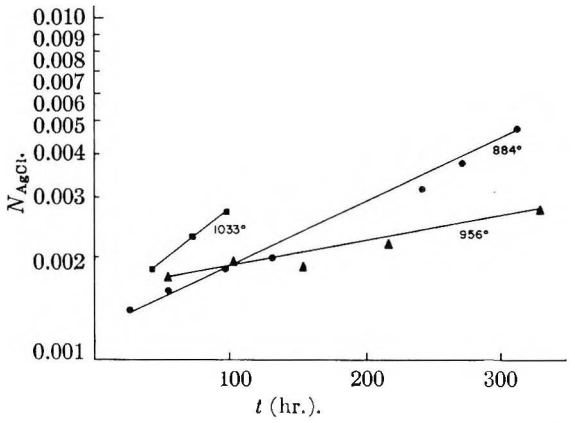

Fig. 3.—Kinetic data for the reaction Ag + NaCl → AgCl + Na: closed system.

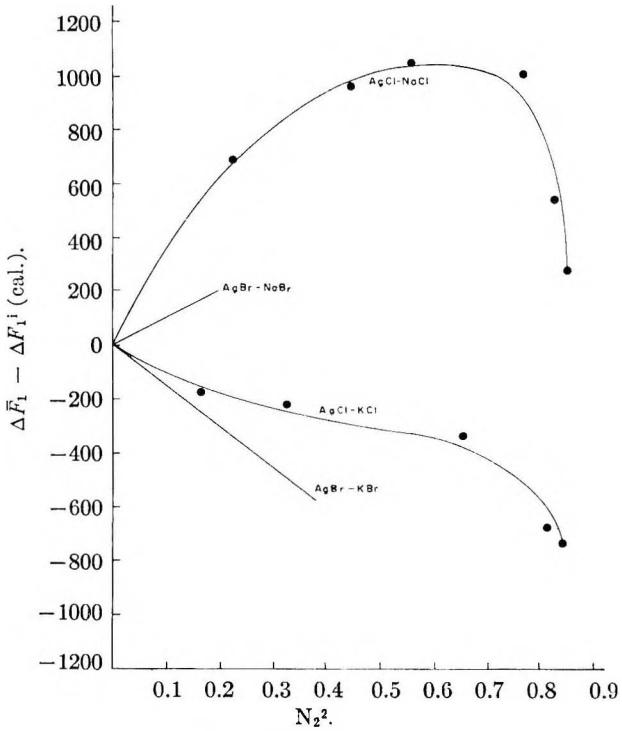

Fig. 4.—Thermodynamic difference function (excess free energy) $\Delta\bar{F}_1 - \Delta\bar{F}_1^i = RT \ln \gamma_1$, for some silver halide–alkali halide systems: AgBr–NaBr, AgBr–KBr at 600°; AgCl–NaCl, AgCl–KCl at 800°; for references see text.

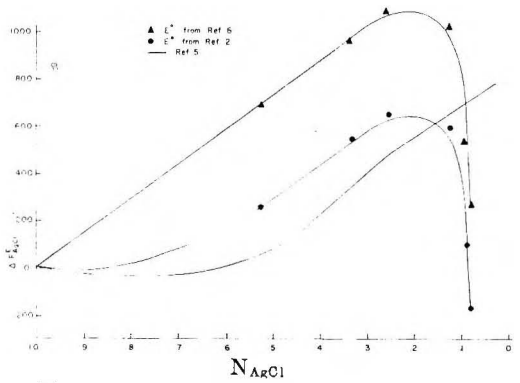

Fig. 5.—Excess free energy ($\Delta F^E = RT \ln \gamma_1$) for the AgCl–NaCl system at 900°.

find. Indeed, after about 100 hours capsules in the 1033° run evidently became permeable to salt after some time since white fumes could be seen coming through the closed capsules.

Discussion

Galvanic Cells.—In their study of the AgBr–alkali bromide systems Hildebrand and Salstrom[3] found that the excess partial molal free energy of AgBr could be represented by an equation of the type $(\bar{F}_1 - \bar{F}_1^i) = BN_2^2$ where $\bar{F}_1 = RT \ln a_1$, $\bar{F}_1^i = RT \ln N_1$ and hence $(\bar{F}_1 - \bar{F}_1^i) = RT \ln \gamma_1$; subscripts 1 and 2 refer to silver bromide and alkali bromide, respectively. This was true, at least, for the solutions rich in AgBr. In Fig. 4 we have plotted $(\bar{F}_1 - \bar{F}_1^i)$ *vs.* N_2^2, where N_2 is the mole fraction of alkali halide, for our data on the AgCl–KCl and AgCl–NaCl systems as well as these functions for the corresponding bromide systems. The data for the bromide systems are given for 650°, for the chloride systems at 900°. However, the entropy is so small as to make the difference negligible. This had been shown by Hildebrand and Salstrom for the bromide systems and also was true for our data; plots of the above functions for several temperatures give virtually the same curve.

From the four systems it seems reasonable to conclude that the anion has virtually no influence on the energies involved in diluting silver ions with alkali metal ions. Over the concentration range studied by Hildebrand and Salstrom our data are also nearly linear, but the deviation from linearity becomes extreme, particularly for the AgCl–NaCl system, on the alkali halide rich side. Parenthetically, our data on the AgCl rich side are also well represented by a first-power concentration dependence, as shown in Fig. 5. Clearly, the choice of E^0 makes a considerable quantitative, but virtually no qualitative, difference. The agreement between our data and those of Panish, *et al.*, is quite good on the silver rich side when the same E^0 is used.

(Since E^0 has now been measured by three independent investigators[2,5,6] whose data agree to within 2 mv. over a large temperature range it would seem that the calculated values of Hamer, *et al.*,[7] may be in error.)

The most striking disagreement with these workers occurs on the NaCl side where our data show a reversal of slope, quite analogous to the abrupt break for the AgCl–KCl system. The slight differences in the experimental arrangement reveal no cause for the discrepancy.

Our data are, however, consistent with the hypothesis that the data below approximately 10 or 12 mole % silver do not represent equilibrium values. For example, in some experiments in which silver was immersed in molten NaCl for several weeks the final composition of the melt was in this range. Since the reaction is very slow it would be possible to measure steady potentials (within a few tenths millivolt) over a period of an hour or two even though the reaction actually was proceeding. It is highly suggestive that the potentials of galvanic cells in which the silver concentration was less than 5 mole % did decrease perceptibly during the time of measurement.

Anticipating the results of our kinetic study in which we found the rate of AgCl buildup to be 7×10^{-5} mole fraction/hr. (at 860°) we get a change of 1 mv./hr. for the galvanic cells, which is in agreement with our observations, and with those reported previously[2] for the cell $Ag/KCl/Cl_2$.

The above results imply that thermodynamic data on silver halide–alkali halide solutions cannot be obtained from measurements on galvanic cells containing silver electrodes for solutions very dilute in silver ion, because silver reacts spontaneously with alkali halides. Thus, even though steady potentials may be measured over an hour or two, they may not represent true equilibrium values.

Of course, thermodynamic data on such solutions may be obtained from methods not involving the presence of metallic silver, *i.e.*, the solutions by themselves are most likely perfectly stable in the absence of the metal except for changes in composition resulting from the preferential vaporization of one component.

Kinetics.—We review first the evidence for our contention that the reaction between silver and sodium chloride is Ag + NaCl → AgCl + Na and that this is a driven reaction.

Consider the equilibrium properties of the system. Using the published E^0 values[7] for AgCl and NaCl we calculate, for 850°, for the reaction Ag + NaCl → AgCl + Na, $E^0 = -2.377$ v., $\Delta F^0 = 54.8$ kcal., $\Delta S^0 = -18.4$ e.u., $\Delta H^0 = 34.6$ kcal. The standard states are the pure substances for Ag, AgCl, and NaCl, and Na vapor at 1 atmosphere pressure. The equilibrium constant $K = 1.91 \times 10^{-11}$. If we let the activity equal the mole fraction we have, in the system at equilibrium

$$K = 1.91 \times 10^{-11} = \frac{P_{Na} N_{AgCl}}{N_{Ag} N_{NaCl}} = \frac{P_{Na} N_{AgCl}}{N_{NaCl}}$$

if the activity of pure silver is unity. Thus, in a closed system in which silver, sodium vapor at 1 atmosphere and NaCl are at equilibrium the concentration of AgCl should be 1.9×10^{-11}, below the limit of detection.

The reverse reaction goes rapidly to completion. This was verified by dropping a piece of sodium into AgCl just above its melting point (480°). The quenched melt contained silver metal.

Unfortunately, the situation in the real system is far more complicated. In addition to the changes in the AgCl/NaCl ratio with time caused by the reaction we must consider the state of the liberated sodium. If the metal and melt were immiscible one might speak of sodium vapor pressure above the melt with some precision. However, at the temperatures of these experiments the solubility of sodium in sodium chloride is considerable,[10] varying from 5 mole % at 850° to 25 mole % at 950° and rising to a consolute temperature near 1060°. Thus it might be more apt to speak of the reaction being driven by the distillation of sodium, not outside the system, but simply into the melt. That sodium does appear in the melt is shown by the blue color of the reaction melts, characteristic of dissolved sodium. Similarly, silver is somewhat soluble in AgCl,[11] 0.06 mole % at 700°. Nothing is known of the solubility of silver in NaCl (as atomic silver). The occurrence of mass-transfer on silver electrodes immersed in NaCl suggests, however, that some solubility exists since otherwise the movement of silver from the hotter to the cooler portions of the electrode would be difficult to explain. It may be that the solution of silver is the initial step in the reaction. Since experimentally we find silver concentrations greater than 0.05 at 860° it is clear that when the solubility of sodium in NaCl is exceeded the metal must distil from the system. Some semi-quantitative experiments in which silver was added to NaCl over a period of two months indicate strongly that the reaction could be driven to completion if enough silver were added.

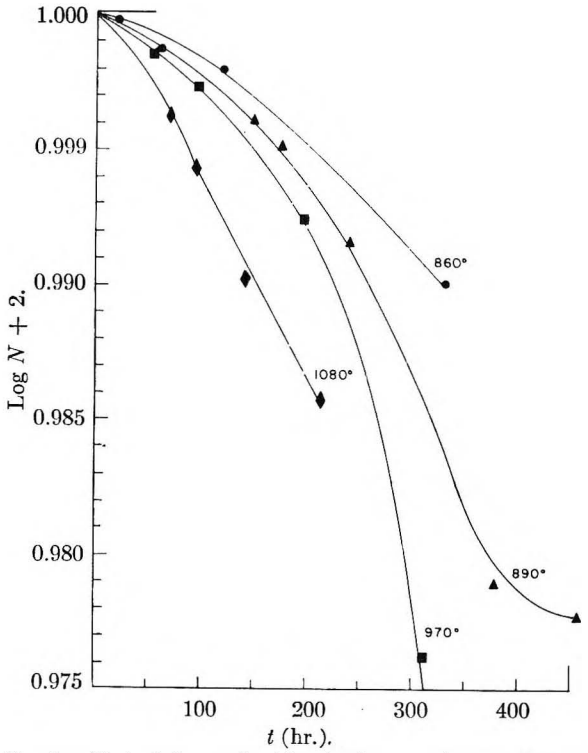

Fig. 6.—Test of first-order kinetics for reaction Ag + NaCl → AgCl + Na data of Fig. 1.

We next consider the order of the reaction. The rate law usually can be determined from a knowledge of reactant or product concentration changes with time. For a zero-order reaction the NaCl concentration is $N_2 = -kt$, whereas for a first-order reaction $\ln N_2 = -kN_2$. Now in the reaction between silver and sodium chloride the mole fraction of the salt, N_2, is between 0.95 and unity. For numbers in this range the number itself and its logarithm are virtually identical. Thus, *a priori*, the data do not distinguish between zero and first-order reactions.

A plot of the log N_2 *vs.* time of the data in Fig. 1 is shown in Fig. 6. A plot of N_2 *vs.* time appears virtually identical. All the curves show an initial slow-rate section and a subsequently more rapid one. The initial period decreases with increasing temperature. Only the 1080° curve is linear over the steep section. Rate constants for this section

(10) M. A. Bredig, J. W. Johnson and W. T. Smith, *J. Am. Chem. Soc.*, **77**, 309 (1955).

(11) J. D. Corbett and S. von Winbush, *ibid.*, **77**, 3964 (1955).

calculated from zero and first-order rate laws are virtually identical, 1.67×10^{-5} mole fraction hr.$^{-1}$ and 1.70×10^{5} hr.$^{-1}$, respectively. The break toward a lower rate in the 890° curve may represent an approach to equilibrium, *i.e.*, the effect of the reverse reaction Na + AgCl → NaCl + Ag.

Since both zero- and first-order treatment yield nearly the same rate constants the same activational energies will apply in either case. The 890 and 970° data do not give very straight lines. However, from the straight-line portion of the 1080° and the 200–300 hour section of the 860° run ($k = 8.9 \times 10^{-5}$ hr.$^{-1}$) we obtain as an estimate for the activational enthalpy $\Delta H^* = 9.7$ kcal. The entropy of activation, ΔS^*, can be calculated from the theory of absolute reaction rates

$$k_T = \frac{kT}{h} e^{\Delta S^*/Re - \Delta H^*/RT} \quad (1)$$

Since k_T is in hr.$^{-1}$, kT/h is in molecules^{-1} hr.$^{-1}$ = 8.35×10^{16}. Solving the equation we get $\Delta S^* = -99.0$ e.u. The free energy of activation is

$$\Delta F^* = \Delta H^* - T\Delta S^* \quad (2)$$

At 861° we get $\Delta F^* = 109$ kcal. The present data are not sufficient to establish a mechanism for the reaction. Broadly it may be described as an electron exchange reaction between atoms and ions characterized by a large negative entropy of activation; this appears to be primarily responsible for the slow rate of reaction, since ΔH^* is relatively small. For reactions of this type in aqueous solution these characteristics have been associated[12,13] with a very low electronic transmission coefficient $k_e = e^{\Delta S^*/R}$. Unfortunately, the equations have been derived only for aqueous solutions, particularly exchange reactions in which the chemical species are indistinguishable, *i.e.*, $\Delta F^0 = 0$. Nevertheless, there is a certain correspondence between the reactions treated by Marcus, Zwolinski and Eyring and the present one.

If it is assumed that $\Delta S^* = R \ln k_e$ and that the reaction is homogeneous (the initial step being the solution of silver in NaCl as atoms) then the tunnel distance r_{ab} at which electron-exchange occurs can be calculated from the expression

$$\ln k_e = -\frac{8\pi}{3h} r_{ab} \left[2me^2 \left(\frac{Z^*}{2r_0} - \frac{f(n)}{Dr_{ab}}\right)\right]^{1/2} \quad (3)$$

where m = mass of the electron, Z^* = the positive charge = 1, $r_0 = n^{*2}a_0$, n^* = effective quantum number for Na = 1.63, $a_0 = 0.528 \times 10^{-8}$ cm., $f(n)$ is a function of charge = 1 for the charge transfer between an atom and a univalent ion, D = dielectric constant. If we let $D = 3$, customary for fused salts, $r_{ab} = 35$ Å., which seems unreasonably large since it is difficult to visualize a mechanism by which an electron can be transferred over such a large distance. However, electron transfer during atom–ion collision in the melt cannot be ruled out.

Alternatively, insufficient evidence is available to establish a heterogeneous mechanism which would have as its initial step the adsorption of sodium ions on the metallic silver surface.

Certainly more work on this reaction, including the effect of surface area and stirring speed on rate, as well as studies on other reactions of this type, is needed.

Acknowledgment.—I wish to thank Mr. Thomas Wilson, a summer research assistant from El Dorado High School, for doing the "closed system" kinetics; Dr. R. W. Fink for his help and advice with the radiochemical experiment, and for the use of his counting equipment; and Mr. K. Okada for the actual counting.

(12) R. J. Marcus, B. J. Zwolinski and H. Eyring, THIS JOURNAL, **58**, 432 (1954).

(13) B. J. Zwolinski, R. J. Marcus and H. Eyring, *Chem. Revs.*, **55**, 157 (1955).

ION-EXCHANGE SEPARATION OF BERYLLIUM BY ELUTION WITH SALICYLATE ANALOGS[1]

BY JACK SCHUBERT, ARTHUR LINDENBAUM AND WILLIAM WESTFALL

Division of Biological and Medical Research, Argonne National Laboratory, Lemont, Illinois

Received June 6, 1957

Rapid quantitative separations of trace quantities of Be from macro-concentrations of salts including those of Cu, U and Ca were devised. The method makes use of the fact that Be forms a relatively strong complex with salicylate analogs in the region *p*H 3–4.5 whereas most cations of the alkaline earths do not react significantly with salicylates, and cations such as Cu^{++} and UO_2^{++} react weakly or not at all in the same *p*H region. The separation of Be from foreign cations is made by means of a cation-exchange resin. Be is eluted selectively with 0.02–0.10 *M* sulfosalicylic acid (SSA) at *p*H 3.5–4.5. Neither Cu^{++}, UO_2^{++} nor Ca^{++} are removed under these conditions. Uranyl ion is eluted by SSA at *p*H 4.5–4.7. The foreign cations can be removed subsequently by a variety of eluting agents such as HCl and H_2SO_4. At *p*H > 6 and in the presence of SSA Be is strongly absorbed by an anion-exchange resin. Evidence is given to show that in the acid regions Be forms an uncharged complex with SSA and a negatively charged complex in neutral and alkaline regions.

The sensitivity of analytical procedures for beryllium is severely limited by the presence of interfering substances.[2a–c] This problem becomes especially acute when it is necessary to isolate micro-quantities of Be from biological and geological materials. Usual methods of extraction and precipitation in such cases are not only laborious and time-consuming but often give low or erratic results. Since the discovery that the radioactive nuclides, Be^7 and Be^{10}, are produced in the atmosphere by cosmic rays,[2b] it is especially worth-

(1) Work performed under the auspices of the U. S. Atomic Energy Commission.

(2) (a) T. Y. Toribara and R. E. Sherman, *Anal. Chem.*, **25**, 1594 (1953); (b) J. R. Arnold and H. A. Al-Salih, *Science*, **121**, 451 (1955); (c) A. J. Cruikshank, G. Cowper and W. E. Grummitt, *Can. J. Chem.*, **34**, 214 (1956).

while to be able to isolate quantitatively trace amounts of Be.

In the separation of a micro-component from large amounts of impurities it is usually desirable to remove the micro-component first. It was decided to utilize the selective metal complexing properties of salicylic acid derivatives in combination with ion exchange. Salicylic acid and derivatives, such as sulfosalicylic and gentisic acids, react negligibly with most alkaline earth cations, *e.g.*, Ca, yielding formation constants with values of log K_1 of 0.14–0.6 for ionic strengths in the region of 0.1–0.16.[3–6] On the other hand, the formation constants for complexes of Be^{++} and UO_2^{++} and for transition elements such as Cu^{++}, Ni^{++} and Fe^{+++} fall in the range log K_1 = 2–5.[7a–f] Since the ratio of the formation constants of Be to that of the other alkaline earths is approximately 10^5, it is possible to devise rapid and efficient schemes for separation of Be from large amounts of mineral substances such as rock and bone without the necessity of resorting to relatively slow chromatographic techniques.

Experimental

The resin used was 8% cross-linked, 60–100 mesh "Dowex 50," a sulfonated polystyrene cation exchanger (Dow Chemical Company, Midland, Michigan). A 5 *N* HCl solution was passed through a column of the resin until all traces of iron were removed. The resin was then alternately converted several times to the sodium and hydrogen forms by use of excess 2*N* NaOH and 2 *N* HCl. The H-form of the resin subsequently was washed with ethanol to remove soluble organic material. Finally, the "fines" were removed by decantation and the resin was air-dried and stored in an air-tight bottle.

In general, a small volume of a Be-containing solution was absorbed at the top of the resin column. Subsequently the Be was eluted with either sulfosalicylic acid or gentisic acid at a given *p*H. When all the Be had been eluted, the remaining bulk cations were usually eluted with either HCl or H_2SO_4. In most instances the effluent was collected by means of an automatic fraction collector.

Radiochemical analyses for Be, Ca and U were made, when specified, by use of the radioactive isotopes Be^7, Ca^{45} and U^{233}. The Cu concentration was determined spectrophotometrically by measurement of the optical density of 3 *M* H_2SO_4 solutions at 455 mμ. Calcium assays were made by precipitation of calcium oxalate from an effluent with 0.01 *N* sodium oxalate and subsequent titration with 0.01 *N* $KMnO_4$. Semi-quantitative tests for Ca were made by adding brom thymol blue to 5-ml. volumes of effluent and then adding NH_4OH dropwise until a blue color persisted in the solution. Upon the addition of 1 ml. of saturated ammonium oxalate a cloudiness proportional to the concentration of precipitated calcium oxalate was observed. The method was sensitive to 0.1 mg. of Ca per 5 ml.

In some experiments a synthetic bone ash solution "spiked" with Be^7 was used. A 20.00-ml. solution consisted of 0.0233 g. of $Mg_3(PO_4)_2 \cdot 8H_2O$, 0.1000 g. of $CaCO_3$, 0.8500 g. of $Ca_3(PO_4)_2$, 0.0106 g. of NaCl and 0.0025 g. of KCl, all dissolved in 1.0 *N* HCl.

Several batch experiments were carried out. In general, a weighed amount of air-dried resin was mixed with a given volume of solution and the mixture shaken mechanically for 2–3 hours. The supernatant solution was assayed for the element, usually Be^7, and the fraction absorbed by the resin was calculated.

(3) C. R. Davies, *J. Chem. Soc.*, 277 (1938).

(4) N. R. Joseph, *J. Biol. Chem.*, **164**, 529 (1946).

(5) R. P. Bell and C. M. Waind, *J. Chem. Soc.*, 2357 (1951).

(6) J. Schubert, *J. Am. Chem. Soc.*, **76**, 3442 (1954).

(7) (a) H. V. Meek and C. V. Banks, *ibid.*, **73**, 4108 (1951); (b) R. T. Foley and R. C. Anderson, *ibid.*, **70**, 1195 (1948); (c) **71**, 909 (1949); (d) S. E. Turner and R. C. Anderson, *ibid.*, **71**, 912 (1949); (e) R. T. Foley and R. C. Anderson, *ibid.*, **72**, 5609 (1950); (f) M. B. Lasater and R. C. Anderson, *ibid.*, **74**, 1429 (1952).

Results

1. Batch Tests. (a) Effects of *p*H and Sulfosalicylic Acid Concentrations.—The system consisted of 100 mg. of air-dried "Dowex 50" in the H-form containing absorbed Be^7, 100 ml. of solution 0.16 *N* in NaCl, *p*H 7, and containing concentrations of sulfosalicylic acid (SSA) varying from 0.01 to 0.08 *M*. With 0.01 *M* SSA only 61% of Be^7 was eluted, but at a concentration of SSA of 0.02 *M* or greater, elution was complete. Next the concentration of SSA was kept constant at 0.02 *M* while the *p*H was varied. It was found that at *p*H 2.5 and below absorption of Be^7 by Dowex 50 was nearly complete while at *p*H 3.2 and greater the absorption dropped sharply to zero, *i.e.*, complete elution.

The above results showed that Be formed a sufficiently strong complex ion with SSA at concentrations of at least 0.02 *M* SSA at *p*H > 2.5, so that rapid elution from a cation-exchange resin could be expected. The observed *p*H of 3.2 in 0.02 *M* SSA at which complex formation became effective was in agreement with the observations of Meek and Banks[8] regarding the stability of the Be–SSA complex as a function of *p*H.

Further information on the nature of the complex ion formed between Be and SSA was obtained from determination of the uptake of Be from SSA solutions by a strongly basic anion resin, "Amberlite IRA-410," a quaternary amine exchanger (Rohm and Haas Company, Philadelphia, Pennsylvania). Up to a *p*H of 4.5 the absorption of Be by this resin was only a few per cent. In terms of the distribution coefficient, K_d, where

$$K_d = \frac{\%\text{ cation in resin}}{\%\text{ cation in soln.}} \times \frac{\text{vol. of soln. } (v)}{\text{mass of resin } (m)} = \lambda \frac{v}{m}$$

the values of K_d (when v was expressed in ml., m in grams) varied from 1 to 4. However, at *p*H 6 and above the uptake rapidly increased to values of K_d several hundred-fold higher.

In the acid regions SSA forms a 1:1 complex with Ni^{++}, Cu^{++}, Fe^{++}, UO_2^{++} and Al^{+++}.[7b–f] The proton binding constant for the carboxyl group in SSA has a pK of about 2.86,[7c] while that of the phenolic–OH group is about 11.7.[9] The phenolic hydroxide group participates in the complex formation even in the *p*H region 3–5 but without the loss of a proton. The $-SO_3$ group gives only a minimum contribution. It is also known that Be forms at best only very weak complexes with aliphatic –OH groups and aliphatic carboxyl-hydroxyl compounds.[10] From such considerations and from the above ion-exchange data we can postulate that in the acid regions (*p*H 3.3) the uncharged complex

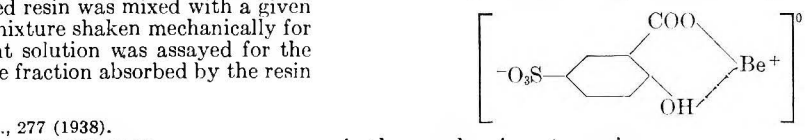

is the predominant species.

(b) Separation in Absence of Salicylates.—Be-

(8) H. V. Meek and C. V. Banks, *Anal. Chem.*, **22**, 1512 (1950).

(9) A. Ågren, *Acta Chem. Scand.*, **9**, 49 (1954).

(10) (a) J. Schubert and A. Lindenbaum, *J. Biol. Chem.*, **208**, 359 (1954); (b) A. Lindenbaum, M. R. White and J. Schubert, *Arch. Biochem. Biophys.*, **52**, 110 (1954).

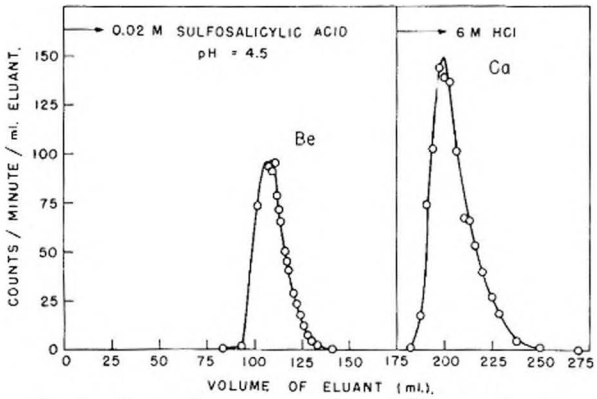

Fig. 1.—Ion-exchange separation of 20 mg. of calcium phosphate from tracer quantities of Be^7 (200–300 mesh "Dowex 50," 1.18 cm.² by 14 cm. deep, hydrogen form; elutriant, as shown, passed at 1 ml./min.). Be^7 did not appear in effluent until *p*H 3–3.5 was reached.

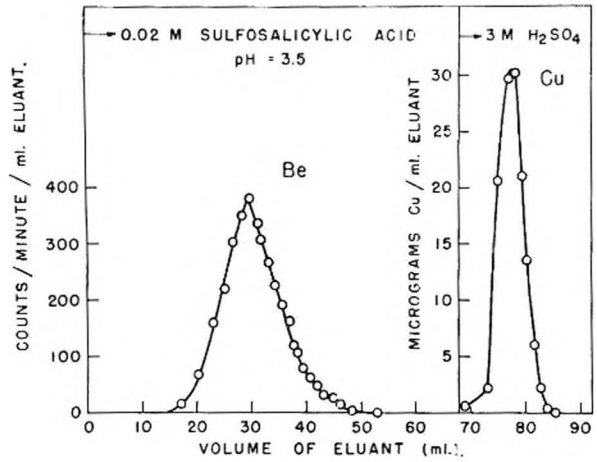

Fig. 2.—Ion-exchange separation of 155 micrograms Cu from tracer quantities of Be^7 (same resin bed and flow rate as in Fig. 1).

cause Be has an extremely small ionic radius and hence a large hydrated radius, its affinity for a cation exchanger in acid media is considerably less than for the other alkaline earth cations.[11] Thus an additional means of separation is possible. In the range of 0.1 to 2 *M* HCl it is possible to separate Be from the other alkaline earths by elution with HCl or simple salts. However, the separation factors are still several orders of magnitude below the values obtained by the use of salicylates.

The uptake of Be^{++} by "Dowex 50" compared to that of Sr^{++} was measured in HCl solutions. In 0.1 *M* HCl the K_d for Sr^{++} (where *m*, the mass of resin, is given in milligrams) was 41 while that for Be^{++} was 2.1—a ratio of $K_d(Sr)/K_d(Be) = 20$. With increasing HCl concentration the ratio diminished to only 6 at 2 *M* HCl. At concentration of HCl 3 to 8 *M* the ratio of uptake of Sr^{++} and Be^{++}, rather than decreasing, remained roughly constant at ~0.25, a reversal of affinities that is in general agreement with previous observations.[12,13]

2. Column Separations. (a) Separation of Be- and Ca-Containing Solutions.—Two ml. of a solution consisting of carrier-free Be^7 and 20 mg. of $Ca_3(PO_4)_2$ labeled with Ca^{45}, and 0.6 *M* in HCl, was added to the top of a Dowex 50 column in the H-form. Sulfosalicylic acid, adjusted to *p*H 4.5 with NH_4OH,[14] was passed through the column. Additional experimental data and results are shown in Fig. 1. No Be was eluted until the *p*H of the effluent rose to approximately 3. At that point the Be was eluted from the column in a sharp band with no detectable Ca^{45} contaminant. When all the Be had been eluted the Ca was eluted readily with 6 *M* HCl. Within experimental error all the Be and Ca were recovered: 1942 counts/min. of Be^7 added, recovered 1937; 3298 counts/min. of Ca^{45} added, recovered 3274.

The effectiveness of salicylate analogs in the separation of trace amounts of Be from synthetic bone ash (see Experimental section) was demonstrated by use of 0.1 *M* gentisic acid (GA) adjusted to a *p*H of 6.0 with NaOH. Pertinent column data include: 15 g. of air-dried "Dowex 50," H-form, 60–100 mesh; column dimensions 12.5 cm. high × 1.0 cm. diameter. Thirty and a half ml. of the synthetic bone ash solution in 0.7 *N* HCl was passed through the column at a flow rate of 1 ml./min. followed by a wash solution of 0.01 *N* HCl to remove residual interstitial ions. Elution with gentisic acid was begun at a flow rate of 1 ml./min. Effluent samples of 5-ml. volumes were taken and analyzed for Be^7 and Ca. When the *p*H of the effluent reached 1.90 (at this point the total effluent volume including holdup was 190 ml.) the Be came off the column in a very sharp band which reached its peak at *p*H 2.74. Within a total volume of 110 ml., or about 10 column volumes, the elution of Be^7 was quantitatively complete while Ca was quantitatively retained on the column. At the end of the elution the *p*H of the effluent was 5.60.

Another approach has the advantage that larger volumes of solution containing Be and foreign ions can be handled. In this procedure, after the Be and foreign salts were dissolved, SSA was added to the solution, the *p*H was adjusted, and the entire solution passed through a resin column previously conditioned with the identical concentration and *p*H of NH_4SSA. With this pretreatment Be broke through immediately and passed through quantitatively without the necessity for additional SSA elutriant. The results of one such separation are shown in Table I, where 150 ml. of a solution containing a mixture of 1.101 g. of $CaCl_2$ and 5 mg. of Be as $BeSO_4$ was completely resolved.

(b) Separation of Be and Cu.—At all *p*H regions Cu forms a complex with SSA that is only one-tenth as strong as the corresponding Be complexes with SSA[7a,d]; consequently it is possible to effect rapid quantitative separations of trace amounts of Be from copper salts. In Fig. 2 is shown a typical separation accomplished by the use of 0.02 *M* SSA at a *p*H of 3.5. The position of the Cu band was unaffected by the SSA; Cu was removed later with 3 *M* H_2SO_4.

(11) T. R. E. Kressman and J. A. Kitchener, *J. Chem. Soc.* (London), 1201 (1949).

(12) K. A. Kraus, F. Nelson and G. W. Smith, THIS JOURNAL, **58**, 11 (1954).

(13) R. M. Diamond, *J. Am. Chem. Soc.*, **77**, 2978 (1955).

(14) The ammonium salts generally are preferable, as they allow a reduction in the bulk of ash to be used for subsequent radiochemical or spectrographic assay of Be.

(c) **Separation of Be and U(VI).**—Uranyl ion, UO_2^{++}, forms a 1:1-complex with SSA at *p*H 4.5–4.7.[7c] Above and below this *p*H-region the stability of the complex decreases markedly. Inasmuch as Be is eluted readily with SSA or GA in the general *p*H region 3 to 4, rapid and complete separations of Be and U(VI) are effected easily. In one run a column of "Dowex 50," 12.5 cm. high × 1.0 cm. in diameter, 60 to 100 mesh, was used. The elutriant was 0.02 *M* SSA at a *p*H of 4.2. Two ml. of a solution consisting of 100 mg. of uranyl nitrate (labeled with 42,000 counts/min. of U^{233}) and 5 μg. of Be (labeled with 6,990 counts/min. of Be^7) as $BeSO_4$ were placed on the top of the column. Be began to break through at *p*H 1.8 and reached a peak at *p*H 3.68. At the point where all the Be had been eluted, *p*H 4.3, no U could be detected. When the concentration of SSA was increased to 0.1 *M* and the *p*H to 6, the U was rapidly and quantitatively removed. The peak of the elution curve came in the *p*H region 4.5–4.7, in agreement with the *p*H region of maximum stability of the complex. When the *p*H of the elutriant varied in either direction from the optimum by more than about 0.5 *p*H unit, considerable tailing of the U elution curve was observed. For optimum Be-U separation it is suggested that 0.1 *M* SSA be used at *p*H 3.5 to 3.8. When all the Be has been eluted, the U(VI) can be removed with 0.1 *M* SSA at *p*H 4.6–4.7.

TABLE I

SEPARATION OF BE FROM CA

Solution: 150 ml. containing 1.101 g. of $CaCl_2$, 5 micrograms Be as $BeSO_4$, 156,300 counts/min. tracer Be^7, all 0.1 *M* in sulfosalicylic acid (SSA) adjusted to *p*H 4.5 with NH_4OH. Column: "Dowex 50" resin, 60–100 mesh, equilibrated with 0.1 *M* SSA adjusted to *p*H 4.5 with NH_4OH; 15.0 g. of resin, 39 cm. in height × 1.0 cm. diameter, flow rate, 2–3 ml./min.

Fraction collected (ml.)	Vol. (ml.)	% Total Be	Ca (mg.)	% Total Ca
0–10	10	0.96	0	0
10–81	71	47.1	0	0
81–151.5	70.5	45.6	0	0
151.5–233 (includes 70 ml. SSA wash)	82	6.0	0	0
233–500 (3 *N* HCl)	26.7	0	295	99

Discussion

When solid materials containing Be are put into solution it is sometimes found that the uptake of Be by a cation exchanger, or its extractability by acetylacetone, is nil or erratic. The difficulty seems to be caused by the conversion of Be into an insoluble oxide when the temperature of dry ashing exceeds 500°.[2,15] However, it has been found that the treatment recommended by Toribara and Chen,[15] namely, to heat the dry ashed residues strongly with concentrated sulfuric acid for several minutes, renders the Be absorbable if the ash has not been lost, wholly or in part, by fusion to the surface of the container.

For samples containing very large amounts of calcium it is possible to use a column large enough to absorb all the polyvalent cations. In the case of "Dowex 50" this would require a minimum of roughly 10 g. of resin per g. of calcium. Calcium may also be removed prior to passage through the column by precipitation of the sulfate from an acidic solution without loss of Be.[15]

Other methods[2,7a,8,16] for minimizing interferences by Ca provide for the addition of EDTA or one of its analogs to the Be-containing solution before passage through the cation exchanger. For example, from a solution at *p*H 5 and containing 2 g. of the tetrasodium salt of EDTA per liter, Be was quantitatively absorbed by the NH_4-form of "Dowex 50,"[16] while those cations which form chelates with EDTA, including Ca, Fe, Mg, Ni and Al, etc., passed through. In many cases, however, as with copper and uranyl ion, the differences in stability of the salicylic acid complexes of Be and many of the transition elements are great enough that the use of a more selective complexing agent such as EDTA is unnecessary.

Iron was eluted along with Be by salicylates at the usual *p*H range employed, namely, 3.5 to 4.5. However, since Fe(III) formed a fairly strong complex with salicylates at *p*H's below 3, it was possible to elute the Fe prior to Be elution. (The polyamino chelating agents also can be used.) In one experiment, for example, from a mixture of Fe, Be and Ca the Fe was eluted with 0.1 *M* gentisic acid at a *p*H of 2.1, then the *p*H was raised to elute the Be, while the Ca was eluted later with HCl.

Another procedure for rapidly removing many interfering elements from Be would be to pass a strong HCl solution of the Be through an anion exchanger first. In such solutions Be is unabsorbed while many elements, including iron and uranium, are strongly absorbed.[17]

Finally there is the problem of how to deal with potential aluminum interference. Since Al is eluted by salicylates in the same *p*H range as Be, the Al must be separated by other means. Kakihana[18] was able to separate Be from Al by passage of a dilute (~0.01 *N*) solution of their salts through a cation exchanger in the calcium form. The Be ran through while Al was retained. Residual Be was eluted free of Al by the use of 0.1 *N* $CaCl_2$. To carry this procedure one step further, the Be could now be reabsorbed by a cation exchanger and eluted with SSA. Other workers[19] have passed the oxalates of Be, Al and Fe through a cation exchanger. The oxalates of Al and Fe are stable at *p*H 4.4 to 4.5 and pass through, while Be is retained on the column.

EDTA forms a chelate with Al under conditions allowing little or no complex formation with Be.[8] Thus, it should be possible to effect a separation of Al from Be either by adding EDTA to the solution at *p*H ~4 before passage through a cation exchanger, or by eluting the Al with EDTA prior

(15) T. Y. Toribara and P. S. Chen, Jr., *Anal. Chem.*, **24**, 539 (1953).

(16) (a) J. Hure, M. Kremer and F. LeBerquier, *Anal. Chem. Acta*, **7**, 37 (1952); (b) M. S. Das and V. T. Athavale, *ibid.*, **12**, 6 (1955); (c) J. Kinnunen and B. Wennerstrand, *Chemist-Analyst*, **44**, 51 (1955).

(17) K. A. Kraus and F. Nelson, "Anion Exchange Studies of the Fission Products," Proceedings of the International Conference on the Peaceful Uses of Atomic Energy, Vol. 7, p. 113, Session 9B.1, P/837, United Nations (1956).

(18) H. Kakihana, *J. Chem. Soc. Japan*, **72**, 200 (1951).

(19) D. I. Ryabchikov and V. E. Bukhtiarov, *Zhur. Anal. Khim.*, **9**, 196 (1954); *C. A.*, **48**, 12610^h (1954).

to Be elution with salicylates.

Acknowledgments.—We are indebted to Mr. Roman V. Lesko for technical assistance in the early stages of this investigation.

THE APPLICATION OF THERMOANALYTICAL TECHNIQUES TO REACTION KINETICS.[1] THE THERMOGRAVIMETRIC EVALUATION OF THE KINETICS OF THE DECOMPOSITION OF CALCIUM OXALATE MONOHYDRATE

BY ELI S. FREEMAN[2] AND BENJAMIN CARROLL

Chemistry Department, Rutgers University, Newark 2, N. J., and The Pyrotechnics Chemical Research Laboratory, Picatinny Arsenal, Dover, N. J.

Received July 30, 1957

The application of thermoanalytical techniques to the investigation of rate processes is discussed. Equations have been derived for non-reversing reactions, which may be used to calculate energy of activation and order of reaction from thermogravimetric and volumetric curves. An equation, recently presented in the literature, for evaluating these parameters by the technique of differential thermal analysis has also been considered, so as to eliminate the trial and error procedure. The thermal decomposition of calcium oxalate monohydrate, which involves dehydration, decomposition of calcium oxalate and calcium carbonate, is used to illustrate the applicability of the derived relationships.

Introduction

Thermoanalytical methods, such as thermogravimetry, thermovolumetry and differential thermal analysis, are being employed increasingly in the investigation of chemical reactions in the liquid and solid states at elevated temperatures. These techniques involve the continuous measurement of a change in a physical property such as, weight, volume, heat capacity, etc., as sample temperature is increased, usually at a predetermined rate. In this article, equations are derived for non-reversing reactions so that rate dependent parameters such as energy of activation and order of reaction may be calculated from a single experimental curve. For this purpose a relationship between specific rate and temperature is assumed

$$k = Ze^{-E^*/RT}$$

A general derivation is presented and applied to thermogravimetry. For the method of differential thermal analysis, the derivation of Borchardt and Daniels[3] has been expanded upon, so that the trial and error procedure now required for evaluating order of reaction and activation energy, may be replaced by a graphical or analytical solution.

It should be kept in mind that the treatment may be applied to the measurement of any physical property which is unaffected by sample temperature. The advantages of evaluating reaction kinetics by a continuous increase in sample temperature are that considerably less experimental data are required than in the isothermal method, and the kinetics can be probed over an entire temperature range in a continuous manner without any gaps. In addition, where a sample undergoes considerable reaction in being raised to the temperature of interest, the results obtained by an isothermal method of investigation are often questionable.

(1) This paper has been presented in part at the North Jersey Meeting in Miniature of the A.C.S. in Jan., 1957, and before the Division of Physical and Inorganic Chemistry at the National Meeting of the A.C.S. in April, 1957.

(2) Pyrotechnics Chemical Research Laboratory, Bldg. 1512, Picatinny Arsenal, Dover, New Jersey.

(3) H. J. Borchardt and F. D. Daniels, *J. Am. Chem. Soc.* **79**, 41 (1957).

Theory and Derivation

Consider a reaction, in the liquid or solid states, where one of the products B is volatile, all other substances being in the condensed state.

$$aA = bB(g) + cC$$

The rate expression for the disappearance of reactant A from the mixture is

$$-\frac{dX}{dt} = kX^x \qquad (1)$$

where

X = conen., mole fraction or amount of reactant, A
k = specific rate
x = order of reaction with respect to A

It is assumed that the specific rate may be expressed as

$$k = Ze^{-E^*/RT} \qquad (2)$$

Solving for k in (1) and substituting (2) for k gives

$$Ze^{-E^*/RT} = \frac{-(dX/dt)}{X^x} \qquad (3)$$

where

Z = frequency factor
E^* = energy of activation
R = gas constant
T = absolute temperature

The logarithmic form of equation 3 is differentiated with respect to, dX/dt, X and T, resulting in equation 4.

$$\frac{E^*dt}{RT^2} = d\ln(-dX/dt) - x\,d\ln X \qquad (4)$$

Integrating the above relationship gives

$$\frac{-E^*}{R} = \Delta\left(\frac{1}{T}\right) = \Delta\ln\left(\frac{-dX}{dt}\right) - x\Delta\ln X \qquad (5)$$

Dividing (4) and (5) by $d\ln X$ and $\Delta\ln X$, respectively, one obtains equations 6 and 7.

$$\frac{E^* \, dT}{RT^2 \, d \ln X} = \frac{d \ln (-dX/dt)}{d \ln X} - x \qquad (6)$$

$$\frac{-\frac{E^*}{R} \Delta \left(\frac{1}{T}\right)}{\Delta \ln X} = \frac{\Delta \ln (-dX/dt)}{\Delta \ln X} - x \qquad (7)$$

From (6) and (7) it is apparent that plots of

$$\frac{dT}{T^2 \log X} \text{ vs. } \frac{d \log (-dX/dt)}{d \log X}$$

and

$$\frac{\Delta (1/T)}{\Delta \log X} \text{ vs. } \frac{\Delta \log (-dX/dt)}{\Delta \log X}$$

should result in straight lines with slopes of + or $-E^*/2.3R$ and intercepts of $-x$.

Let us consider the cases where X refers to mole fraction of A, molar concentration and amount of reactant.

1. Mole fraction of A, $X = n_a/M = N_A$

where: n_a = no. of moles of A at time t
M = total no. of moles in reaction mixture

(a) Total number of moles is constant during reaction. Substituting for X in (3) results in the relationships

$$\ln k = \ln M^{x-1} + \ln (-dn_a/dt) - x \ln n_a \qquad (8)$$

and

$$\frac{-(E^*/R)\Delta(1/T)}{\Delta \ln n_a} = -x + \frac{\Delta \ln (-dn_a/dt)}{\Delta \ln n_a} \qquad (9)$$

Equation 9 also may be written in differential form as equation 4.

(b) Total number of moles is not constant. For this case

$$\ln k = (x - 2) \ln M - x \ln n_a + \ln \left(n_a \frac{dM}{dt} - M \frac{dn_a}{dt}\right) \qquad (10)$$

$$\frac{\frac{E^*}{RT^2} dT}{d (\ln M - \ln n_a)} = x + \frac{d \ln \left(n_a \frac{dM}{dt} - M \frac{dn_a}{dt}\right) - 2 \, d \ln M}{d (\ln M - \ln n_a)} \qquad (11)$$

and

$$\frac{\frac{-E^*}{R} \Delta \left(\frac{1}{T}\right)}{\Delta (\ln M - \ln n_a)} = x + \frac{\Delta \ln \left(n_a \frac{dM}{dt} - M \frac{dn_a}{dt}\right) - 2 \Delta \ln M}{\Delta (\ln M - \ln n_a)} \qquad (12)$$

2. Molar concn. $X = n_a/V$

where V = volume of reaction mixture

The equations which result are identical to the case of mole fraction with the exception that V replaces M.

3. $X = n_a$

For this case

$$\ln k = -x \ln n_a + \ln (-dn_a/dt) \qquad (13)$$

The final equation is identical to (9).

The above relationships may be applied simply to measurements of weight or volume changes by the appropriate substitutions for M and n_a. After evaluating x and E^* the frequency factors may be calculated by combining equations 2 and 1.

Let us consider the case of differential thermal analysis.

In a recent article[3] an equation was derived from which order of reaction and energy of activation was determined using differential thermal analysis. The expression given was

$$k = \left(\frac{KAV}{n_0}\right)^{x-1} \frac{C_p \frac{d\Delta T}{dt} + K\Delta T}{(K(A - a) - C_p \Delta T)^x} \qquad (14)$$

where

K = heat transfer coefficient
A = area under curve
ΔT = differential temp. at a particular time
$d\Delta T/dt$ = rate of change of differential temp. at the point where ΔT is measured
V = volume of solution
n_0 = initial number of moles of reactants
Cp = total heat capacity of reactant solution or liquid
a = area under curve up to time where ΔT and $d\Delta T/dt$ is taken
x = order of reaction with respect to one component

The method used by the authors[3] to determine x and E^* is as follows. A value of x is chosen and used to calculate k over an entire temperature range using equation 14. A graph of log k *vs.* T^{-1} was then plotted. If a linear relationship was obtained, it was assumed that the value of x was valid and the energy of activation could then be calculated from the slope of the line.

A method of evaluating x and E^* which eliminates this trial and error procedure becomes apparent if equation 2 is substituted in (14). The resulting expression written in logarithmic form is

$$\ln Z - \frac{E^*}{RT} = (x - 1) \ln \frac{KAV}{n_0} - x \ln (K(A - a) - C_p \Delta T) - \ln \left(C_p \frac{d\Delta T}{dt} + K\Delta T\right) \qquad (15)$$

Differentiating and integrating (15) gives equations 16 and 17, respectively.

$$\frac{\frac{E^* \, dT}{RT^2}}{d \ln (K(A - a) - C_p \Delta T)} = -x + \frac{d \ln \left(C_p \frac{d\Delta T}{dt} + K\Delta T\right)}{d \ln (K(A - a) - C_p \Delta T)} \qquad (16)$$

$$\frac{\frac{-E^*}{R} \Delta \left(\frac{1}{T}\right)}{\Delta \ln (K(A - a) - C_p \Delta t)} = -x + \frac{\Delta \ln \left(C_p \frac{d\Delta T}{dt} + K\Delta T\right)}{\Delta \ln (K(A - a) - C_p \Delta T)} \qquad (17)$$

From the above it is clear that plots of

$$\frac{\frac{dT}{T^2}}{d \log (K(A - a) - C_p \Delta T)} \text{ vs. } \frac{d \log \left(\frac{d\Delta T}{dt} + K\Delta T\right)}{d \log (K(A - a) - C_p \Delta T)}$$

and

$$\frac{\Delta \left(\frac{1}{T}\right)}{\Delta \log (K(A - a) - C_p \Delta T)} \text{ vs. } \frac{\Delta \log \left(\frac{d\Delta T}{dt} + K\Delta T\right)}{\Delta \log (K(A - a) - C_p \Delta T)}$$

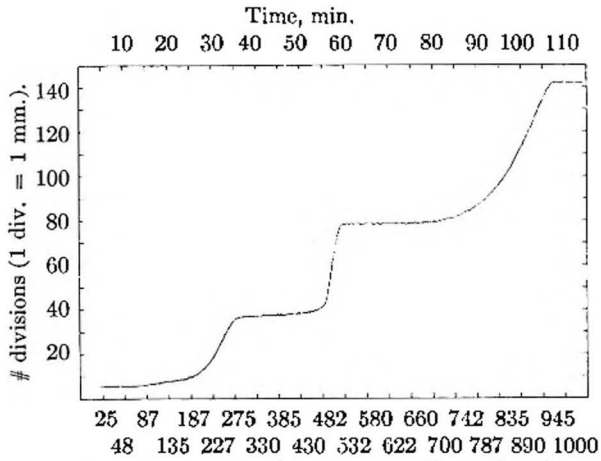

Fig. 1.—Thermogram for decomposition of calcium oxalate monohydrate, weight (mg.) *vs.* temp. and time: 2 mm. on X-axis = 1 min.; 1 mm. of Y-axis = 2.05 mg.

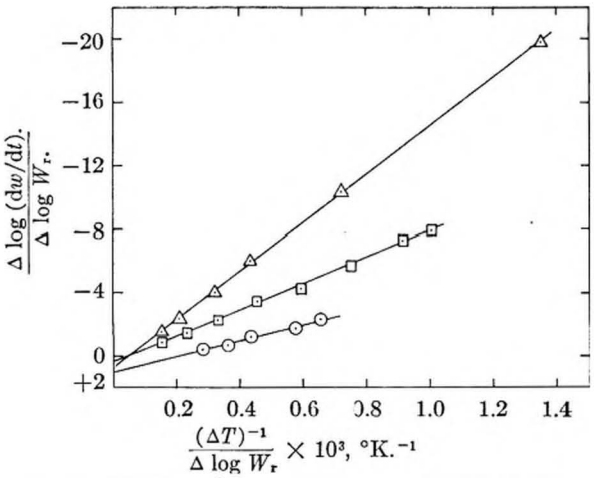

Fig. 2.—Kinetics of decomposition: ○, $CaC_2O_4 \cdot H_2O(s) = CaC_2O_4(s) + H_2O(g)$; △, $CaC_2O_4(s) = CaCO_3(s) + CO(g)$; □, $CaCO_3(s) = CaO(s) + CO_2(g)$.

should result in straight lines with intercepts at $-x$ and slopes of $+$ or $-E^*/2.3R$ for any unique physical or chemical reaction. It should be noted, however, that (14) and subsequent equations are valid only where the volume of the reaction mixture does not change appreciably.

Experimental

The Testut magnetic transmission type continuously recording thermobalance[4] employed for the thermogravimetric studies, was supplied by the Testut Company of Paris, France.[5] A weight of 423 mg. of calcium oxalate monohydrate was placed in #000 Coors glazed porcelain crucible and heated in air, from room temperature to 1000° at a rate of 10°/min. A Marshall Product's furnace was used for this purpose. A chromel-alumel thermocouple was located directly beneath the sample. The increase in furnace temperature was regulated by a Guardsman Indicating Pyrometric Stepless Program Controller which was purchased from the West Instrument Company. A continuous record of weight change as a function of time and temperature was obtained as shown in Fig. 1. The calcium oxalate monohydrate was of C.P. grade and purchased from the Fisher Scientific Company.

(4) An article describing and evaluating this balance will be submitted for publication in the Journal of Analytical Chemistry. Also see Abst. Paper #12, Div. of Analytical Chem. Natl. Meeting, A.C.S., April 1957.

(5) Testut Company, 9, Rue Brown Sequard, Paris XV, France.

The rate of change in sample weight was obtained by going, horizontally, two divisions to the right and two divisions to the left of a particular point on the curve and extending two vertical lines in opposite directions at these positions to the curve. The vertical distance between the points on the curve was taken as the measure of the rate of change in weight. Since two horizontal divisions is equal to 1 min., the rate of change in weight is given as change in the number of divisions for every 2 min. Substantially the same results were obtained by drawing tangents to the curve. The sample was weighed before and after heating, on an analytical balance, and was within 2% of the theoretical weight loss.

Results and Discussion

Figure 1 is a continuous tracing of change in sample weight as a function of time and temperature where $CaC_2O_4 \cdot H_2O$ is heated from 25 to 1000°. Three distinct reactions are apparent, dehydration, decomposition of CaC_2O_4 to $CaCO_3$ and CO, and decomposition of $CaCO_3$ to CaO and CO_2. The weight losses are within 2% of the theoretical values. Since the reactions under consideration involve solid state decomposition it is assumed that the rate expression may be given in terms of amount of reactant where equations 9 and 13 apply.

The following relationships may be used to relate number of moles of reactant to weight

$$-\frac{dn_a}{dt} = -\frac{n_0}{w_c}\frac{dw}{dt} \qquad (18)$$

and

$$W_r = w_c - w \qquad (19)$$

where

n_0 = initial number of moles of A
w_c = weight loss at completion of reaction
w = total weight loss up to time, t

combining (18) and (19) with (9), equation 20 is obtained, which is used to evaluate the reaction kinetics

$$\frac{\frac{-E^*}{2.3R}\Delta\left(\frac{1}{T}\right)}{\Delta \log W_r} = -x + \frac{\Delta \log dw/dt}{\Delta \log W_r} \qquad (20)$$

Figure 2 is a graph of

$$\frac{\Delta \log dw/dt}{\Delta \log W_r} \text{ vs. } \frac{\Delta(T^{-1})}{\Delta \log W_r}$$

for the three reactions. For the purpose of this plot, dw and W_r can be determined directly from the thermogram in terms of number of divisions. The values of order of reaction and energy of activation for dehydration, decomposition of CaC_2O_4 and $CaCO_3$ were found to be 1.0, 0.7, 0.4 and 22, 74 and 39 kcal./mole, respectively. See Table I.

Table I compares these results with those reported in the literature. The referenced rate studies were conducted under vacuum. There appears to be general agreement among investigators that the kinetics of decomposition is dependent on particle size, which may partially account for the lack of better agreement shown in Table I. For calcium carbonate the order of reaction falls between zero and unity with an energy of activation in the neighborhood of 42 kcal./mole, for decomposition under vacuum. This is in reasonable agreement with the values determined

TABLE I

COMPARISON OF RESULTS WITH REPORTED VALUES

Reaction	Order of reaction Exp.	Order of reaction Lit.	Energy of activation (kcal./mole) Exp.	Energy of activation (kcal./mole) Lit.
$CaC_2O_4 \cdot H_2O = CaC_2O_4 + H_2O$	1.0		22	
$CaC_2O_4 = CaCO_3 + CO$	0.7[6]		74	
$CaCO_3 = CaO + CO_2$	0.4	0.20–0.53[7]	39	
		0–1[8]		49[8]
		0.3[9]		35–42[9]
		1[10]		95[10]
		1[11]		41–44[11]
		0.3[12]		37-39[12]
				48[13]

(6) E. Moles and C. D. Vallamil, *Anal. soc. espan. fis. quim.*, **24**, 465 (1926).

(7) P. Vallet and A. Richer, *Compt. rend.*, **238**, 1020 (1954).

(8) G. F. Hüttig and H. Kappal, *Angew. Chem.*, **53**, 57 (1940).

(9) H. T. S. Britton, S. J. Gregg and G. W. Winsor, *Trans. Faraday Soc.*, **48**, 63 (1952).

(10) Maskill and W. E. S. Turner, *J. Soc. Glass Tech.*, **16**, 80 (1932).

(11) G. Slonim, *Z. Elektrochem.*, **36**, 439 (1930).

(12) J. Splichel, St. Skramovsky and J. Goll, *Collection Czechoslov. Chem. Commun.*, **9**, 302 (1937).

(13) J. Zawadzki and S. Bretsznajder, *Z. Elektrochem.*, **41**, 215 (1935).

in this investigation, in air, 0.4 and 39 kcal./mole, respectively.

The reported order of reaction for the decomposition of calcium oxalate is unity. The order of reaction determined in this study is 0.7. No previous work has been found in the literature dealing with the kinetics of the dehydration of calcium oxalate monohydrate.

Acknowledgment.—The authors wish to express their appreciation to Mr. Jean Carton and the Testut Company of Paris, France for providing the thermobalance for this research.

The value of 0.3 was derived from the author's equation[9]

$$(w/w_0)^n = kt + a$$

where

$$n = 0.7$$

The above equation was differentiated with respect to (w/w_0) and t. This gives

$$\frac{-\mathrm{d}\,(w/w_0)}{\mathrm{d}t} = nk\left(\frac{w}{w_0}\right)^{1-n}$$

where

$1 - n$ = order of reaction

HEATS OF COMBUSTION OF SOME ORGANIC COMPOUNDS CONTAINING CHLORINE

BY G. C. SINKE AND D. R. STULL

Thermal Laboratory, Dow Chemical Company, Midland, Michigan

Received October 3, 1957

The heats of combustion of several organic compounds containing chlorine were determined by bomb calorimetry. A solution of arsenious oxide supported on glass filter cloth in a platinum lined bomb was used to reduce free chlorine to chloride ion. Heats of formation from graphite and gaseous hydrogen, oxygen and chlorine at 25° in kcal. mole^{-1} were derived: 1,2-dichloroethane(l), -39.6 ± 0.4; *o*-dichlorobenzene(l), -4.4 ± 0.3; 2,5-dichlorostyrene(l), $+8.3 \pm 0.4$; pentachlorophenol(s), -70.6 ± 0.7; hexachlorobenzene(s), -31.3 ± 1.0; 1,1-dichloroethylene(l), -6.0 ± 0.3. Heats of combustion of polyvinyl chloride and poly-1,1-dichloroethylene were measured and used to calculate the heats of polymerization at 25° in kcal. mole^{-1} of gaseous vinyl chloride and liquid 1,1-dichloroethylene as -31.5 ± 0.6 and -18.0 ± 0.7, respectively. Heats of formation of 1,2-dichloroethane and *o*-dichlorobenzene agreed well with literature values obtained by other methods.

Introduction

The methods and apparatus used for the bomb calorimetry of compounds containing only carbon, hydrogen, oxygen and nitrogen is unsuitable for compounds containing chlorine. First, the ordinary steel bomb is severely corroded by the combustion products and, second, some free chlorine is formed during combustion which continues to react slowly with water and oxygen during the final period. The historical development of techniques to cope with these problems is given in a recent publication.[1] The extensive researches by Smith and co-workers at the University of Lund employed a platinum lined bomb to reduce corrosion and a solution of arsenious oxide supported on quartz fibers to cause rapid reduction of free chlorine. A summary of this work with complete references has been published.[2] A later development of this group has been the use of a rotating bomb to ensure a homogeneous final solution and eliminate the need for quartz fibers.[3] A third method developed by Hubbard, Knowlton and Huffman[4] used a tantalum or platinum-lined bomb and a solution of hydrazine hydrochloride supported on glass filter cloth. In the present investigation, a solution of arsenious oxide supported on glass filter cloth in a platinum lined bomb proved to be satisfactory. All these methods have been used to determine the heat of combustion of *o*-dichlorobenzene and the results, as will be shown, agree within experimental error.

(1) L. Smith and W. N. Hubbard, "Combustion in a Bomb of Organic Chlorine Compounds," Chapter 8 of "Experimental Thermochemistry," edited by F. D. Rossini, Interscience Publishers, Inc., New York, N. Y., 1956.

(2) L. Smith, L. Bjellerup, S. Krook and H. Westermark, *Acta Chem. Scand.*, **7**, 65 (1953).

(3) L. Bjellerup and L. Smith, *Kgl. Fysiograph. Sällskap. Lund Forh.*, **24**, 21 (1954).

(4) W. N. Hubbard, J. W. Knowlton and H. M. Huffman, THIS JOURNAL, **58**, 396 (1954).

TABLE I

CALIBRATION OF CALORIMETER SYSTEM

Series[a]	q_B, cal.	q_{oil}, cal.	q_{fuse}, cal.	q_{HNO_3}, cal.	q_{As}, cal.	q_W, cal.	C, cal.	ΔT, °C.	C_0, cal. deg.$^{-1}$
B	5413.5	647.6	7.3	2.2		12.5	47.7	1.9816	3045.7
B	5501.7	625.4	8.1	2.2		12.5	48.2	2.0020	3047.8
B	5318.5	773.8	7.7	2.2		12.5	47.9	1.9912	3046.8
B	5350.4	725.3	8.2	2.2		12.5	47.7	1.9857	3047.2
B	5379.3	656.6	9.8	2.2		12.5	47.1	1.9727	3048.3
B	5448.9	668.1	7.6	2.2		12.5	47.3	1.9992	3047.2
C	5365.7	717.7	6.2	2.2		12.5	47.1	1.9887	3045.8
C	5392.0	654.1	7.4	2.2		12.5	46.8	1.9769	3045.9
C	5339.5	714.5	5.8	2.2		12.5	46.4	1.9772	3048.8
D	5361.8	678.3	6.7	2.2	4.3	12.5	46.6	1.9752	3047.4
D	5376.7	720.5	7.8	2.2	4.1	12.5	47.0	1.9925	3049.8
D	5348.8	707.1	8.5	2.2	2.7	12.5	46.6	1.9802	3047.8
								Av.	3047.4

[a] "B" series—20 ml. pure water; "C" series—20 ml. 0.5 N HCl; "D" series—20 ml. 0.34 N As_2O_3.

TABLE II

RESULTS OF COMBUSTION EXPERIMENTS

q_{oil}, cal.	q_{fuse}, cal.	q_{As}, cal.	q_{HNO_3}, cal.	q_{Pt}, cal.	q_{HCl}, cal.	q_W, cal.	C, cal.	ΔT, °C.	m, g.	$-\Delta U_B/M$, cal. g.$^{-1}$
					1,2-Dichloroethane					
3031.1	4.5	82.6	2.0	1.2	5.4	8.0	44.2	1.9686	0.97377	2997.9
3110.4	6.3	81.2	1.5	1.0	5.5	8.2	44.8	1.9955	0.97857	2986.7
2872.1	6.1	87.0	1.4	0.5	6.4	8.3	45.1	2.0050	1.06535	2990.6
3903.8	5.7	56.3	2.0	.1	3.1	8.1	44.7	1.9993	0.72334	2992.2
3511.7	5.9	64.9	1.3	.1	4.2	8.2	44.6	1.9961	.84672	2999.2
4101.5	6.5	44.3	1.7	.1	2.5	8.1	44.3	1.9876	.64697	3000.9
4218.0	5.1	44.9	2.0	.2	2.3	8.1	44.4	1.9957	.61734	2996.7
3801.7	5.6	66.2	1.5	.2	3.4	8.2	44.5	2.0013	.75674	2990.7
									Av.	2994.4
									σ =	1.8
					o-Dichlorobenzene					
2075.3	5.7	57.4	2.4	0.3	2.0	11.1	45.0	2.0212	0.84170	4816.6
796.5	6.0	79.3	2.4	.5	3.3	11.7	45.4	2.0183	1.10146	4814.3
865.6	6.2	71.5	2.0	.4	3.2	11.5	44.9	2.0096	1.08357	4812.7
982.6	7.3	75.5	2.0	.3	3.1	11.3	45.0	2.0149	1.06145	4813.4
1619.9	5.5	62.1	3.7	.3	2.4	11.1	44.7	2.0057	0.92554	4815.1
960.4	6.7	75.7	2.3	.4	3.0	11.2	38.8	1.9866	1.04755	4810.3
									Av.	4813.7
									σ =	0.9
					2,5-Dichlorostyrene					
1744.5	6.2	47.9	1.9	0.4	1.4	10.7	47.5	2.0660	0.80367	5640.5
1836.0	7.1	42.4	2.4	.2	1.2	10.2	45.8	1.9968	.74960	5647.8
1156.4	5.7	49.7	2.4	.2	1.7	11.0	47.4	2.0718	.91034	5643.2
1168.5	6.2	56.7	2.4	.2	1.7	10.9	47.4	2.0682	.90451	5645.8
1126.3	6.1	58.9	1.9	.2	1.6	10.6	46.0	2.0094	.88070	5639.7
1226.8	6.4	56.0	2.2	.1	1.5	10.5	45.7	1.9979	.85674	5641.7
									Av.	5643.1
									σ =	1.3
					Pentachlorophenol					
4485.8	6.2	73.6	1.6	0.4	3.5	10.4	46.5	2.0305	0.79184	2095.9
4116.2	5.5	113.0	1.5	.8	5.1	11.1	47.5	2.0692	1.00910	2091.1
4092.2	4.6	88.7	3.0	.8	4.0	10.4	45.1	1.9710	0.88556	2095.5
4148.0	6.1	93.9	1.8	.8	4.0	10.5	45.7	1.9936	.89123	2091.3
4216.1	4.8	93.7	2.2	.7	4.0	10.6	46.0	2.0103	.88460	2089.1
									Av.	2092.6
									σ =	1.3
					Hexachlorobenzene					
4572.2	7.5	88.6	1.5	0.7	4.0	10.1	46.5	2.0394	0.79507	1993.2
4414.7	6.3	79.3	1.5	.7	3.5	9.6	44.2	1.9432	.73035	1995.2

TABLE II (*Continued*)

q_{oil}, cal.	q_{fuse}, cal.	q_{As}, cal.	q_{HNO_3}, cal.	q_{Pt}, cal.	q_{HCl}, cal.	q_W, cal.	C, cal.	ΔT, °C.	m, g.	$-\Delta U_R/M$, cal. g.$^{-1}$
4331.5	6.4	85.5	1.5	.5	3.7	9.7	43.4	1.9302	.75137	1988 4
4447.0	5.0	81.7	1.5	.7	3.7	9.7	44.3	1.9704	.75278	2001.8
4768.6	5.1	77.3	1.5	.5	3.6	10.2	46.6	2.0697	.74705	2000.0
4475.3	5.5	80.5	1.5	.7	3.7	9.8	44.5	1.9803	.75498	1999.5
4478.3	4.2	80.3	1.5	.7	3.7	9.8	44.5	1.9807	.75412	2001.4
4562.1	3.8	83.9	1.5	.6	3.5	9.8	44.8	1.9956	.73753	1990.3
4602.7	4.7	80.1	0.9	.7	3.5	9.8	45.0	2.0015	.72878	1988.1
									Av.	1995.3
									σ =	1.8
					1,1-Dichloroethylene					
4191.8	4.8	76.2	2.5	0.5	3.8	9.3	47.1	2.0808	0.78066	2698.6
3750.8	5.3	82.2	2.5	.6	4.3	9.1	44.9	1.9858	.83370	2698.9
3809.5	6.2	79.1	2.2	.5	4.0	9.0	44.8	1.9803	.80464	2705.6
3780.0	5.6	84.1	2.1	.6	4.3	9.0	45.1	1.9984	.83522	2703.2
4207.8	6.0	63.3	1.8	.3	2.9	8.9	44.8	1.9902	.67527	2701.7
									Av.	2701.6
									σ =	1.3
					Poly-1,1-dichloroethylene					
3920.7	4.2	81.3	2.2	0.5	4.1	9.2	44.5	1.9717	0.81276	2508.7
3993.4	4.5	71.2	2.2	.4	4.0	9.3	44.8	1.9912	.80727	2521.7
3996.0	4.3	72.6	2.2	.5	4.1	9.3	45.1	1.9998	.81785	2516.8
4000.8	3.3	69.3	2.2	.5	4.0	9.3	44.8	1.9935	.81068	2514.3
4001.8	2.7	71.0	2.2	.4	4.0	9.3	44.8	1.9894	.80501	2514.0
									Av.	2515.1
									σ =	2.1
					Polyvinyl chloride					
1278.3	6.5	85.9	1 2	0.7	4.1	8.8	44.7	1.9495	1.05387	4372.6
1400.4	8.0	86.1	1.2	.5	4.1	9.0	45.6	1.9881	1.05175	4376.4
1532.1	6.8	84.6	1.5	.5	3.8	8 9	45.3	1.9812	1.01601	4381.9
1876.2	4.9	77.7	1.3	.5	3.4	8.9	45.6	1.9967	0.95101	4378.6
1755.5	6.1	84.8	1.6	.6	3.7	9.1	46.3	2.0289	1.00175	4367.5
1889.0	4.4	80.0	1.5	.5	3.5	9.1	46.4	2.0345	0.97553	4372.2
									Av.	4374.9
									σ =	1.7

TABLE III

HEATS OF FORMATION AT 25° IN KCAL. MOLE^{-1}

Substance	Mol. wt.	Purity (mole %)	$\Delta U°_R$	$\Delta H°_R$	$\Delta H°_f$
1,2-Dichloroethane(l)	98.968	99.9	−296.35	−296.65	−39.6 ± 0.4[b]
o-Dichlorobenzene(l)	147.012	99.9	−707.67	−707.97	− 4.4 ± .3
2,5-Dichlorostyrene(l)	173.050	99.5	−976.54	−977.13	+ 8.3 ± .4
Pentachlorophenol(s)	266.359	99.7	−557.38	−556.49	−70.6 ± .7
Hexachlorobenzene(s)	284.808	99.9	−568.28	−567.39	−31.3 ± 1.0
1,1-Dichloroethylene(l)	96.952	99.8	−261.93	−261.93	− 6.0 ± 0.3
Poly-1,1-dichloroethylene(s)[a]	96.952	99.9	−243.84	−243.84	−24.0 ± .4
Polyvinyl chloride(s)[a]	62.503	99.7	−273.44	−273.74	−22.6 ± .3

[a] Per monomer unit. [b] Uncertainty is twice the standard deviation, σ.

Experimental

Apparatus.—The calorimetric system was similar to that described by Hubbard, Knowlton and Huffman.[5] The platinum lined bomb[6] was self-sealing with a rubber O-ring and had an internal volume of 0.360 liter. Electrodes and crucible support were of platinum and other internal fittings were of titanium. The bomb was used in an inverted position and the walls and ceiling in this position were lined with about 20 g. of Owens Corning Glass Cloth CSS-28. The cloth readily absorbed and held the 20 ml. of arsenious oxide solution. Since the titanium fittings were at the bottom and not subjected to the combustion flame, conditions were not severe and no corrosion of these parts was detected. A small amount of chloroplatinic acid was formed on the platinum crucible and electrodes.

Materials.—Sample purities were determined by freezing curve analysis and are given in Table III. Impurities were probably similar in nature to the compounds themselves and did not seriously affect results.

Calibration.—The energy equivalent of the system was determined using NBS benzoic acid 39f. Three series of calibration experiments were made with the glass cloth in place and wet with 20 ml. of pure water, 0.5 *N* hydrochloric acid and 0.34 *N* arsenious oxide, respectively. The heat of combustion of benzoic acid was first reduced to the standard bomb process in which all products and reactants

(5) W. N. Hubbard, J. W. Knowlton and H. M. Huffman, *J. Am. Chem. Soc.*, **70**, 3259 (1948).

(6) Constructed by Parr Instrument Co., Moline, Illinois.

are in their standard states at 25° as described by Jessup.[7] The result, $-\Delta U_R/M$, is 6313.05 thermochemical calories per gram mass. The "Washburn corrections" for the new conditions of 20 ml. of water in the bomb were then calculated by the method of Prosen[8] and added to each calibration experiment. Corrections for 0.5 N HCl and 0.34 N As_2O_3 were assumed to be the same as for pure water. No systematic difference could be detected when the solutions were used instead of pure water. A correction was made for the small amount of arsenious oxide oxidized during the actual combustion period.

All experiments were initiated very near 24° and ended at near 26°. For each experiment the heat absorbed by the glass cloth, the initial solution, and the sample in warming from the initial temperature to 25° and the heat absorbed by the glass cloth and the final solution in warming from 25° to the final temperature was calculated. The heat capacity of the glass cloth was taken as 0.17 cal. $g.^{-1}$ $deg.^{-1}$ and of the 0.5 N HCl and 0.34 N As_2O_3 as 0.977 cal. $ml.^{-1}$ $deg.^{-1}$. The sum was termed C and was subtracted from each experiment before calculating the energy equivalent. C also included a small correction term for the replacement of the oxygen used by the carbon dioxide formed in the combustion. The energy equivalent of the system minus the above items was termed C_0 and found to be 3047.4 cal. $deg.^{-1}$ with a standard deviation of 0.35 cal. $deg.^{-1}$.

Procedure.—Liquid samples were placed in thin-walled soft-glass ampules similar to those described by Hubbard, Knowlton and Huffman.[4] Solid samples were formed into pellets. The amount of sample varied according to chlorine content, and was adjusted so that not more than two-thirds of the arsenious oxide was oxidized. Paraffin oil was added to ignite the samples and to furnish the heat required to raise the temperature two degrees. The paraffin oil was ignited by a fuse of cotton thread tied to a fine (No. 40 B & S) platinum wire. Application of an electrical potential of 12 volts melted the wire and ignited the fuse. The electrical firing energy was very small and very nearly the same in all experiments and was not included in the calculations.

Twenty ml. of 0.34 N As_2O_3 solution was added to the glass cloth lining and the bomb charged with oxygen to 30 atmospheres in all experiments. Temperatures were measured with a platinum resistance thermometer. The corrected temperature rise was calculated by the method of Dickinson.[9] After the combustion, the bomb was carefully opened while still inverted and the platinum lid was rinsed off with distilled water. The crucible and electrodes were then rinsed and the washings kept separate. The glass cloth was placed in a beaker, the bomb was carefully rinsed with the distilled water and the washings together with the washings from the lid were added to the glass cloth. The solution was divided into two parts. The major portion was saturated with sodium bicarbonate and unreacted arsenious oxide determined by titration with 0.1 N iodine using starch as indicator. A small portion was used to determine nitrate ion by a colorimetric method.[10] The chloroplatinic acid from the crucible and electrodes also was determined by a colorimetric method.[11]

Auxiliary Data.—As discussed by Smith and Hubbard,[1] the combustion reactions can be represented by the equations

$$C_aH_bO_cCl_d + [a + (b - d)/4 - c/2]O_2(g) + [dn - (b - d)/2]\,H_2O(l) \longrightarrow a CO_2(g) - d[HCl \cdot nH_2O](l) \quad (1)$$

$$As_2O_3(aq.) + O_2(g) \longrightarrow As_2O_5(aq.) \quad (2)$$

$$6HCl(aq.) + O_2(g) + Pt(s) \longrightarrow H_2PtCl_6(aq.) + 2H_2O(l) \quad (3)$$

$$1/2N_2(g) + 5/4O_2(g) + 1/2H_2O(l) \longrightarrow HNO_3(aq.) \quad (4)$$

In the first equation, n was taken as 600 and all combustions were corrected to this value using the heat of dilution of HCl given by Rossini and co-workers.[12] The heat of oxidation of arsenious oxide at constant volume was measured by Bjellerup, Wadsö and Sunner[13] as -77.4 ± 0.1 kcal. $mole^{-1}$. Values for reactions 3 and 4 of -63.2 and -14.07 kcal. $mole^{-1}$, respectively, are from Smith and Hubbard.[1] The heats of combustion, ΔU_R, of the paraffin oil and cotton thread were measured as $-10{,}989.5 \pm 1.5$ and -3800 ± 50 cal. $g.^{-1}$, respectively. The heat capacity of the average final bomb solution was measured as 0.93 cal. $g.^{-1}$ $deg.^{-1}$.

Results

Data for calibration experiments are given in Table I and for combustion experiments in Table II. Column headings have the following significance: q_B, q_{oil} and q_{fuse} are the heat released by the weighed quantities of benzoic acid, oil and fuse, respectively, when all products and reactants are in their standard states at 25°; q_{As}, q_{Pt} and q_{HNO_3} are the heats of reactions 2, 3 and 4 as determined by analysis of the combustion products, q_{HCl} is the heat of dilution of the final bomb solution to $n = 600$, q_W is the total "Washburn correction" calculated by the outline of Prosen[8] assuming values for pure water apply to the bomb solutions, C is the heat absorbed by the bomb contents as described under calibration, ΔT is the corrected temperature rise, m is the mass (wt. *in vacuo*) of sample, and $-\Delta U_R/M$ is the heat of combustion per gram of substance at constant volume with all reactants and products in their standard states. The calculation is

$$-\Delta U_R/M = \frac{[C_0\Delta T - q_{oil} - q_{fuse} - q_{As} - q_{Pt} - q_{HNO_3} + q_{HCl} - q_W + C]}{m}$$

For the calibration experiments, the calculation is reversed to obtain C_0 from $-\Delta U_R/M$ for benzoic acid.

Table III gives the derived heats of combustion at constant pressure and the heats of formation from graphite and gaseous oxygen, hydrogen and chlorine. The heats of formation of gaseous carbon dioxide, liquid water and hydrochloric acid (1 in 600 H_2O) were taken as -94.054, -68.317 and -39.885 kcal. $mole^{-1}$ from reference 12. The value for CO_2 is corrected for the new atomic weight of carbon.

The difference between the heats of formation of monomeric and polymerized 1,1-dichloroethylene gives the heat of polymerization as -18.0 ± 0.7 kcal. $mole^{-1}$. Lacher, Emery, Bohmfalk and Park[14] have determined the heat of formation of gaseous vinyl chloride as $+8.9 \pm 0.3$ kcal. $mole^{-1}$. Combined with the heat of formation of the polymer this gives the heat of polymerization of gaseous vinyl chloride as -31.5 ± 0.6 kcal. $mole^{-1}$.

Accuracy.—Although some of the thermochemical corrections applied are not strictly accurate because mixtures were involved rather than pure water or solutions of one component, these effects are largely eliminated by running calibration experiments under essentially the same conditions as combination experiments. Comparison with results of other investigations lends weight to this

(7) R. S. Jessup, *J. Research Natl. Bur. Standards*, **29**, 247 (1942).

(8) E. J. Prosen, National Bur. Standards Report 1119, Aug. 6, 1951.

(9) H. C. Dickinson, *Bull. Natl. Bur. Standards*, **11**, 189 (1914).

(10) I. M. Kolthoff and G. E. Noponen, *J. Am. Chem. Soc.*, **55**, 1448 (1933).

(11) O. I. Milner and G. F. Shipman, *Anal. Chem.*, **27**, 1476 (1955).

(12) F. D. Rossini, D. D. Wagman, W. H. Evans, S. Levine and I. Jaffe, Natl. Bur. Standards Circ. 500, 1952.

(13) L. Bjellerup, I. Wadsö and S. Sunner, Thermochemical Bull., March, 1957.

(14) J. R. Lacher, E. Emery, E. Bohmfalk and J. D. Park, THIS JOURNAL, **60**, 492 (1956).

claim. Conn, Kistiakowsky and Smith[15] measured the heat of addition of chlorine to ethylene at 355°K. as $-43{,}653 \pm 100$ cal. mole^{-1}. ΔC_p for the reaction is small and this result can be applied to 25° without appreciable error. From the heat of formation of ethylene from reference 12 and a heat of vaporization[16] of dichloroethane at 25° of 8,470 $\pm$ 20 cal. mole^{-1} there is calculated for liquid 1,2-dichloroethane $\Delta H_f = -39.6 \pm 0.2$ kcal. mole^{-1}, in excellent agreement with the combustion value of -39.6 ± 0.4 kcal. mole^{-1}. For *o*-dichlorobenzene, the result of Hubbard, Knowlton and Huffman[4] when calculated to an HCl dilution of 1 in 600 H_2O is $-\Delta U_R/M = 4813.8 \pm 1.0$ cal. g.$^{-1}$. The value found by Bjellerup and Smith[3] by the rotating bomb method, when calculated to 25° and corrected to the new value of ΔE_{oxid} of As_2O_3 is $-\Delta U_R/M = 4815.2 \pm 2.7$ cal. g.$^{-1}$. These figures are in agreement with our combustion value of 4813.7 $\pm$ 1.8 cal. g.$^{-1}$ well within experimental error.

Of historical interest is the value found by Berthelot[17] for the heat of formation of hexachlorobenzene, -83 kcal. mole^{-1}, which is in error by more than 50 kcal. Other results given by Berthelot for highly chlorinated compounds are similarly inaccurate.[18]

Acknowledgment.—We wish to thank R. A. McDonald of this Laboratory for determining the sample purities.

(15) J. B. Conn, G. B. Kistiakowsky and E. A. Smith, *J. Am. Chem. Soc.*, **60**, 2764 (1938).

(16) R. A. McDonald, unpublished measurements, Dow Chemical Co.

(17) M. P. E. Berthelot, *Ann. chim. phys.*, [6] **28**, 126 (1893).

(18) L. Smith, *Svensk Kem. Tidskr.*, **62**, 61 (1950).

THE TIME LAG IN DIFFUSION. II[1]

BY H. L. FRISCH

Bell Telephone Laboratories, Murray Hill, N. J.

Received October 22, 1957

It is shown that provided we know or can guess the functional form of the concentration dependence of the diffusion coefficient, measurements of the time lag in (vacuum) transmission experiments through a membrane at several diffusant reservoir pressures (or concentrations) allows us to determine both the diffusion coefficient (and its parameters) as well as the solubility of the diffusant in the membrane. Under some weak restrictions, even if nothing is known concerning the functional dependence, a knowledge of the time lag allows one to estimate the order of magnitude of the integral diffusion coefficient.

Introduction

In a previous paper[2] we gave an expression for the time lag, $L(c_0)$, for the diffusion of a species through a thin membrane of thickness l, whose sides are maintained at the constant concentrations c_0 (at $x = 0$) and 0 (at $x = l$), in which the transport of the diffusing species is governed by a concentration dependent diffusion coefficient, $\mathfrak{D}(c)$. If the membrane is initially free of the diffusing species we found that

$$L(c_0) = -\frac{l^2 \int_0^{c_0} w\mathfrak{D}(w) \int_w^{c_0} w\mathfrak{D}(u)\, du\, dw}{\left[\int_0^{c_0} \mathfrak{D}(u)\, du\right]^3}$$

The purpose of this paper will be to explore how much information concerning $\mathfrak{D}$ (as well as the solubility coefficient S of the diffusing species in the membrane) can be obtained from measurements of $L(c_0)$.

In principle, equation 1 can be inverted to give $\mathfrak{D}(c)$ from the experimentally determined function $L(c_0)$.[3] Practically this requires a prohibitively detailed and accurate knowledge of $L(c_0)$ as a function of c_0. A further difficulty arises from the fact that in the usual transmission experiment described above the concentration c_0 is not known and has to be determined from a separate solubility measurement relating the known constant ambient pressure p_0 (or concentration c_0') over the membrane side at $x = 0$ to c_0. If the solubility coefficient is known

$$S(c_0) = c_0/p_0 \qquad (2)$$

then the integral diffusion coefficient $\bar{D}(c_0)$ can be found from the steady state flux $q_s(c_0)$ without a knowledge of the time lag from the experimentally known permeability coefficient, $P(p_0)$, since

$$\bar{D}(c_0) = \int_0^{c_0} \mathfrak{D}(u)\, du/c_0 = -q_s l/c_0 \qquad (3)$$

and

$$P(p_0) = -j_s l/p_0 = \bar{D}(c_0)S(c_0) \qquad (4)$$

We show in the next section that if the functional form of $\mathfrak{D} = \mathfrak{D}(c)$ is known or can be guessed then from measurements of L and q_s at several different pressures $p_0^{(i)}$, D and S can be found without recourse to a separate solubility measurement. The examples of $\mathfrak{D}$ we shall discuss apply principally to the diffusion of organic vapors through polymer membranes although the theory is quite general and would apply equally well, say, to the diffusion of Li into a Ga doped specimen of Ge where the concentration dependence arises[4] from chemical

(1) This research was supported in part by the United States Air Force Office of Scientific Research and Development Command under Contract no. AF 18(603)-142 with the University of Southern California.

(2) H. L. Frisch, THIS JOURNAL, **61**, 93 (1957); the nomenclature and definitions used throughout this paper are identical with those used in reference 2.

(3) Equation 1 leads to the ordinary differential equation

$$\frac{1}{l^2}\frac{d^2}{dc_0^2}(\Phi^3 L(c_0)) = c_0\left(\frac{c_0\Phi}{dc_0}\right)^2;\ \Phi = \int_0^{c_0} D(u)\, du$$

which can be numerically integrated to give Φ and this on differentiation D.

(4) H. Reiss, C. S. Fuller and F. J. Morin, *Bell Syst. Tech. J.*, **35**, 535 (1956).

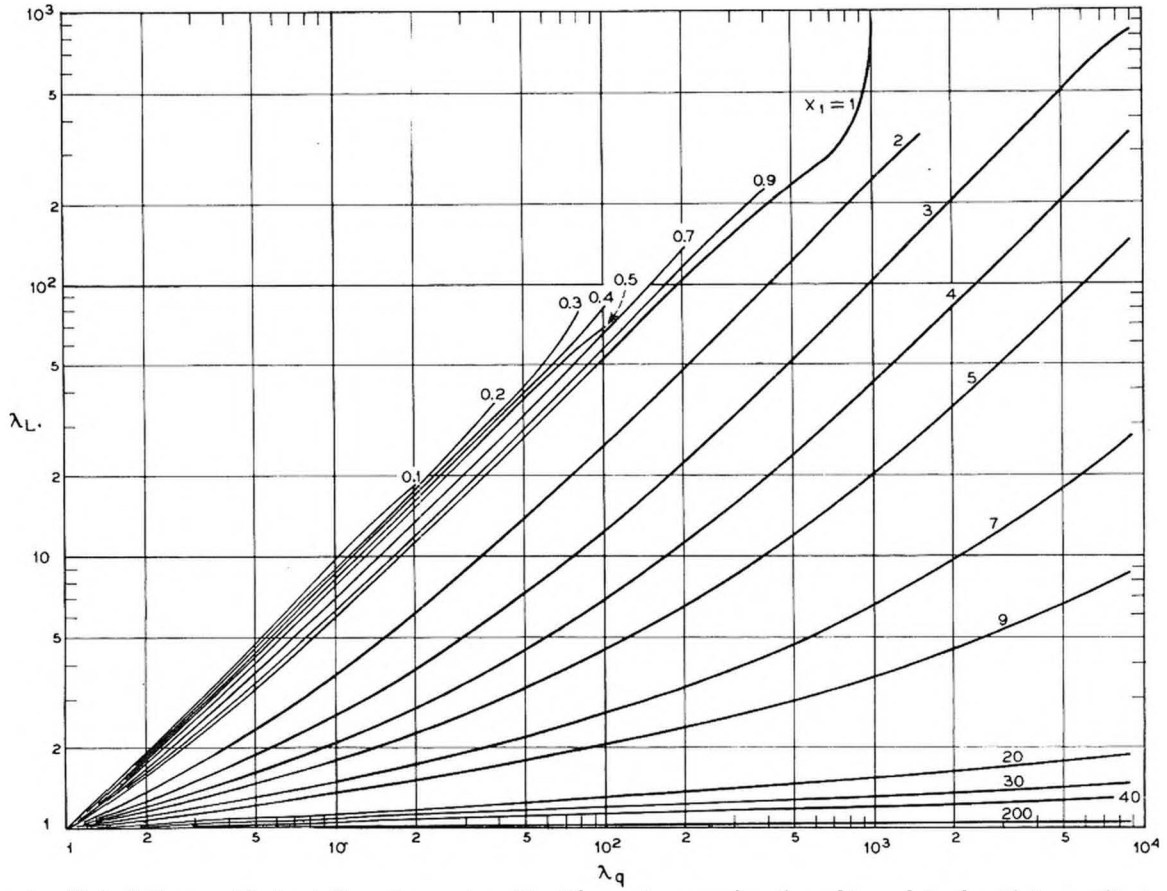

Fig. 1.— Plot of the graphical solution of equation 10. The root x_1 as a function of λ_q and λ_L for $h(x) = e^x(1 + x)$, $x_1 = \alpha c_0^{(1)}$.

interactions (*e.g.*, ion pairing).

Treatment of Experimental Data. A useful dimensionless function of c_0 is

$$F(c_0) = \frac{L(c_0)\bar{D}(c_0)}{l^2} = -\frac{L(c_0)q_s(c_0)}{lc_0} = \tag{5}$$
$$\int_0^{c_0} w\mathfrak{D}(w)\int_w^{c_0}\mathfrak{D}(u)\,du\,dw/c_0\left[\int_0^{c_0}\mathfrak{D}(u)du\right]^2$$

which can be thought of as the "reduced (dimensionless) time lag." Furthermore without loss in generality we can set

$$\bar{D}(c_0) = D_0H(\alpha c_0) = D_0H(x) \tag{6}$$
$$= D_0\int_0^{c_0} h(\alpha u)\,du/c_0 = D_0\left[\int_0^x h(w)\,(dw)/x\right]$$

where D_0 the least value of $\mathfrak{D}$ (for all $c \geq 0$), is independent of c_0 and possesses the dimensions of $\bar{D}$, α is a characteristic parameter of the diffusion system possessing the units of reciprocal concentration, and $h(x)$ and $H(x)$ are dimensionless functions of the reduced (dimensionless) concentration

$$x = \alpha c \tag{7}$$

Dimensional analysis assures us of the existence of at least one such parameter as α. $h(x)$ and $H(x)$ thus completely specify the functional dependence of $\mathfrak{D}$ and $\bar{D}$, respectively, on the concentration. We note from equation 5 that $F(c_0)$ is also a function of x and independent of D_0 since

$$F(x) = \int_0^x y\,h(y)\int_y^x h(z)\,dz\,dy/x\left[\int_0^x h(y)\,dy\right]^2$$

The functions $H(x)$ and $F(x)$ are particularly useful if the diffusion in a given system can be completely characterized by only one such parameter as α for then H and F are free of further parameters. This is actually the case for most proposed functional forms of $\mathfrak{D}$ (or h) describing the diffusion of vapors through polymer films. These together with the computed H and F functions are shown in Table I.

Consider now the results of typical vacuum vapor transmission experiments at a fixed temperature on a given vapor–membrane system. These consist of a number of different pressures of vapor $p_0^{(i)}$ on the high pressure side of the membrane, the thickness of the membrane l_i (note that we may have $l_i = l_j$), the measured time lags $L_i = L_i(p_0^{(i)})$ and steady-state fluxes $q_i = q_s(p_0^{(i)})$ with $i = 1, 2, \ldots$. Assuming we know or can guess the correct form of $h = h(x)$ we form from any pair of data, say for $i = 1, 2$, the ratios (*cf.* equations 3–7.)

$$\lambda_q = \frac{q_1}{q_2}\times\frac{l_1}{l_2} = \frac{\bar{D}(c_1)c_1}{\bar{D}(c_2)c_2} = \frac{H(x_1)x_1}{H(x_2)x_2} \tag{8}$$

and

$$\lambda_L = \frac{L_1}{L_2}\times\frac{q_1}{q_2}\times\frac{l_2}{l_1} = \frac{F(x)x_1}{F(x_2)x_2} \tag{9}$$

where $x_i = \alpha c_0^{(i)}$ and $c_0^{(i)}$ is the concentration of vapor at $x = 0$ corresponding to the pressure $p_0^{(i)}$ *i.e.*, $c_0^{(i)} = S(c_0^{(i)})\,p_0^{(i)}$. We can rewrite these relations in the form

TABLE I

THE FUNCTIONS $H(x)$ AND $F(x)$[5]

Case	$h(x)$	$H(x)$	$F(x)$	Ref.
0	1 ($\alpha = 0$)	1	1/6	6
1	$1 + 2x$ ($\alpha = b/2$)	$(1 + x)$	$\left(1 + \frac{5x}{2} + \frac{8x^2}{5}\right)/6(1 + x)^2$	7
2	$\exp(2x)$ ($\alpha = \delta/2$)	$[\exp(2x) - 1]/2x$	$\frac{1}{8}[(4x - 3)\exp(4x) + 4\exp(2x) - 1]/x[\exp(2x) - 1]^2$	8
3	$(1 + x)\exp(x)$ ($\alpha = \alpha$)	$\exp x$	$\frac{1}{2} - \frac{3}{4x} + \frac{3}{4x^2} + \frac{1}{8x^3} - \frac{e^{-x}}{x^2} - \frac{e^{-2x}}{8x^3}$	9

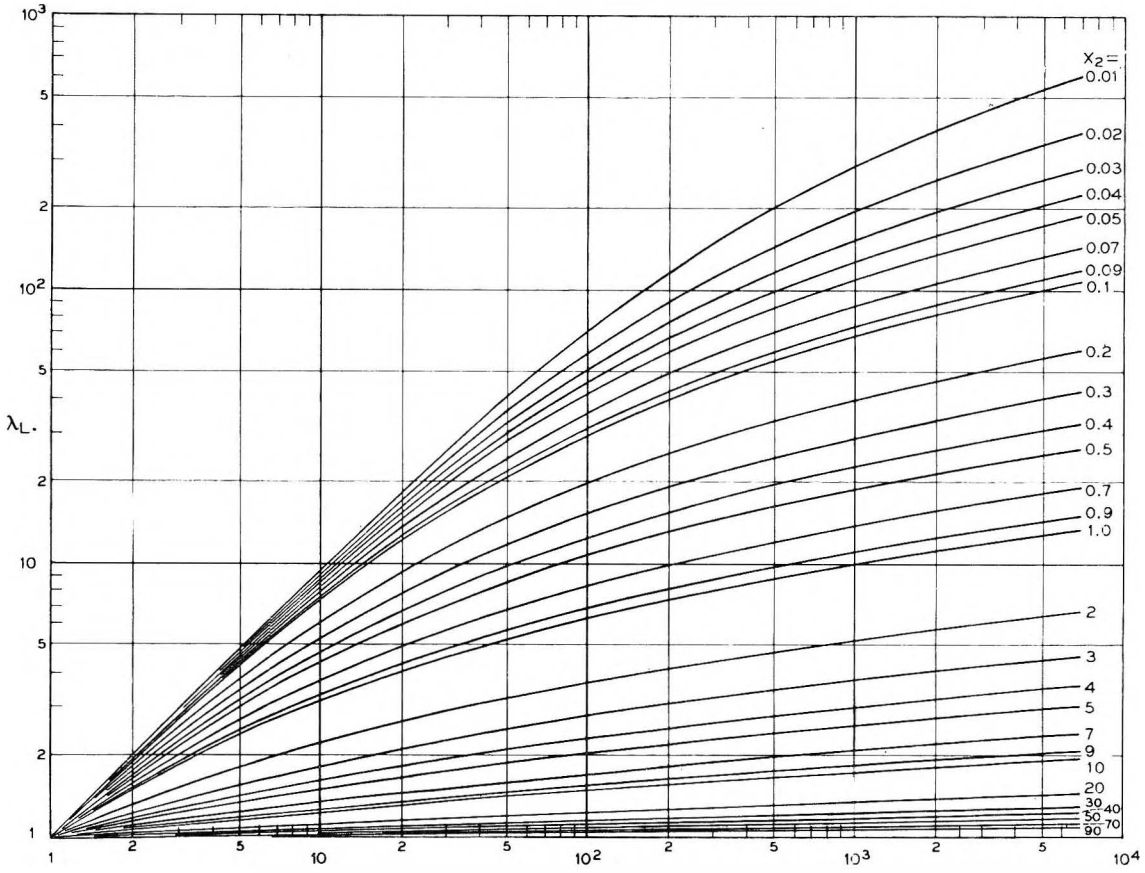

Fig. 2.—Plot of the graphical solution of equation 10. The root x_2 as a function of λ_q and λ_L for $h(x) = e^x(1 + x)$, $x_2 = \alpha c_0^{(2)}$.

$$g_H(x_1,x_2;\lambda_q) = \lambda_q \frac{x_2}{x_1} - \frac{H(x_1)}{H(x_2)} = 0$$
$$g_F(x_1,x_2;\lambda_L) = \lambda_L \frac{x_2}{x_1} - \frac{F(x_1)}{F(x_2)} = 0 \qquad (10)$$

The solution of this pair of simultaneous equations gives in general two unique roots, the desired values of $x_1 = x_1(\lambda_q, \lambda_L)$ and $x_2 = x_2(\lambda_q, \lambda_L)$. Figures 1 and 2 are graphs of x_1 and x_2 as functions of λ_q and λ_L obtained from a graphical solution of eq. 31 for the rather ubiquitous case 3, *i.e.*, $h(x) = (1 + x)e^x$.

Once x_1 (and x_2) are known we can find the values of $F(x_1)$ and $H(x_1)$ from the graphs of $F(x)$ and $H(x)$ *versus* x. Now the value of D_0 and $\bar{D}$ can be found since

$$D_0 = l_1^2 F(x_1)/L_1 H(x_1) \qquad (11)$$

by virtue of equations 5 and 6. The unknown concentration $c_0^{(1)}$ can now be found from

$$c_0^{(1)} = -q_1 L_1/l_1 F(x_1) \qquad (12)$$

say, and in turn α and $S(c_0^{(1)})$ can be solved for from

$$\alpha = x_1/c_0^{(1)}, \; S(c_0)^{(1)}) = c_0^{(1)}/p_0^{(1)} \qquad (13)$$

In a similar fashion $\bar{D}(c_0^{(2)})$ and $S(c_0^{(2)})$ can be found. Data for a third, different pressure $p_0^{(3)}$ can serve as a test of the correctness of the assumed functional form of h since α and D_0 are at a given temperature characteristics of the vapor–membrane system.

To summarize we have shown that in principle at least time lag and steady-state data from vacuum vapor transmission experiments at several pressures can give the characteristic parameters de-

(5) The parametrization of h is so chosen that in all cases $h(x) = 1 + o(x)$.

(6) R. M. Barrer, "Diffusion in and through Solids," Cambridge at the University Press, 1951.

(7) A. Aitken and R. M. Barrer, *Trans. Faraday Soc.*, **51**, 116 (1955).

(8) D. W. McCall, *J. Polymer Sci.*, **26**, 151 (1957).

(9) S. Prager and F. A. Long, *J. Am. Chem. Soc.*, **73**, 4072 (1951).

scribing the diffusion and solubility of a vapor in a membrane without recourse to a separate solubility measurement. In practice it is clear from the foregoing that in order to obtain even the correct order of magnitude of these characteristic parameters the basic experimental observables must be known to within a few per cent. of their accurate values. The methods described above can be extended to cases where h contains other parameters besides α; *e.g.*, even if nothing is known concerning the form of h we could fit a polynomial to the time lag data to any desired degree of accuracy. Needless to say the degree of complication of such procedures increases sharply with the number of parameters.

It should also be noted that if besides time lag and steady-state data we know the solubility at one pressure (only one α) we can still use the foregoing formulas (*cf.*, equations 2, 12 and 13, etc.) to find D_0 and α separately if we assume a suitable functional form for h. Without time lag data only $\bar{D}(c_0)$ can be found.

If an isotope of the given vapor (preferably a radioactive one) is available then a transmission experiment can yield directly (if we neglect a small isotope effect) $\mathfrak{D}$ without the necessity of knowing anything about the functional form of $\mathfrak{D}$. The membrane is initially uniformly saturated at a concentration of c_0 of isotope 1; the vapor reservoirs (at $x = 0$ and l) being maintained at a constant pressure $p_0 = c_0/S(c_0)$ of isotope 1. At time $t = 0$ the reservoir at $x = 0$ is exchanged for another maintaining a pressure p_0 of isotope 2. The amount of isotope 2 appearing at the reservoir at $x = l$ is now measured as a function of time.[10] Since the total vapor concentration is constant throughout the membrane the time lag of isotope 2 is given by

$$L = l^2/6\mathfrak{D}(c_0)$$

(10) The author is indebted to Prof. M. Saware for a discussion of this method clarifying certain details.

Isotope experiments such as this are necessary in any case if we desire to know the true binary diffusion coefficients in order to make frame of reference corrections. We will not comment further here on this topic.

Discussion

We can conclude from the foregoing that if we can guess the form of the concentration dependence of $\mathfrak{D}$ then time lag data are as useful as in the case where $\mathfrak{D}$ is constant. Even if we cannot say anything about the concentration dependence of $\mathfrak{D}$ we can still use L to obtain an idea of the order of magnitude of $\mathfrak{D}$ it we make certain assumptions (generally rather harmless ones) concerning $\mathfrak{D}$.

Thus in the absence of phase separation (in the diffusant-membrane system), phenomenological diffusion theory and the thermodynamics of irreversible processes (since entropy production is positive) assure us that

$$0 < D_0 \leq \mathfrak{D}(c) \quad 0 \leq c < c_s \tag{14}$$

where c_s is the equilibrium saturation concentration, *i.e.*, "up-hill" diffusion does not occur. In this case $F(c_0)$ satisfies the inequality

$$0 \leq \frac{1}{6}\left[\frac{D_0}{\bar{D}(c_0)}\right]^2 \leq F(c_0) \leq \frac{1}{2} \tag{15}$$

Since $\bar{D}(c_0)$ is bounded (15) allows us to estimate the order of magnitude of $\bar{D}(c_0)$. In particular for a large class of D's including all shown in Table I and $\mathfrak{D}$'s which are polynomials $\mathfrak{D} = D_0[1 + \sum_{i=1}^{n} b_i c^i]$ with $b_i \geq 0$ the lower bound on F is $1/6$. Thus the estimate

$$\bar{D}(c_0) \sim l^2/6L(c_0)$$

is at worst too small by a factor of three.

The author is indebted to Miss M. C. Gray and her computing staff for the numerical calculations leading to Figs. 1 and 2 and to Prof. R. M. Barrer for his continued interest in this work.

MUTUAL DIFFUSION IN NON-IDEAL BINARY LIQUID MIXTURES[1]

By D. K. Anderson, J. R. Hall and A. L. Babb

Department of Chemical Engineering, University of Washington, Seattle, Washington

Received October 23, 1957

As part of a comprehensive study of the mutual and self-diffusion behavior of non-ideal binary liquid mixtures, experimental data for six systems are presented. Mutual diffusion data for the following solutions are given over the complete composition range: acetone–benzene at 25.15°; acetone–water at 25.15°; acetone–chloroform at 25.15 and 39.95°; acetone–carbon tetrachloride at 25.15°; ethanol–benzene at 25.15 and 39.98°; and methanol–benzene at 39.95°. For the two systems involving ethanol and methanol, the new results are combined with previously reported data to evaluate the activation energies of both the diffusion and viscous flow mechanisms. Curves for the function $D\eta/(c \ln a_1/d \ln N_1)$ also have been evaluated for the systems studied experimentally. At present no attempt will be made to interpret the results theoretically.

Introduction

Diffusion studies in this Laboratory have two general aims.[2-4] For both ideal and non-ideal liquid systems, current theories relating mutual and self-diffusivities may be compared with recently available results. Secondly, for systems where association of one component is known to occur, or where there are solvent–solute interactions, it is hoped that with the present knowledge of association mechanisms some progress may be made toward predicting experimental diffusion.

As part of this comprehensive program, mutual diffusion data for six non-ideal systems are reported

(1) This work was supported in part by the Office of Ordnance Research, U. S. Army.

(2) C. S. Caldwell and A. L. Babb, This Journal, **60**, 51 (1956); **59**, 1113 (1955).

(3) P. A. Johnson and A. L. Babb, *ibid.*, **60**, 14 (1956).

(4) P. A. Johnson and A. L. Babb, *Chem. Revs.*, **56**, 387 (1956).

TABLE I

SUMMARY OF EXPERIMENTAL DIFFUSION DATA

System A	System B	Temp., °C.	Av. compn. of A mole fraction	$D \times 10^5$, cm.²/sec.
Methanol	Benzene	40.0	0.00470	4.67
			.01536	4.22
			.1094	1.88
			.2559	1.30
			.5034	1.28
			.6567	1.68
			.8163	2.22
			.9966	3.15
Ethanol	Benzene	25.15	.00225	3.02
			.00471	2.86
			.09574	1.30
			.2034	0.993
			.3415	0.901
			.5068	1.01
			.7022	1.35
			.9961	1.81
Ethanol	Benzene	39.98	.00372	3.72
			.00372	3.76
			.09574	1.89
			.2034	1.46
			.3415	1.30
			.5068	1.42
			.7022	1.76
			.9961	2.36
			.9961	2.38
Acetone	Water	25.0	.00216	1.28
			.08309	0.854
			.2392	0.635
			.4893	0.819
			.8036	2.39
			.0653	1.43
			.9265	3.80
			.9696	4.56
Acetone	Carbon tetrachloride	25.15	.00390	1.69
			.00390	1.71
			.2056	1.45
			.3942	1.65
			.7934	2.63
			.9953	3.59
			.9953	3.54
Acetone	Chloroform	25.15	.00548	2.35
			.2081	2.97
			.3903	3.29
			.6061	3.45
			.7472	3.52
			.8641	3.59
			.9948	3.63
			.9953	3.63
Acetone	Chloroform	39.95	.00548	2.90
			.00548	2.87
			.2013	3.57
			.2013	3.59
			.3984	4.05
			.4989	4.14
			.4989	4.16
			.6040	4.24
			.8592	4.27
			.8641	4.28
			.9948	4.31
Acetone	Benzene	25.15	.00369	2.75
			.00369	2.74
			.1000	2.58
			.2027	2.55
			.2027	2.56
			.3941	2.70
			.3939	2.69
			.3939	2.70
			.5994	2.98
			.5994	2.96
			.7808	3.35
			.9967	4.14
			.9973	4.18
			.9973	4.15

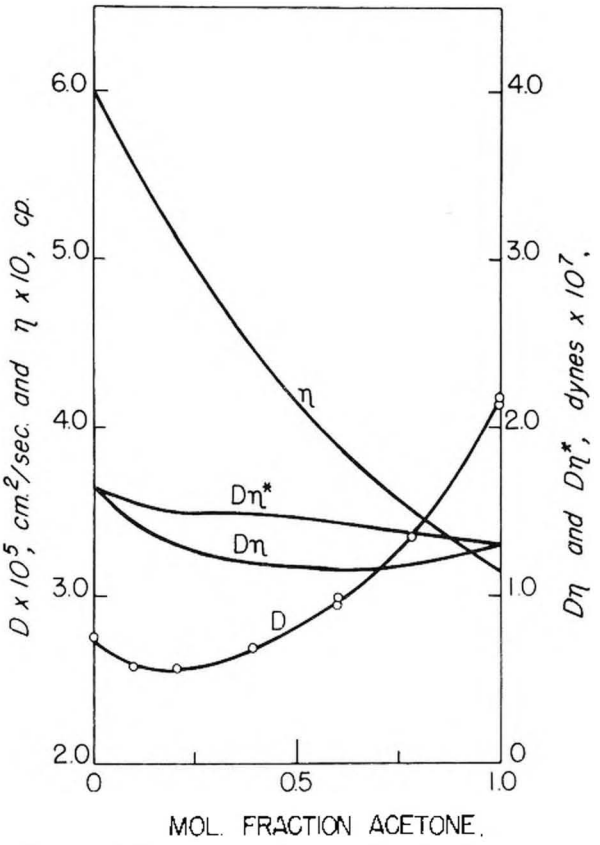

Fig. 1.—Diffusion and viscosity data for the acetone–benzene system at 25.15°, left hand scale; $D\eta$ and activity corrected $D\eta(D\eta^*)$, right hand scale.

in this paper together with some energies of activation for both viscosity and diffusion. At present, no attempt will be made to interpret the results theoretically.

Experimental

The solvents used were the highest grades commercially available and were for the most part used without further purification. Particular care was taken in handling hygroscopic liquids, as the slightest traces of water were found to affect the diffusion results markedly. The ethanol stabilizer was removed from chloroform with anhydrous calcium chloride, and benzene was stored over metallic sodium.

The mutual diffusion measurements were made with a Mach–Zehnder type diffusiometer, described fully elsewhere.[5]

(5) C. S. Caldwell, J. R. Hall and A. L. Babb, *Rev. Sci. Inst.*, **28**, 816 (1957).

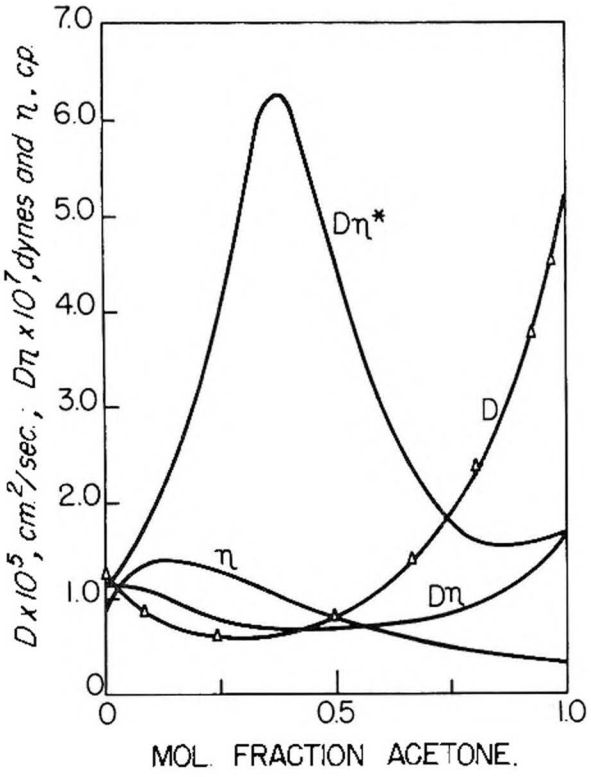

Fig. 2.—Mutual diffusion, viscosity, uncorrected and activity corrected $D\eta$ product for acetone–water system at 25.15°.

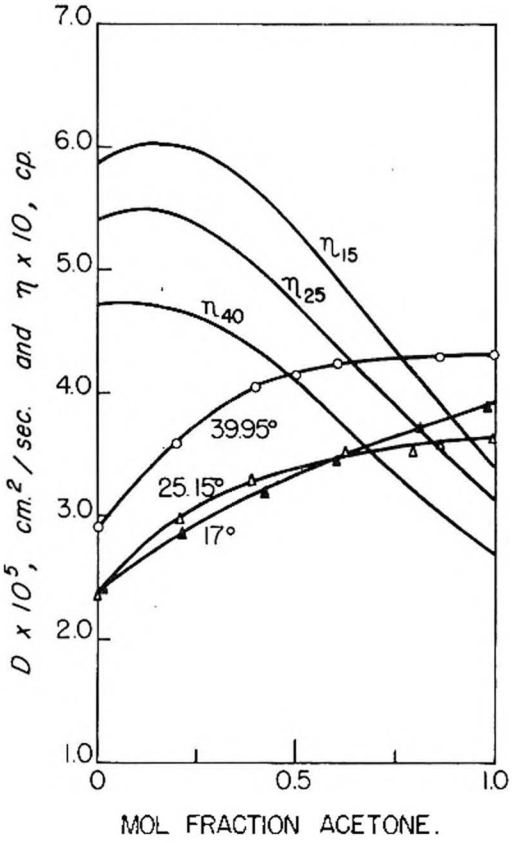

Fig. 3.—Mutual diffusion and viscosity data for the acetone–chloroform system: ○, this work 39.95°; △, this work 25.15°; ▲, Lemonde 17° (ref. 7).

Results and Calculations

Mutual diffusion results for the following systems are presented: acetone–benzene (25.15°, Fig. 1); acetone–water (25.15°, Fig. 2); acetone–chloroform (25.15°, 39.95°, Fig. 3); acetone–carbon tetrachloride (25.15°, Fig. 4); ethanol–benzene (25.15°, 39.98°, Fig. 5); methanol–benzene (39.95°, Fig. 6), and a summary of the experimental data is given in Table I. In addition, a summary of the experimental data for the acetone systems is given in Fig. 8.

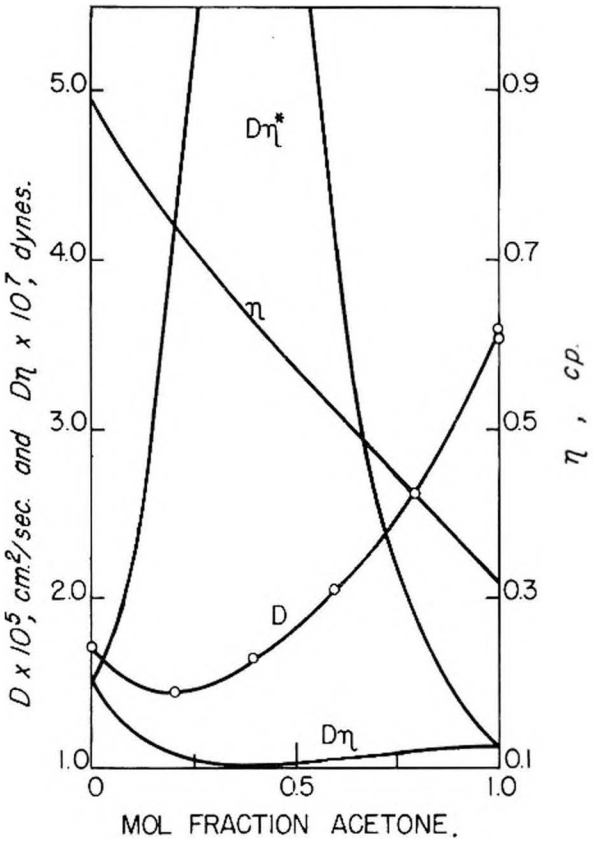

Fig. 4.—Mutual diffusion data for acetone–carbon tetrachloride system at 25.15°; $D\eta$ and activity corrected $D\eta(D\eta^*)$, left hand scale; viscosity on right hand scale.

Being the prime basis of selection, the degree of non-ideality of the results for these systems is not surprising. All the systems except one exhibit a marked minimum in the diffusivity–composition curves. The exception, the chloroform–acetone system, is the classic example of a system which deviates negatively from Raoult's law,[6] while all the other systems for which results are presented have positive deviations.

From the diffusion results, values of the $D\eta$ product and $D\eta/(\mathrm{d}\ \ln a_1/\mathrm{d}\ \ln N_1)$ were calculated where D, η, a_1 and N_1 are the mutual diffusivity, the solution viscosity, the activity of one component and the mole fraction of that component, respectively. The required viscosity data were selected for the most part from the literature. For the chloroform–acetone system available

(6) J. v. Zadwidski, *Z. physik. Chem.*, **35**, 129 (1900).

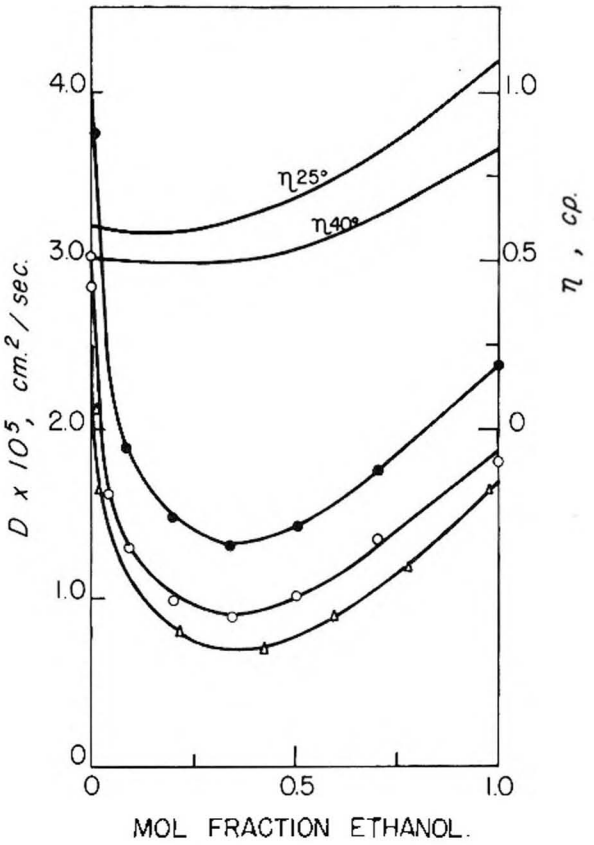

Fig. 5.—Mutual diffusion and viscosity data for the ethanol–benzene system; ●, this work 39.98°; ○, this work 25.15°; △, Lemonde 15° (ref. 7); viscosity data on right hand scale.

data[7-9] showed some scatter, so the viscosity isotherms were determined in this Laboratory.[10] Likewise for the ethanol-benzene systems, the required measurements were repeated and compared with previously published data.[11,12] In the case of benzene–acetone solutions, interpolation of the data of Bingham and Brown[13] appeared to give more reliable viscosities than the direct measurements of Fischler[14] at 25°. The data of Davis, *et al.*,[15] were used for acetone–water mixtures, and for acetone–carbon tetrachloride interpolations were made from the smoothed data of Yajnik, *et al.*[8]

The activity term was evaluated from available thermodynamic data with the help of the Van Laar equation. Only for the acetone-chloroform system were isothermal data available[16] at the temperatures required. For the remaining three acetone systems, isobaric boiling point–composition data were used.[17-20] Such measurements provide

(7) H. Lemonde, *Ann. Phys.*, **9**, 399 (1938).
(8) N. A. Yajnik, M. D. Bhalla, R. C. Talwar and M. A. Soofi, *Z. physik. Chem.*, **118**, 305 (1925).
(9) D. E. Tsakalotos, *ibid.*, **71**, 667 (1910).
(10) N. T. Anderson, unpublished notes, Univ. of Wash., 1957.
(11) A. E. Dunstan, *J. Chem. Soc. (London)*, **85**, 817 (1904).
(12) F. H. Eetman, *J. chim. phys.*, **4**, 386 (1906).
(13) "International Critical Tables," Vol. V, McGraw Hill Book Co., New York, N. Y., 39 (1929).
(14) J. Fischler, *Z. Elektrochem.*, **19**, 126 (1913).
(15) P. B. Davis, H. Hughes and H. C. Jones, *Z. physik. Chem.*, **85**, 513 (1913).
(16) H. Röck and W. Schröder, *ibid.*, N.F., **11**, 41 (1957).

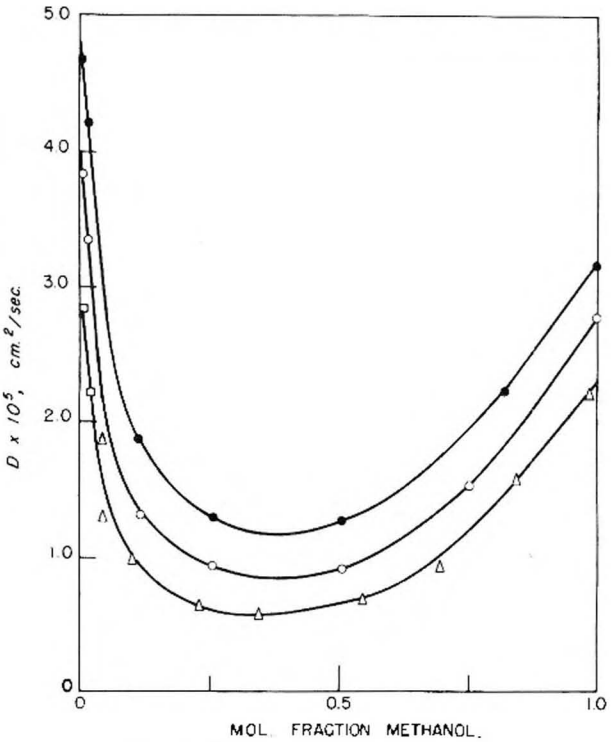

Fig. 6. Mutual diffusion data for the methanol–benzene system; ●, this work 39.95°; ○, Caldwell and Babb 27.06° (ref. 2); □, Caldwell and Babb 11.0°; △, Lemonde 11.0° (ref. 7).

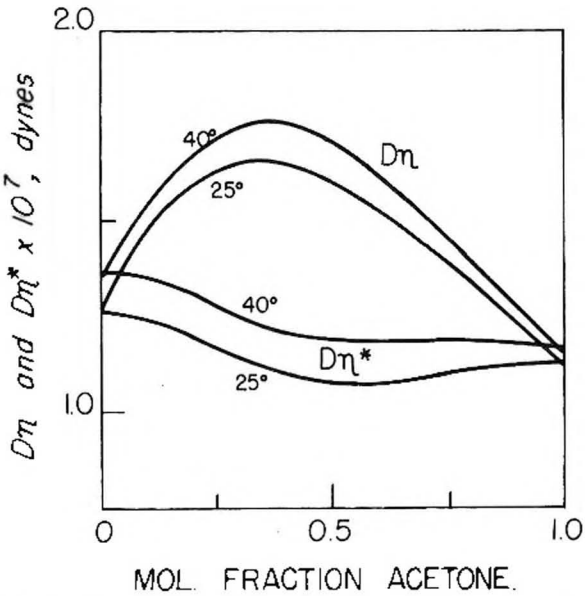

Fig. 7.—Uncorrected and activity corrected $D\eta$ products for the acetone–chloroform system at 25.15 and 39.15°.

activity coefficients at variable temperatures higher than those at which the diffusion measurements were made. It may be argued, however, that the activity corrections at the required lower temperatures, were they available, would be certainly greater than those used. For the systems ethanol–

(17) K. C. Bachman and E. L. Simmons, *Ind. Eng. Chem.*, **44**, 203 (1952).
(18) R. York and R. C. Holmes, *ibid.*, **34**, 345 (1942).
(19) A. S. Brunjes and M. J. P. Bogart, *ibid.*, **35**, 258 (1943).
(20) F. J. Soday and G. W. Bennett, *J. Chem. Ed.*, **7**, 1336 (1930).

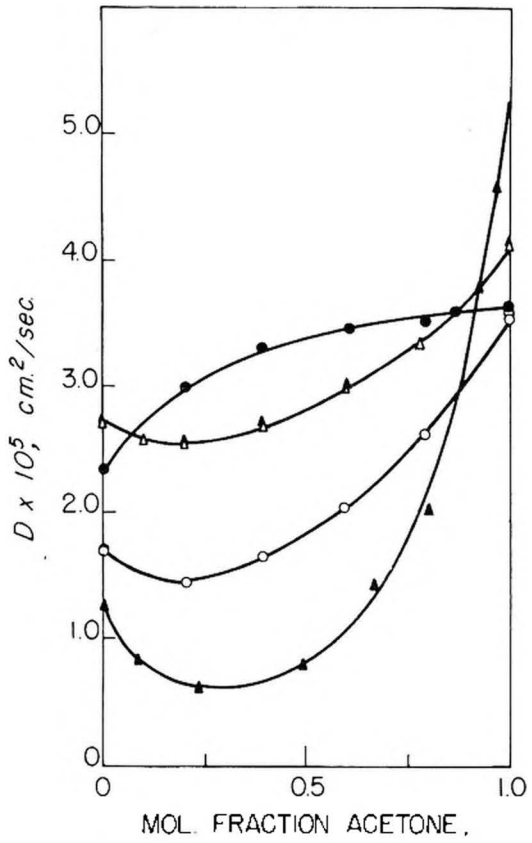

Fig. 8.—Mutual diffusion data for acetone systems at 25.15°: ●, acetone–chloroform; △, acetone–benzene; ○, acetone–carbon tetrachloride; ▲, acetone–water.

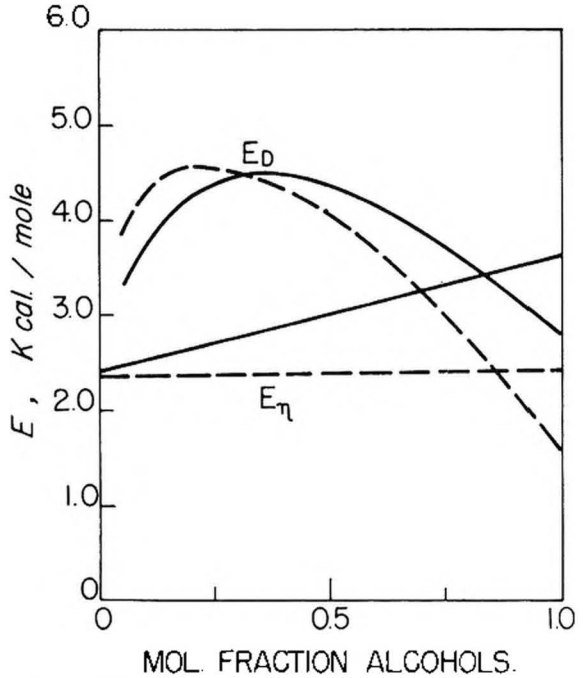

Fig. 9.—Energies of activation for viscosity and diffusion: ———, ethanol–benzene system; — — —, methanol–benzene system.

benzene and methanol–benzene, the activity corrected curves have been presented elsewhere.[3] For the acetone–water and acetone–carbon tetrachloride systems, examination of the $D\eta/(\mathrm{d}\ln a_1/\mathrm{d}\ln N_1)$ curves shows that even with the activity data used, the effect of the corrections is too great. The acetone–benzene and acetone–chloroform curves, however, are more nearly linear.

In the case of acetone–benzene the activity correction is relatively small, having a maximum difference from unity of only 20%. On the other hand, it has been shown by Stokes and Hammond[21] for the system cyclohexane–carbon tetrachloride, where the maximum difference of the activity term from unity is 5.6%, that the quantity $D\eta/(\mathrm{d}\ln a_1/\mathrm{d}\ln N_1)$ still deviates from linearity by amounts up to 4%. Eyring, *et al.*,[22] have presented data for the acetone–chloroform and chloroform–ether systems showing the term $D\eta/(\mathrm{d}\ln a_1/\mathrm{d}\ln N_1)$ linear with composition. Eyring appeared to have used the data of Lemonde[7] at 17°, which appear to be inconsistent with the data shown in Fig. 3. The activity corrected diffusion curves for this system, shown in Fig. 7, deviate from linearity by amounts up to 9%. The thermodynamic properties of the acetone–chloroform system have been well established[16,23,24] and it thus appears that the observed linearity may be a coincidence, considering the complexity of the system. For both the alcohol systems and those involving acetone, one thus has further evidence that conventional thermodynamic corrections alone are insufficient to account for the diverse kinds of deviations from ideality.

It is interesting to note the qualitative similarity between the variation of D, excess enthalpy of mixing (ΔH^m), and $1/(\mathrm{d}\ln a_1/\mathrm{d}\ln N_1)$ with composition. The system ethanol–chloroform provides an illustration of this. Both the $1/(\mathrm{d}\ln a_1/\mathrm{d}\ln N_1)$ and excess enthalpy of mixing[25] curves show a change from positive to negative deviation and the diffusivity curve likewise shows a point of inflection at approximately the same mole fraction. Although the proportionality between ΔH^m and $1/(\mathrm{d}\ln a_1/\mathrm{d}\ln N_1)$ for symmetrical regular solutions is known, the ΔH^m data available for the systems discussed here[26–33] suggest a possible relation between ΔH^m and D. Recent work by the authors indicates that for systems containing one associating component a quantitative relationship between ΔH^m and D can be derived from association theory.

(21) R. H. Stokes and B. R. Hammond, *Trans. Faraday Soc.*, **52**, 781 (1956).
(22) R. E. Powell, W. E. Roseveare and H. Eyring, *Ind. Eng. Chem.*, **33**, 430 (1941).
(23) L. Sarolea-Mathot, *Trans. Faraday Soc.*, **49**, 8 (1953).
(24) A. Nikuradse and R. Ulbrich, *Z. physik. Chem., N.F.*, **2**, 9 (1954).
(25) G. Scatchard and C. L. Raymond, *J. Am. Chem. Soc.*, **60**, 1278 (1938).
(26) G. C. Schmidt, *Z. physik. Chem.*, **121**, 221 (1926).
(27) J. Hirobi, *J. Fac. Sci. Tokyo. Imp. Univ.*, Section I, Part 4, *1*, 155 (1926).
(28) B. H. Carroll and J. H. Mathews, *J. Am. Chem. Soc.*, **46**, 30 (1924).
(29) A. Winkelman, *Ann. Physik Chem.*, **226**, 592 (1873).
(30) Ref. 13, Vol. V, 1929, p. 156.
(31) W. Jost, H. Rock, W. Schröder, L. Sieg and H. Wagner, *Z. physik. Chem., N. F.*, **10**, 133 (1957).
(32) G. Scatchard, L. B. Ticknor, J. R. Goates and E. R. McCartney, *J. Am. Chem. Soc.*, **74**, 3721 (1952).
(33) G. Scatchard, S. E. Wood and J. M. Mochel, *ibid.*, **68**, 1957 (1946).

Activation energies for diffusion and viscosity of the ethanol–benzene and methanol–benzene systems are shown in Fig. 9. These were determined in the conventional manner by plotting ln D and ln η against reciprocal temperature. Eyring's theory[34] predicts viscosity and diffusion equations of the form: $\eta = AT^{1/2}\exp(E_0/RT)$ and $D = BT^{1/2}\exp(-E_0/RT)$ from which it follows that

$$E_\eta = R\left(\mathrm{d}\ln\eta/\mathrm{d}\left(\frac{1}{T}\right)\right) = E_0 - \frac{1}{2}RT \quad (1)$$

and

$$E_D = -R\left(\mathrm{d}\ln D/\mathrm{d}\left(\frac{1}{T}\right)\right) = E_0 + \frac{1}{2}RT \quad (2)$$

where E_0 is the activation energy at 0°K., and E_D, E_η, are the respective activation energies for diffusion and viscous flow as defined by equations 1 and 2. Thus, E_D and E_η should differ by the amount RT.

It has been suggested[35] that $\ln(D/T)$, rather than ln D, should be plotted to obtain the activation energy for diffusion. This requires the assumption that the partition function ratio in the original form of the Eyring equation is independent of temperature. Since it is entirely a matter of definition of E_0 the more usual method of plotting ln D *versus* $1/T$ was used in preparing Fig. 9. For six ideal systems, Caldwell and Babb[2] have verified that the difference between E_η and E_D is approximately 0.6 kcal./mole. In the case of the non-ideal alcohol systems presented here, such a simple relationship was not expected to be valid, as shown in Fig. 9.

(34) H. Eyring, *J. Chem. Phys.*, **4**, 283 (1936).
(35) R. E. Meyer and N. H. Nachtrieb, *ibid.*, **23**, 1951 (1955).

Discussion

It is difficult to make any general statements which would cover all of the systems for which data are presented here, as several kinds of molecular interaction may be distinguished. The problem of association in alcohols has been the subject of considerable investigation,[36–38] and as Kretschmer and Wiebe[39] have pointed out, the presence of an aromatic as the second component introduces additional and complicating interactions. The two acetone systems, those with benzene and chloroform, were chosen for comparison with the acetone–carbon tetrachloride system, for which the second component may be considered inert. It was hoped that the effects of introducing an aromatic component in one case, and of the hydrogen atom in the other, could easily be characterized. It was surprising to find, therefore, that the carbon tetrachloride system behaved least ideally of the three, at least insofar as diffusion behavior is concerned. Most data exist for the acetone–chloroform system, and thus this system is the best understood. The possible molecular interactions of acetone–water solutions precludes discussion of this system, and the measurements presented here were made for comparison with self-diffusion studies,[40] rather than in the hope of theoretical progress.

(36) R. Mecke, *Disc. Faraday Soc.*, **9**, 161 (1950).
(37) K. L. Wolf, H. Dunken and K. Merkel, *Z. physik. Chem.*, **B46**, 287 (1940).
(38) I. Prigogine and A. Desmyter, *Trans. Faraday Soc.*, **47**, 1137 (1951).
(39) C. B. Kretschmer and R. Wiebe, *J. Chem. Phys.*, **22**, 1697 (1954).
(40) B. W. Mar and A. L. Babb, unpublished data, University of Washington.

VISIBLE AND ULTRAVIOLET ABSORPTION SPECTRA OF $NiCl_2$ DISSOLVED IN FUSED LiCl–KCl MIXTURES[1]

BY CHARLES R. BOSTON AND G. PEDRO SMITH

Metallurgy Division, Oak Ridge National Laboratory, Oak Ridge, Tennessee[2]

Received October 24, 1957

Absorption spectra were measured for solutions of $NiCl_2$ in fused LiCl–KCl mixtures near the eutectic composition over the wave length range of 220 to 750 mμ and at temperatures of 360 to 550°. In the ultraviolet region an absorption band was found with maximum at 260 mμ and a molar absorbancy index of $(3.6 \pm 0.2) \times 10^3$ at 395°. The visible spectrum consisted of four overlapping bands with maxima at 512, *ca.* 590, 625 and 695 mμ at 398°. The highest of these bands (625 mμ) had a molar absorbancy index of 61 ± 3 at a temperature of 398° and a solvent salt composition of 41.0 mole % KCl. The absorbancy indices of all bands changed considerably with temperature. Furthermore, the ultraviolet band broadened and its maximum shifted to longer wave lengths with increasing temperature. It was shown that these absorption bands were caused by at least two light-absorbing species derived from $NiCl_2$. With increasing temperature the concentration of one species decreased while the concentration of another species increased. At a constant temperature the concentration of all species giving rise to observed light absorption was proportional to the concentration of total nickel. The spectra were changed by a small but measurable amount with small changes in the composition of the solvent salt.

Introduction

The absorption spectra of fused salts have been of interest for some time as aids in studying the chemical constitution and electronic structure of these media.[3–8] This paper is concerned with the determination of molar absorbancy indices from the

(1) Throughout this paper the nomenclature and symbols recommended by K. S. Gibson, National Bureau of Standards Circular 484, September 1949, are used where applicable.
(2) Operated by Union Carbide Nuclear Company for the U. S. Atomic Energy Commission.
(3) K. Schaum and M. Funk, *Z. wiss. Phot.*, **23**, 73 (1924).
(4) E. Mollwo, *Z. Physik*, **124**, 118 (1947).
(5) H. Lux and T. Niedermaier, *Z. anorg. allgem. Chem.*, **285**, 246 (1956).
(6) B. R. Sundheim and J. Greenberg, *Rev. Sci. Inst.*, **27**, 703 (1956).
(7) D. M. Gruen, *J. Inorg. Nuclear Chem.*, **4**, 74 (1957).
(8) K. Sakai, THIS JOURNAL, **61**, 1131 (1957).

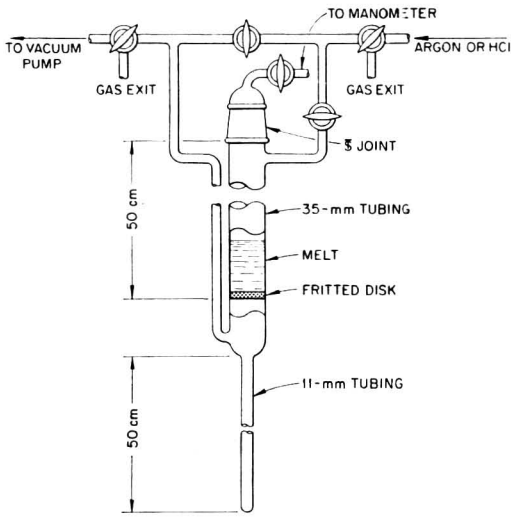

Fig. 1.—Apparatus used for the purification of LiCl–KCl mixtures.

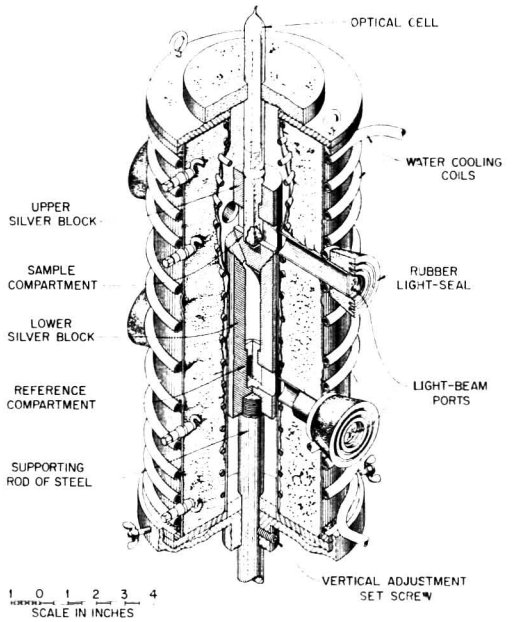

Fig. 2.—Furnace assembly used as a cell compartment in the spectrophotometer.

spectra of solutes existing in dilute solutions in fused salt media. Such measurements should give useful information concerning the chemical nature of species in fused salt solution. The particular system chosen for initial study was a solution of $NiCl_2$ in mixtures of LiCl and KCl. Measurements of this sort have recently been reported by Lux and Niedermaier,[5] who measured absorbancy values for manganese oxysalts dissolved in NaOH and KOH fusions, and by Gruen,[7] who determined absorbancy values for a variety of metal chlorides in fused $LiNO_3$–KNO_3 eutectic.

Experimental

Preparation of Materials.—Commercial, anhydrous HCl gas was purified by passing over activated charcoal and silica gel. Argon was purified by passing first over hot copper and then over P_2O_5. Anhydrous $NiCl_2$ was made from reagent grade, "cobalt-free" $NiCl_2 \cdot 6H_2O$. This material was first heated slowly to 450° over a period of 4 hr. under an atmosphere of flowing HCl gas. Then it was sublimed at 800 to 900° under an HCl atmosphere. The cobalt content of the final product was 0.0037% as determined by spectroscopic analysis.

Most of the LiCl–KCl mixtures used had a composition close to that of the eutectic (*ca.* 41 mole % KCl, m.p., *ca.* 350°). A convenient method for purifying this material is described in detail inasmuch as it is applicable to the preparation of a variety of low melting halide mixtures in a form suitable for quantitative spectral measurements. The apparatus is schematically illustrated in Fig. 1. The Pyrex fritted disk was of a "fine" porosity. By maintaining a suitable pressure differential on either side of the fritted disk the melt could be supported on the disk or filtered through at will. The apparatus was heated over the distance from the bottom of the 11 mm. tube to a position well above the top of the melt in the 35 mm. tube.

A mixture of reagent grade LiCl and KCl was placed on the fritted disk and the entire apparatus was evacuated with a mechanical pump. Exposure time of LiCl to room air was held to a minimum. The solid was heated under vacuum to 300° by gradually raising the temperature over a period of two hours. At 300°, argon followed by anhydrous HCl was admitted. While HCl passed through the filter disk and solid salt mixture, the temperature was raised over a period of ½ hr. to 500° to fuse the mixture. Initially the melt was cloudy. HCl was then passed through the melt, dispersed as fine bubbles by the fritted disk, until the cloudiness disappeared and for about 10 min. thereafter. The argon was bubbled through the melt for 5 min. to remove excess HCl. Next a vacuum was applied to the lower side-arm and the melt filtered through the disk to remove the solid impurities. The molten salt flowed into the lower, 11 mm., tube where it was quickly frozen by opening the lower furnace. The tube containing the purified mixture was then sealed off under vacuum, checked for vacuum leaks and stored until needed.

The mixture was removed easily from these tubes in a dry box by cracking the glass tubing and sliding out the solid rod of mixture. The rod of mixture was broken into segments and loaded into optical absorption cells.

The purity of the solvent mixture prepared in this way was evidenced by the complete absence of etch on the highly polished cell windows after 20 hr. exposure and by the reproducibility of the absorption spectra.

Spectrophotometer and Furnace.—Measurements of absorption spectra were made with a Cary Model 11 MS recording spectrophotometer which was modified for high temperature work by replacing the cell compartment with a furnace assembly described below. Furnace radiation did not interfere with the spectral measurements reported. This absence of interference was ensured by two design features of the Cary instrument. First, the light beam was pulsed at a low audio frequency and the output current was filtered to pass only the fundamental frequency of the pulses. Second, the light sensing units were a pair of matched 1P28 multiplier phototubes which had a low sensitivity to light of wave lengths greater than 750 mμ.

The furnace assembly is shown in Fig. 2. It consisted, essentially, of two silver blocks which held the optical cells, a furnace, and a supporting rod made from stainless steel pipe. This supporting rod was screwed into the lower silver block and carried a brass platform on which the furnace rested. The furnace could be unbolted from its platform and raised to give easy access to the silver blocks. The furnace assembly and the phototube housing were held on carriages which rode on a lathe-bed type of optical bench which was accurately aligned with the light beams from the monochromator.

The lower silver block, shown in Fig. 2, was designed to hold an optical cell containing a reference material. This cell was omitted in the measurements reported here and is not illustrated in the diagram. The upper silver block held the optical cell which contained the sample material. A cone on the bottom of the upper block rested in a precisely mating conical socket at the top of the lower block. Rotary alignment of the two blocks was ensured by means of a steel pin. Silver shims in the upper block held each cell in a reproducible position in the light beam.

In order to prevent heating of other components, the furnace shell was cooled with water and the light-beam ports were closed off with optical-grade fused silica windows. In order to prevent volatile products from the furnace insula-

tion and refractory cement from reaching and condensing on the furnace windows, the interior of the furnace and the adjacent light-beam ports were lined throughout with an all-welded Inconel shield.

The furnace winding was provided with shunts so that different power in-puts could be applied to the top, middle and lower sections in order to help reduce thermal gradients. Further reduction in thermal gradients was provided by the silver blocks which held the optical cells. Inasmuch as a reference cell was not placed in the lower silver block in the research described here, the elimination of a thermal gradient between the two silver blocks was not important. However, such a gradient can be reduced to a very small value with this apparatus when it is desired to measure absorbancy directly.

Such gradients as existed together with the temperature of each cell compartment were measured by means of five calibrated platinum to platinum–rhodium thermocouples placed into holes drilled at suitable positions in the silver blocks and read with a Leeds and Northrup Model K-3 Universal potentiometer. The temperature level was controlled by means of a chromel–alumel thermocouple which actuated a Leeds and Northrup Model G Speedomax coupled with a Leeds and Northrup "DAT" controller. Temperature control was within a precision of 0.5° as measured by couples adjacent to the optical cells. The temperature of a melt was calibrated with a platinum-sheathed thermocouple immersed therein. It is estimated that the absolute temperature of a melt was known to within 1°.

The absorbance range of the spectrophotometer as supplied by the manufacturer was 0 to 3.5 absorbance units. For a few high absorbance measurements this range was increased to about 5.5 by insertion in the reference light beam of screens made from accurately perforated steel plates supplied by the Pyramid Screen Corporation. This extension of the absorbance range was permissible because of the very low level of stray light achieved by the Cary double monochromator. The absorbances of the screens were accurately measured.

Optical Cells.—The types of optical cells used in this work are illustrated in Fig. 3. (Cells were supplied by Pyrocell Manufacturing Company.) The cell shown in Fig. 3a was used largely for preliminary work in which some risk of atmospheric contamination was accepted in order to gain experimental flexibility. This type of cell will be referred to as a "stoppered" cell. The other type of cell, shown in Fig. 3b, initially had a standard taper joint on the upper end as shown. However, after loading it was sealed off under vacuum by fusing the glass several centimeters above the melt so as to avoid any chance of atmospheric contamination during a run. This type of cell is referred to as a "sealed" cell.

The lower end of both types of cells consisted of a square cross section, Beckman optical-cell made of fused silica. This Beckman cell was fastened to the upper Pyrex tubing by means of a graded seal. The cell windows were 40 mm. high by 10 mm. wide and the inside distance between windows was 10 mm. For some measurements the light path length through the melt was reduced to 0.5 mm. This was accomplished with precision-grade quartz inserts, supplied by Pyrocell Manufacturing Company, which are shown in place in Fig. 3. Values of the average path length for each measurement were determined to within 1% by micrometer measurements on the cell and the insert.

In the stoppered cells purified argon was admitted through a quartz capillary tube which had a side opening near the liquid level. Below this side opening the capillary tube was collapsed to form a rod which was fused to a quartz insert. Argon left the cell through a side arm which was closed with a valve that permitted gas to leave but not to enter the cell.

Procedure.—Optical cells were loaded with salt in a vacuum-type dry box under a high purity nitrogen atmosphere. The cells were weighed on an analytical balance before and after loading in order to obtain the weight of the LiCl–KCl mixture. $NiCl_2$ was added in the dry box from a weighing bottle which was likewise weighed before and after the addition. After loading, the cells of the sealed type were pumped down to about 10^{-5} mm. and sealed off.

For all spectral measurements, air was the reference material. That is, the measured quantity was log (incident intensity/transmitted intensity). Absorbancy values were obtained by subtracting measured values for a cell containing only the solvent from measured values for an identical cell containing a solution. Light absorption by the solvent over the range 280 to 750 mμ was small and did not change much with temperature. However, at wave lengths approaching 220 mμ the light absorption of the solvent rose rapidly and changed considerably with temperature.

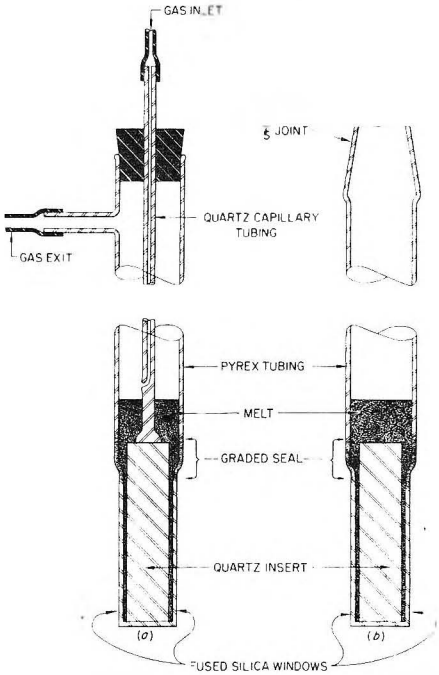

Fig. 3.—Types of optical cells used: (a) "stoppered" cell; (b) "sealed" cell. After loading this cell was sealed off under vacuum at a point below the standard taper joint.

In measurements made with the stoppered type of optical cell weighed amounts of $NiCl_2$ were added as desired by momentarily unstoppering the cell. After each addition the cell was flushed with argon and the $NiCl_2$ mixed with the melt by raising and lowering the quartz insert a number of times. It is to be noted that anhydrous $NiCl_2$ is not hygroscopic. Following each addition of $NiCl_2$ adequate time was allowed for thermal equilibration.

The vaporization of $NiCl_2$ was appreciable only for a few melts containing a high concentration of this material, and then only after a prolonged time at temperature. In these instances the contents of the cell, including vapor deposited $NiCl_2$, were remixed before each spectral measurement.

At the termination of measurements on a given sample contained in a sealed cell, the cell was inverted and allowed to cool. Then the cell was cut open, the entire contents dissolved in 0.1 *M* HNO_3, and portions of the solution submitted for analytical determination of Li and K. If the cell was not inverted before cooling, the cell windows usually cracked as the salt solidified.

Values for the molar absorbancy index a_m (also known as the molar extinction) were computed from weights of $NiCl_2$ and LiCl–KCl mixture added to the optical cell and from the density of the fused LiCl–KCl mixture at the temperature and KCl concentration involved. It is not unlikely that a small amount of $NiCl_2$ was lost in the loading operation. This would cause the absolute values of a_m reported here to be too great. However, the precision in the a_m values for different weighings of $NiCl_2$ was very good (standard deviation <2%) considering sources of error other than weighing. The absolute values of a_m are estimated to be within 5%. The density of the solutions was taken to be the density of the solvent. The error involved in this assumption is considered to be less than experimental errors inasmuch as the $NiCl_2$ concentrations were for the most part very small. Density values of the LiCl–KCl mixtures were obtained from the work of Van Artsdalen and Yaffee.[9] They gave empirical equations in two constants, *a* and *b*, which express density as a function of temperature at several

(9) E. R. Van Artsdalen and I. S. Yaffee, THIS JOURNAL, **59**, 118 (1955).

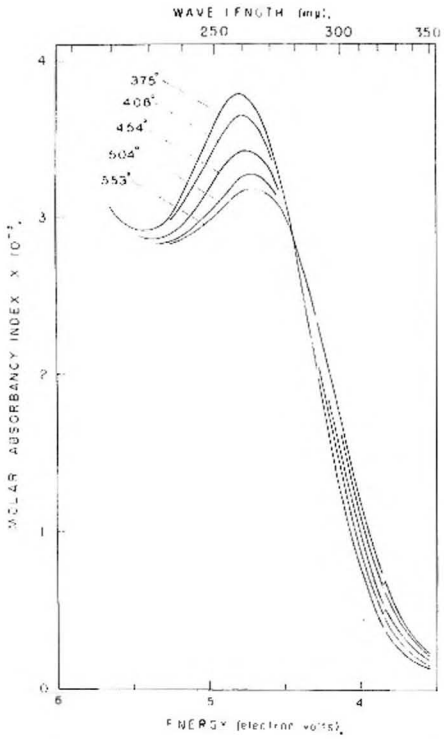

Fig. 4.—Ultraviolet absorption spectra of a solution of $NiCl_2$ in a fused LiCl–KCl mixture at several temperatures. Measurements made in sealed optical cells. Melt contained 1.11×10^{-3} g. $NiCl_2$ per g. solution. Molar absorbancy indices computed from concentration of total nickel.

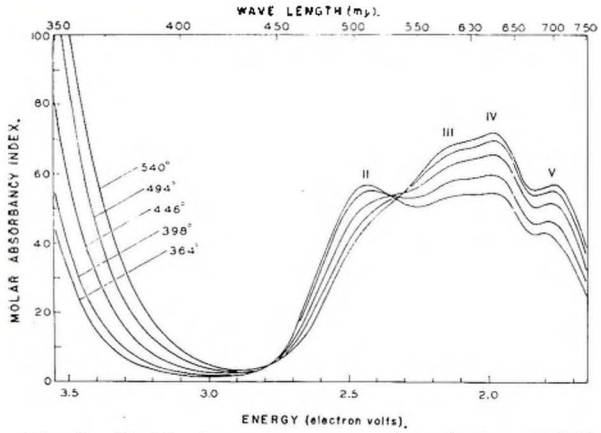

Fig. 5.—Visible absorption spectra of a solution of $NiCl_2$ in a fused LiCl–KCl mixture at several temperatures. Measurements made in a sealed optical cell. Melt contained 0.0246 g. $NiCl_2$/g. solution and solvent salt contained 41.0 mole % KCl.

fixed concentrations of KCl. In the measurements reported here, density values were needed at intermediate concentrations in the neighborhood of the eutectic composition. For this purpose the constants of Van Artsdalen and Yaffee were represented by the equations

$$a = 1.860 + 0.00225(X - 30)$$
$$b \times 10^3 = 0.5073 + 0.0018(X - 30)$$

where

$$X = \text{mole \% KCl, and } 30 < X < 60$$

Results and Discussion

Typical results of the spectral measurements are illustrated for the ultraviolet in Fig. 4 and for the visible in Fig. 5. The data shown were obtained with sealed cells. Along the ordinates in these figures is plotted the molar absorbancy index computed in terms of the molar concentration of nickel atoms without regard to the chemical composition of the light absorbing species. Five absorption bands were found over the range of 220 to 750 mμ and these will be designated as bands I through V taken in the order of increasing wave length. Band I is shown in Fig. 4 and bands II through V are indicated in Fig. 5. The shape of the short wave length side of band I shows the presence of another absorption band at shorter wave lengths. With increasing temperature bands I and II decreased in molar absorbance index while bands III, IV and V increased. The temperature coefficient of the molar absorbance index was found to have the same value for all wave lengths between the maxima of bands III and V. The spectra for different temperatures were found to intersect twice between bands I and II and once between bands II and III. The two intersections between bands I and II were caused by a broadening and shift toward longer wave lengths of band I, whereas the intersection between bands II and III was caused by the simultaneous downward movement of band II and upward movement of band III. At 398° the band maxima occurred as follows: I at 260 mμ, II at 512 mμ, III at *ca.* 590 mμ, IV at 625 mμ and V at 695 mμ. As may be seen, there was a considerable overlapping of bands so that the above values are somewhat different from those of the true band centers. A Gaussian analysis of the group of bands in the visible indicates that there may be one or two additional bands not evidenced by an inflection in the absorbancy curves, and shows unquestionably that band II decreases much more with increasing temperature than does the composite a_M curve shown in Fig. 5.

No attempt will be made in this report to deduce, precisely, the chemical constitution of the light absorbing species or to make an assignment of the observed bands. However, Gruen[7] gives evidence which indicates that the observed bands are due at least in part to various chloro-nickel complexes. The authors have conducted similar studies in which spectra were measured for a solution of $NiCl_2$ in fused KNO_3 to which additions of KCl were made. With increasing additions of KCl the 440 mμ absorption band of $NiCl_2$ in pure KNO_3 disappeared and there appeared the complex of overlapping bands reported here for the visible absorption spectrum of $NiCl_2$ in fused LiCl–KCl mixtures. Details of this study will be reported later.

A consideration of the effect of temperature on the absorption spectrum strongly suggests that there is more than one light absorbing species present in the melt, but first it will be demonstrated that all such species were derived from $NiCl_2$.

It was found that at constant temperature and constant solvent salt composition the molar absorbancy index computed from the molar concentration of nickel atoms was a constant independent of nickel atom concentration over the range of about 0.01 to 0.4 *M*. This result, the experimental evidence for which is described below, shows, first,

that the concentrations of all light-absorbing species are proportional to the total concentration of nickel atoms and, second, that the molar absorbancy index computed as described could be employed for analytical purposes in the way which is customary for more conventional solutions at ordinary temperatures. Experimental verification of the constancy of the molar absorbancy index computed using the total concentration of nickel is described in the following paragraphs.

Spectra were measured over the visible range after each of seven successive additions of $NiCl_2$ to a LiCl–KCl melt contained in a stoppered cell at 409°. The concentration range covered was about 0.01 to 0.4 *M* $NiCl_2$. Molar absorbancy indices were computed at 10 mμ intervals over the range of 350 to 750 mμ for all seven spectra. The resultant values obtained at the same wave lengths but different $NiCl_2$ concentrations were in agreement. Similar measurements were made in the ultraviolet. The absorbancy values at the band maximum formed a straight line function of concentration of $NiCl_2$ except that for an absorbance of 4.8 and greater negative deviations and a small shift in band maxima toward longer wave lengths were observed. These systematic deviations were probably caused by stray light. The concentration range covered was about 0.01 to 0.038 *M* $NiCl_2$.

In order to determine the constancy of the molar absorbancy index over a wide range of temperature, visible spectra were measured for five sealed absorption cells. Each cell contained a different concentration of $NiCl_2$ over the range of about 0.013 to 0.32 *M* and each was measured at five temperatures from 364 to 540°. Resultant values and their standard deviations were as follows: for band II at 364° $a_M = 58.9 \pm 0.4$, at 398° $a_M = 55.4 \pm 0.2$; for band IV at 364° $a_M = 55.9 \pm 1.0$, at 398° $a_M = 61.1 \pm 0.9$, at 445° $a_M = 66.5 \pm 0.8$, at 490° $a_M = 70.1 \pm 1.0$ and at 540° $a_M = 73.1 \pm 0.9$. In each of these five sets of measurements the composition of the solvent salt was unavoidably somewhat different. As would be expected from the results described below, these variations in solvent composition had a small effect on the molar absorbancy indices. Consequently, the data were corrected to 41.0 mole % KCl, the eutectic composition, on the basis of plots of a_M *vs.* mole % KCl for each of the two band maxima. These corrections were small.

As seen in Figs. 3 and 4 changes in temperature produced substantial changes in the absorption spectrum of $NiCl_2$ dissolved in a LiCl–KCl mixture. Any quantitative interpretation of a change in shape of an absorption curve with a large change in temperature must be made with caution. In general, three rather different kinds of temperature effects are to be expected. First, a change in temperature may cause a change in concentration of the light absorbing species apart from that associated with the change in density. Second, an increase in temperature will cause a given absorption band to broaden and may cause a shift in the wave length of the band maximum. This latter effect is caused by thermal motions of the light absorbing species and the magnitude of this

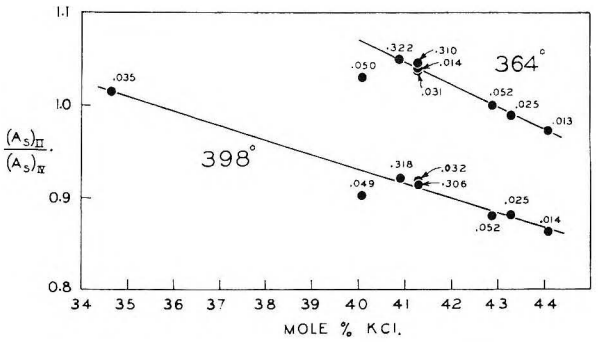

Fig. 6.—Effect of small changes in solvent composition on the visible absorption spectrum as measured by changes in the ratio of the absorbancy of band II to that of band IV at each of two temperatures. Upper line for measurements at 364°, and lower line for measurements at 398°. The number by each point indicates the molar concentration of total nickel in the melt. The point at 34.4 mole % KCl on the 398° line was obtained by extrapolation from data obtained at 416° and above.

effect is determined in a complex way by the electronic structures of the ground and excited states. Third, if an absorption band is associated with a forbidden transition which has been perturbed, and if the perturbations are temperature dependent, then the integrated absorbancy index (or integrated optical cross section) must change with a change in temperature. As a consequence of the latter two effects, the absorbancy per unit path length will change for each wave length in a way which is independent of any change in concentration of the light absorbing species; that is, the absorbancy index will be a function of temperature.

The observed ultraviolet band (band I) would seem most likely to arise from an allowed transition, whereas the complex of bands in the visible is due probably to transitions between the degenerate 3d orbitals of Ni^{2+} in which the degeneracy has been removed by the field of the neighboring ions. The substantial decrease in peak amplitude of the ultraviolet band with increasing temperature is no doubt attributable in part to band broadening. Approximate computations, however, show that no more than one-half of the observed decrease can be accounted for in this way. The remaining decrease arises from a decrease in concentration of the species giving rise to this band. For band II the very considerable drop in amplitude (shown by Gaussian analysis) is much too great to be attributable to band broadening and its strong negative coefficient is not the behavior expected from known kinds of thermal perturbations which might relax its forbidden character. Consequently, this band is also associated with a species which decreases in concentration with an increase in temperature. The remaining identified bands increase in amplitude with increasing temperature. Thermal perturbations no doubt contribute to this effect while band broadening is in the wrong direction. However, the thermal perturbation effect should be most effective at relatively low thermal energies, and it seems doubtful that it could account for more than a fraction of the observed decrease in absorbancy index of about 20% for a temperature decrease of about 20% at the 700°K. level. For this reason a substantial portion of this decrease in

absorbancy index is attributed to a decrease in concentration of light absorbing species with decreasing temperature.

It is concluded that when $NiCl_2$ dissolves in a LiCl–KCl mixture at least two light absorbing species are formed, and that these species are in equilibrium such that those associated with bands I and II decrease in concentration with increasing temperature while those associated with bands III, IV and V increase in concentration with increasing temperature.

Small changes in the composition of the solvent salt were found to have a small but measurable effect on the absorption spectra. This effect is best shown in terms of the ratio of the absorbancy values of bands II and IV, that is, $(A_s)_{II}/(A_s)_{IV}$. In Fig. 6 this ratio is plotted against mole % KCl at two temperatures, 364 and 398°. These temperatures are near the freezing point of the eutectic so that the accessible composition range for LiCl–KCl mixtures was quite small. Values of the molar concentration of $NiCl_2$ are indicated for each point in Fig. 6. It will be noted that, to within experimental error, the effect of solvent composition is independent of the $NiCl_2$ concentration for the range of compositions measured. The absorbancy ratio for the 34.4 mole % KCl mixture was extrapolated from measurements at 416° and above. This extrapolation was necessary because this mixture freezes at the lower temperature while for mixtures near the eutectic at temperatures above 400°, band II is obliterated by overlap of band III.

At a constant temperature a change in the relative absorbancies of bands II and IV could be a measure of a change in the relative concentrations of the two species which give rise to them (ignoring the effect of band overlap), and these relative concentrations might be expected to shift with a change in the cation ratio of the solvent salt because of a corresponding shift either in the activity coefficients of the two species or in the equilibrium constant. On the other hand, chloronickel(II) complex anions should be surrounded by Li^+ and K^+ cations which differ greatly in their ability to polarize neighboring ions. Consequently, a change in the average of the ratio of Li^+ to K^+ ions surrounding a chloronickel(II) complex anion might well be expected to have some effect on the width or even on the oscillator strength of absorption bands of the anion. The existing experimental data do not permit a separation of the contribution of the latter effects from that of a change in concentration.

Absorption spectra measurements will be continued on this and other fused salt systems. In addition, consideration is being given to measurements of paramagnetic susceptibility for fused salt systems. Such measurements, particularly in the case of nickel, should provide information regarding the electronic and spatial configurations of the complex species present.

Acknowledgment.—The authors gratefully acknowledge the assistance of Mr. D. E. LaValle who prepared the compounds, Mr. D. F. Anthrop who made many numerical computations, and Dr. W. R. Laing and co-workers who did the Li and K analyses.

KINETICS OF OXIDATION–REDUCTION REACTIONS OF PLUTONIUM. THE REACTION BETWEEN PLUTONIUM(VI) AND VANADIUM(III) IN PERCHLORATE SOLUTION[1]

BY SHERMAN W. RABIDEAU

Contribution from the University of California, Los Alamos Scientific Laboratory, Los Alamos, N. M.

Received October 28, 1957

The kinetics of the reaction between PuO_2^{+2} and V^{+3} has been studied by spectrophotometric measurements at 8304 Å. The stoichiometry of the reaction is given by the equation $PuO_2^{+2} + V^{+3} + H_2O \rightarrow PuO_2^{+} + VO^{+2} + 2H^+$. This second-order reaction has been found to be dependent upon both an inverse first and an inverse second power of the hydrogen ion concentration. Values of k' and k'', the rate constants associated with the inverse first and the inverse second power of the hydrogen ion concentration, have been found to be 2.12 ± 0.03 sec.$^{-1}$ and 0.228 ± 0.005 mole liter^{-1} sec.$^{-1}$, respectively, for perchlorate solutions of ionic strength two at a temperature of 25°.

Introduction

In view of the observation that the rate of reaction between PuO_2^{+2} and Pu^{+3} can be followed spectrophotometrically,[2] interest has developed in the kinetics of other oxidation–reduction reactions previously thought to be too rapid to measure without the use of very rapid-mixing techniques. Also, since the absorption peak of plutonyl ion at 8304 Å. (molar absorptivity *ca.* 550 M^{-1} cm.$^{-1}$) can be used to follow the progress of the reaction with spectrophotometric recording methods, the reactant concentrations can be as low as 10^{-4} M to bring the reaction rates into a conveniently measurable range without the loss of precision.

Experimental

Preparation of Reagents.—Plutonium(VI) perchlorate solutions were prepared from oxide-free plutonium metal especially selected from a lot of high purity. A known weight of metal was dissolved in a weighed quantity of standardized 70% perchloric acid. The oxidation to the plutonyl state was accomplished by prolonged ozonization, *ca.* 24 hours. An additional period of oxidation with ozone was performed on the diluted stock solution prior to

(1) This work was done under the auspices of the U. S. Atomic Energy Commission.

(2) A. E. Ogard and S. W. Rabideau, THIS JOURNAL, **60**, 812 (1956); S. W. Rabideau and R. J. Kline, *ibid.*, to be published.

use in the reaction with vanadium(III). At the termination of the period of oxidation, the solution was flushed with helium to remove dissolved ozone.

Baker and Adamson reagent grade 70% perchloric acid was boiled to remove traces of organic material; then filtered through a sintered glass disc prior to use. Standardization of this acid was performed on a weight aliquot basis with mercuric oxide used as the primary standard. All solutions were prepared with distilled water which had been redistilled from alkaline permanganate in an all-Pyrex apparatus. Sodium perchlorate was prepared by neutralizing C.P. sodium carbonate with perchloric acid, then recrystallizing the sodium perchlorate from water. Lithium perchlorate was similarly prepared as the trihydrate and recrystallized from water. This salt was analyzed for water and for perchlorate content before use. Mallinckrodt AR grade acetone and ammonium thiocyanate together with Baker and Adamson reagent grade stannous chloride were used in the spectrophotometric analysis of vanadium(III).

Vanadium(V) oxide was prepared by the ignition in air of Fisher purified grade ammonium metavanadate which had been recrystallized from water. Vanadium(III) perchlorate was prepared by the electrolytic reduction of a 1 M perchloric acid suspension of vanadium(V) oxide with platinized platinum electrodes. The reduction apparatus consisted of a 50/50 Pyrex joint the male section of which was formed into a flat-bottomed container, was fitted with a wide tube for the entrance of the platinum cathode through a Teflon plug, and was provided with a stopcock through which the vanadium(III) perchlorate was removed at the termination of the electrolysis. The female section of the joint was equipped with a Dewar-sealed re-entrant tube terminating in a sintered glass disc of medium porosity which served to separate the anode and cathode compartments. A gas inlet tube was provided through which nitrogen purified with chromous chloride was admitted in the cathode compartment of the electrolysis cell to prevent the air oxidation of the vanadium(III) perchlorate. The anode was supported in the re-entrant tube with a Teflon plug. Suitably located gas outlet tubes were provided.

Analysis of Vanadium(III) Solutions.—The stock solutions of vanadium(III) were analyzed spectrophotometrically at 3960 Å. as the thiocyanate complex using a minor modification of the procedure given by Crouthamel, *et al.*[3] It was found that freshly prepared vanadium(III) solutions when converted into the thiocyanate complex gave identical optical densities either with or without added stannous chloride. Thus, since it appears that the vanadium(III) perchlorate is not significantly oxidized to vanadium(IV) under the conditions of this analysis, even in the absence of added stannous chloride, the vanadium(III) solutions were analyzed without added reductant. Solutions of known total vanadium content were analyzed routinely as controls. Standard vanadium solutions were prepared by dissolving 99.7% pure fused vanadium metal obtained from A. D. McKay Co. in nitric acid solution; then removing the nitric acid by boiling with hydrochloric acid. The molar absorptivity ϵ of the vanadium thiocyanate complex at a temperature of 25° was measured to be 12,250 ± 93. In good agreement with the results of Furman and Garner,[4] the molar absorptivities of vanadium(III) perchlorate at 4000 and 5900 Å. at a temperature of 25° were found to be 8.42 and 5.57, respectively. Estimations of the vanadium(III) perchlorate stock solution concentrations were made by use of these molar absorptivities, and the final concentrations of the diluted stock solutions were obtained with the thiocyanate method.

Spectrophotometric Measurement. The progress of the reaction was followed by means of measurements at 8304 Å. with the Cary Model 14 recording spectrophotometer. The solutions of vanadium(III) and plutonium(VI) perchlorate were placed in the separate legs of a double-chambered 10 cm. spectrophotometric cell which had been flushed with nitrogen. The solutions were then brought to constant temperature within ±0.1° by immersing the cell in a constant-temperature water-bath without mixing the solutions. At time zero, the solutions were mixed by removing the mixing cell from the constant temperature bath and tilting the cell back and forth several times. The mixing cell was placed in the thermostated cell holder within 30 seconds of the time of mixing. In the spectrophotometric cell compartment, the cell was submerged in the water-bath surmounting a modified[5] Cary cell holder which was maintained at a temperature constant to within ±0.2° by circulation of water through the heavy metal base of the modified cell holder. The walls of the cell compartment bath contained gasketed quartz windows for transmission of the light beam from the spectrophotometer. At temperatures below the dew point of the room, it was necessary to pass a current of dry helium across the faces of the windows to prevent fogging.

(3) C. E. Crouthamel, B. E. Hjelte and C. E. Johnson, *Anal. Chem.*, **27**, 507 (1955).

(4) S. C. Furman and C. S. Garner, *J. Am. Chem. Soc.*, **72**, 1785 (1950).

(5) The modified cell holder was designed by T. W. Newton and F. Baker of this Laboratory.

Results and Discussion

Reaction Stoichiometry.—In a set of experiments designed to examine the stoichiometry of the reaction between plutonium(VI) and vanadium(III), the rate of disappearance of PuO_2^{+2} was followed at 9512 Å. (molar absorptivity = 24.8 M^{-1} cm.$^{-1}$) and the rate of appearance of PuO_2^{+} was observed at 5690 Å. (molar absorptivity = 17.1 M^{-1} cm.$^{-1}$) at a temperature of 2.4°. The initial reactant concentrations in the two experiments were essentially equal (*ca.* 3×10^{-3} M). The rate of disappearance of PuO_2^{+2} was matched by a corresponding rate of increase of PuO_2^{+} in accord with the assumption that the stoichiometry is given by the reaction

$$PuO_2^{+2} + V^{+3} + H_2O = PuO_2^{+} + VO^{+2} + 2H^{+} \quad (1)$$

Although the usual procedure in this study has been to follow the disappearance of PuO_2^{+2} through the absorption at 8304 Å., the progress of the reaction was followed by another stoichiometry check by observing the rate of formation of VO^{+2} from measurements at 7500 Å. A rate constant of 0.24 liter mole^{-1} sec.$^{-1}$ was obtained which is in good agreement with the values obtained at this temperature from measurements of the rate of disappearance of PuO_2^{+2} (*vide infra*). It would appear that under the conditions of this study the rate of reaction between V^{+3} and PuO_2^{+} is rather small in comparison with the rate of reduction of PuO_2^{+2}. Also, at the plutonium concentrations used, the disproportionation of PuO_2^{+} appears to be negligibly small especially in the early phases of these experiments, because of the low plutonium(V) concentrations.

Order of Reaction.—In Table I are given some of the results of experiments in which the second-order character of the reaction between PuO_2^{+2} and V^{+3} was demonstrated. The apparent rate constant, k_1, was calculated from the integrated equation for a bimolecular process

$$k_1 = \frac{2.303}{t[(PuO_2^{+2})_0 - (V^{+3})_0]} \log \frac{(V^{+3})_0[(PuO_2^{+2})_0 - x]}{(PuO_2^{+2})_0[(V^{+3})_0 - x]} \quad (2)$$

in which the subscript zero refers to initial concentrations and x is the concentration of PuO_2^{+} or VO^{+2} formed at time t. The linear relation between plots of the logarithmic term in equation 2 *versus* time has been observed.

Acidity and Ionic Strength Dependence.—The hydrogen ion concentration dependence of the reaction rate was obtained in a series of measurements

TABLE I

EVALUATION OF SPECIFIC RATE CONSTANTS FOR Pu(VI)–V(III) REACTION IN MOLAR PERCHLORIC ACID AT 2.4°

$(PuO_2^{+2})_0 \times 10^4$, M	$(V^{+3})_0 \times 10^4$, M	k_1, l. mole^{-1} sec.$^{-1}$
1.911	2.201	0.23
1.736	6.818	.20
24.61	24.52	.24

at a constant ionic strength of two at a temperature of 25°. Sodium perchlorate was substituted for perchloric acid to maintain the ionic strength at a constant value. The results are given in Table II.

TABLE II

HYDROGEN ION CONCENTRATION DEPENDENCE OF REACTION BETWEEN Pu(VI) AND V(III) IN PERCHLORATE SOLUTION

$[PuO_2^{+2}]_0 \times 10^4$, M	$[V^{+3}]_0 \times 10^4$, M	$[H^+]$, M	k_1 (obsd.), l. mole^{-1} sec.$^{-1}$	k_1 (calcd.), l. mole^{-1} sec.$^{-1}$
1.939	5.328	2.000	1.16	1.12
1.718	9.121	2.000	1.15	
2.119	10.138	1.500	1.56	1.51
2.123	5.067	1.500	1.59	
2.122	5.371	1.000	2.23	2.34
1.666	9.333	1.000	2.25	
1.704	4.493	0.500	4.88	4.80
1.910	5.291	.500	4.70	
2.085	3.055	.250	12.49	12.11
1.731	4.963	.250	12.42	
1.734	2.226	.150	24.49	24.24
2.049	2.179	.150	24.67	
2.081	1.293	.100	43.6	43.96
2.003	2.028	.100	43.75	

The values of $k_{1(calcd)}$ given in Table II were obtained by use of the equation

$$k_1 = (k'/[H^+] + k''/[H^+]^2) \qquad (3)$$

in which k' and k'' are the specific rate constants associated with an inverse first and an inverse second power of the hydrogen ion concentration, respectively. Values of k' and k'' obtained by the method of least squares are 2.12 ± 0.03 sec.$^{-1}$ and 0.228 ± 0.006 mole liter^{-1} sec.$^{-1}$, respectively, for perchlorate solutions of ionic strength two and at a temperature of 25°. The uncertainties given represent twice the standard deviation of the average values of the intercept and slope. A possible mechanism which is in accord with the second-order nature of the reaction and with the observed hydrogen ion concentration dependence is

$$V^{+3} + H_2O \rightleftharpoons VOH^{++} + H^+ \quad \text{(rapid)} \qquad (4)$$

$$PuO_2^{+2} + VOH^{+2} \xrightarrow{k'} PuO_2^{+} + VO^{+2} + H^+ \quad \text{(slow)} \qquad (5)$$

$$PuO_2^{+2} + V(OH)_2^{+} \xrightarrow{k''} PuO_2^{+} + VO^{+2} + H_2O \quad \text{(slow)} \qquad (6)$$

It should be pointed out that alternative possibilities to reactions 5 and 6 consist of the reaction of PuO_2OH^+ with V^{+++} and of PuO_2OH^+ with VOH^{+2}, respectively. Since these reactions are kinetically indistinguishable, both must be considered as possibilities. Measurements of the rate of reaction between PuO_2^{+2} and V^{+3} also were made as a function of acidity in solutions of unit ionic strength and at a temperature of 25°. The results of these experiments are given in Table III. By the method of least squares the values of k' and k'' for the perchlorate solutions of unit ionic strength and 25° have been computed to be 1.81 ± 0.05 sec.$^{-1}$ and 0.200 ± 0.010 mole liter^{-1} sec.$^{-1}$, respectively. Thus, from a comparison of Tables II and III it is seen that the effect of an increase in the ionic strength from one to two has been to increase both k' and k''. The magnitude of the increase is about 10% for both k' and k''.

TABLE III

HYDROGEN ION CONCENTRATION DEPENDENCE OF REACTION BETWEEN PuO_2^{+2} AND V^{+3} IN PERCHLORATE SOLUTION

$[PuO_2^{+2}]_0 \times 10^4$, M	$[V^{+3}]_0 \times 10^4$, M	$[H^+]$, M	k_1 (obsd.)	k_1 (calcd.)
1.620	3.161	1.000	2.08	2.01
1.584	1.583	1.000	2.08	
1.347	1.271	0.500	4.20	4.42
1.387	1.244	.500	4.20	
1.170	1.186	.250	10.26	10.44
1.245	1.227	.250	10.35	
1.953	1.882	.150	22.4	20.96
1.669	1.918	.150	21.4	
1.586	1.819	.100	37.3	38.1
2.289	2.390	.100	37.5	

In an experiment devised to illustrate the effect of the substitution of lithium perchlorate for sodium perchlorate as the added salt in maintaining the ionic strength of the solution at unity, the rate of reaction between PuO_2^{+2} and V^{+3} was measured in 0.500 M perchloric acid–0.500 M lithium perchlorate at 25°. Values of 4.55 and 4.53 liters mole^{-1} sec.$^{-1}$ were obtained in these solutions for k_1 as compared to 4.20 liters mole^{-1}sec.$^{-1}$ in solutions in which sodium perchlorate was the added salt (see Table III). Thus the substitution of lithium perchlorate for sodium perchlorate occasions no large change in the specific rate constant for this reaction.

Temperature Dependence.—The effect of the variation of temperature upon the rate of reaction has been studied in molar perchloric acid solutions between 2.4 and 34.5°. In Table IV the variation of the apparent rate constant, k_1, is given as a function of temperature. From a linear plot of log k_1 *versus* $1/T$ is computed a least squares slope of 3517 ± 81 which corresponds to an experimental Arrhenius activation energy of 16.1 ± 0.4 kcal./mole. Since $k_1 = k' + k'' = A' e^{-E'/RT} + A'' e^{-E''/RT}$, the activation energy for the principal path is not necessarily equal to the experimentally observed value of 16.1 kcal. However since the plot of k_1 *versus* $1/T$ is linear, the activation energies E' and E'' are not greatly different from this

TABLE IV

TEMPERATURE DEPENDENCE OF THE RATE OF REACTION BETWEEN PuO_2^{+2} AND V^{+3} IN MOLAR PERCHLORIC ACID

Temp., °C.	k_1, l. mole^{-1} sec.$^{-1}$	log k_1
34.5	4.57	0.660
25.0	2.08	.318
15.2	0.74	− .131
2.4	.22	− .658

value. At a temperature of 25° the values of k' and k'' have been determined and the values of k_1 are known with a precision of ±2%; hence, by a trial and error procedure extreme values which E' and E'' can have were found. From these calculations it has been possible to show that $E' = 15.8 \pm 0.5$ kcal. The uncertainty in the value of E'' is considerably larger; the value obtained was 16.0 ± 2.5 kcal. From expressions of the transition state theory,[6] values of the heat, free energy and entropy of activation were computed for the reaction between plutonyl ion and trivalent vanadium ion in terms of the principal species, *i.e.*, $PuO_2^{+2} + V^{+3} \rightarrow$ (activated complex) $+ H^+$. These quantities are $\Delta F^{\ddagger} = 17.03 \pm 0.01$ kcal./mole, $\Delta H^{\ddagger} = 15.5 \pm 0.4$ kcal./mole and $\Delta S^{\ddagger} = -5 \pm 2$ cal./deg. The magnitudes of the rate constants k' and k'' show the relative importance of the two paths which appear to be indicated in the reaction between plutonyl ion and vanadium(III). Thus at 25° about 90% of the over-all reaction occurs through the path in which a single hydrogen ion is liberated.

Acknowledgment.—The author wishes to express his appreciation to Drs. J. F. Lemons, Charles E. Holley, Jr., and Thomas W. Newton for valuable discussions and interest shown in this research.

(6) S. Glasstone, K. Laidler and H. Eyring, "The Theory of Rate Processes," McGraw–Hill Book Co., Inc., New York, N. Y., 1941, p. 417.

COMPLEX IONS IN FUSED SALTS

BY F. R. DUKE AND M. L. IVERSON

Contribution No. 545 from the Institute for Atomic Research and Department of Chemistry, Iowa State College, Ames, Iowa. Work was performed in the Ames Laboratory of the U. S. Atomic Energy Commission

Received October 31, 1957

The complex formation constants for a series of bivalent metal halides were determined using fused KNO_3-$NaNO_3$ eutectic as solvent. The method involved measuring the increase in solubility of the slightly soluble metal chromate as halide ion was added.

The existence of complex ions in fused salts has been fairly well substantiated by previous studies. The main sources of evidence have been freezing point depression,[1] conductance,[2] spectrophotometric[3] and electrometric titration[4] studies in fused salts.

Solubility data have been used in aqueous solutions to study complex ions, *e.g.*, cadmium chloride[5] and silver chloride[6] complex ions. In the present research the effect of alkali halides upon the solubility of slightly soluble chromate salts in molten sodium nitrate–potassium nitrate eutectic is interpreted in terms of complex ion formation.

Experimental

ACS reagent grade chemicals were used. The chromate salts of barium, calcium, lead and magnesium were precipitated from aqueous nitrate solutions with a potassium chromate solution. Cadmium chromate was prepared by mixing solutions of stoichiometric amounts of cadmium nitrate and potassium chromate dissolved in the eutectic solvent of KNO_3–$NaNO_3$. The solvent was then drawn off and the precipitate equilibrated with a second portion of the fused solvent. After the second portion had been drawn off, the eutectic solvent–cadmium chromate residue was analyzed and used for the cadmium chromate solubility studies.

The solubilities of the chromate salts in the fused sodium nitrate–potassium nitrate eutectic were determined in the following manner. An amount of the chromate salt in excess of its solubility was added to 50 g. of the fused solvent in a test-tube. The test-tube was immersed in a fused salt bath maintained at the desired temperature ±1°. The solutions were stirred from 15 to 30 minutes and then the excess chromate salt was allowed to settle. Usually one hour was sufficient settling time. A medicine dropper was used to withdraw samples which were then analyzed for their chromate and chloride content. The absence of undissolved particles of the chromate salts in excessive amounts was reasonably assured by visual observation of the molten sample. The solutions were then stirred again for one-hour periods and samples again withdrawn. The constancy of the chromate concentration within the experimental error of the measurement indicated that the desired equilibrium was attained. The equilibrium temperatures were approached from above and below for the $PbCrO_4$ determinations. All the other values for solutions containing halide ions were obtained approaching the equilibrium temperature from below.

The chromate content of the samples was determined following the diphenylcarbazide colorimetric method.[7] For the high concentrations of chromate in the more soluble cases, the iodine-thiosulfate method[8] was used.

Results and Discussion

The solubility of lead chromate in a fused KNO_3-$NaNO_3$ eutectic solvent increases with increasing sodium chloride content up to the limiting solubility of sodium chloride as shown in Fig. 1. A similar increase in solubility with addition of sodium bromide is shown by the data of Table I. The solubility of cadmium chromate in the same solvent also increases with the addition of either chloride or bromide as shown in Table II. The solubilities of the chromate salts of magnesium, calcium and barium are not affected significantly by the addition of halide ions as shown by the data in Table III.

The increase in solubility of a salt such as lead chromate in fused KNO_3-$NaNO_3$ eutectic solvent on adding chloride can be interpreted on the basis

(1) E. Kordes, W. Bergmann and W. Vogel, *Z. Elektrochem.*, **55**, 600 (1951); E. Kordes, G. Ziegler and H. Proeger, *ibid.*, **58**, 168 (1954); E. Van Artsdalen, THIS JOURNAL, **60**, 172 (1956).

(2) H. Bloom and E. Heymann, *Proc. Roy. Soc. (London)*, **A188**, 392 (1947).

(3) D. M. Gruen and P. Graf, Abstract of Papers, 131st meeting of the American Chemical Society, April, 1957, 52R.

(4) S. N. Flengłass and E. K. Rideal, *Proc. Roy. Soc. (London)*, **A233**, 442 (1956).

(5) E. King, *J. Am. Chem. Soc.*, **71**, 319 (1949).

(6) J. H. Jonte and D. S. Martin, *ibid.*, **74**, 2052 (1952).

(7) Snell and Snell, "Colorimetric Method of Analysis," Vol. II, D. Van Nostrand Co., Inc., New York, N. Y., 1926, p. 274.

(8) Kolthoff and Sandell, "Textbook of Quantitative Analysis," The Macmillan Co., New York, N. Y., 1943, p. 624.

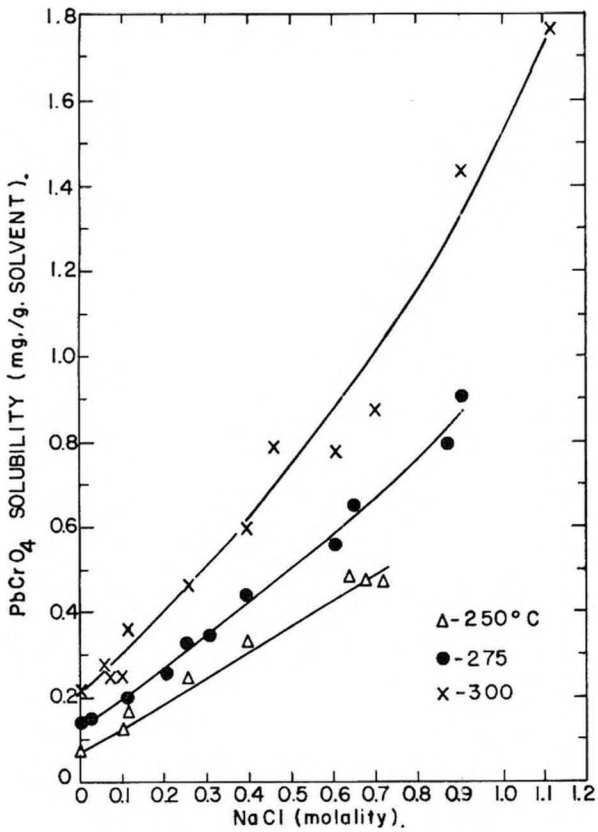

Fig. 1.—Effect of added sodium chloride on the solubility of lead chromate in fused sodium nitrate–potassium nitrate eutectic.

TABLE I

LEAD CHROMATE SOLUBILITY IN SODIUM NITRATE–POTASSIUM NITRATE EUTECTIC CONTAINING SODIUM BROMIDE

Sodium bromide, m	$PbCrO_4$ solubility[a] (mg./g. solvent) 250°	275°	300°
0.0	0.071	0.13	0.21
.05	.10	.18	.27
.10	.14	.22	.32
.20	.22	.30	.44
.30	.29	.39	.55
.40	.38	.48	.69
.50	.48	.59	.85
.60	.59	.72	1.04

[a] Values taken from smoothed curves through original data.

TABLE II

$CdCrO_4$ SOLUBILITY DEPENDENCE ON TEMPERATURE AND HALIDE CONCENTRATION IN KNO_3–$NaNO_3$ EUTECTIC

NaBr (and NaCl) concn. in eutectic solvent, m	$CdCrO_4$ solubility ($m \times 10^2$) 250°	300°
0.00	0.59 ± 0.07	0.80 ± 0.07
.10	1.2	1.7
.20	1.7	2.6
.30	2.3	3.5
.40	2.9	4.4
.50	3.5	5.3

[a] Values taken from a smoothed curve through the original data. Accuracy of data is approximately ±15%.

of complex ion formation. If one assumes that stable complex ions of the type $PbCl_n^{2-n}$ are formed, the solubility of lead chromate should vary with the

TABLE III

SOLUBILITY OF ALKALINE EARTH CHROMATES IN FUSED KNO_3–$NaNO_3$ EUTECTIC CONTAINING HALIDE IONS

Chromate salt	Solubility, $m \times 10^2$	Solvent
	300°	
$BaCrO_4$	0.20 ± 0.02	Pure eutectic
	.25	0.41 m NaCl
	.27	1.00 m NaCl
$CaCrO_4$	1.3 ± 0.1	Pure eutectic
	1.4	0.64 m NaBr
	250°	
$MgCrO_4$	0.55 ± 0.09	Pure eutectic
	.44	0.36 m KCl
	.67	0.71 m KCl
	.47	0.23 m NaBr
	.55	Saturated NaBr solu.

chloride concentration according to the expression

$$K_S' = K_S [1 + \beta_1(Cl^-) + \beta_2(Cl^-)^2 + \beta_3(Cl^-)^3 - \ldots] \quad (1)$$

where K_S' is the apparent solubility product of lead chromate, K_S is the solubility product of lead chromate in the pure solvent, and β_n is the constant.

$$\beta_n = \frac{(PbCl_n^{2-n})}{(Pb^{++})(Cl^-)^n}$$

The curves of Fig. 1 represent the equation

$$S = K_S'^{1/2} = \{K_S [1 + \beta_1(Cl^-) + \beta_2(Cl^-)^2 + \ldots]\}^{1/2} \quad (2)$$

where S is the solubility of the chromate salt. The change in solubility with respect to chloride concentration is given by the derivative

$$\frac{dS}{d(Cl^-)} = \frac{K_S [\beta_1 + 2\beta_2(Cl^-) + \ldots]}{2S} \quad (3)$$

It is apparent from the curves shown in Fig. 1 that one must start with MX^+ as the first complex ion species since the slope of the curve as the chloride concentration goes to zero is some positive value. The highest complex species which needs to be considered to explain the data is the MX_3^- ion. This does not necessarily rule out the existence of others nor prove absolutely the existence of MX^+, MX_2 and MX_3^-. Exceedingly accurate data are required to settle this as an absolute and unique answer because of the numbers of adjustable parameters involved in such a solution. The values for stability constants of the various complex ions shown in Table IV were determined by the graphical method of obtaining successive intercepts.[9] The estimated probable errors in the values for MX^+, MX_2 and MX_3^- are 20, 50 and 100%, respectively.

The effect of halides on the solubility of lead chromate and cadmium chromate in molten alkali nitrates is good evidence for the formation of stable complexes of the type MX_n^{2-n} where n is one, two and three. The data show that the cadmium ion forms slightly more stable complex ions with chloride and bromide than does lead. It is evident that the trend is toward a decrease in stability

(9) I. Leden, *Z. physik. Chem.*, **A188**, 160 (1941).

TABLE IV

STABILITY CONSTANTS[a] FOR METAL-HALIDE COMPLEX IONS IN FUSED KNO_3-$NaNO_3$ EUTECTIC

Complex species	Stability constant 250°	275°	300°
$PbCl^+$	18	8	6
$PbCl_2$	2	3	3
$PbCl_3^-$	2	1	1
$PbBr^+$	18	13	11
$PbBr_2$	5	2	2
$PbBr_3^-$	1	1	2
CdX^+	20	..	24
CdX_2	5	..	5
CdX_3^-			

[a] Stability constant $= K_r = (MX_n^{2-n})/[(MX_{n-1}^{3-n})(X^-)]$ where X^- is either Cl^- or Br^-.

of the complex with an increase in temperature in the case of lead.

The slight difference in stability of the chloride and bromide complexes is interesting in view of the ten-fold difference in stability of the cadmium bromide and cadmium chloride species in molten sodium nitrate as observed by Van Artsdalen.[1]

On the basis of the nearly equal ionic radii of calcium (0.99 Å.) and cadmium (0.97 Å.) and of barium (1.35 Å.) and lead (1.21 Å.), forces other than purely electrostatic appear to be important. Van Artsdalen's basis for the argument that the bonds of the complex are more of the chemical type because the predominant species are the ones with two and four halide ions is not substantiated in this work. In view of the similarities between this solvent and water with respect to the stability of the metal halide complexes of lead and cadmium, one might expect some degree of association between these metal cations and the nitrate ion of the solvent.[10] Therefore, an interpretation of the data on the basis of stable complex ions of the type MX_n^{2-n} where n is one, two and three, does not indicate whether the complex is of the ionic type or of the chemical type since, among other things, the role of the solvent is not known.

(10) A. I. Biggs, N. H. Parton and R. A. Robinson, *J. Am. Chem. Soc.*, **77**, 5844 (1955), give a value of 0.67 for the stability constant of the $PbNO_3^+$ complex in aqueous solution.

HEATS OF FORMATION AND HYDRATION OF ANHYDROUS ALUMINUM CHLORIDE

BY JAMES P. COUGHLIN

Minerals Thermodynamics Experiment Station, Region II, Bureau of Mines, United States Department of the Interior, Berkeley 4, California

Received January 6, 1958

Heat of solution measurements of crystalline anhydrous aluminum chloride, aluminum chloride hexahydrate and aluminum were conducted at 303.15°K. in 4.360 *m* hydrochloric acid solution. Based upon these data, the following heats of formation from the elements at 298.15°K. were derived: $-168{,}570 \pm 200$ cal./mole for anhydrous aluminum chloride and $-643{,}600 \pm 210$ cal./mole for aluminum chloride hexahydrate. In addition, the heat of hydration of the anhydrous chloride to the hexahydrate at 298.15°K. was evaluated as $-65{,}130 \pm 80$ cal./mole.

Recent articles from this Laboratory dealt with the heats of formation of several aluminum compounds.[1,2] In continuation of this activity the present paper reports the heats of formation of anhydrous aluminum chloride and aluminum chloride hexahydrate. The previously accepted value of the heat of formation of the hexahydrate[3] is based upon work of Sabatier[4] in 1889, and that of the anhydrous compound was obtained indirectly by combining thermochemical values in the literature.

Materials.—The two samples of aluminum used in the measurements were in the form of thin lathe turnings of 99.995 and 99.998% pure metal as described in an earlier paper.[1]

Anhydrous aluminum chloride was prepared from the same high-purity metal by direct reaction with dry chlorine gas at 500–600° in an all-glass apparatus. The product was resublimed in a stream of dry chlorine gas at 280–300°, transferred to the sample bulbs in a closed system, and finally glass-sealed with minimum exposure to air. One bulb of sample was used for analysis. The bulb was broken under water in a calibrated, 2-l. volumetric flask. The resulting solution was diluted to the mark (account being taken of the volume of glass in the broken sample bulb) and aliquots were removed for analysis. Aluminum was determined by precipitation as hydroxide, followed by ignition to oxide, and chlorine by precipitation as silver chloride. The results were 20.28% aluminum and 79.62% chlorine, as compared with the theoretical 20.23 and 79.77%.

The aluminum chloride hexahydrate sample was reagent-grade quality. Analysis showed 11.18% aluminum and 44.09% chlorine, with 44.73% water by difference (theoretical: 11.17, 44.06 and 44.77%, respectively). An attempt was made to make up the slight water deficiency by sealing a sample in glass with the required amount of water and aging at several different oven temperatures; however, the added water was never absorbed uniformly, and so the substance was used without this treatment.

The hydrochloric acid solution (4.360 molal or $HCl \cdot 12.731H_2O$) was prepared by dilution of reagent-grade acid in the manner previously described.[1]

Method and Results.—The apparatus for the heat of solution measurements is that described by Southard,[5] with minor improvements reported earlier by the author.[6] The results are expressed in defined calories (1 cal. = 4.1840 abs. joules), and all molecular weights are based upon the 1954 - 1955 Report on Atomic Weights.[7] All sample weights were corrected to vacuum.

In all measurements, 1936.2 g. of 4.360 *m* hydro-

(1) J. P. Coughlin, *J. Am. Chem. Soc.*, **78**, 5479 (1956).

(2) J. P. Coughlin, *ibid.*, **79**, 2397 (1957).

(3) F. D. Rossini, D. D. Wagman, W. H. Evans, S. Levine and I. Jaffe, Natl. Bur. Standards Circular 500, 1952.

(4) P. Sabatier, *Bull. soc. chim., France*, **1**, 88 (1889).

(5) J. C. Southard, *Ind. Eng. Chem.*, **32**, 442 (1940).

(6) J. P. Coughlin, *J. Am. Chem. Soc.*, **77**, 868 (1955).

(7) E. Wichers, *ibid.* **78**, 3235 (1956).

TABLE I

HEAT OF FORMATION OF ANHYDROUS ALUMINUM CHLORIDE
(Mol. wt. = 133.35)

	Reaction	$\Delta H_{303.15}$, cal.
(1)	$Al(c) + 3H^+(sol) = Al^{+++}(sol) + 3/2H_2(g)$	$-127,050 \pm 120$
(2)	$3(HCl\cdot 12.731H_2O)(l) = 3H^+(sol) + 3Cl^-(sol) + 38.193H_2O(sol)$	0 ± 10
(3)	$AlCl_3(c) = Al^{+++}(sol) + 3Cl^-(sol)$	$-72,510 \pm 50$
(4)	$38.193H_2O(l) = 38.193H_2O(sol)$	$-3,050 \pm 20$
(5)	$Al(c) + 3(HCl\cdot 12.731H_2O)(l) = AlCl_3(c) + 38.193H_2O(l) + 3/2H_2(g)$	$-51,490 \pm 140$

At 298.15°K., $\Delta H_5 = -51,870 \pm 140$ cal.

chloric acid was employed as the solution medium. The amounts of samples used were 0.5296 g. of aluminum (0.02 gram-atom) and corresponding quantities of all other materials, as they appear below in reactions 5 and 11.

It was not necessary to determine ΔC_p of the reactions under study, as all heat measurements were made within 0.05 of 30° and required no correction. A small correction was involved in bringing the electrical calibrations to exactly 30°. This amounted to −20 cal./mole in the case of anhydrous aluminum chloride and was negligibly small for the other substances. (The corrections applied to the measurements on aluminum metal, reaction 1, were discussed earlier.[1])

Anhydrous Aluminum Chloride.—Table I gives the skeleton equations for the reactions measured to obtain the heat of formation of anhydrous aluminum chloride. Reactions 1 and 2 were measured consecutively in the same acid solution. Reactions 3 and 4 were measured consecutively in a fresh portion of the acid. Thus the final solution from reactions 1 and 2 is identical with that from reactions 3 and 4; consequently, $\Delta H_5 = \Delta H_1 + \Delta H_2 - \Delta H_3 - \Delta H_4$.

The time required for completion of the reactions in Table I (and also those in Table III) was less than 15 minutes, except for the reaction of aluminum metal with the acid which required 36 to 82 minutes, depending upon the thickness of the lathe cuttings.

Reaction 1 was discussed in an earlier paper.[1] The molal heat of solution of aluminum in 4.360 *m* hydrochloric acid (including all corrections) is −127,050 ± 120 cal. at 303.15°K. A single measurement was made of reaction 2, the heat of mixing of approximately 15 ml. of the original hydrochloric acid with the final solution of reaction 1, merely to confirm that the heat is virtually zero.

The data for reaction 3 appear in Table II. In all, ten glass bulbs were filled with sample and sealed. Three were unsuitable for the measurements, because they were found to contain amounts of sample over 1 g. in excess of the desired quantity (2.6670 g.); two other bulbs were lost in apparatus failures. Within experimental error, there is no trend in the results in Table II because of sample size or filling order of the bulbs.

Three measurements of reaction 4 (−79.9, −79.9 and −79.6 cal./mole) were combined with three measurements of subsequent reaction 10 (−80.5, −79.0 and −79.6 cal./mole) to give an over-all average of −79.8 cal./mole of water for both reactions.

The heat of reaction 5 was corrected to 298.15°K., using heat capacity data of Kelley[8,9] and Rossini.[10] (The apparent molal heat capacity of hydrogen chloride in 4.360 *m* solution was taken as −17.3 cal./deg., by extrapolating Rossini's data.)

TABLE II

HEAT OF SOLUTION OF ANHYDROUS ALUMINUM CHLORIDE

Sample wt., g.	Filling order	$\Delta H_{303.15}$, cal./mole
2.2057	6	−72,440
2.4019	10	−72,510
2.5061	3	−72,520
2.6213	4	−72,570
2.8957	5	−72,510
	Mean	−72,510 ± 50

The heat of formation from the elements

$$Al(c) + 3/2Cl_2(g) = AlCl_3(c)$$
$$\Delta H_{298.15} = -168,570 \pm 200 \text{ cal./mole} \quad (6)$$

was obtained by combining the heat of reaction 5 with the heat of formation of $HCl\cdot 12.731H_2O$ from NBS Circular 500.[3]

Aluminum Chloride Hexahydrate.—The reactions measured to obtain the heat of formation of aluminum chloride hexahydrate are shown in Table III. The sequence of reactions followed the pattern outlined for the anhydrous compound, and exact stoichiometry again was maintained so that $\Delta H_{11} = \Delta H_7 + \Delta H_8 - \Delta H_9 - \Delta H_{10}$.

Reactions 7, 8 and 10 are discussed above as reactions 1, 2 and 4. The data for obtaining the heat of reaction 9 are in Table IV. Four measurements were made of the original material (the composition of which was taken as $AlCl_3\cdot 5.99H_2O$) and four of material from which small amounts of water had been removed. The results were plotted against per cent. water and extrapolated to the theoretical water content. The equation

$$\Delta H_{303.15} = -143.45 + 2.5 \times (\%\ H_2O) \quad (12)$$

fits the data with a precision uncertainty of ±0.2% and yields −31.52 ± 0.07 cal./g. or −7,610 ± 17 cal./mole for aluminum chloride hexahydrate. The uncertainty is increased to ±40 cal./mole to allow for ±0.05% possible error in the determinations of water content.

The heat of reaction 11 was corrected to 298.15°K., using data of Kelley[8,9] and Rossini.[10] Employing literature values[3] of the heat of formation of water and hydrochloric acid, the following reaction heats are obtained

(8) K. K. Kelley, U. S. Bur. Mines Bull. 477, 1950.

(9) K. K. Kelley, personal communication. The heat capacities of anhydrous aluminum chloride and aluminum chloride hexahydrate were estimated as 19.8 and 77.0 cal./deg. mole.

(10) F. D. Rossini, *J. Research Natl. Bur. Standards*, 4, 313 (1930).

TABLE III

HEAT OF FORMATION OF ALUMINUM CHLORIDE HEXAHYDRATE

(Mol. wt. = 241.45)

	Reaction	$\Delta H_{303.15}$, cal.
(7)	$Al(c) + 3H^+(sol) = Al^{+++}(sol) + 3/2H_2(g)$	$-127,050 \pm 120$
(8)	$3(HCl\cdot 12.731H_2O)(l) = 3H^+(sol) + 3Cl^-(sol) + 38.193H_2O(sol)$	0 ± 10
(9)	$AlCl_3\cdot 6H_2O(c) = Al^{+++}(sol) + 3Cl^-(sol) + 6H_2O(sol)$	$-7,610 \pm 40$
(10)	$32.193H_2(l) = 32.193H_2O(sol)$	$-2,570 \pm 20$
(11)	$Al(c) + 3(HCl\cdot 12.731H_2O)(l) = AlCl_3\cdot 6H_2O(c) + 32.193H_2O(l) + 3/2H_2(g)$	$-116,870 \pm 130$

At 298.15°K., $\Delta H_{11} = -117,000 \pm 130$ cal.

TABLE IV

HEAT OF SOLUTION OF HYDRATED ALUMINUM CHLORIDE

H_2O, %	$\Delta H_{303.15}$, cal./g.	$\Delta H_{303.15} - 2.5(\%\ H_2O)$
44.73	−31.63	−143.45
44.73	−31.64	−143.46
44.73	−31.59	−143.41
44.73	−31.67	−143.49
44.71	−31.77	−143.55
44.64	−31.97	−143.57
44.62	−31.74	−143.29
44.61	−31.89	−143.41
	Mean	-143.45 ± 0.07

$$Al(c) + 3/2Cl_2(g) + 6H_2O(l) = AlCl_3\cdot 6H_2O(c) \quad (13)$$

$\Delta H_{298.15} = -233,700 \pm 200$ cal.,

$$Al(c) + 3/2Cl_2(g) + 6H_2(g) + 3O_2(g) = AlCl_3\cdot 6H_2O(c) \quad (14)$$

$\Delta H_{298.15} = -643,600 \pm 210$ cal.

The heat of reaction 15 was evaluated at 303.15°K. by combining the data for reactions 3, 4, 9 and 10. Correction to 298.15°K. was made, using an estimated $\Delta C_p = -51$ cal./deg.

$$AlCl_3(c) + 6H_2O(l) = AlCl_3\cdot 6H_2O(c) \quad (15)$$

$\Delta H_{303.15} = -65,380 \pm 80$ cal.

$\Delta H_{298.15} = -65,130 \pm 80$ cal.

Discussion

Previously accepted values[3] of the heats of reactions 6 and 15 (the heats of formation and hydration of anhydrous aluminum chloride) are −166,200 and −65,000 cal., respectively. The present work agrees with the value for the hydration reaction but differs on the heat of formation of the anhydrous compound by 2370 cal. From examination of the bibliography of NBS Circular 500,[3] it appears that the "best" values of the heats of solution of aluminum metal, the anhydrous chloride and the hexahydrated chloride of necessity were taken from the work of at least three different investigators. This involves possible errors due to variations in sample purity, solution concentration, temperature of measurement, and variation in systematic errors in apparatus, all of which are avoided in the new values presented here.

THERMAL DIFFUSION IN DENSE GASES[1]

BY J. E. WALTHER AND H. G. DRICKAMER

Department of Chemistry and Chemical Engineering, University of Illinois, Urbana, Illinois

Received November 4, 1957

Thermal diffusion measurements have been made on a series of binary mixtures of gases to 500 atm. (Several systems were studied to 1000 atm.). Mixtures far from the critical temperature showed only small pressure effects. For systems where one component is near its critical temperature, a large negative value of the thermal diffusion ratio α is obtained. Neither present kinetic theories, nor the thermodynamics of irreversible processes offer a satisfactory explanation, but it is possible to get some insight into the phenomenon from each theory.

There have been numerous studies of thermal diffusion in gases at or near atmospheric pressure[2]; the theory is well developed and gives good agreement with experiment. There also have been rather frequent investigations of the phenomenon in liquids and it can be described with reasonable qualitative accuracy[3] in terms of activated motion. There are only a very few investigations in the dense gas region, and these have been over a very limited pressure range,[4] or have used the thermal diffusion column.[5] The theory of the column is at best only semi-quantitative and, in dense gases, particularly near the critical point, its applicability is very doubtful.

Therefore thermal diffusion measurements have been made, in a single stage cell, on a series of binary gas mixtures. In most cases the pressure range was to 500 atm., although a few data were obtained to 1000 atm. In all cases the gases were pure grade commercial products used as purchased.

The defining equation for the thermal diffusion ratio in a binary system is

$$\vec{J}_1 = -\rho D\,(\overrightarrow{\text{grad}\ X_1} - \alpha X_1(1 - X_1)\,\overrightarrow{\text{grad ln}\ T}) \quad (1)$$

(1) This work was supported in part by the A.E.C.

(2) J. O. Hirschfelder, C. F. Curtiss and R. B. Bird, "Molecular Theory of Liquids and Gases," John Wiley and Sons, Inc., New York, N. Y., 1954, p. 582 ff.

(3) L. J. Tichacek, W. S. Kmak and H. G. Drickamer, THIS JOURNAL, **60**, 660 (1956); E. L. Dougherty, Jr., and H. G. Drickamer, *ibid.*, **59**, 443 (1955); *J. Chem. Phys.*, **23**, 295 (1955).

(4) E. W. Becker, *Naturforschung*, **5a**, 457 (1950).

(5) N. C. Pierce, R. B. Duffield and H. G. Drickamer, *J. Chem. Phys.*, **18**, 950 (1950); E. B. Giller, R. B. Duffield and H. G. Drickamer, *ibid.*, **18**, 1027 (1950); F. E. Caskey and H. G. Drickamer, *ibid.*, **21**, 153 (1953).

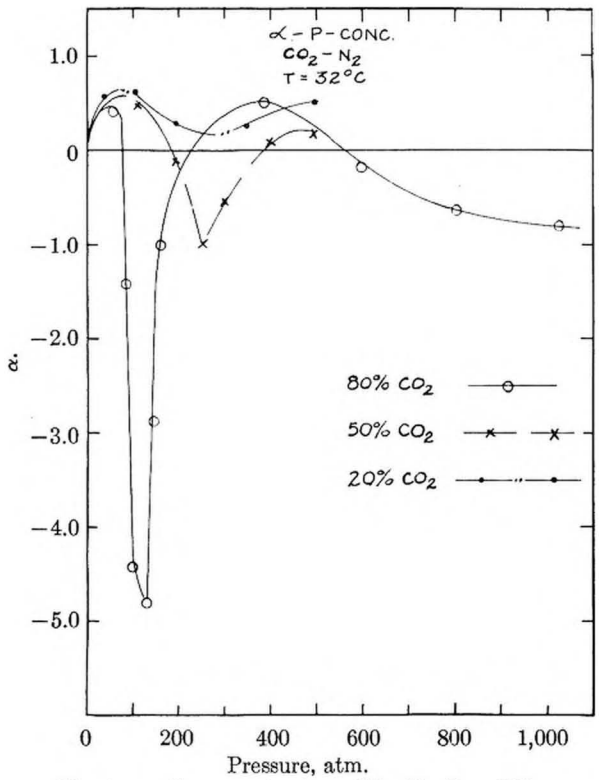

Fig. 1.—α–P–concentration: CO_2–N_2, T = 32°.

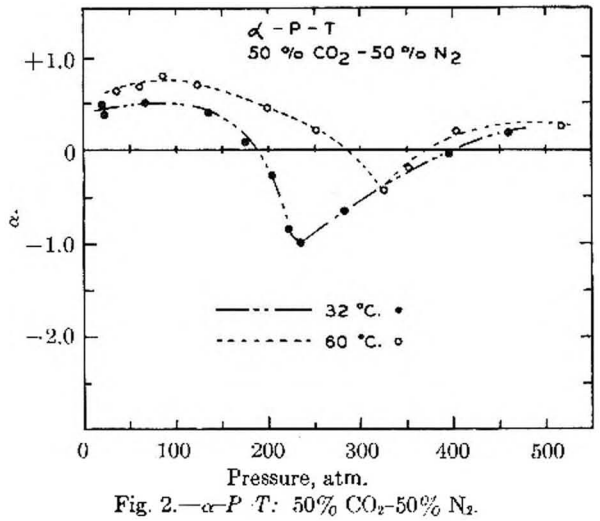

Fig. 2.—α–P T: 50% CO_2–50% N_2.

where

$\vec{J}_1$ = flux of component 1
ρ = density
D = diffusion coefficient
X_i = mole fraction component i
T = absolute temperature
α = thermal diffusion ratio

The steady state solution is

$$\ln\left(\frac{X_1}{1-X_1}\right)_C\left(\frac{1-X_1}{X_1}\right)_H = \alpha \ln\frac{T_H}{T_C} \qquad (2)$$

from which α can be calculated if the temperature difference and concentration difference across an appropriate membrane are known for the steady state.

Equipment and Procedure.—The gas mixtures were made up in a large U tube consisting of two high pressure cylinders connected by high pressure tubing. Oil transmitted pressure to mercury which transmitted pressure to the gases. Mixing was obtained by raising and lowering pressure for several cycles and by letting the mixture stand 24–72 hours.

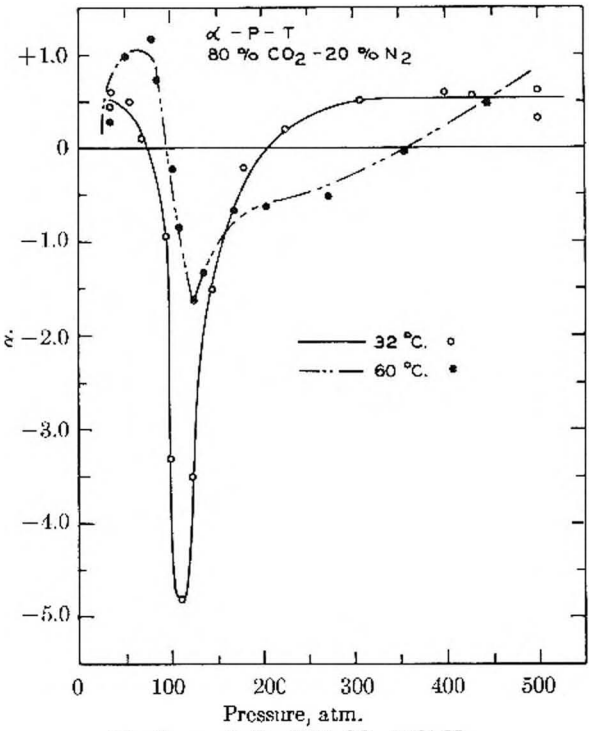

Fig. 3.—α–P–T: 80% CO_2–20% N_2.

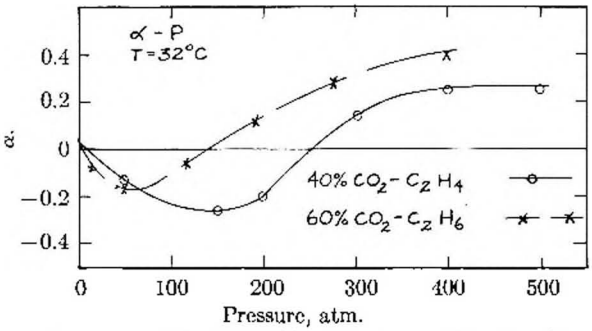

Fig. 4.—α–P: 40% CO_2–60% C_2H_4; T = 32°, 60% CO_2–40% C_2H_6.

The thermal diffusion cell consisted of a large hot chamber and a much smaller cold chamber, separated by a layer of porous glass. Convection from the heater provided mixing and uniform temperature in the lower chamber. The upper chamber was filled with high porosity bronze which provided a uniform temperature. The chamber was designed so that diffusion provided mixing rapidly compared with the rate of transport across the porous glass. Thermocouples were inserted on each side of the porous glass. The lower couple was protected from radiation by a thin porous bronze disc. The temperature difference averaged 8°. The upper chamber could be sampled by means of a valve built in the head. The lower chamber could be sampled through a line which also served as entry for the gas. The lines could be evacuated up to the bomb. In practice, however, the lower chamber never deviated significantly from the feed. The analysis was performed by use of a thermal conductivity bridge. For each mixture the bridge was calibrated from mixtures of known composition. The analysis could be performed either by measuring both lower and upper samples against a known standard, or by measuring the upper sample against the lower. Where both methods were employed, no difference in the measured separation was noted. It was possible to estimate relaxation times from measured or estimated diffusion coefficients. The duration of runs

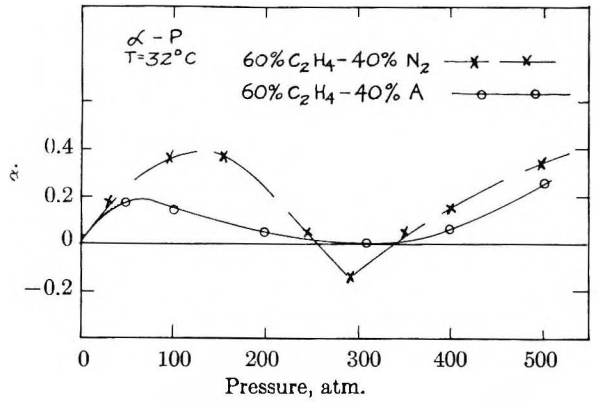

Fig. 5.—α–P: 60% C_2H_4–40% N_2; T = 32°, 60% C_2H_4–40% A.

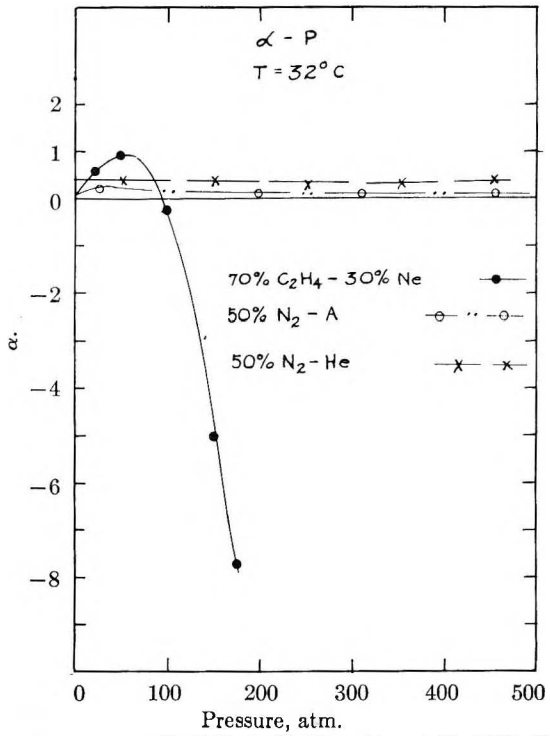

Fig. 6.—α–P: 70% C_2H_4–30% Ne; T = 32°, 50% N_2–50% A; 50% N_2–50% He.

was at least 5–6 relaxation times. In all cases in doubt runs were made at several time lengths to ensure steady-state conditions.

Results

The results are shown in Figs. 1–9. The sign of α as originally assigned is arbitrary, as long as one adheres to a consistent convention. Here α is considered positive when the species with the larger molecular weight concentrated in the cold chamber. For systems where the average temperature of operation was far above the critical temperature of either component (and presumably that of the mixture) the effect of pressure on α is not large. For systems were T_{av} was reasonably near T_C for one of the components, α usually started at a small positive value, became large and negative, passed through a minimum (apparently near the critical density of the mixture) and then increased in value. It usually became positive again within the pressure range studied. For the mixture 80% CO_2–

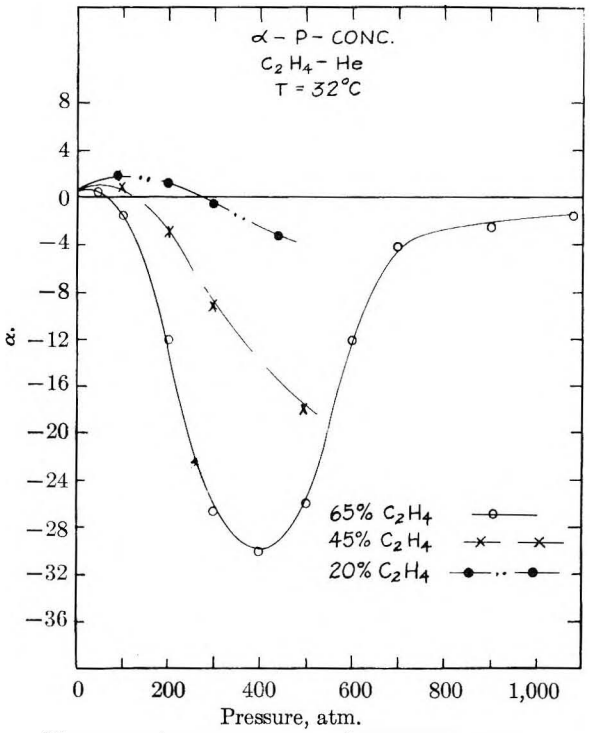

Fig. 7.—α–P–concentration: C_2H_4–He, T = 32°.

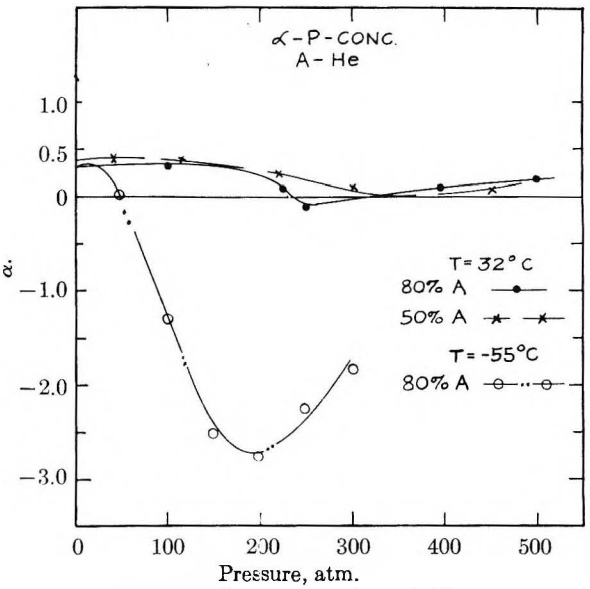

Fig. 8.—α–P–concentration: A–He.

20% N_2 α became negative again at the highest pressures. The minimum in α was larger, the larger the difference in the critical temperatures of the two components. The results are qualitatively consistent with previous column data[5] on other systems.

Discussion

For dilute gases of simple molecules, the transport behavior can be characterized by two parameters, using the Lennard-Jones model, the maximum attractive energy of interaction ϵ, and the collision diameter r_0. These are listed for the pure components as obtained from viscosity and

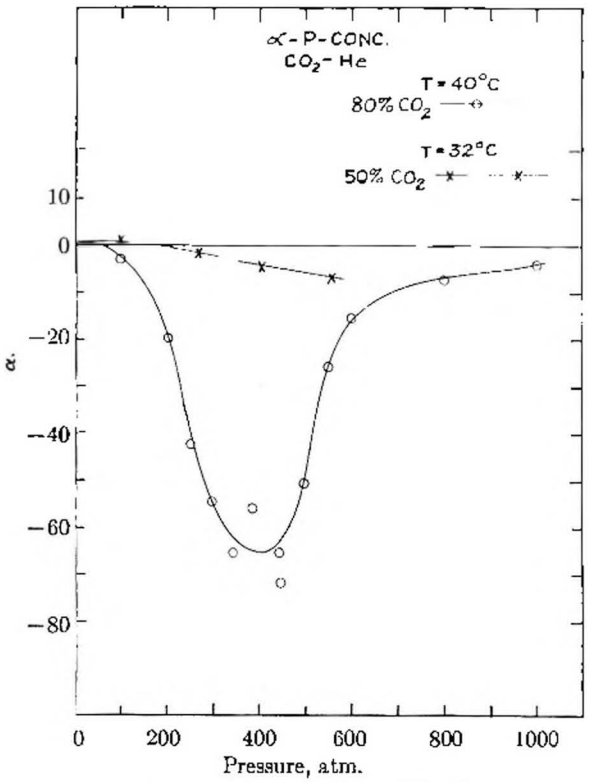

Fig. 9.— α–P–concentration: CO_2–He.

p–v–t data[6] in Table I. It is usually assumed for unlike molecules that $r_{0_{12}} = 1/2\ (r_{0_1} + r_{0_2})$ and $\epsilon_{12} = (\epsilon_1\epsilon_2)^{1/2}$.

TABLE I

MOLECULAR PROPERTIES

Substance	ϵ/k (°K.)[a] A	ϵ/k (°K.)[a] B	r_0 (Å.)[a] A	r_0 (Å.)[a] B	Mol. wt.
He	10 22	10.2	2.576	2.56	4.003
Ne	35.7	34.9	2.789	2.78	20.18
Ar	124.0	122.0	3.418	3.40	39.94
N_2	91.5	95.0	3.681	3.698	28.02
CO_2	13.0	205.0	3.897	4.07	44.01
C_2H_4	205.0	199.2	4.232	4.52	28.05
C_2H_6	230.0	243.0	4.418	3.95	30.07

[a] A—from viscosity data; B—from second virial coefficients.

Thorne[7] has applied Enskog's dense gas theory to thermal diffusion, obtaining a complex result which can be written

$$\alpha = (C - 1)S \qquad (3)$$

S is a complex function which contains parameters depending on density. It changes very slowly with density (only about 10% from one atmosphere to the critical density). $(C - 1)$ can be expressed in terms of collision cross section integrals averaged so as to weight more or less heavily collisions at high relative kinetic energy[8]

$$C - 1 = \frac{2W_{12}^{(1)}{}_{(2)} - 5W_{12}^{(1)}{}_{(1)}}{5W_{12}^{(1)}{}_{(1)}} \qquad (4)$$

$(C - 1)$ is a function of ϵ and T but not of density in this form of theory. The factor $(C - 1)$ appears also in the theory of dilute gases. The Lennard-Jones model predicts negative values of α below about $0.7T_c$ at low densities. This prediction is confirmed by experiment. If one ignores for the moment the fact that the dense gas theory was developed only for solid elastic spheres, it is of interest to note that one could predict a negative α at higher densities if ϵ_{12} were larger than ϵ_1, or ϵ_2. More generally, an increase in $W^{(1)}{}_{(1)}$ relative to $W^{(1)}{}_{(2)}$ (*i.e.*, an increase in the importance of low relative kinetic energy collisions relative to high relative kinetic energy collisions, would give a negative α). Since one approaches the phase envelope by increasing pressure as well as by lowering temperature it is qualitatively consistent with theory that α would become negative particularly near the critical density. It is also reasonable that low relative kinetic energy collisions be emphasized near saturation. There appears at present to be no way to formulate these generalizations quantitatively and in particular, no hint in the available theory of the very *large* negative values of α near the critical density.

A second, quite different, approach to thermal diffusion is supplied by the thermodynamics of irreversible processes. From this theory one obtains for $\alpha^{(2)}$

$$\alpha = \frac{\bar{V}_1\bar{V}_2}{\bar{V}} \frac{1}{X_1 \dfrac{\partial \mu_1}{\partial X_1}} \left[\frac{Q_2^*}{\bar{V}_2} - \frac{Q_1^*}{\bar{V}_1}\right] \qquad (5)$$

where

$\bar{V}_i$ = partial molar volume of component i
μ_i = chemical potential of component i
X_i = mole fraction of component i
Q_i^* = net heat of transport of component i. This quantity is discussed in detail in the references on liquid thermal diffusion[5]

The lack of p–v–t data for mixtures and the complex nature of the net heat of transport make it difficult to extract quantitative results from equation 5, but some interesting qualitative considerations are available. $X_1(\partial\ \mu_1/\partial\ X_1) = RT$ for an ideal gas mixture. From a few data for mixtures $X_1\ (\partial\mu_1/\partial X_1) = 0.3RT$ near the critical density and some 20–30° above T_c. One would need a value of $0.005RT$ to account for the minimum value of α for CO_2–He by this means alone. Available data indicate that the factor $\bar{V}_1\bar{V}_2/\bar{V}$ cannot contribute significantly to the change of α with pressure. The subscript 2 refers to the component with the larger value of ϵ, hereafter called the "heavier" component, although it need not always have the higher molecular weight. It seems then, that the heavier component must have a large negative net heat of transport Q_2^*. Q_2^* is the total energy transported isothermally with one mole of component two, above the average (thermodynamic) value of the partial molar enthalpy of component two. It is generally assumed, based on a variety of evidence, that molecules tend to form clusters, on nuclei of the condensed phase, near saturation. The clustering process is greatly intensified in the critical region. The clusters presumably have less energy per molecule than single molecules.

(6) Ref. 2, pp. 1110–1111.

(7) S. Chapman and T. G. Cowling, "Mathematical Theory of Non-Uniform Gases," Cambridge University Press, 1939, pp. 292–294.

(8) Ref. 2, p. 541.

If the average entity of component two moving from the cold to the hot chamber were a cluster of a size larger than the average cluster in the cold chamber, and if this cluster disintegrated at the hot wall and returned (in the steady state) as individual molecules, this would result in a negative net heat of transport. There is certainly no *a priori* reason for assuming that the moving entity is a cluster of larger than average size, and it seems inconsistent with a simple kinetic picture. One could assume that there is significant clustering in each chamber but that the entities leaving the hot chamber were smaller relative to the average size at that temperature than those leaving the cold chamber. Again, there is no independent supporting evidence, nor is it intuitively reasonable.

The possibility that the "lighter" component (one) might have a large positive heat of transport seems rather unlikely, particularly for helium.

Neither the present kinetic theory nor the thermodynamics of irreversible processes gives a satisfactory explanation of thermal diffusion in dense gases where motion is neither completely "collisional" nor completely "activated." These data provide a significant and important test of any more refined theory of molecular motion in this region.

The authors wish to acknowledge most gratefully the work of R. E. Harder who developed and erected the equipment as his M.S. thesis. J. E. Walther wishes to acknowledge assistance from the Standard Oil Company (Ohio) Fellowship.

THE INTENSITY OF THE S–H STRETCHING FUNDAMENTAL; DIMERIZATION OF MERCAPTANS[1]

By Robert A. Spurr[2] and H. Franklin Byers

Contribution from the Department of Chemistry, University of Maryland, College Park, Md.

Received November 4, 1957

Integrated absorption coefficients were determined for the 3.8–3.9 μ band (the S–H stretching fundamental) of six mercaptans at concentrations ranging from 0.1 to 7.5 M in carbon tetrachloride. This band is formed by two components at about 2530 and 2560 cm.$^{-1}$, which are attributed to monomer and dimer forms of the mercaptans, respectively. The variation with concentration of the total integrated absorption coefficient can be accounted for on the basis of a monomer–dimer equilibrium. For all compounds studied, the integrated absorption coefficient for the monomer is about 0.03 intensity unit; that of the dimer is about 0.3 unit for the aliphatic mercaptans and 0.7 unit for thiophenol. The equilibrium constant at 24° for the reaction $(RSH)_2 \rightleftarrows 2RSH$ is about 50.

Introduction

The intensity of the S–H stretching fundamental apparently has not been measured previously. Bell[3] pointed out that the 3.8–3.9 μ band is peculiar to mercaptans, and Ellis and others[4-7] established it as the S–H stretching vibration.

Hydrogen bonding of the S–H . . . S type has generally been considered unlikely. Pauling[8] concluded on the basis of physical properties that hydrogen sulfide does not associate. Molecular weights determined by the freezing point method[9] do not reveal any tendency to polymerization. Gordy and Stanford[10] scanned the S–H band using a 0.1 M solution of thiophenol and of pure thiophenol, failed to observe a shift of the peak to a lower frequency at the higher concentration, and concluded that thiophenol is not associated.

Copley, Marvel and Ginsberg[11] found that thiophenol associates with nitrogen- and oxygen-containing solvents forming S–H . . . N and S–H . . .O hydrogen bonds. They measured heats of mixing of thiophenol with the various solvents. Gordy and Stanford[10] confirmed the S–H . . . N hydrogen bond spectroscopically by noticing that the S–H peak of thiophenol shifts to slightly lower frequencies when the thiophenol is dissolved in solvents of the amine type.

On the basis of boiling point and melting point data of thioamides and other compounds containing sulfur and nitrogen, Hopkins, Burrows and Hunter[12] claimed to have evidence for the N–H . . . S hydrogen bond. This claim may be doubted, for, although their compounds are undoubtedly associated, the association more probably takes place through the N–H . . . N hydrogen bond, the possibility of which the authors apparently overlooked.

Experimental

The model 12-C Perkin–Elmer infrared spectrophotometer was equipped with double-pass optics and a lithium fluoride prism. Slits were set at 0.2 mm., corresponding to a spectral slit width of 3.6 cm.$^{-1}$ at 2580 cm.$^{-1}$. Sodium chloride absorption cells varied in length from 0.01 to 1.5 cm. "Spectral-grade" carbon tetrachloride was the solvent. The mercaptans were obtained commercially and were purified by fractional distillation. Temperature was maintained at 24 ± 1°.

Integrated absorption coefficients A are defined by the equation

(1) Presented at the Pittsburgh Conference on Analytical and Applied Spectroscopy, March 3, 1955.

(2) Research Laboratories, Hughes Aircraft Co., Culver City, Calif.

(3) F. K. Bell, *Chem. Ber.*, **60B**, 1749 (1927); **61B**, 1918 (1928).

(4) J. W. Ellis, *J. Am. Chem. Soc.*, **50**, 2113 (1928).

(5) D. Williams, *Phys. Rev.*, **54**, 504 (1938).

(6) H. W. Thompson and N. P. Skerrett, *Trans. Faraday Soc.*, **37**, 81 (1941).

(7) I. F. Trotter and H. W. Thompson, *J. Chem. Soc.*, 481 (1946).

(8) L. Pauling, "The Nature of the Chemical Bond," Cornell Univ. Press, Ithaca, N. Y., 1940, p. 290.

(9) E. N. Lassettre, *Chem. Revs.*, **20**, 259 (1939).

(10) W. Gordy and S. C. Stanford, *J. Am. Chem. Soc.*, **62**, 497 (1940).

(11) M. J. Copley, C. S. Marvel and E. H. Ginsberg, *ibid.*, **61**, 3161 (1939).

(12) G. Hopkins and L. Hunter, *J. Chem. Soc.*, 638 (1942); A. A. Burrows and L. Hunter, *ibid.*, 4118 (1952).

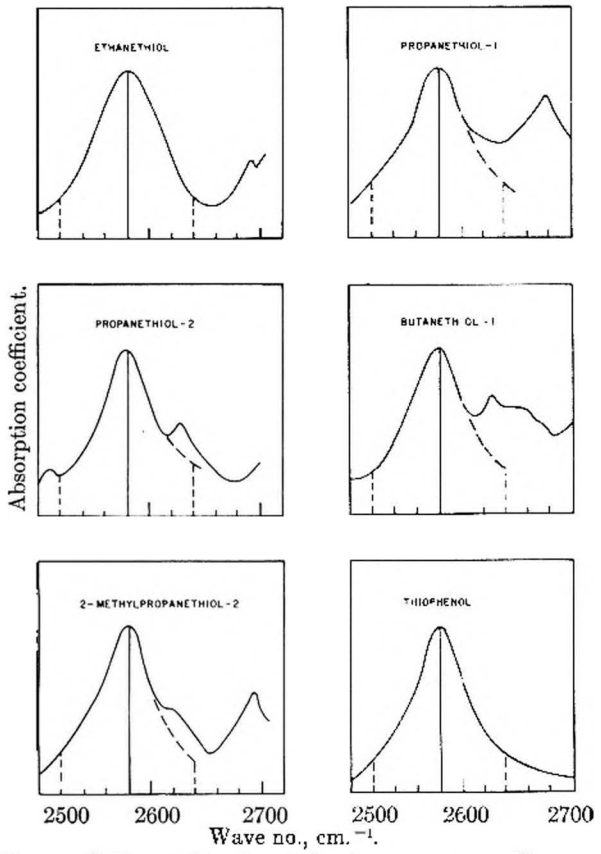

Fig. 1.—S–H stretching bands for six mercaptans. Concentration about 0.1 *M* in carbon tetrachloride.

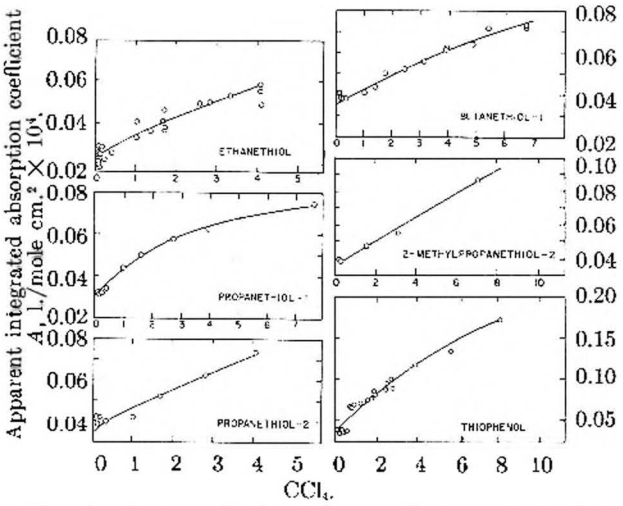

Fig. 2.—Integrated absorption coefficients of the S–H stretching band at 3.8-3.9 μ as a function of mercaptan concentration.

$$A = \int_{\text{band}} \alpha \, d\nu = \frac{1}{lC} \int_{\text{band}} \ln (I_0/I) d\nu \quad (1)$$

where α is the absorption coefficient, ν the wave number, l the cell thickness, C the apparent molarity based on monomer molecular weight and I_0 and I are the intensities of the incident and emergent beams, respectively. The units of A, called "intensity units," are (liters/mole cm.²) × 10^4.

Estimation of the integrated absorption coefficients was complicated by two effects: (a) the S–H stretching absorption is made up of two strongly overlapping bands, and (b) neighboring bands due to other vibrations interfere to a greater or less extent. After a number of methods had been tried, the technique selected as giving the most reproducible

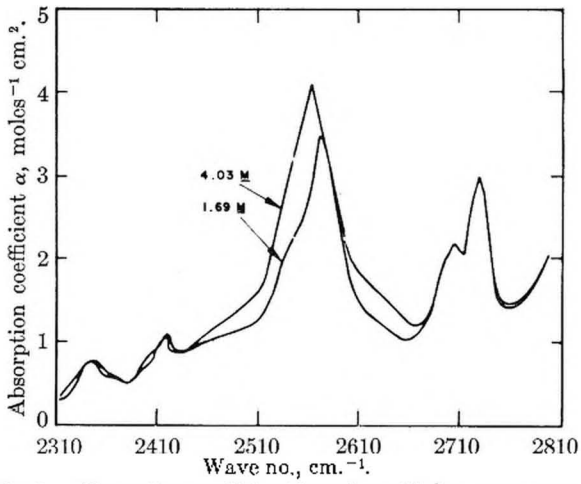

Fig. 3.—Absorption coefficient for ethanethiol *vs.* wave number for two concentrations in carbon tetrachloride.

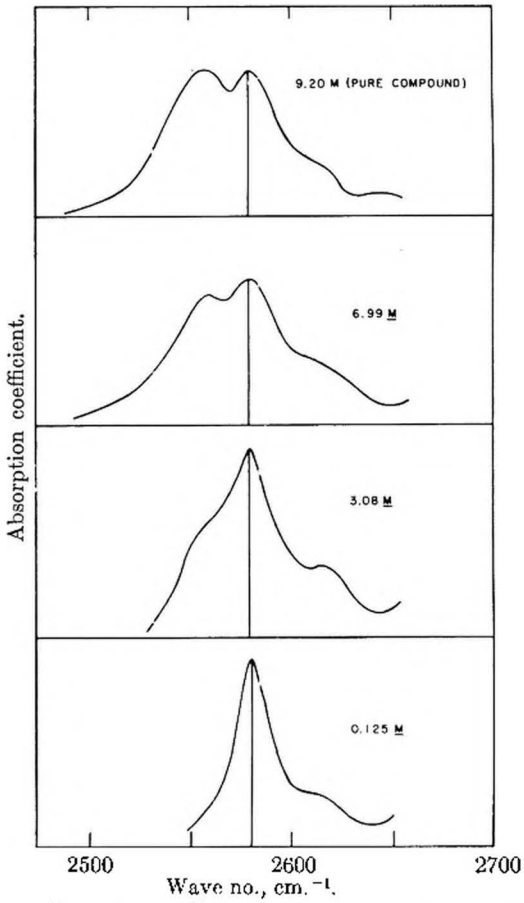

Fig. 4.—Absorption coefficient *vs.* wave number for solutions of 2-methylpropanethiol-2 in carbon tetrachloride.

results was to integrate α *versus* wave number out to 60 cm.$^{-1}$ on each side of the peak maxima. Wing corrections were then added, independently for each wing, based on Ramsey's equation[13]

$$\% \text{ correction} = \frac{\pi/2 - \tan^{-1} \frac{\nu - \nu_0}{b}}{\tan^{-1} \frac{\nu - \nu_0}{b}} \times 100 \quad (2)$$

where ν_0 is the wave number at the peak maximum, ν is the wave number at the point where graphical integration is ter-

(13) D. A. Ramsay, *J. Am. Chem. Soc.*, **74**, 72 (1952).

minated ($\nu - \nu_0 = 60$ cm.$^{-1}$ in this case), and b is the half-intensity band width, calculated for each side of the band individually. Separate corrections for the two wings are necessary because the band is in many cases unsymmetrical. Where interference from a neighboring band arose, it was corrected for by a graphical extrapolation. Fortunately such interferences appear mainly at the high-frequency side of the maximum, while the phenomenon of special interest, the appearance with increasing concentration of a new peak due to the dimer, occurs on the low-frequency side of the maximum.

Results

The 3.8–3.9 μ bands for six mercaptans at concentrations of about 0.1 M in carbon tetrachloride are shown in Fig. 1. The curves for ethanethiol and thiophenol are symmetrical; it may be assumed that those for the other mercaptans would also be symmetrical if it were not for the interference of C–H bands on the high-frequency side. The effect of these interfering bands is therefore subtracted away as shown by the dashed lines. The resulting curves are approximately of the same size and shape for all the mercaptans, corresponding to the fact that about the same value of the monomer integrated intensity coefficient was found for all. Figure 2 shows that the integrated coefficients increase for all the mercaptans with increasing apparent concentration. For the case of 2-methylpropanethiol-2 each point plotted is the average of three determinations. Examination of the complete spectrum of a mercaptan in the range 2–15 μ reveals that the 3.8–3.9 μ band is the only one whose integrated coefficient changes with concentration. An indication of this fact is given in Fig. 3. Figure 4 shows for one compound how the plot of absorption coefficient *versus* wave number varies with increasing concentration. The broadening on the low-frequency side of the band and the associated increase of integrated absorption coefficient are attributed by us to the appearance of a band associated with the mercaptan dimer.

Extrapolation of the plots of A *versus* C in Fig. 2 yielded the integrated absorption coefficients for the monomers (Table I). These were in all cases approximately 0.03 intensity unit, indicating weak absorption.

TABLE I

INTEGRATED ABSORPTION COEFFICIENTS

Compound	A_M	A_D	A pure compd.	Dimer dissociation constant, moles/l. K
	(l./mole cm.^{2}) $\times 10^4$			
Ethanethiol	0.023	0.30	0.105	47
Propanethiol-1	.033	.16	.098	19
Propanethiol-2	.033	.34	...	55
Butanethiol-1	.035	.28	.097	61
2-Methylpropanethiol-2	.036	.28	.091	61
Thiophenol	.038	.70	.173	53

Monomer–Dimer Theory

It is now of interest to obtain A values for the dimer species and to estimate the equilibrium constant of the dimerization reaction. The apparent concentration C is given by the expression

$$C = M + D \qquad (3)$$

where M is the concentration of monomer-located S–H groups and D is the concentration of dimer-located S–H groups. The concentration of dimer molecules is thus $^1/_2 D$. The apparent integrated coefficient A is given by the equation

$$AC = A_M M + A_D D \qquad (4)$$

where A_M is the integrated absorption coefficient characteristic of monomer-located S–H groups, and A_D is the corresponding quantity for dimer-located groups. For the equilibrium reaction

$$(RSH)_2 \rightleftharpoons 2RSH \qquad (5)$$

the equilibrium expression may be written

$$K = M^2/^1/_2 D = (C - D)^2/^1/_2 D \cong (C^2 - 2CD)/^1/_2 D \qquad (6)$$

In the second and third equalities use has been made of (3) and D^2 has been neglected in comparison with C^2. This approximation is justified by the value of the equilibrium constant obtained, which indicates that the dimer concentration is comparatively low even at high total concentrations. Equations 3, 4 and 6 may be combined to give the relation

$$\frac{1}{A - A_M} = \frac{2}{A_D - A_M} + \frac{K}{2(A_D - A_M)}\left(\frac{1}{C}\right) \qquad (7)$$

As shown by (7), the quantity $1/(A - A_M)$ may be plotted against $1/C$. If the theory is correct, a straight line will be obtained, and A_D and K may be calculated from slope and intercept. Other relations which do not involve approximations can be obtained from (3), (4) and (6). Results obtained with the use of these relations are the same, within experimental error, as those obtained with (7).

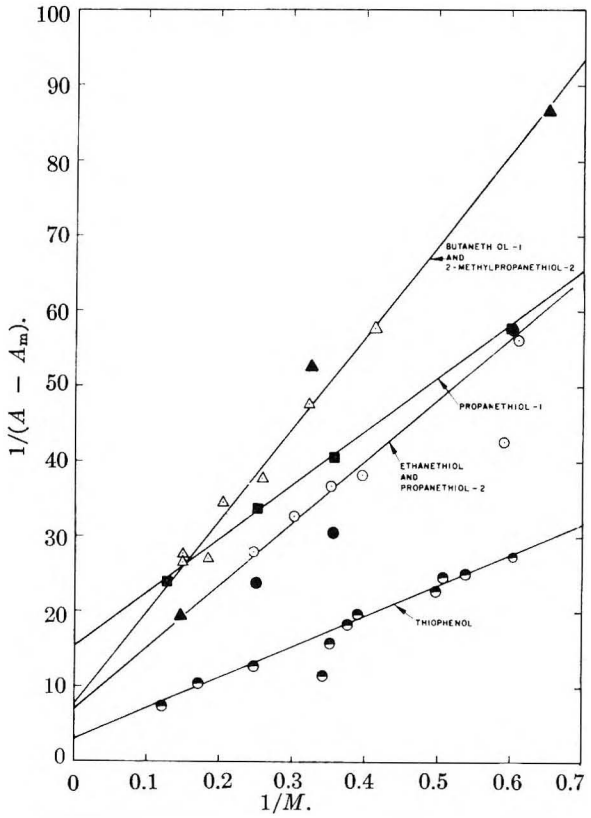

Fig. 5.—Plots of $1/(A - A_m)$ *vs.* $1/M$ (see text); △, butanethiol-1; ▲, 2-methylpropanethiol-2; ■, propanethiol-1; ○, ethanethiol; ●, propanethiol-2; ◓, thiophenol.

It was found more convenient, therefore, to make use of the simple equation 7.

Plots of $1/(A - A_M)$ *versus* $1/C$ are shown in Fig. 5. Data chosen for plotting were those obtained at apparent concentrations greater than 1.4 M, where the contribution to the total intensity by the dimer-located S–H groups was considerable. Values obtained from these plots for A_D and K are given in Table I.

The most important sources of error are (1) wings of neighboring peaks extending into the 3.8–3.9 μ band, (2) failure of the Beer–Lambert law at the higher concentrations and (3) failure of the equilibrium expression at the higher concentrations. The first error probably is not important because a difference of areas is used in arriving at the expression $A - A_M$. It is possible that the second and third effects tend to cancel one another. The values of A_M, A_D and K are very sensitive, however, to the manner in which the extrapolation is made to obtain A_M values. The type of precision obtained indicates that they are reproducible to within about 30%. In the calculations made it is assumed that the equilibrium expression 6 holds for a wide range of concentrations, from 0 to about 70 mole per cent. of "solute." While this assumption would be highly inappropriate for aqueous solutions, it has greater validity for mercaptans in carbon tetrachloride, which may be expected, on the basis of calculations of internal pressures, to approach ideal solutions. It also may be noted that the dimer concentration is small in all solutions.

Discussion

It would be difficult to understand the results of this work except on the basis of a monomer–polymer equilibrium. If it is assumed that the free energy decrease on formation of trimer from dimer is no greater than that on dimer formation, the concentration of trimers and higher polymers must be negligible, and it is sufficient to consider a monomer–dimer equilibrium. It may, therefore, be concluded that in concentrations greater than about 0.5 M in carbon tetrachloride appreciable quantities of dimers are formed. (The equilibrium expression predicts that about 2% of the S–H groups are located in dimers at 0.5 M.) The fact that this slight dimerization can be detected and measured by infrared spectroscopy is due to the circumstance that the intensity of the dimer S–H vibration is approximately 10 times that of the monomer for the aliphatic compounds. This is the same ratio of intensities as found for the carboxylic O–H group in dimeric and monomeric acids.[14] The especially large effect of dimerization upon intensity in the case of thiophenol may be attributed to inhibition through hydrogen bonding of the formation of resonating structures of the type

so that dimerization produces a greater increase of negative charge on sulfur in the case of thiophenol than in the cases of the aliphatic mercaptans.

(14) J. Wenograd and R. A. Spurr, *J. Am. Chem. Soc.*, **79**, 5844 (1957).

PERCHLORIC ACID TITRATIONS OF PORPHYRINS IN NITROBENZENE[1]

BY S. ARONOFF

Iowa State College, Institute for Atomic Research and Departments of Botany and Chemistry, Ames, Iowa

Received November 7, 1957

Although porphyrins as a class are diacidic bases, spectrophotometric titration of chlorins derived from chlorophyll display no unique monosalt spectrum. Uroporphyrin octamethyl ester and tetraphenylchlorin possess sharply-defined monosalt spectra, while various other porphyrins (tetraphenylporphine, phylloerythrin, protoporphine) are of an intermediate type. Apparent dissociation constants may be calculated.

Introduction

Although porphyrins as a class form disalts[2] the isolation of monosalts has never been accomplished, and proof of their existence has been the subject of considerable effort,[3] in large measure because of the general insolubility of the free bases or their salts in aqueous solutions. Consequently, titrimetry has been confined, for the most part, to non-aqueous solutions as glacial acetic acid (potentiometric)[4] pyridine–sulfuric acid[5] (spectrophotometric), ethanol–HCl[2b] and ether–glacial acetic acid.[6] Attempts to use the limited solubility of selected carboxylic and sulfonated porphyrins in buffered aqueous solutions have eventually resulted, with a single exception, in precipitation, figuratively and factually beclouding the data.[3] By the use of nitrobenzene in which all porphyrins and their perchlorates thus far tested are sufficiently soluble for spectrophotometric titrimetry, a set of relative basicities may be obtained. By inclusion of a pair of common indicators, also soluble in this solvent, a rough calculation of apparent pK's may be made, assuming unit activity coefficients in nitrobenzene.

(1) This research was sponsored, in part, by the National Science Foundation.

(2) (a) A. Treibs, *Ann.*, **476**, 1 (1929); (b) S. Aronoff and M. Calvin, *J. Org. Chem.*, **8**, 205 (1943).

(3) A. Neuberger and J. J. Scott, *Proc. Roy. Soc. (London)*, **213A**, 307 1952), and references therein.

(4) J. B. Conant, B. F. Chow and E. M. Dietz, *J. Am. Chem. Soc.*, **56**, 2185 (1934).

(5) S. Aronoff and C. A. Weast, *J. Org. Chem.*, **6**, 550 (1941).

(6) G. Niemann, *Hoppe-Seyl. Z. physiol. Chem.*, **146**, 181 (1925).

Experimental

All curves were obtained with a Cary spectrophotometer, model 12.

The pigments were dissolved in a convenient amount of nitrobenzene (E. K. reagent grade, used without further purification) and diluted to convenient optical density. This solvent is useful down to approximately 400 mμ. Since the compounds were all of known structure and adequately characterized, concentrations were determined from the optical densities, assuming absorption coefficients in nitrobenzene equal to those in dioxane[7] after allowance for small shifts in wave length in the different solvent.

The perchloric acid solution was prepared by addition of approximately 6 μl. of concd. (70%) reagent grade acid to 10 ml. of purified dioxane, providing a solution of about 0.01 *M*, the exact value being determined by titration in aqueous solution. Either a 10 or 25 μl. aliquot of this acid dioxane solution was added to the pigment in nitrobenzene (around 5 to 10 ml.), the spectrum being recorded after each addition. The original water content of the perchloric acid allowed a final concentration in the nitrobenzene of 10^{-6} to 10^{-7} *M*. Comparable concentrations of pigment and acid were twenty to one-hundred-fold greater.

The two indicators, *p,p'*-dimethylaminoazobenzene ("Reagent grade," Fisher Scientific) and *p*-aminonaphtholbenzein ("less than 0.5% chloride," Eastman Kodak) were used without further purification, as other studies[8] had shown this to be unnecessary.

Pheophorbide *a*, phylloerythrin, pyropheophorbide *a* and protoporphine IX were prepared by procedures described by Fischer, *et al.*[9] Chlorin p_6 and purpurin 18, similarly prepared, were generously supplied by Prof. M. M. Hendrickson, Univ. of Nebraska Medical School. Uroporphyrin octamethyl ester, furnished through the kindness of Prof. L. Bogorad, Univ. of Chicago, was initially obtained as the free acid from a porphinuric cow.

Discussion

The titration of the porphyrin free base to a monosalt and then to a disalt is expected to result in spectral changes according to the concentration of the three microspecies, unless the spectrum of the monosalt is identical with one or the other of the microspecies or unless it exists over so narrow a range that it is undetected by discontinuous titration. From the spectral families shown in Figs. 1 to 3, which are typical of the porphyrins employed as a whole, it is apparent that these may be divided into three groups: (a) those clearly providing intermediate spectra between the free base and the disalt and presumably corresponding to the monosalt (uroporphine octamethyl ester and tetraphenyl chlorin); (b) those providing *no* evidence of a monosalt (the chlorophyll chlorins—pheophorbide *a*, pyropheophorbide, chlorin p_6 and purpurin 18); and (c) those where an intermediate spectrum is indicated, either by shift of a maximum during titration or by shift of an isosbestic point (phylloerythrin, protoporphine IX, and tetraphenylporphine).

The absence of a monosalt spectrum in the chlorophyll chlorins is not associated with the isocyclic ring since purpurin 18, which has no such ring, is within this category. Furthermore, phylloerythrin, whose isocyclic ring is intact, but which has been tautomerized to a porphine, is not in this group. The effect presumably is associated with the dihydroporphine nature of these compounds.

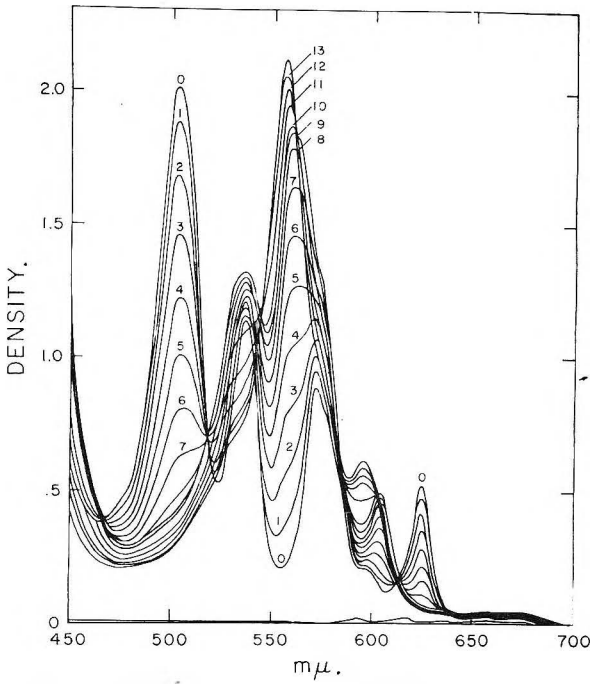

Fig. 1.—The family of curves obtained by titrating uroporphyrin octamethyl ester in nitrobenzene (4.85 ml.) with 10-μl. aliquots of 0.0137 *N* perchloric acid in dioxane. Maxima of the free base are at 625, 572, 537 and 502 mμ. The reversal of optical density in going from the free base to a monosalt and then to a disalt is most noticeable at 537 mμ. The monosalt–disalt curves also result in an isosbestic point at 603 mμ, the transition from free base to monosalt being characterized only by a shift of maxima in that region.

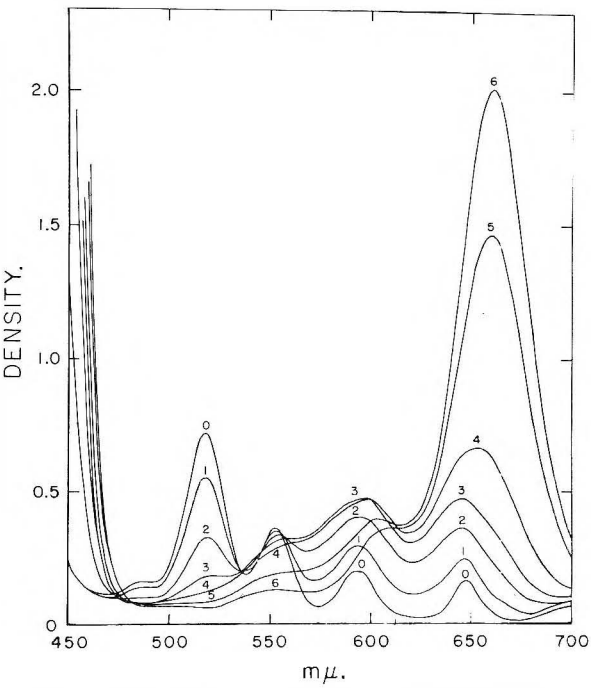

Fig. 2.—The family of curves obtained by titrating α,β, γ,δ-tetraphenylporphine (12.3 ml.) with 10-μl. aliquots of 0.0164 *N* perchloric acid in dioxane. Transition from the monosalt to the free base is accompanied by a shift in the absorption maximum at 645 to 660 mμ. The "floating" isosbestic points of the region 557–562 mμ is also evidence of the existence of a monosalt.

(7) A. Stern, *et al.*, *Z. physik. Chem.*, [A] **174**, 81, 321 (1935); **175**, 38, 405 (1935); **176**, 81, 209 (1936); **177**, 165, 365 (1936); **178**, 161, 420 (1937); **180**, 321 (1937); **182**, 117 (1938).

(8) I. M. Kolthoff and S. Bruckenstein, *J. Am. Chem. Soc.*, **79**, 1 (1957).

(9) (a) H. Fischer and H. Orth, "Die Chemie des Pyrrols," Vol. I, Akad. Verlags., Leipzig, 1934, 1937, 1940; (b) H. Fischer and A. Stern, ref. 9a, Vol. II, parts 1 and 2.

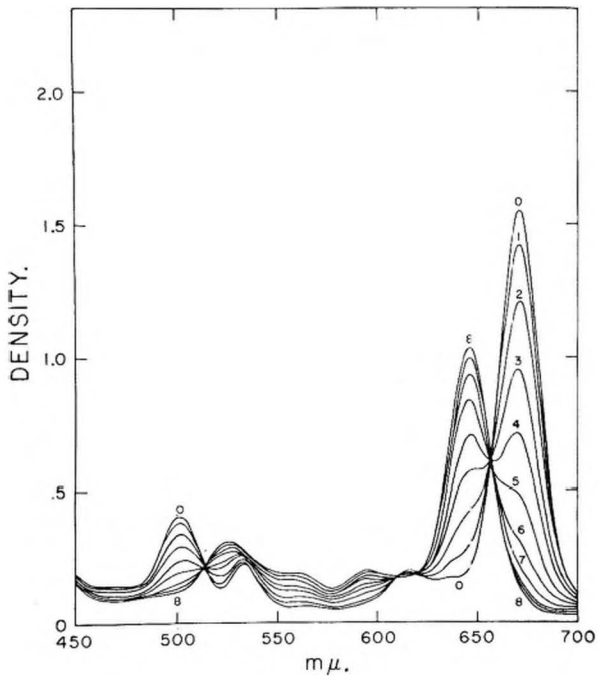

Fig. 3.—The family of curves obtained by titrating chlorin p_6 in nitrobenzene (15 ml.) with 10-μl. aliquots of 0.0137 *N* perchloric acid in dioxane. The absence of monosalt spectra is apparent from the stability of the isosbestic points.

This explanation does not account, however, for the intermediate spectrum of tetraphenyl chlorin, assuming its structure as a dihydroporphine to be valid[10] and the inductive effect of the substituted phenyls to be a minor one. It is interesting to note, however, that whereas tetraphenyl-chlorin and -porphine have virtually identical disalt spectra, a corresponding chlorophyll chlorin and porphine, pyropheophorbide and phylloerythrin, are completely different. The latter is similar, in its disalt spectrum, with other porphines of divergent origin, *e.g.*, protoporphine IX and uroporphine octamethyl ester. There appears, then, to be a structural factor in the chlorophyll chlorins which affects the monosalt spectra uniquely and which is at present unknown. It is not the result of hydrogen tautomerism amongst the nitrogens, since these are presumably rapidly interconvertible at room temperature.[11]

All porphyrins contain (at least) two "active" hydrogens, presumably attached to the nitrogens.[12] However, there are no generally accepted values for the acidity of these hydrogens[13] or the basicity of the nitrogens. The most commonly used criterion of porphyrin basicity is the "acid number,"[14] that is, the percentage of aqueous HCl required to extract two-thirds of the pigment from an equal volume of ether. Unfortunately, the acid number is a function of *two* parameters: the basicity of the nitrogens and the partition coefficient of the porphyrin dihydrochloride between HCl and Et_2O.[15] Of the various solvents which have been used for determinations of acidity functions (H_0)[16] none is entirely adequate for both potentiometric and spectrophotometric titration of porphyrins. Nitrobenzene, with a moderate dielectric constant and a fair solubility for most porphyrins, is at present a good possibility. Perchloric acid is a considerably stronger acid in nitrobenzene than in acetic acid. Furthermore, since the ionization of indicator dyes, as dimethylaminoazobenzene, is considerably less in this solvent than in acetic acid,[8] it is not necessary to suppress the ionization by the addition of a base, as pyridine. Calculation of the apparent ionization constants of the porphyrin free bases from spectral data at various acid strengths requires knowledge of the absorption coefficients of all these microspecies and the (over-all) hydrogen ion concentration at which each curve was determined.[2b] The absorption coefficient of the free base is, of course, known and one may presume that of the disalt from the limiting values in acid solution. It is not known for the monosalt. Unfortunately, for any one point on any one curve we presume, for purposes of calculation, that H^+ is given by $\bar{H}^+$–PH^+–PH^{++}, ($\bar{H}^+$ being the total H^+ added up to and including that point). Consequently, in addition to the three unknowns (the absorption coefficient of the monosalt and the two ionization constants), the H^+ becomes in effect a fourth parameter. In theory it is feasible to utilize three wave lengths on three curves to obtain a set of nine equations whose solution yields the eight unknowns, K_1, K_2, H_1^+, H_2^+, H_3^+, ϵ_{1a}, ϵ_{1b}, ϵ_{1c}, where $\epsilon_{0,1,2}$ are the absorption coefficients of the free base,

TABLE I

APPARENT DISSOCIATION CONSTANTS OF VARIOUS PORPHYRINS AND REFERENCE COMPOUNDS IN NITROBENZENE, TITRATED WITH PERCHLORIC ACID (IN DIOXANE)

The K's are defined as $K_1 = (H^+)(B)/(BH^+)$ and $K_2 = (H^+)(BH^+)/(BH^{++})$ where B is the concentration of the free base, B^+ is the assumed monoion and BH^{++} the presumed diion. The perchloric acid is also assumed to be completely ionized. The pK H_2O of DMAAB is approximately 3.2×10^{-4} and that for PNB is 7.9×10^{-12}.

Compound	Acid no.	$K_1 \times 10^5$	$K_2 \times 10^5$
Distinct monoion			
Uroporphyrin monomethyl ester	7	4.3	32
Tetraphenylchlorin	19-20	14	42
Indistinct monoion			
Tetraphenylporphine	13–14	4.2	14
Phylloerythrin	7–8	0.69	14
Protoporphine	2	1.2	11
Indistinguishable monoion			
Pheophorbide *a*	15	8.7	
Purpurin 18	18	5.6	
Pyropheophorbide *a*	12	1.9	
Chlorin p_6	5	1.5	
Reference compd.			
p,p'-Dimethylaminoazobenzene (DMAAB)		2.3	
p-Naphtholbenzein (PNB)		7.6	

(10) R. Ball, G. D. Dorough and M. Calvin, *J. Am. Chem. Soc.*, **68**, 2278 (1946).

(11) G. D. Dorough and K. T. Shen, *ibid.*, **72**, 3939 (1950).

(12) H. Fischer and S. Goebel, *Ann.*, **522**, 168 (1936).

(13) Except for N-methyletioporphine and etioporphine I, where *pK*'s of 14–15 and 16, respectively, have been given: W. K. McEwen, *J. Am. Chem. Soc.*, **58**, 1124 (1936).

(14) R. Willstätter and U. A. Stoll, "Untersuchungen über Chlorophyll," Berlin, 1913.

(15) K. Zeile and R. Rau, *Hoppe-Seyl. Z. physiol. Chem.*, **250**, 197 (1937).

(16) M. A. Paul and F. A. Long, *Chem. Revs.*, **57**, 1 (1957).

monosalt and disalt at wave lengths a, b and c, K_2 is the disalt dissociation constant ($PH^{+2} \rightleftarrows PH^{+} + H^{+}$) and K_1 the corresponding monosalt constant ($PH^{+} \rightleftarrows P + H^{+}$). In practice this is prohibitive and one is forced to approximate values of ϵ_1 by use of fortuitous wave lengths and at which the ratios of microspecies may be approximated, so that the K's and H^{+}'s follow directly. This approximation procedure is, of course, not required for the chlorophyll chlorins, where, pending potentiometric titration, one assumes that $K_1 = K_2$ and this may be calculated directly from the data.

The results of both the calculations and approximations are presented in Table I. The strength of perchloric acid in nitrobenzene is apparent from the narrow limits of the reference compounds whose aqueous dissociation constants are approximately 3.2×10^{-4} and 7.9×10^{-10}. It is interesting to note that the K's of the chlorophyll chlorins follow their "acid numbers" roughly, the inversion of pheophorbide a and purpurin 18 presumably arising from a solubility effect in Et_2O. The very small values of K_2 imply, by comparison with p-naphtholbenzein, much weaker basicity for the second N than has generally been supposed. From these values, and by the assumption of a Hammett acidity function, one may calculate apparent, approximate aqueous over-all dissociation constants. This hardly appears warranted at the present stage.

Acknowledgment.—The author wishes to express his appreciation for the excellent tracings made in the Medical Arts and Scientific Exhibits Section of the National Institutes of Health, Bethesda, Maryland.

THE DENSITIES OF HEAVY WATER LIQUID AND SATURATED VAPOR AT ELEVATED TEMPERATURES[1]

BY G. M. HEBERT, H. F. MCDUFFIE AND C. H. SECOY

Contribution from the Chemistry Division of the Oak Ridge National Laboratory, Oak Ridge, Tennessee

Received November 8, 1957

In connection with studies of the homogeneous catalysis of the deuterium–oxygen reaction in heavy water systems, it became desirable to know the densities for the liquid and saturated vapor of heavy water at temperatures above 250°. Previous studies had provided information concerning the density of the liquid up to 250° [2] and information concerning the critical properties.[3] No data relating to the vapor densities appeared to be available.

An experimental method used for determining the volume of uranyl sulfate solutions as a function of concentration, temperature and fractional filling of sealed quartz tubes[4] appeared suitable for application to the determination of the fractional filling, at various temperatures, of tubes containing heavy water. Such determinations were made for heavy water and light water samples. From the relationship between fractional filling and temperature it was possible to calculate the desired densities of the liquid and saturated vapor.

Experimental

Method.—Mass balance considerations lead to a relationship between fractional filling at room temperature, F_0, and that, F_T, at some elevated temperature: If

V = total volume of tube
F_0, F_T (fractional filling) = vol. of liquid ÷ V
m_0, m_T = total mass of water in the tube
d = density
v = vapor
l = liquid

then

$$m_0 = VF_0d_{l_0} + V(1 - F_0)d_{v_0} \quad (1)$$

$$m_T = VF_Td_{l_T} + V(1 - F_T)d_{v_T} \quad (2)$$

Since no mass is added $m_0 = m_T$; hence, equating the right-hand portions of (1) and (2) and cancelling V

$$F_0d_{l_0} + (1 - F_0)d_{v_0} = F_Td_{l_T} + (1 - F_T)d_{v_T} \quad (3)$$

Equation 3 reveals a linear relationship between F_0 and F_T. This equation could be used for work of the highest accuracy. When, however, as in the present case, $d_{v_0} \approx 0$, equation 3 can be reduced to a simpler form

$$F_0 = F_T\frac{d_{l_T} - d_{v_T}}{d_{l_0}} + \frac{d_{v_T}}{d_{l_0}} \quad (4)$$

When the relationship between F_0 and F_T is established experimentally, the slope and intercept may be used to calculate d_{l_T} and d_{v_T} if d_{l_0} is known (as it is).

Procedure.—Samples of heavy water of known weight and density were sealed in quartz tubes (approximately 14 cm. long, 1.6 mm. i.d. and 4 mm. o.d.) which had been selected for uniform bore. The total volume of the sealed portion of the tube was determined in the following manner which automatically corrects for the distortion introduced by the two seals.

1. With reference to Fig. 1 measure the height of the liquid h_1 with a cathetometer and the total height (tip to tip of the inner space) of the inner volume of the tube, h_2. The height of the liquid is measured to a position one third the distance from the bottom to the top of the meniscus.
2. Invert the tube and measure the height of the liquid again, as h_3, and remeasure h_2 to obtain an average.
3. Calculate $h_4 = h_2 - h_1 - h_3$ as the length of undistorted tubing in the center of the tube which is never (or always) wet by the liquid in the vertical position, depending on whether the tube is more or less than half full.
4. The total volume of the tube is, then, twice the liquid volume plus the volume $h_4\pi r$ (this volume will be positive or negative depending on whether $h_2 - h_1 - h_3$ is positive or negative) (r = half the measured tube diameter).
5. The liquid volume is known from its weight and density.

Six tubes were prepared as described above and placed in a circulating air-bath furnace, shown with its instrumentation in Fig. 2. The temperature was measured with a calibrated

(1) This paper is based upon work performed at Oak Ridge National Laboratory, which is operated by Union Carbide Nuclear Company for the Atomic Energy Commission.

(2) J. R. Heiks, *et al.*, THIS JOURNAL, **58**, 488 (1954).

(3) "The Reactor Handbook (USAEC)," Vol. 2, (Engineering), 1955, p. 22.

(4) G. M. Hebert, D. W. Sherwood and C. H. Secoy, HRP Quar. Prog. Rep. Oct. 31, 1954, ORNL 1813, p. 164.

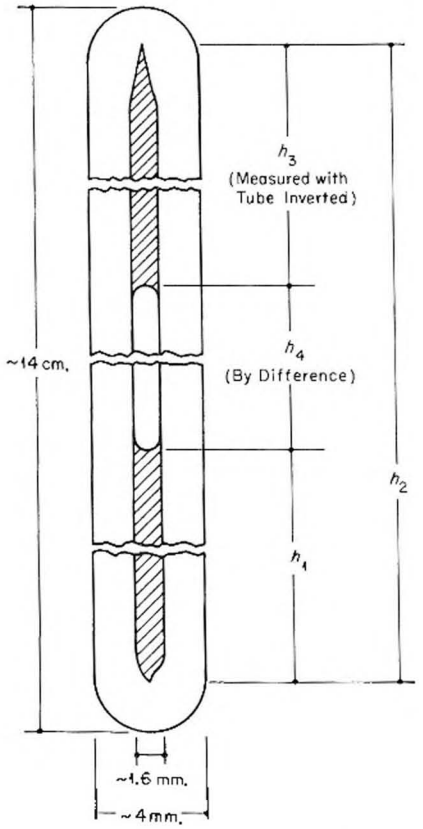

Fig. 1.—Measurements of liquid heights in quartz tubes.

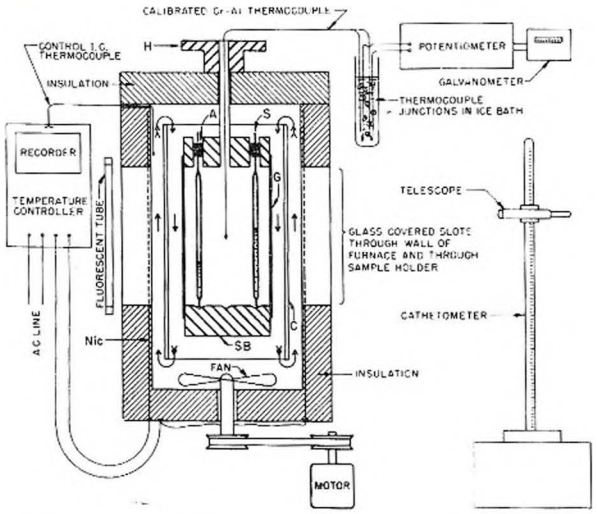

Fig. 2.—Air-bath furnace and instrumentation: S, sample tube; SB, sample block (6 samples); G, glass tube around sample holder; asbestos packing around top and bottom; Nic, nichrome heater wire (wound vertically); H, handle for rotating sample holder; A, asbestos cord packing; C, glass chimney.

chromel–alumel thermocouple, and the temperature control precision was better than 0.1°. Readings of the liquid heights in each tube were made at various temperatures after temperature stabilization. The change in volume accompanying each change in temperature was calculated from the measured change in the height of the liquid and the measured diameter of the tube. It was assumed that the change in height was occurring in a section of the tube which had not been distorted by the sealing process. It was also assumed that the change in volume of the tube, due to thermal expansion of the quartz, was negligible when compared with other experimental uncertainties. From the known liquid

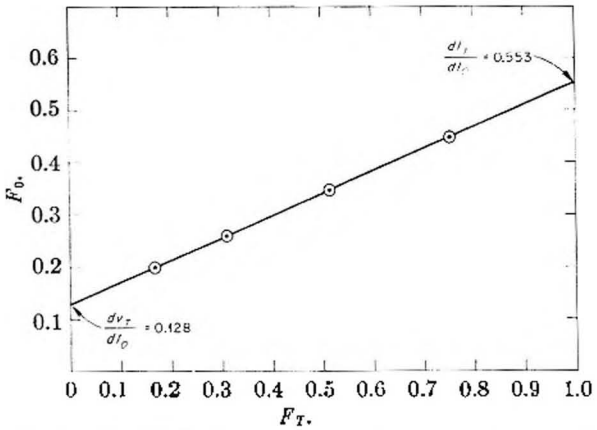

Fig. 3.—Graphical determination of relative liquid and vapor densities of D_2O at 353.4°.

volume and fractional filling at room temperature and the change in volume on heating to elevated temperature, it was possible to calculate the liquid volume and fractional filling at each of the elevated temperatures.

Of the six experimental tubes prepared, four contained heavy water and two contained light water. The tubes containing light water were present to serve as an internal check upon the agreement of the experimental data with the known properties of light water liquid and vapor. This check also established the reliability of the measured temperature and made possible the direct comparison of the data for heavy and light water in the same experiment.

Data and Calculations.—The experimentally determined fractional fillings at room temperature and at the various elevated temperatures are presented in Table I.

TABLE I

FRACTIONAL FILLING *vs* TEMPERATURE

Temp. (°C.)	H_2O Fr_1	Fr_2	Fr_3	D_2O Fr_4	Fr_5	Fr_6
Room temp.[a]	0.261	0.348	0.198	0.260	0.346	0.447
113.2	.272	.366	.208	.274	.362	.491
229.1	.303	.409	.226	.310	.406	.533
268.5	.314	.430	.230	.314	.429	.567
305.6	.320	.455	.227	.322	.455	.613
353.4	.315	.508	.168	.311	.514	.753
367.0	.250	.560		.252	.601	
371.5	.215	.583			.608	
372.6	.207	.603				
373.8	.112	.646				
374.8	.074	.668				

[a] 24°.

Values for d_{v_T} and d_l can be derived from these data either by graphical or mathematical procedures. A graphical solution for the heavy water data at 353.4° is presented as Fig. 3. Multiplying the intercepts by 1.1047, the density of heavy water liquid at room temperature (d_{l_0}), gives 0.6109 g./cc. and 0.1414 g./cc. as the values for d_{l_T} and d_{v_T}, respectively. A mathematical solution can be obtained for each pair of experimental points by means of simultaneous equations; for four tubes at one temperature there are six such sets of equations, and the average of all such values was determined at each temperature. Figure 4 presents the graphical and mathematical values for the liquid and vapor densities so determined for light and heavy water, together with appropriate values from the literature for comparison. Table II presents values for D_2O taken from the smoothed curve at convenient temperature intervals.

Discussion

The expected linear relationship between fractional filling at room temperature and fractional filling at elevated temperatures was demonstrated,

TABLE II

LIQUID AND VAPOR DENSITIES OF D_2O

Temp. (°C.)	Density (g./cc.) Vapor	Liquid
175	0.004	0.989
180	.005	.983
190	.006	.970
200	.007	.957
210	.009	.943
220	.010	.929
230	.013	.913
240	.016	.898
250	.020	.881
260	.024	.864
270	.029	.847
280	.034	.829
290	.040	.809
300	.048	.787
310	.058	.763
320	.070	.735
330	.087	.705
340	.105	.668
350	.129	.626
360	.163	.573
370	.248	.462
371.5	.363	.363[a]

[a] Critical point.

and the agreement of the experimental data with this relationship was sufficiently close to permit calculation of the densities of the liquid and the saturated vapor. The values so calculated were in good agreement with the available data for heavy water and the established data for light water. The precision of the method may be estimated from the deviations between accepted values for light water and those found by the present technique. Between 200 and 370° the average deviation in liquid densities was less than 1% of the accepted value and the average deviation in vapor densities was less than 10% of the accepted value. Above 370° the effects of small temperature errors are so much magnified, and below 200° the vapor densities are so low, that larger deviations occur.

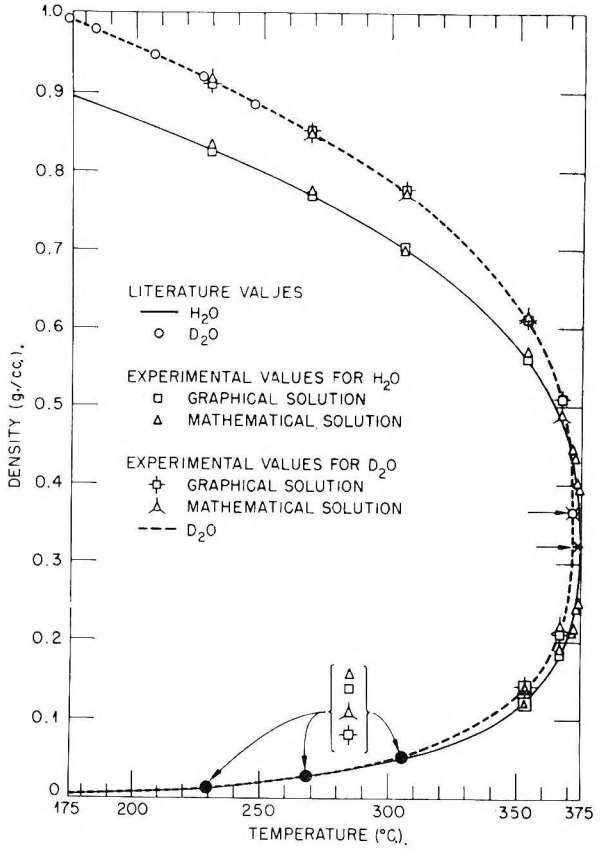

Fig. 4.—Liquid and saturated vapor density of H_2O and D_2O.

This method is so simple to apply, and the opportunities for direct comparison with liquids of known properties in order to establish internal checks of the consistency and temperature in a particular experiment are so attractive, that the method might be considered for use with other liquids, such as pure hydrocarbons, for which it may become desirable to know the vapor and liquid densities at elevated temperatures.

VAPOR–SOLID EQUILIBRIA IN THE IRON–CHLORINE SYSTEM

BY LAURENCE E. WILSON[1] AND N. W. GREGORY

Contribution from the Department of Chemistry, University of Washington, Seattle 5, Washington

Received November 12, 1957

The vaporization and thermal decomposition equilibria of iron(III) chloride have been investigated by gas saturation flow and diaphragm gage techniques. A brief summary and discussion of results of previous investigators is given. Based on the present study, equations for the pressures of Fe_2Cl_6 and Cl_2 in equilibrium with $FeCl_3(s)$ and/or $FeCl_2(s)$ as a function of temperature are presented. Solid solution of $FeCl_3$ and $FeCl_2$ is not significant below 300°.

Vaporization of solid iron(III) chloride is complex. Three equilibria (or alternate combinations thereof) must be considered

$$2FeCl_3(s) \rightleftharpoons Fe_2Cl_6(g) \quad (1)$$

$$Fe_2Cl_6(g) \rightleftharpoons 2FeCl_3(g) \quad (2)$$

$$Fe_2Cl_6(g) \rightleftharpoons 2FeCl_2(s) + Cl_2(g) \quad (3)$$

Although a number of studies involving these equilibria have been made previously, a survey of published results reveals inconsistencies such that one cannot, with confidence, predict the equilibrium partial pressures of the various components as a function of temperature.

Four independent measurements of the total pressure above solid iron(III) chloride have been

(1) National Science Foundation Fellow, 1954–1957.

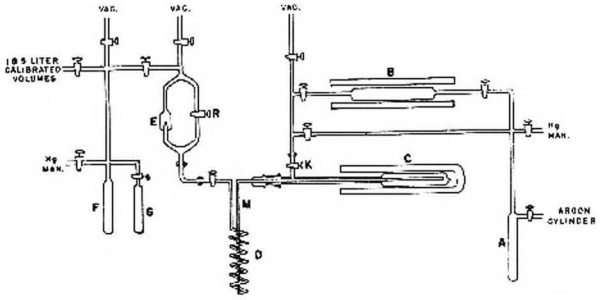

Fig. 1.—Gas saturation flow (transpiration) apparatus.

made by Maier,[2] Stirnemann,[3] Sano[4] and Johnstone, *et al.*[5] Results of Stirnemann and Johnstone are in fairly close agreement but do not follow the observations of either of the other two, which are also not in mutual accord. In all four cases, calculation of pressures of Fe_2Cl_6 from reported data cannot be made without further knowledge of the partial pressures of chlorine and of monomeric $FeCl_3$.

Kangro and Bernstorff[6] have made a direct study of the dissociation equilibrium (2) between 487 and 741°; this work is supported by observations of Schafer[7] in a study of the Fe_2O_3–HCl system. Extrapolation of their results indicates that the partial pressure of $FeCl_3(g)$ in equilibrium vapor pressure mixtures is less than 1% of that of the dimer at temperatures below 300°; hence it has been assumed that the monomer may be neglected unless, as was the case in the study of equilibrium (3), total iron(III) chloride pressures are significantly below saturation values.

Jellinek and Koop[8] and Ringwald[9] have made independent gas saturation flow studies of the vaporization process. Results of Jellinek and Koop differ appreciably from those of all other investigators. Ringwald employed nitrogen as a carrier gas at flow rates of 0.01 mole/hour (measured at room temperature) between 251 and 302° and measured the weight of iron(III) chloride vapor, condensed in a water-cooled trap, and of chlorine, collected in a soda lime, magnesium perchlorate filled trap, transported during a given run. Schafer and Oehler[10] conducted similar experiments at lower temperatures, 160 to 210°, determining only chlorine pressures, which give equilibrium constants for the reaction

$$2FeCl_3(s) \rightleftharpoons 2FeCl_2(s) + Cl_2(g) \qquad (4)$$

The chlorine pressures of Ringwald and of Schafer and Oehler are compared in Fig. 4. Their results appear generally compatible, although, considered independently, significantly different heats of reaction are derived and extrapolation of Ringwald's curve predicts pressures well above those of Schafer and Oehler.

Kangro and Petersen[11] have studied reaction 3 at higher temperatures, 333 to 697° (in the absence of a condensed iron(III) phase), using a quenching technique. Combining an extrapolation of their results with those of Schafer and Oehler leads to predicted saturation vapor pressures of Fe_2Cl_6 which differ by a factor of more than two from those observed by Ringwald.

In view of these discrepancies we have felt it necessary to make an additional study of both the thermal decomposition and vaporization reactions. The gas saturation flow method has been used to study reaction 1 in a lower temperature range, 160 to 227°, than used by other investigators. Reaction 3 has been investigated by the same technique from 160 to 420° and reaction 4 from 160 to 220°. A Pyrex diaphragm gage has been used to measure the combined pressures of chlorine and Fe_2Cl_6, between 225 and 300°, above solid iron(III) chloride and various mixtures of iron(III) and iron(II) chlorides to confirm results of the flow experiments and to ascertain whether solid solution effects are important.

Experimental

Gas Saturation Flow Studies.—The apparatus, Fig. 1, is an adaptation of one used in the study of the iron–bromine system.[12] To study equilibrium 3 anhydrous $FeCl_2$, prepared from Reagent Grade $FeCl_2 \cdot 4H_2O$ by vacuum dehydration followed by sublimation, was resublimed under high vacuum directly onto the walls of the reaction chamber C (the sublimation tube at the end of the reactor was subsequently sealed off). The system was then filled with argon and the inner tube placed in position *via* the standard taper joints shown. It was found possible to complete the assembly with the system filled with dry argon without observable hydrolysis of $FeCl_2$ (or later $FeCl_3$) in the reactor. The apparatus was evacuated immediately after closing to minimize chances of contact of water vapor from the atmosphere with the sample.

Argon (Matheson, 99.9%, and Linde, C.P.; initially purified by bubbling through liquid potassium; this step was later found unnecessary) was condensed with liquid nitrogen (v.p. argon *ca.* 270 mm.) in table A in sufficient quantity for the anticipated flow experiment. Prior to entry into the sample tube, the desired initial pressure of chlorine was introduced by permitting the argon to flow over a sample of $CuCl_2$, maintained at a temperature between 360 and 435° by furnace B; chlorine is produced by thermal decomposition of $CuCl_2$.

A run was conducted as follows. After bringing furnaces B and C to the desired temperature the coolant on trap A was changed to liquid oxygen (v.p. argon *ca.* 1050 mm.) and the entire system allowed to fill with argon and come to thermal equilibrium in its various parts. Flow was then initiated by opening the appropriate stopcocks, after immersing trap F in liquid nitrogen. The flow rate was controlled at desired values between 2 and 70 ml./minute (calculated at reaction temperature and pressure) by inserting selected capillary tubes at E. The by-pass stopcock R was closed during a run. The mixture of argon and chlorine entered the reactor through K and passed over the $FeCl_2$ sample; the resulting gas mixture left the reactor *via* the small exit tube extending down the center. The iron(III) chloride vapor condensed almost immediately outside the hot zone; chlorine subsequently was trapped in the spiral tube D, immersed in liquid oxygen, and argon in trap F.

To stop the run, the stopcocks were closed, the furnace removed from the reactor, and the latter evacuated *via* the stopcock K. The spiral was separated by sealing the glass tube at M. The total moles of argon which had passed

(2) C. Maier, U. S. Bur. Mines, Tech. Paper 360 (1925).

(3) E. Stirnemann, *Neues Jahrb. Mineral., Geol., Palaont.*, **52A**, 334 (1925).

(4) K. Sano, *J. Chem. Soc. Japan*, **59**, 1073 (1938).

(5) H. F. Johnstone, H. C. Weingartner and W. E. Winsche, *J. Am. Chem. Soc.* **64**, 241 (1942).

(6) W. Kangro and H. Bernstorff, *Z. anorg. allgem. Chem.*, **263**, 316 (1950).

(7) H. Schafer, *Z. anorg. Chem.*, **259**, 53 (1949).

(8) K. Jellinek and R. Koop, *Z. physik. Chem.*, **145A**, 305 (1929).

(9) O. E. Ringwald, Doctoral Dissertation, Princeton Univ., 1949.

(10) H. Schafer and E. Oehler, *Z. anorg. allgem. Chem.*, **271**, 206 (1953).

(11) W. Kangro and E. Petersen, *Z. anorg. Chem.*, **261**, 157 (1950).

(12) N. W. Gregory and R. O. MacLaren, THIS JOURNAL, **59**, 110 (1955).

through the system in the measured time was determined by evaporating the condensate in F into calibrated volumes. Chlorine was determined by drawing KI solution into the evacuated spiral and titrating the liberated iodine with sodium thiosulfate by the "dead stop" method.[13] This method made it possible to determine quantities of chlorine as small as 10^{-8} mole within 5% uncertainty; in the majority of cases amounts of chlorine were between 10^{-4} and 10^{-6} mole, determined within an uncertainty of 1%. Iron(III) chloride was washed from the center tube (after removal) and determined after reduction by titration with 0.01 *N* potassium dichromate, when amounts were larger than 3×10^{-5} mole, or by a colorimetric method[12,14] using the orange tris-(1,10-phenanthroline)-iron(II) ion when amounts were smaller. The colorimetric method permitted determination of quantities of iron as small as 5×10^{-7} mole within 2% uncertainty. Color comparisons were made on a Beckman DU spectrophotometer at a wave length of 510 mμ.

During a given flow experiment the temperature of the reaction chamber, maintained uniform and constant within two degrees, was measured by four 24 gage calibrated chromel–alumel thermocouples taped to various positions on the outside surface of the reactor. An electric furnace with independent Nichrome windings at each end and in the center was used to produce a uniform temperature zone.

For most of the saturation vapor pressure measurements in the flow experiments, iron(III) chloride was sublimed onto the walls of the reactor in place of $FeCl_3$ and argon introduced directly, by-passing the copper(II) chloride furnace. In these experiments chlorine detected in the exit gas came from decomposition of iron(III) chloride. To minimize error from diffusion of vapor from the reactor, argon (from G, Fig. 1) flow was reversed during the thermal equilibration period. In other respects these experiments were conducted in the same manner as described in the preceding paragraphs.

Vapor pressures of $FeCl_2$ have not been measured in the temperature range of this work. However, from results at higher temperatures[2,15,16] and observed sublimation behavior in this work, it is apparent that the contribution of $FeCl_2$ to the iron halide vapor may be neglected in our experiments.

Diaphragm Gage Measurements.—A Pyrex diaphragm gage of a type described previously[12] was used. Motion of the pointer was detected with a 40 power microscope enabling pressures to be measured within 1 mm. Total pressures were measured as a function of temperature for four different samples: (a) iron(III) chloride sublimed into the gage and an excess of chlorine, 96 mm. pressure at 100°, added; (b) a mixture of $FeCl_3$ and $FeCl_2$, sublimed into the gage independently (7.4 mole % $FeCl_2$); (c) a mixture of $FeCl_3$ (30.4 mole %) and $FeCl_2$, prepared by subliming $FeCl_2$ into the gage and adding a limited amount of chlorine. (In this series a small residual pressure (2 mm.) was observed at room temperature after the first preliminary measurements. This was removed by opening a "break-in-ski" which permitted pumping on the sample without intermediate exposure to an inert atmosphere, after which the gage was resealed. No residual pressure could be detected following subsequent measurements); (d) a sample of pure $FeCl_3$, prepared by subliming $FeCl_3$ *in vacuo* into the gage and treating the sample with excess chlorine at 300°. The excess chlorine was removed through a "break-in-ski" at room temperature and the gage resealed. No residual gas was observed following subsequent pressure measurements. The composition of the last three samples was confirmed by analysis.

Temperatures were produced and measured as described for the flow experiments.

Results and Discussion

The Iron(II) Chloride–Chlorine Reaction.—From the total amount of iron(III) chloride collected and the amount of argon flowing through the system in a given run, partial pressures of Fe_2Cl_6 and $FeCl_3$ were calculated using the equation

$$\log \frac{P^2_{FeCl_3}}{P_{Fe_2Cl_6}} (\text{mm.}) = \frac{-6907}{T} + 9.391 \qquad (5)$$

based on results of Kangro and Bernstorff.[6] From pressures of Fe_2Cl_6 and chlorine, apparent equilibrium constants for reaction 3 were calculated. Below 220°, the ratio of these pressures at a given temperature showed a dependency on flow rate, with the relative pressure of chlorine decreasing as flow rates were decreased. Further evidence of a slow reaction was seen in the observation that, for a given flow rate and temperature, the ratio of Fe_2Cl_6 to chlorine leaving the reactor decreased as the initial chlorine pressure was decreased.[17] Insufficient data were obtained below 220° to permit quantitative estimate of equilibrium constants by extrapolation to zero flow. However, the data were in qualitative agreement with the equilibrium behavior anticipated from extrapolation of results at higher temperatures.

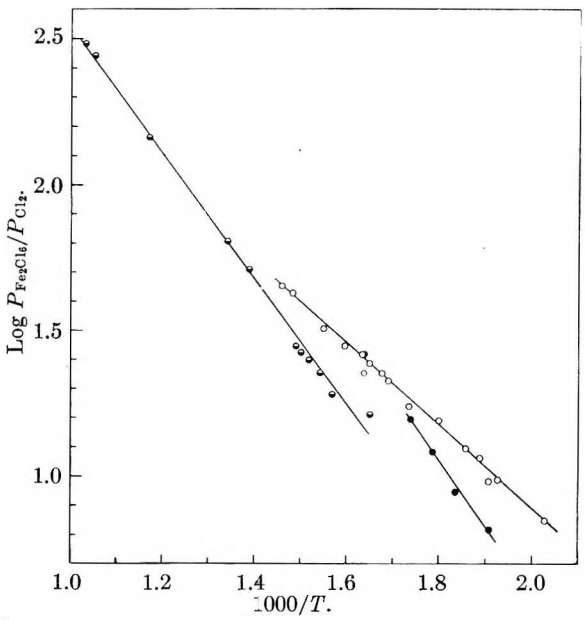

Fig. 2.—Equilibrium characteristics of reaction 3: ●, Ringwald; ◒, Kangro and Petersen; ○, this work.

Between 220 and 400° and at flow rates between 3 and 60 ml./min., a series of measurements were made in which the chlorine to Fe_2Cl_6 ratio showed no dependency on flow rate. These data are shown in Fig. 2. The variation of K_3 with temperature may be expressed by the equation

$$\log \frac{P_{Cl_2}}{P_{Fe_2Cl_6}} = \frac{1408}{T} - 3.710 \qquad (6)$$

At the lower end of this temperature range, however, it was still noted that a combination of high initial chlorine pressure and high flow rate gave non-equilibrium mixtures (excess chlorine). At the highest temperatures no rate of reaction problem was encountered. However, it was found necessary to use high flow rates (50–70 ml./min.) to avoid deposition of iron(III) chloride from the exit

(13) G. Wernimont and F. J. Hopkinson, *Ind. Eng. Chem., Anal. Ed.*, **12**, 308 (1940).

(14) W. B. Fortune and M. G. Mellon, *ibid.*, **10**, 60 (1938).

(15) H. Schafer and K. Krehl, *Z. anorg. allgem. Chem.*, **268**, 35 (1952).

(16) H. Schafer, *ibid.*, **278**, 300 (1955).

(17) A detailed account of these and of all experiments discussed in this paper may be found in the Doctoral Thesis of Laurence E. Wilson, University of Washington, 1957.

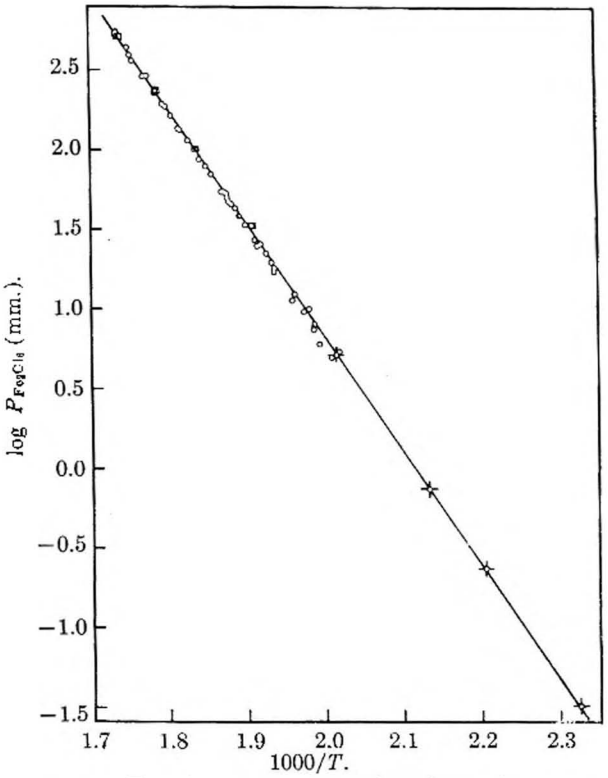

Fig. 3.—Equilibrium characteristics of reaction 1: □, Ringwald; O, this work, diaphragm gage method; ⊠, this work, gas saturation flow method.

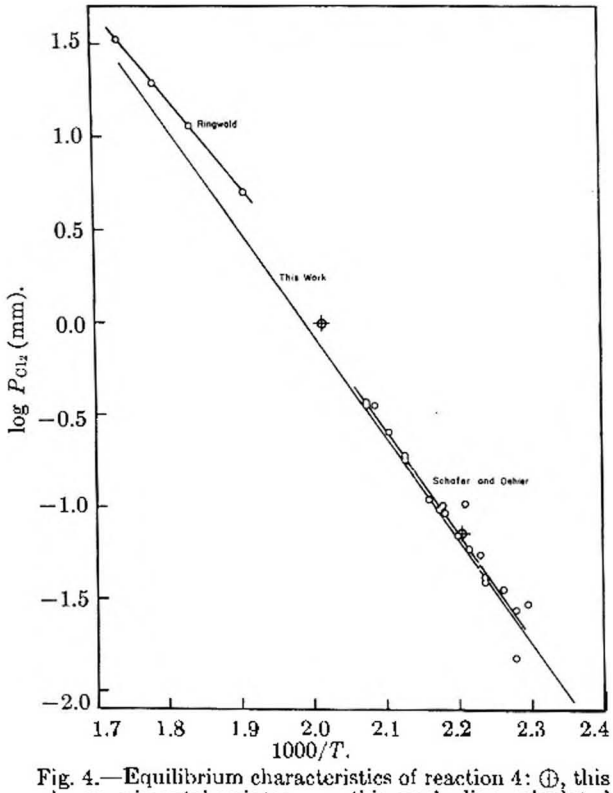

Fig. 4.—Equilibrium characteristics of reaction 4: ⊕, this work, experimental points; —, this work, line calculated from equations 6 and 7.

gas mixture close to the reactor furnace. When this occurred, at lower flow rates, amounts of chlorine collected were larger than expected. Since only very small amounts of chlorine were collected in these high temperature runs, decomposition of a small amount of iron(III) chloride made a significant contribution to the total chlorine. At high flow rates deposition of $FeCl_3$ occurred far enough from the furnace zone (at lower temperatures) to prevent significant decomposition. This problem was not encountered at lower furnace temperatures.

It is seen, Fig. 2, that equilibrium constants obtained in this work lie somewhat above those observed by Ringwald, and give an appreciably different heat of reaction. At higher temperatures equation 6 extrapolates into the line drawn through the data of Kangro and Peterson but at lower temperatures deviates markedly from their findings.

Vapor Pressures of Solid Iron(III) Chloride.—In flow experiments in which chlorine pressures over $FeCl_2$ were sufficiently high, condensation of solid $FeCl_3$ occurred in the reactor. In this case, and in others in which argon was passed over an initially pure sample of solid iron(III) chloride, measured pressures of Fe_2Cl_6 characterize equilibrium 1. Twenty such experiments were completed between 150 and 230°, giving vapor pressures between 0.02 and 8 mm. A plot of calculated pressures *versus* flow rate was made at four temperatures to determine equilibrium values shown on Fig. 3. These results are in good agreement with those predicted by extrapolation of a line through vapor pressures given by Ringwald and with pressures obtained from our diaphragm gage measurements.

Total pressures measured in the diaphragm gages represent the sum of chlorine and Fe_2Cl_6 pressures. For samples (b), (c) and (d) partial pressures of each component were calculated with the aid of equation 6. For (a), in which an excess of chlorine was present, the chlorine pressure was calculated at each temperature (assuming ideal gas behavior) from measured chlorine pressures at low temperatures where the contribution of Fe_2Cl_6 was negligible. Data from all four samples, described in the experimental part, are shown on Fig. 3. As results are indistinguishable, it is concluded that appreciable solid solution of $FeCl_2$ in $FeCl_3$ does not occur below 300°. The line drawn on Fig. 3 corresponds to the equation

$$\log P_{Fe_2Cl_6}(\text{mm.}) = \frac{-7142}{T} + 15.111 \qquad (7)$$

Total pressures of iron(III) chloride vapor and chlorine measured in the diaphragm gage are in good agreement with the results of Stirnemann[3] and of Johnstone, *et al.*[5] near the melting point, though somewhat higher at lower temperatures.

Chlorine pressures were measured in a number of flow experiments in which both $FeCl_2$ and $FeCl_3$ solid phases were present, thus characterizing reaction 4. It was observed in this case that equilibrium is established very slowly from both directions (*i.e.*, reaction of excess chlorine with $FeCl_2$ or by decomposition of $FeCl_3$) which makes the system difficult to study by flow methods. At two temperatures sufficient information was obtained to make a plot of chlorine pressures *versus* argon flow rate for the decomposition of $FeCl_3$; however, con-

TABLE I

SUMMARY OF RESULTS OF VARIOUS INVESTIGATORS

Ref.	Temp. range, °C.	$\log P = -(A/T) + B$ A	B	ΔH^0, kcal. (mean)	ΔS^0, e.u.[a] (mean)	Pressure Fe_2Cl_6 (mm.) 220°	260°	300°
			Reaction 1					
2	216–304	6674	14.161	30.5	51.62	4.3	44.1	330
3	253–301	7498	15.733	34.3	58.81	3.4	46.9	449
4	240–296	6575	13.928	30.1	50.55	4.0	39.5	286
5	232–289	7511	15.778	34.4	59.02	3.5	49.1	472
8	200–280	8070	17.366	36.9	66.28	10.1	170.1	1936
9	251–302	7038	14.941	32.2	55.19	4.7	55.1	460
10, 11	Extrapol.	7817	16.01	35.8	60.09	1.4	22.4	237
This work	160–304	7142	15.111	32.7	55.97	4.3	52.0	448
			Reaction 3 $K = \frac{P_{Cl_2}}{P_{Fe_2Cl_6}}$					
		$\log K = -(A/T) + B$						
9	251–302	−2228	−5.058	−10.2	−23.14			
11	333–697	−2147	−4.682	− 9.82	−21.42			
This work	220–400	−1408	−3.710	− 6.44	−16.98			

[a] P^0 = 1 atm.

trary to customary flow data, these plots did not show a plateau. Extrapolation to zero flow led to the predicted equilibrium pressures shown on Fig. 4.

A summary of results of various investigators for reactions 1 and 3 is given in Table I. To facilitate comparison of Fe_2Cl_6 vapor pressures, partial pressures of chlorine, calculated from equation 6 and the total pressures, have been subtracted from results of investigators who reported only total pressures.

Using heat capacity data of Moore[18] ($FeCl_2$) and Kelley[19] (Cl_2) and the function suggested by Kangro and Petersen[11] for $Fe_2Cl_6(g)$, $\Delta C_p^0 = 13.9$ was estimated for reaction 3 and used to correct the constants in equation 6 from a mean temperature of 575°K. to the mean temperature for equation 7, 519°K. Combination of the two then gives the expression

$$\log P_{Cl_2}(\text{mm.}) = \frac{-5565}{T} + 11.085 \qquad (8)$$

for reaction 4. This line is shown on Fig. 4 in comparison with chlorine pressures measured in this work and with data of Schafer and Oehler[10] and of Ringwald.[9]

A ΔC_p^0 of −4.6 for reaction 4, estimated from the heat capacity data cited above, and results for $FeCl_3(s)$ reported by Todd and Coughlin[20] leads to values of $\Delta H^0 = 26.5$ kcal. and $\Delta S^0 = 40.1$ e.u. (standard state of $Cl_2(g)$ taken as one atmosphere) at 25°. Taking −81.5 kcal. and 28.19 e.u. as the standard heat of formation[21] and entropy[22] of $FeCl_2(s)$, respectively, and 53.3[21] for $S_{Cl_2}^0$, values of $\Delta H^0 = -94.7$ kcal. and $S^0 = 34.8$ e.u. are calculated for $FeCl_3(s)$ at 25°. Todd and Coughlin obtained 32.2 ± 0.4 e.u. for the entropy of $FeCl_3(s)$ from their heat capacity data, measured from 50 to 298°K., neglecting possible transitions between 0 and 50°K. The heat of formation is somewhat larger than the value −93.4 kcal. observed in heat of solution studies in this Laboratory,[23] but the difference is within experimental and extrapolation uncertainties.

Correcting the constants in equation 6 (reaction 3) to 25° with the estimated ΔC_p^0 of 13.9 and using the standard values for $FeCl_2$ and Cl_2 cited above, ΔH^0 and S^0 are calculated to be −152.6 kcal. and 135.9 e.u. for $Fe_2Cl_6(g)$ at 25°. These values are confirmed by equation 7 assuming $\Delta C_p^0 = -19$ and thermodynamic properties of $FeCl_3(s)$ calculated above. The latter is not entirely an independent check, however, as about half of the data used to establish equation 7 were obtained with the aid of equation 6. If ΔH^0 is taken as −93.4 kcal. for $FeCl_3(s)$, equation 7 gives $\Delta H^0 = -150.2$ kcal. for $Fe_2Cl_6(g)$ at 25°.

(18) G. E. Moore, *J. Am. Chem. Soc.*, **65**, 1700 (1943).

(19) K. K. Kelley, U. S. Bureau of Mines, Bulletin 476, 1950.

(20) S. S. Todd and J. P. Coughlin, *J. Am. Chem. Soc.*, **73**, 4184 (1951).

(21) National Bureau of Standards, Circ. 500, "Selected Values of Chemical Thermodynamic Properties," U. S. Government Printing Office, Washington, D. C., 1950.

(22) Private communication from E. F. Westrum, Jr., Department of Chemistry, University of Michigan.

(23) J. C. M. Li and N. W. Gregory, *J. Am. Chem. Soc.*, **74**, 4670 (1952).

HEATS OF VAPORIZATION OF MOLECULES AT LIQUID–VAPOR INTERFACES

BY BERT H. CLAMPITT AND DALE E. GERMAN

Boeing Airplane Company, Wichita Division, Wichita, Kansas

Received November 18, 1957

A theory is developed whereby it is shown quantitatively that the heat of vaporization of the surface layer at a liquid vapor interface is appreciably lower than the heat of vaporization of bulk liquid. The BET adsorption theory is reviewed in light of the present theory and it has been found that the BET "c" constant assumes a new meaning allowing calculations of heats of adsorption in closer agreement with experiment. By calculation of the ratio of heats of vaporization of surface and bulk molecules it is possible to establish whether a given liquid is hydrogen bonded and its type and degree of hydrogen bonding.

Introduction

The assumption is commonly made in gas adsorption theories that the heat of adsorption of the second and higher layers of molecules is equal to the heat of vaporization of bulk liquid and is independent of the number of adsorbed layers.[1] It should be pointed out, however, that the heat of vaporization of the final adsorbed layer is substantially different from bulk liquid. This causes the total heat of vaporization of the liquid above the first adsorbed layer to be a function of the thickness. This note is for the purpose of demonstrating a simple method of calculating the heat of vaporization of the final adsorbed layer.

Method.—Consider two drops of liquid, one of infinitely large radius, and one of small radius (r). The Clausius–Clapeyron equation may be assumed to hold in each case and equation 1 may be written.

$$\frac{\mathrm{d}\ln p/p^0}{\mathrm{d}T} = \frac{\Delta H - \Delta H^0}{RT^2} \qquad (1)$$

where p refers to the vapor pressure, T the temperature, R the gas constant, ΔH the heat of vaporization and the superscripted symbols refer to the drop of infinite radius.

Considering each drop as composed of a bulk component (b) and a surface component (s), a modified form of Raoult's law yields the equations

$$\Delta H = X_b\,\Delta H_b + X_s\,\Delta H_s \qquad (2)$$

$$\Delta H^0 = X_b^0\,\Delta H_b + X_s^0\,\Delta H_s \approx \Delta H_b \qquad (3)$$

Substituting equation 3 into equation 2 and imposing the obvious restriction $X_b = 1 - X_s$ yields

$$\Delta H - \Delta H^0 = X_s(\Delta H_s - \Delta H^0) \qquad (4)$$

The composition of the surface and bulk being the same for pure liquids, volume fraction may be substituted for mole fraction

$$X_s = \frac{4\pi r^2 t}{4/3\pi r^3 + 4\pi r^2 t} \approx \frac{3t}{r} \qquad (5)$$

where (t) is the thickness of the surface layer and (r) is the radius of the drop. Combining equations 1, 4 and 5 yields

$$\frac{\mathrm{d}\ln p/p^0}{\mathrm{d}T} = \frac{3t(\Delta H_s - \Delta H^0)}{rRt^2} \qquad (6)$$

In this form equation 6 cannot be solved for ΔH_s; however it contains terms found in the Kelvin equation

$$\ln p/p^0 = \frac{2M\gamma}{r\rho RT} \qquad (7)$$

where in addition to the previously defined terms, M is the molecular weight, γ the surface tension and ρ the density. Differentiating (7) with respect to temperature (assuming ρ to be independent of temperature) yields

$$\frac{\mathrm{d}\ln p/p^0}{\mathrm{d}T} = \frac{2M}{r\rho R}\left[\frac{1}{T}\frac{\mathrm{d}\gamma}{\mathrm{d}T} - \frac{\gamma}{T^2}\right] \qquad (8)$$

(1) S. Brunauer, "The Adsorption of Gases and Vapors," Princeton University Press, Princeton, N. J., 1945, pp. 151–168.

Combining equations 6 and 8

$$\frac{\mathrm{d}\gamma}{\mathrm{d}T} - \frac{\gamma}{T} = \frac{3t\rho}{2MT}(\Delta H_s - \Delta H^0) \qquad (9)$$

Integrating (9)

$$\frac{\gamma}{T} = \frac{3t\rho}{2M}\int \frac{\Delta H_s - \Delta H^0}{T^2}\,\mathrm{d}T \qquad (10)$$

t may be any integral number of molecular layers and the mathematics that follow are applicable. Due to the short range nature of intermolecular forces, the surface layer will be assumed to be unimolecular, in which case t can be estimated as the cube root of the molecular volume. Equation 10 therefore becomes

$$\gamma\left(\frac{M}{\rho}\right)^{2/3} = 0.74T\int \frac{\Delta H_s - \Delta H^0}{T^2}\,\mathrm{d}T \qquad (11)$$

where the ΔH terms are expressed in calories per mole. Differentiating equation 11 with respect to temperature gives

$$\frac{\mathrm{d}[\gamma(M/\rho)^{2/3}]}{\mathrm{d}T} = 0.74\left[\int \frac{\Delta H_s - \Delta H^0}{T^2}\,\mathrm{d}T + \frac{\Delta H_s - \Delta H^0}{T}\right] \qquad (12)$$

The negative of the differential term is the well known Eotvos constant (k) which has been evaluated for a large number of liquids. Solution of equation 11 for the integral and substitution into equation 12 yields

$$\Delta H_s = \Delta H^0 - 1.35[kT + \gamma(M/\rho)^{2/3}] \qquad (13)$$

Equation 13 contains terms that are easily obtainable from the literature and provides a means of directly calculating the heats of vaporization of the surface layers of pure liquids.

Results and Discussion

Table I gives values for ΔH_s for various substances calculated by means of equation 13. Using these tabulated values of ΔH_s equation 2 yields the heat of vaporization for that liquid (n layers) above the first adsorbed layer. A plot of n *versus* the total heat of vaporization of the n layers for several liquids is shown in Fig. 1. It is seen that the total heat of vaporization approaches the heat of vaporization of bulk liquid asymptotically and that the ΔH values are significantly lower that that ΔH^0 for n less than ten.

The Brunauer–Emmett–Teller (BET) theory assumes that for all layers above the first adsorbed layer the heat of adsorption is equal to the heat of vaporization of bulk liquid. This assumption fails to take into account that even if the molecules behaved as if they were in a true liquid, the heat of vaporization is dependent upon the number of layers of liquid present. Following the notation of Brunauer[1] but without imposing the restriction

$$E_2 = E_3 = E_i = E_L$$

$$s_i = s_0 y (p/g)^{i-1} \exp(E_2 + E_3 - - - + E_i)/RT \qquad (14)$$

TABLE I

HEAT OF VAPORIZATION OF THE SURFACE LAYER OF VARIOUS LIQUIDS AT THEIR BOILING POINTS

Substance	ΔH^0 (cal./mole)	ΔH_s (cal./mole)	$\Delta H_s/\Delta H^0$
Carbon tetrachloride	7180	5535	0.771
Benzene	7345	5685	.774
n-Hexane	7190	5610	.780
m-Xylene	8690	6895	.793
Toluene	7985	6325	.792
Diethyl ether	6210	4810	.775
Hydrogen	216	168	.778
Nitrogen	1330	995	.750
Oxygen	1630	1235	.758
Argon	1560	1170	.750
Neon	450	350	.778
Acetone	7220	5910	.818
Water	9720	8565	.881
Methyl alcohol	8410	7650	.910
Ethyl alcohol	9400	8555	.910
n-Propyl alcohol	9865	8770	.889
n-Butyl alcohol	10455	8955	.857
Acetic acid	5810	4735	.815
Propionic acid	7310	6090	.833
Butyric acid	10030	8655	.865
Hydrogen cyanide	6025	5310	.881

The BET theory replaces $(E_2 + E_3 - - - + E_i)$ with $(i - 1)E_L$ and this is probably permissible if E_L is assumed to be a function of i. According to equation 2 E_L is

$$E_L = \frac{i-2}{i-1}\Delta H^0 + \frac{1}{i-1}\Delta H_s \qquad (15)$$

Equation 14 therefore becomes

$$s_i = s_0 y (p/g)^{i-1} \exp(i\Delta H^0 - 2\Delta H^0 + \Delta H_s)/RT \qquad (16)$$

According to reference 1

$$y = (a_1/b_1)p \exp(E_1/RT) \qquad (17)$$

Equation 16 then becomes

$$s_i = s_0(a_1 g/b_1)(p/g)^i \exp(i\Delta H^0 + E_1 - 2\Delta H^0 + \Delta H_s)/RT \qquad (18)$$

or

$$s_i = s_0 c x^i \qquad (19)$$

where

$$x = (p/g) \exp(\Delta H^0/RT) \qquad (20)$$

as in the derivation of the BET equation. Significantly, however, the constant "c" now assumes a new meaning

$$c = (a_1 g/b_1) \exp(E_1 - 2\Delta H^0 + \Delta H_s)/RT \qquad (21)$$

as opposed to the BET

$$c = (a_1 g/b_1) \exp(E_1 - E_L)/RT \qquad (22)$$

In the latter two equations E_L and ΔH^0 have the same meaning, namely, the heat of vaporization of bulk liquid. Since equations 19 and 20 are identical to those used in the derivation of the BET equation, the adsorption equations obtained are the same, with the important exception that the constant "c" now has the revised meaning [equation 21].

$E_1 - E_L$ values often are calculated from the BET "c" values; however, they are actually $E_1 - 2\Delta H^0 + \Delta H_s$ values. This is borne out by the work of Harkins and Boyd[2] who measured the true $E_1 - E_L$ for crystalline powders from heat of emersion experiments. They found $E_1 - E_L$ equals 5.2 kcal./mole for benzene on TiO_2 at 25° while the BET energy was 2.6 kcal./mole. As has been indicated, it is not correct to compare these values, but rather

$$2.6 = E_1 - E_L + (\Delta H_s - E_L)$$

The term in the parentheses is, according to Table I, −1.7 kcal./mole, and therefore $E_1 - E_L$ equals 4.3 kcal./mole according to the revised BET plot. It is readily seen that the revised BET theory yields $E_1 - E_L$ values in better agreement with experimental $E_1 - E_L$ data than does the original theory.

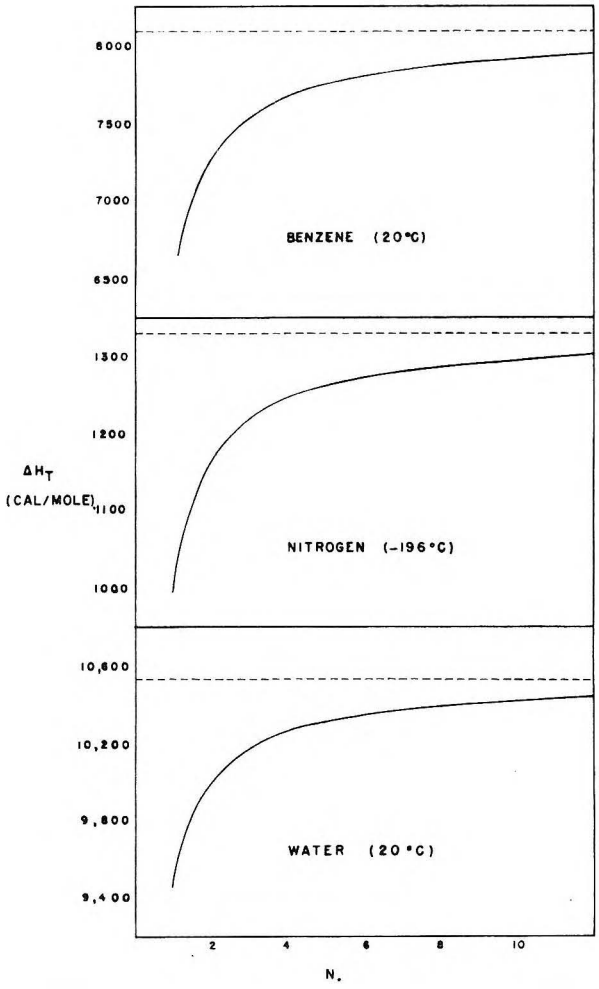

Fig. 1.—Total heat of vaporization *versus* the number of adsorbed layers above the first.

The heat of vaporization of a liquid is a measure of the ease with which a molecule may be removed from the liquid. The ratio between the heats of vaporization of surface and bulk molecules should represent, therefore, a measure of the strength of bonding between molecules in the liquid state. From geometric considerations it is often assumed that surface molecules experience approximately three-fourths the forces experienced by bulk molecules. Table I shows that for non-associated liquids

(2) W. D. Harkins and G. E. Boyd, *J. Am. Chem. Soc.*, **64**, 1195 (1942).

at their boiling point $\Delta H_s/\Delta H^0$ is between 0.75 and 0.79. For hydrogen bonded liquids this ratio is larger, the magnitude of the ratio increasing as the strength of hydrogen bonding increases. The values indicate that the lower alcohols show stronger hydrogen bonding than water which is in conformity with the findings of Pauling.[3]

Table I indicates that $\Delta H_s/\Delta H^0$ values for alcohols decrease with increasing chain length; while the reverse is true for organic acids. Because an increase in chain length results in an increase in the boiling point of a given homologous series a decrease in bond strength at the boiling point would be expected. The results for acids suggest a change in type of bonding with increasing chain length. Both acids and alcohols are strongly hydrogen bonded; however, acids show a great tendency to form dimers. It appears, therefore, that with increasing chain length the acids decrease in dimeric hydrogen bonding and increase in infinitic lattice hydrogen bonding.

The theory presented above for the heat of vaporization of the liquid–vapor surface layer should prove of value to workers investigating surface phenomena. It also should be useful in differentiating types of bonding.

(3) L. Pauling, "The Nature of the Chemical Bond," Cornell Press, Ithaca, N. Y., 1948, p. 304.

COMPARATIVE HEAT STABILITIES OF SOME METAL ACETYLACETONATE CHELATES

BY ROBERT G. CHARLES AND M. ARLENE PAWLIKOWSKI

Westinghouse Research Laboratories, Pittsburgh 35, Pennsylvania

Received November 19, 1957

The heat stabilities of the acetylacetonates derived from a number of different metals have been compared at 191° in an inert atmosphere. The observed stability is markedly dependent upon the nature of the metal present. No very general correlations were observed between the heat stabilities and other properties of the acetylacetonates, or with the properties of the parent metal ions.

Few quantitative data are available for the heat decomposition of metal acetylacetonates (I, x = 1,2,3 or 4).[1] The Cr(III)[2] and Be(II)[3] acetylacetonates reportedly boil at atmospheric pressure without decomposition. On the other hand the rare earth acetylacetonates decompose at temperatures below that required to volatilize these chelates.[3] Relatively little is known of the temperature sensitivity of the numerous other acetylacetonates which have been synthesized.[4] Because of recent interest in organic polymers containing metal-(β-diketone) units,[5,6] it was thought of value to study the relative heat stabilities of acetylacetonates derived from a variety of metals.

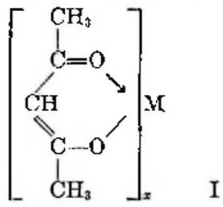

I

The experimental method chosen for this study involved measuring the pressure increase caused by the formation of volatile decomposition products in a closed system containing metal acetylacetonate and an inert gas.

(1) The quantity x = 1 for monovalent metals, 2 for divalent, 3 for trivalent, and 4 for tetravalent. Only neutral chelates formed by acetylacetone with metals are considered here.

(2) G. Urbain and A. Debierne, *Compt. rend.*, **129**, 302 (1899).

(3) "The Chemistry of the Coördination Compounds," J. C. Bailar, Jr., Ed., Reinhold Publ. Corp., New York, N. Y., 1956, p. 42.

(4) G. T. Morgan and H. W. Moss, *J. Chem. Soc.*, **105**, 189 (1914).

(5) J. P. Wilkins and E. L. Wittbecker, U. S. Patent 2,659,711 (Nov. 17, 1953).

(6) W. C. Fernelius, Wright Air Development Center, WADC 56-203 (Oct. 1956).

Experimental

Preparation of Compounds.—All of the compounds used here have been described in the literature.[4,6-8] In certain instances, however, it was found desirable to modify the literature method of preparation or to replace it by a more convenient procedure.

The three alkali metal acetylacetonates, and the Ba chelate, were prepared by treating the corresponding metal hydroxide with acetylacetone in methanol or water solution. The Ca and Sr chelates were prepared from the metal nitrates, acetylacetone, and a stoichiometric quantity of KOH in water solution.

The Ni(II) acetylacetonate was prepared in the following manner. To a solution of 59.4 g. (0.25 mole) $NiCl_2 \cdot 6H_2O$ in 250 ml. of water was added a solution of 50 g. of acetylacetone (0.5 mole) in 100 ml. of methanol, while stirring. To the resulting mixture was added a solution of 0.5 mole of sodium acetate in 150 ml. of water. The mixture was heated briefly on a hot plate, cooled to room temperature, and placed in the refrigerator for several hours. The green solid was filtered off on a buchner funnel, washed with water, and dried in a vacuum desiccator.

Most of the remaining divalent metal acetylacetonates (plus the Fe(III) compound) were prepared in a manner similar to that used for the nickel chelate. The gallium and indium chlorides were prepared from the metals and reacted with acetylacetone in water in the presence of aqueous NH_3. The Co(III) acetylacetonate was prepared from $CoCO_3$, acetylacetone and hydrogen peroxide. The Mn(III) chelate was prepared by the method of Cartledge[9] and the Zr(IV) chelate by the method of Larsen, Terry and Leddy.[10] We are indebted to the members of the Insulation Department, Westinghouse Research Laboratories, for providing us with pure samples of the Be(II), Cr(III) and Al(III) acetylacetonates.

The majority of the acetylacetonates were recrystallized, one or more times, using the solvents listed in Table I.

(7) W. C. Fernelius and B. E. Bryant, *Inorganic Syntheses*, **5**, 105 (1957).

(8) N. V. Sidgwick, "The Chemical Elements and Their Compounds," Oxford University Press, 1950.

(9) G. H. Cartledge, *J. Am. Chem. Soc.*, **73**, 4416 (1951).

(10) E. M. Larsen, G. Terry and J. Leddy, *ibid.*, **75**, 5107 (1953).

The Be(II), Fe(III), Al(III), Cr(III), Co(III) and Zn(II) acetylacetonates were dried overnight in a vacuum desiccator over anhydrous $CaSO_4$. The remainder of the compounds were dried four hours at 100° and 1 mm. in an Abderhalden drying apparatus. The chelates were stored in tightly capped bottles in a desiccator to prevent hydration.

TABLE I

PREPARATION OF METAL ACETYLACETONATES

Metal	Recrystallized from	Metal, % Calcd.[d]	Found
Li	Methanol	6.54	6.62
Na	Benzene–methanol[a]	18.8	19.1
K	Methanol	28.3	27.8
Be(II)	Benzene–pet. ether[a]		[e]
Mg(II)	Methanol	10.9	10.8
Ca(II)	Methanol[b]	16.8	16.6
Sr(II)	Methanol[b]	30.6	30.2
Ba(II)	Methanol	40.9	39.4
Cr(III)	Benzene–pet. ether[a]		[f]
Mn(II)	[c]	21.7	21.8
Mn(III)	Benzene–pet. ether[a]		[g]
Fe(III)	Methanol–water	15.8	15.7[h]
Co(II)	Methanol	22.9	23.3
Co(III)	Benzene–pet. ether[a]		[i]
Ni(II)	Methanol	22.8	22.8
Cu(II)	Methanol	24.3	24.0
Zn(II)	Acetylacetone–pet. ether[a]	24.8	24.8
Cd(II)	Acetylacetone–pet. ether[a]	36.4	35.9
Al(III)	Methanol–water		[j]
Ga(III)	Methanol		[k]
In(III)	Methanol		[l]
Zr(IV)	Benzene–pet. ether[a]	18.7	18.5

[a] The chelate was dissolved in the first named solvent and precipitated with the second. [b] Not recrystallizable. Purified by extraction with solvent. [c] Too easily oxidized to permit recrystallization by the usual means. [d] Calculated for the anhydrous compound. [e] M.p. 108–109°. [f] M.p., 213–215°. [g] Calcd. for $Mn(C_5H_7O_2)_3$: C, 51.1; H, 6.01; ash (as Mn_3O_4), 21.6. Found: C, 51.2; H, 6.34; ash, 22.0. [h] M.p. 178–183°. [i] Calcd. for $Co(C_5H_7O_2)_3$: C, 50.6; H, 5.94. Found: C, 49.8; H, 5.80. [j] M.p. 194–195°. [k] M.p. 197–199°. [l] M.p. 189–190°.

The identity and purity of the dried compounds were established, in most cases, by metal analysis. Table I lists the values obtained. The Be(II), Al(III), Ga(III), In(III) and Cr(III) acetylacetonates were characterized by their melting points which were sharp, reproducible and in agreement with literature values. The significant thermal decomposition of many of the remaining compounds, at or below the melting point, makes melting point an unreliable criterion of purity for these cases.

Experimental Method and Apparatus.—Of the various experimental approaches possible for this type of work the measurement of the volatile decomposition products produced appeared the most promising. Methods based on weight loss of the chelate as a function of time were rejected because of the tendency of a number of the acetylacetonates to sublime. Methods based on analysis for unchanged acetylacetonate were also considered unsuitable for survey work since each chelate would necessitate a separate experimental technique.

The method adopted consisted in measuring pressure changes in an all glass system containing nitrogen gas and the acetylacetonate. The Pyrex glass apparatus used is shown in Fig. 1. Decomposition took place within the lower portion of the flask G within a constant temperature metal block oven. The close fitting removable glass plug D served to minimize the volume of gas outside the oven and also retarded the diffusion of volatile materials out of the hot zone. The clearance between the glass plug and flask neck was sufficient to allow instantaneous pressure equilibrium between G and the manometer. The temperature within the oven was maintained at 191 ± 0.2° by means of the metal block oven F. The temperature in G was determined in blank runs by means of a precision mercury-in-glass thermometer, the neck of the flask in this case being filled with glass wool.

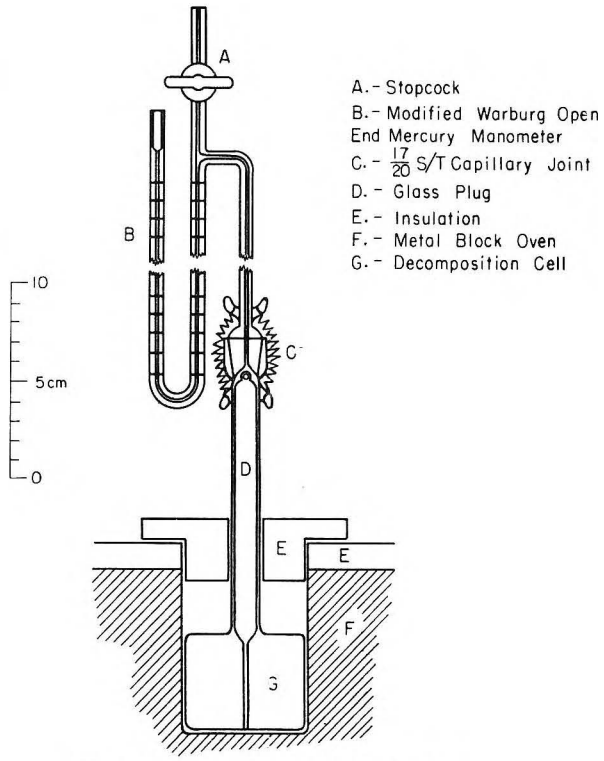

Fig. 1.—Heat decomposition apparatus.

Three pieces of apparatus of the type shown in Fig. 1 were, in general, used simultaneously, using three ports in the same metal block oven. The reproducibility of results was found to be nearly the same for simultaneous runs in different apparatus as that obtained for successive runs in the same apparatus. Some runs were also made in apparatus similar to that shown in Fig. 1 but having a shorter flask neck (without the glass plug D) and with the joint C completely within the oven F. In the latter case the joint was lubricated with high-temperature silicone stopcock grease which showed no decomposition under the conditions used. This apparatus gave essentially the same results as the apparatus in Fig. 1 but, being somewhat less convenient than the apparatus shown, was abandoned in favor of the latter.

The gas volume of the apparatus was determined by weighing the amount of water necessary to fill the apparatus above the capillary joint. To the volume obtained was added a small correction term calculated from the diameter of the capillary in the manometer and its length from the joint to the mercury meniscus.

For a run, approximately 0.2 g. of the pure dry acetylacetonate was weighed accurately into a small glass vial. This was dropped through the neck of the flask (plug D removed) into G and allowed to spill over the bottom of the flask. The size of the crystals were those obtained from recrystallization and no attempt was made to grind to a finer powder. The apparatus was then assembled as shown in Fig. 1, greasing the stopcock A and joint C with silicone stopcock grease. The tube above A was then connected by rubber pressure tubing to a stopcock arrangement in such a way that a partial vacuum or a small positive pressure of dry nitrogen could be applied alternately. The apparatus was partially evacuated (nearly to the capacity of the manometer) and then nitrogen introduced to a pressure somewhat above atmospheric. This process was repeated a total of twenty times in order to remove oxygen as completely as possible. Finally the nitrogen pressure within the apparatus was adjusted to about 450 mm. at room temperature and the stopcock A closed.

Manometer readings, together with barometer and room temperature readings, were recorded and the apparatus placed in the oven. Manometer and barometer readings were then taken as a function of time. Blank experiments (no chelate present) indicated that temperature equilibrium

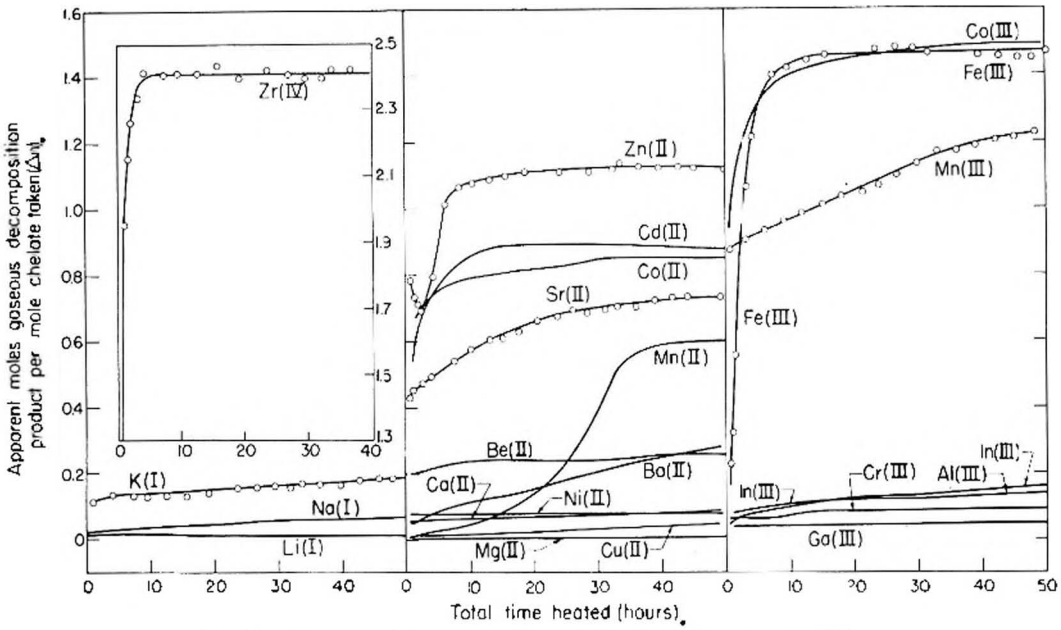

Fig. 2.—Decomposition curves for metal acetylacetonates at 191°.

was reached within the first half hour. Most of the experiments were run for a total of either one or 50 hours. At the conclusion of these time intervals the apparatus was removed from the oven and allowed to cool to room temperature. Manometer, barometer and room temperature readings were then again taken.

Calculations and Calibrations.—Results obtained in these experiments were most conveniently expressed in terms of the quantity Δn given by 1

$$\Delta n = (\Delta P)V/RTm \qquad (1)$$

where ($\Delta P = P_2 - P_1$) is the pressure rise at the end of a given time interval above the equilibrium pressure P_1, attained in the absence of chelate; V is the gas volume of the system; R is the gas constant; T is the absolute temperature; and m is the number of moles of metal chelate taken for the experiment.

Since a small but significant fraction of the total gas volume for the apparatus is out of the oven (Fig. 1), the actual value of P_1 in any experiment is somewhat lower than the value calculated from 2.

$$P_1 = \frac{T_{191}P_r}{T_r} \qquad (2)$$

where P_r and T_r are the pressure and absolute temperature at room temperature. For this reason an empirical relationship between P_1 and P_r was determined using various amounts of nitrogen in blank experiments. This relationship was then used to calculate P_1 for each decomposition experiment. The values of P_1 calculated in this way were about 2% smaller than those calculated from (2).

Also for the reason just mentioned an effective value, b, of (V/RT) at 191° was calculated from 3.

$$b = \frac{P_r}{P_1}\left(\frac{V}{RT_r}\right) \qquad (3)$$

The value b was found to be about 3% larger than that calculated from V/RT assuming all the gas to be at 191°. The experimentally determined value of b for each apparatus was used to calculate Δn for experiments performed in that apparatus.

In order to obtain some estimate of the amount of gaseous decomposition product present at room temperature, the apparatus was cooled for an hour at the conclusion of each run and the quantity Δn calculated from 1 using the values of ΔP and T determined at room temperature.

Results and Discussion

In Fig. 2 the quantity Δn at 191° is plotted as a function of time for each of the acetylacetonates investigated. Table II compares the values of Δn obtained at the conclusion of the experiments at 191°, when measured at 191°, with the values measured at room temperature for the same runs.[11]

For the ideal case, where the simple gas laws are obeyed and the metal chelate has no appreciable vapor pressure, Δn can be taken as a measure of the number of moles of decomposition product which are gaseous at the temperature of measurement (per mole of chelate taken). In practice some of the chelates may be expected to have a measurable vapor pressure at 191° and Δn, when measured at 191°, would then be correspondingly larger than the quantity just mentioned.

Vapor pressure data for the metal acetylacetonates at 191° are completely lacking. For some of the compounds, however, an estimate of the vapor pressure at this temperature can be obtained from reported data at other temperatures.[7,12] From such data the vapor pressures at 191° for the Al(III), Cr(III), Ni(II) and Be(II) acetylacetonates are estimated to be 8, 4, 3 and 63 mm. respectively.[13] The values of Δn corresponding to these vapor pressures are, respectively, 0.04, 0.02, 0.01 and 0.22.

Vapor pressures have not been reported for the other metal acetylacetonates investigated. It may be assumed, however, that all of these will have vapor pressures that are appreciably lower than the vapor pressure of the Be compound, considering (a) the higher molecular weights of most of these

(11) The curves in Fig. 2 and the values in Table II are for typical individual runs. For many of the compounds two or more runs were made. In general Δn for a given time of heating was reproducible to 0.03 unit or less for duplicate runs. For the sake of clarity, experimental points are included only for representative curves in Fig. 2.

(12) I. E. Coop and L. E. Sutton, *J. Chem. Soc.*, 1269 (1938).

(13) The vapor pressures of the Al(III), Cr(III) and Ni(II) acetylacetonates were calculated from existing data making the approximation that the latent heat of vaporization is the same as that found for aluminum isovalerylacetonate (20.3 kcal./mole).[14] The vapor pressure of Be(II) acetylacetonate was calculated from the reported boiling point of 270°[7] and the approximate vapor pressure at 185°.[12]

(14) R. G. Charles, *J. Inorg. Nucl. Chem.*, in press.

compounds, and (b) the greater intermolecular forces in these chelates, as evidenced by their higher melting points. It seems likely, therefore, that only in the case of the Be chelate does the vapor pressure make a large contribution to Δn.

TABLE II

DECOMPOSITION OF METAL ACETYLACETONATES AT 191°

	Δn			
	Heated 1 hr. at 191° measured at		Heated 50 hr. at 191° measured at	
Metal	191°	27°	191°	27°
Li			0.01	0.02
Na			.07	.07
K	0.10	0.03	.19	.17
Be(II)	.17	.02	.26	.06
Mg(II)			.01	.03
Ca(II)			.09	.08
Sr(II)	.51	.45	.73	.68
Ba(II)			.28	.27
Cr(III)			.09	.09
Mn(II)			.60	.39
Mn(III)	.92	.23	1.23	.86
Fe(III)	.33	.19	1.47	1.24
Co(II)	.59	.72	0.85	0.76
Co(III)	1.05	.27	1.49	1.27
Ni(II)	0.08	.04	0.07	0.06
Cu(II)			0.04	.04
Zn(II)	.74	.47	1.12	.92
Cd(II)	.52	.46	0.88	.70
Al(III)			.14	.06
Ga(III)			.04	.04
In(III)	.01	.03	.16	.16
Zr(IV)	1.77	1.08	2.36	1.99

It can be seen from Fig. 2 that many of the acetylacetonates, derived from metal ions of all four charge types, decompose significantly under the conditions employed. Both the rate and ultimate extent of decomposition are markedly dependent on the nature of the metal present in the chelate. For many of the more unstable acetylacetonates much of the decomposition takes place during the first few hours, after which the value of Δn tends toward a limit. An obvious exception is Mn(II) acetylacetonate which reaches its maximum rate of decomposition only after 30 hours of heating. An even more peculiar curve is given by Zn(II) acetylacetonate. A rather high value of Δn is reached after 0.5 hour then decreases with time to a minimum at 2.5 hours and finally increases rapidly to a constant value. The differences in shape of the curves obtained and the fact that the same ultimate value of Δn is not reached in all cases indicates that the nature, as well as the rate, of decomposition may be a function of the metal present. Among the most heat stable acetylacetonates are the Li(I), Mg(II), Be(II), Cu(II), Ni(II), Ga(III) and Cr(III) compounds. It would seem that the last six of these metals would also be the metals most likely to yield heat stable polymers of the β-diketone type.[5,6] The acetylacetonate studied having the lowest heat stability was found to be Zr(IV) acetylacetonate.

No very general correlations were noted between the heat stabilities of the acetylacetonates and parameters associated with the metal, such as cation charge, cation size, electronic configuration, or position in the periodic table. Also, no general relationship was observed relating the heat stability to other properties of the metal chelates, such as the stability toward dissociation to ions in aqueous solution.[15-17] For limited groups of metals, however, some trends were noted.

For the alkali metal acetylacetonates the heat stability decreases with increasing atomic weight of the metal. This is also the order for decreasing stability toward dissociation in solution for this type of chelate.[18] The same trend is observed for the group IIA elements, with, however, Sr (and possibly Be) out of place. The order is reversed for the IIB elements Zn and Cd, the compounds both being quite unstable. The group IIIA elements Al, Ga and In all give rather stable acetylacetonates but, within the group, there is no obvious correlation with atomic weight.

A considerable variation in heat stability was noted among the acetylacetonates derived from the metals of the first transition series. The trivalent Mn, Co and Fe chelates were found to be quite unstable while the Cr(III) acetylacetonate was one of the most stable compounds. The Mn(II) and Co(II) compounds were also found to be unstable. The extent of decomposition after 50 hours was found to be less for the latter compounds than for the corresponding trivalent metal chelates. This may be related to the fact that the Mn(III) and Co(III) chelates have three acetylacetone residues per molecule while the corresponding divalent compounds have only two. The other two divalent metal chelates of this series, Ni(II) and Cu(II) acetylacetonates, were found to be much more stable than the Mn(II) and Co(II) compounds. It is interesting that the Cu(II) and Ni(II) chelates are also the most stable of the divalent transition metal acetylacetonates studied toward dissociation in aqueous solution.[15,15]

A property of the acetylacetonates which was expected to be of importance in this work was melting point since, at 191°, some of the chelates are (at least initially) liquid and others solid.[19] Unstable and stable compounds were, however, found in both groups. It appears that a study of decomposition as a function of temperature would be necessary to evaluate the importance of the physical state to the decomposition for these compounds.

The final values of Δn for each of the experiments is compared in Table II with Δn calculated from the data obtained at room temperature. In nearly all cases the value of Δn at 27° is lower than that calculated from data at 191°, presumably due to condensation of some of the decomposition products.

(15) L. G. Van Uitert, W. C. Fernelius and B. E. Douglas, *J. Am. Chem. Soc.*, **75**, 2736 (1953).

(16) R. M. Izatt, W. C. Fernelius and B. P. Block, THIS JOURNAL, **59**, 80 (1955).

(17) R. M. Izatt, W. C. Fernelius, C. G. Haas, Jr., and B. P. Block, *ibid.*, **59**, 170 (1955).

(18) W. C. Fernelius and L. G. Van Uitert, *Acta Chem. Scand.*, **8**, 1726 (1954).

(19) The literature melting points of the Be(II), Zn(II), Mn(III), Fe(III) and In(III) acetylacetylacetonates are below 191°, while the Al(III), Ga(III) and Zr(IV) chelates melt within a few degrees of 191°. The rest of the acetylacetonates studied melt considerably above 191°.

The value of Δn at 27° is a measure of the amount of decomposition product still gaseous at room temperature. The fact that Δn at 27° is still large, in many cases, indicates that at least some of the decomposition products are of low molecular weight. The nature of the volatile decomposition products for certain of these compounds is currently being investigated. The results of this study will be reported in a later paper.

The nature of the solid residues obtained from the decomposition of the acetylacetonates was not determined. In general the change in appearance of the chelates paralleled the extent of decomposition, as indicated by Δn. Those acetylacetonates undergoing extensive decomposition generally gave very dark colored, and frequently resinous, residues. It is planned to study the nature of some of these materials.

Acknowledgment.—The authors are grateful to Miss M. I. Mistrik for certain of the analyses.

A THERMODYNAMIC STUDY OF SOME COMPLEXES OF METAL IONS WITH POLYAMINES[1]

BY CHARLES R. BERTSCH, W. CONARD FERNELIUS AND B. P. BLOCK

The Department of Chemistry, The Pennsylvania State University, University Park, Pennsylvania

Received November 22, 1957

The dissociation constants of these several amines have been determined at 10, 20, 30 and 40°: N,N,N′,N′-tetramethylmethanediamine (I), 1,3-propanediamine (II), 1,4-butanediamine (III), *cis*- and *trans*-1,2-cyclohyexanediamines (IV and V, resp.), 2,2′,2″-triaminotriethylamine (VI) and 1,3-diamino-2-propanol (VII), and at 10° for *trans*(?)-1,2-cycloheptanediamine (VIII). Formation constants and enthalpy and entropy changes have been determined for II with Ag^+, Cu^{++} and Ni^{++}; III with Ag^+; IV and V with Cu^{++}, Ni^{++}, Zn^{++} and Cd^{++}; VI with Cu^{++}; and VII with Ag^+ and Ni^{++} at the four temperatures. Formation constants have been determined for VIII with Cu^{++}, Ni^{++}, Zn^{++} and Cd^{++} at 10°. These quantities are compared from one ligand to another with the same metal ion. The difference in stability for the formation of different sized rings is primarily an entropy effect which is related to the strain introduced in the ring and the loss of freedom of the diamine in the chelate. The chelates formed with the cyclic diamines are generally more stable because of a more favorable entropy effect; however, there appear to be exceptions when the metal ion is not the proper size to fit a given diamine and weaker bonds result. An ion-exchange process for preparing diamine solutions directly from diamine salts is described.

Introduction

The publication in 1941 of J. Bjerrum's thesis[2] on equilibria involving metal ion–amine complexes initiated a series of investigations which have demonstrated the effect of (1) chelates *vs.* monodentate ligands,[3] (2) ring size for bidentate amines,[4–6] (3) number of points of attachment,[3] (4) C[3,7–9] and N-substitution,[2,7–11] (5) *d,l*-diamines *vs.* the *meso* forms,[9b] (6) *cis*- *vs.* *trans*-1,2-cyclohexanediamines[12] and (7) substitution of >NH by >S[13] and >O.[14] Many of the values for the equilibrium expressions given in the literature are not strictly comparable one to the other because the measurements were made in solutions of different ionic strength and at varying temperatures. Unfortunately, the measurements for any one system seldom include measurements at more than one temperature. Hence, although there is considerable information about approximate free energies of reaction, very little is known about enthalpies or entropies of reaction.

With these equilibrium constants at hand for a range of temperatures, more satisfactory values for the enthalpies and entropies of reaction can be calculated. In continuation of previous studies[14,15] there are presented here studies of N,N,N′N′-tetramethylmethanediamine, 1,3-propanediamine, 1,-4-butanediamine, *cis*- and *trans*-1,2-cyclohexanediamine, *trans*(?)-1,2-cycloheptanediamine, 2,2′,2″-triaminotriethylamine and 1,3-diamino-2-propanol.

Experimental

Procedure.—The general procedure involved the titration of 100 ml. of solution 0.001 *M* in metal ion and 0.002 *M* in acid with *ca.* 10 ml. of 0.04 to 0.10 *M* amine under nitrogen at 10, 20, 30 and 40°. A Beckman Model G *p*H meter equipped with a saturated calomel electrode and a Beckman Model E No. 1190-80 glass electrode was used to follow the titrations. For the titrations involving silver ion a salt bridge containing saturated potassium nitrate solution (in contact with excess solid) was used to isolate the calomel electrode from the solution in the titrating flask.

The method used to calculate the constants was reported earlier.[16] For these calculations concentrations were converted to activities by application of the Debye–Hückel equation.[15]

(1) From a dissertation presented by Charles R. Bertsch in partial fulfillment of the requirements for the degree of Doctor of Philosophy, August, 1955.

(2) J. Bjerrum, "Metal Ammine Formation in Aqueous Solution," P. Haase and Son, Copenhagen, 1941.

(3) G. Schwarzenbach, Report No. BRL/146, May 1951. Presented at Discussion on Coordination Chemistry held by Imperial Chemical Industries, Ltd. at Welwyn, Herts, September, 1950.

(4) G. R. Hares, W. C. Fernelius and B. E. Douglas, *J. Am. Chem. Soc.*, **78**, 1816 (1956).

(5) F. A. Cotton and F. E. Harris, THIS JOURNAL, **59**, 1203 (1955).

(6) I. Poulsen and J. Bjerrum, *Acta Chem. Scand.*, **9**, 1407 (1955).

(7) J. Bjerrum, *Chem. Revs.*, **46**, 381 (1950).

(8) R. J. Bruehlman and F. H. Verhoek, *J. Am. Chem Soc.*, **70**, 1401 (1948).

(9) (a) F. Basolo and R. K. Murmann, *ibid.*, **74**, 5243 (1952); (b) F. Basolo, Y. T. Chen and R. K. Murmann, *ibid.*, **76**, 956 (1954).

(10) H. Irving, see ref. 3.

(11) F. Basolo and R. K. Murmann, *J. Am. Chem. Soc.*, **76**, 211 (1954).

(12) G. Schwarzenbach and R. Baur, *Helv. Chim. Acta*, **39**, 722 (1956).

(13) E. Gonick, W. C. Fernelius and B. E. Douglas, *J. Am. Chem. Soc.*, **76**, 4671 (1954); C. R. Bertsch, W. C. Fernelius and B. P. Block, THIS JOURNAL, **60**, 384 (1956).

(14) J. R. Lotz, Ph.D. Thesis, The Pennsylvania State University, 1954.

(15) R. M. Izatt, C. G. Haas, Jr., B. P. Block and W. C. Fernelius, THIS JOURNAL, **58**, 1133 (1954).

(16) B. P. Block and G. H. McIntyre, Jr., *J. Am. Chem. Soc.*, **75**, 5667 (1953).

Reagents.—All metal perchlorate and perchloric acid solutions were prepared from G. F. Smith Chemical Co. reagent-grade materials. The concentrations of the solutions were determined by means of standard analytical methods.

The amine solutions were prepared using freshly boiled, distilled water. The normality of each solution was determined by titration with a standardized perchloric acid solution.

Amines.—N,N,N′,N′-Tetramethylmethanediamine (Peninsular ChemResearch, Inc.) was distilled over sodium through a 24″-column packed with glass helices, and the fraction boiling at 82.5° collected; Picon[17] reports 82.5°. 1,3-Diamino-2-propanol (Distillation Products Industries) could not be distilled through a packed column because of its high viscosity and hence was distilled over barium oxide in a simple distillation flask: m.p. 38–40°.

The preparation of pure anhydrous polyamines usually involves large losses and presents difficulties in storage and handling. Therefore, aqueous solutions of several amines were obtained by passing an aqueous solution of the purified hydrochloride or sulfate (twice recrystallized from an alcohol–water mixture) through a column filled with the hydroxide form of Amberlite IRA-400. 1,3-Propanediamine dihydrochloride (L. Light and Co.), 1,4-butanediamine dihydrochloride (Distillation Products Industries), 2,2′,2″-triaminotriethylamine trihydrochloride, *cis*-1,2-cyclohexanediamine dihydrochloride, *trans*-1,2-cyclohexanediamine sulfate,[18] and *trans*(?)-1,2-cycloheptanediamine hydrochloride were treated in this manner. Although the complete recovery of the amine from the column involves too great a dilution for most purposes, complete recovery can be obtained, and, when this is done, the equivalent weight of the amine agrees with that expected

Cycloheptanone (Columbia Organic Chemicals Co.) was converted to the dione and dioxime by the method of Vander Haar.[19] The dione was obtained in 75% yield and boiled at 116–117° at 20 mm. (as compared to 85% and 107–109° at 17 mm.). The dioxime was obtained in 50% yield and melted at 182° as compared to 179–180°.[19] One-tenth mole of 1,2-cycloheptanedionedioxime was added with stirring over a period of 4 hr. to a slurry of 31 g. of $LiAlH_4$ in 500 ml. of anhydrous ether. The mixture was then refluxed for 48 hr. with constant stirring and hydrolyzed successively with wet ether and with water. The ether layer was decanted and extracted with dilute HCl. The white hydrolysis residue was treated with KOH and steam distilled into dilute HCl. The combined HCl solutions were evaporated to dryness. The resulting amine dihydrochloride was purified by recrystallizing several times from an alcohol–water mixture. A 10% yield of 1,2-cycloheptanediamine dihydrochloride was obtained. *Anal.* Calcd. for $C_7H_{18}Cl_2N_2$: Cl, 35.25; N, 13.93. Found: Cl, 35.31, N, 13.97. Presumably this is the *trans* isomer since similar reactions produce *trans*-1,2-cyclohexanediamine.[20]

The preparation of *trans*-1,2-cyclopentanediamine was tried unsuccessfully a number of times. 1,2-Cyclopentanedione was made in 50% yield by the method of Jaeger and Blumendal,[21] but not by oxidation of cyclopentanone with SeO_2 either at 0° or 35°,[22] or by hydrolysis of 2-chlorocyclopentanone followed by oxidation with $FeCl_3$.[23] Reduction of the dioxime of the dione with sodium and alcohol was unsuccessful.

Results.—The log K_n values are given in Table I together with the calculated thermodynamic quantities ΔF_n, ΔH_n and ΔS_n. The ± values are the 95% confidence intervals based on three or more calculations for each constant. Plots of log K_n *vs.* $1/T$ were constructed in order to determine ΔH_n. The formation curves for the titrations at 20° involving silver ion are plotted in Fig. 1, together with the theoretical formation curve for the case $N = 1$.

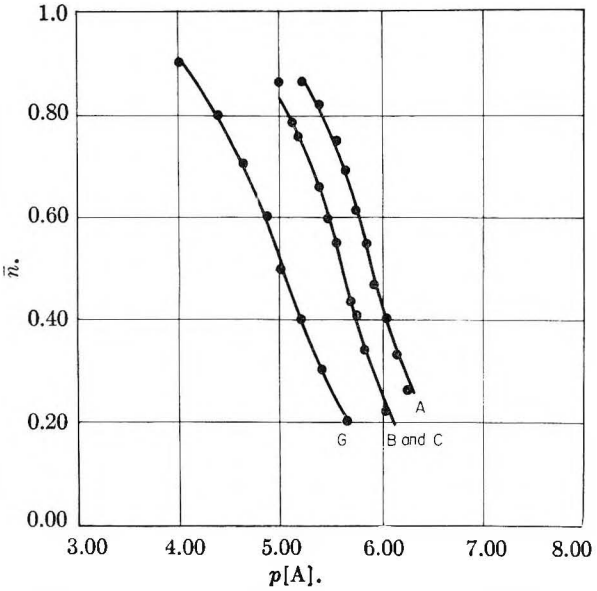

Fig. 1.—Formation curves of silver in titration at 20°: A, 1,3-propanediamine; B, 1,4-butanediamine; C, 1,3-diamino-2-propanol; G, theoretical formation curves for the $N = 1$.

The log K_2 values for the chelation of Cu^{++} with 1,3-propanediamine are not reported since they varied when different data points were used in the calculation. In the titrations run in the presence of cobalt(II) ion, the *p*H of the solutions continually dropped with time after a small amount of amine was added. No precipitation was observed, and the color of the solutions indicated that coördination was taking place. A possible explanation is that the cobalt(II) was being oxidized to cobalt(III). McIntyre reports a similar difficulty in attempts to titrate cobalt(II) solutions with amines.[24]

Precipitation occurred during the titrations of Ag^+, Cu^{++}, Ni^{++}, Zn^{++} and Cd^{++} with N,N,N′,N′-tetramethylmethanediamine, of Cu^{++}, Ni^{++}, Zn^{++} and Cd^{++} with 1,4-butanediamine, of Zn^{++} and Cd^{++} with 1,3-propanediamine and of Zn^{++} with 1,3-diamino-2-propanol. Although no precipitation was noted during the titration of the latter amine and Cd^{++}, the calculated constants were not consistent.

Discussion

In general 5-membered chelate rings are the most stable in systems with saturated rings.[25] The failure of N,N,N′,N′-tetramethylmethanediamine to form stable chelates with the usual bivalent ions under conditions in which N,N,N′,N′-tetramethyl-1,2-ethanediamine does form stable chelates with both copper(II) and silver ions[26] is in agreement with this general observation. Another qualita-

(17) M. Picon, *Bull. soc. chim.*, [4] **33**, 89 (1923).

(18) We wish to express our appreciation to Dr. H. Kroll of Alrose Chemical Company for the gift of *trans*-1,2-cyclohexanediamine sulfate and *cis*-1,2-cyclohexanediamine (b.p. 70–73° at 12 mm.), and to Mr. G. S. Burch of Carbide and Carbon Chemicals Company for the gift of 2,2′,2″-triaminotriethylamine.

(19) R. W. Vander Haar, R. C. Voter and C. V. Banks, *J. Org. Chem.*, **14**, 836 (1949).

(20) L. D. Berg, unpublished observations in this Laboratory.

(21) F. M. Jaeger and H. B. Blumendal, *Z. anorg. Chem.*, **176**, 161 (1928).

(22) H. L. Riley, J. F. Morley and N. Friend, *J. Chem. Soc.*, 1875 (1932).

(23) Dutch Patent 58,279 (Sept. 16, 1946); *C. A.*, **41**, 4807 (1947).

(24) G. H. McIntyre, Jr., Ph.D. Thesis, The Pennsylvania State University, 1953.

(25) A. E. Martell and M. Calvin, "Chemistry of the Metal Chelate Compounds," Prentice-Hall, Inc., New York, N. Y., 1952, p. 137.

(26) B. P. Block, unpublished observations.

TABLE I

VALUES FOR THE THERMODYNAMIC QUANTITIES LOG K_n, $-\Delta F_n$, $-\Delta H_n$ AND ΔS_n, INVOLVED IN THE REACTION AT 10, 20, 30 AND 40° OF SEVERAL BIVALENT METAL IONS WITH SEVERAL POLYAMINES

t, °C.	H^+	Ag^+	Cu^{++}	Ni^{++}	Zn^{++}	Cd^{++}	H^+	Cu^{++}	Ni^{++}	Zn^{++}	Cd^{++}	H^+	Ni^{++}	Zn^{++}
1,2-Ethanediamine[a]														
			log K_1					log K_2					log K_3	
10	10.39		11.01	7 74	5.85	5.53	7.28	9.57	6.44	5.13	4.74		4.67	3.26
	±0 01		±0 03	±0.05	±0 01		±0 04	±0 02	±0.04	±0.03			+0.02	±0 04
20	10.09		10.67	7 52	5.77	5.47	7 00	9.23	6.32	5.06	4.52		4.49	3 28
	±0.01		±0 04	±0 06	±0.06		±0 02	±0.05	±0.06	±0.02			±0.05	±0.05
30	9.81		10 36	7.27	5.55	5.34	6.79	8.99	6.11	4.89	4.38		4.20	3.22
	±0.01		±0.03	±0 02	±0.09		±0 03	±0 01	±0.03	±0 05			±0.03	±0 07
40	9.53		10 06	7.04	5.31	5.06	6.50	8.66	5.89	4.76	4.25		4 05	3.18
	±0.01		±0.02	±0 03	±0.14		±0.02	±0 04	±0.03	±0.06			±0.51	±0.10
			$-\Delta F_1$(kcal./mole)					$-\Delta F_2$(kcal./mole)					$-\Delta F_3$(kcal./mole)	
10	13.5		14.3	10.0	7.5	7 1	9.4	12.4	8 3	6.6	6.1		6.1	4.2
20	13.5		14.3	10.1	7.7	7 3	9.4	12 4	8.5	6.8	6.2		6.0	4.4
30	13.6		14 4	10.1	7.3	7.4	9 4	12.4	8.5	6.8	6.3		5.8	4.5
40	13.7		14.4	10 1	7.3	7.2	9 3	12.4	8 4	6.8	6.3		5.8	4.6
			$-\Delta H_1$(kcal./mole)					$-\Delta H_2$(kcal./mole)					$-H_3$(kcal./mole)	
10 40	11.5		12.8	9.5	5.3	6.2	10 3	12.3	7.5	5 2	7.5		8.7	1 8
			$-\Delta S_1$(cal./mole-deg.)					$-\Delta S_2$(cal./mole-deg.)					$-\Delta S_3$(cal./mole-deg.)	
10	7		5	2	9	3	−3	0	3	5	−5		−9	8
20	7		5	2	9	4	−3	0	3	5	−4		−9	9
30	7		5	2	9	4	−3	0	3	5	−5		−10	9
40	7		5	2	9	3	−3	0	3	5	−5		−9	9
1,3-Propanediamine														
			log K_1					log K_2						
10	10.94	6.35	10.13	6.67			9.03	4.71						
	±0.02	±0.07	±0.05	±0.02			±0.03	±0.04						
20	10.62	5.92	9.72	6.40			8.64	4.44						
	±0.03	±0 04	±0.05	±0 04			±0.03	±0.08						
30	10.32	5 56	9.45	6.18			8 33	4.28						
	±0.02	±0 02	±0.02	±0 03			±0 02	±0.04						
40	9 99	5.27	9.16	5.94			8 02	4.09						
	±0.02	±0 06	±0 04	±0.01			±0.03	±0.04						
			$-\Delta F_1$(kcal./mole)					$-\Delta F_2$(kcal./mole)						
10	14 2	8 2	13 1	8.6			11.7	6.1						
20	14 3	7.9	13 0	8.6			11.6	6.0						
30	14.3	7 7	13 1	8 6			11.6	5.9						
40	14.3	7.6	13 1	8.5			11.5	5.9						
			ΔH_1(kcal./mole)					$-\Delta H_2$(kcal./mole)						
10–40	13.3	14.6	13.9	10.2			13.9	8.2						
			ΔS_1(cal./mole-deg.)					ΔS_2(cal./mole-deg.)						
10	3	23	−3	−6			−8	−7						
20	3	−23	−3	−6			−8	−8						
30	3	−23	−3	−5			−8	−8						
40	3	−22	−2	−5			−8	−7						
1,4-Butanediamine														
			log K_1					log K_2						
10	11.15	6.00					9.71							
	±0 05	±0 07					±0.03							
20	10.80	5 67					9.35							
	±0.06	±0.04					±0.01							
30	10.50	5.30					9.04							
	±0.04	±0.05					±0.05							
40	10.26	5.19					8.83							
	±0.05	±0.09					±0.03							
			$-\Delta F_1$(kcal./mole)					$-\Delta F_2$(kcal./mole)						
10	14.4	7.7					12.6							
20	14 5	7.6					12.6							
30	14.6	7.4					12.5							
40	14.7	7.4					12.7							
			$-\Delta H_1$(kcal./mole)					$-\Delta H_2$(kcal./mole)						
10 40	12.0	10.7					12.0							
			ΔS_1(cal./mole-deg.)					ΔS_2(kcal./mole-deg.)						
10	8	−11					2							
20	9	−11					2							
30	9	−11					2							
40	9	−11					2							

TABLE I (*Continued*)

1,3-Diamino-2-propanol

			log K_1		log K_2
10	9.95 ±0.05	5.96 ±0.09	5.68 ±0.09	8.12 ±0.04	4.41 ±0.02
20	9.69 ±0.03	5.84 ±0.02	5.56 ±0.02	7.93 ±0.02	4.32 ±0.09
30	9.42 ±0.06	5.31 ±0.06	5.42 ±0.03	7.68 ±0.02	4.16 ±0.09
40	9.14 ±0.00	4.97 ±0.04	5.25 ±0.02	7.38 ±0.05	4.05 ±0.12
			$-\Delta F_1$(kcal./mole)		$-\Delta F_2$(kcal./mole)
10	12.9	7.7	7.4	10.5	5.7
20	13.0	7.5	7.5	10.6	5.8
30	13.1	7.4	7.5	10.7	5.7
40	13.1	7.1	7.5	10.6	5.8
			$-\Delta H_1$(kcal./mole)		$-\Delta H_2$(kcal./mole)
10–40	11.2	13.2	5.8	10.4	5.0
			ΔS_1(cal./mole-deg.)		ΔS_2(cal./mole-deg.)
10	6	−19	6	0	2
20	6	−19	6	1	3
30	6	−19	6	1	2
40	6	−19	5	1	3

2,2′,2″-Triaminotriethylamine

		log K_1	log K_2	log K_3
10	10.45 ±0.03	19.09 ±0.10	9.55 ±0.08	8.28 ±0.10
20	10.15 ±0.02	18.71 ±0.04	9.26 ±0.02	7.98 ±0.12
30	9.91 ±0.06	18.40 ±0.04	9.00 ±0.09	7.71 ±0.11
40	9.63 ±0.15	17.91 ±0.07	8.65 ±0.10	7.48 ±0.10
		$-\Delta F_1$(kcal./mole)	$-\Delta F_2$(kcal./mole)	$-\Delta F_3$(kcal./mole)
10	13.5	24.7	12.4	10.7
20	13.6	25.1	12.4	10.7
30	13.7	25.5	12.5	10.7
40	13.8	25.7	12.4	10.7
		$-\Delta H_1$(kcal./mole)	$-\Delta H_2$(kcal./mole)	$-\Delta H_3$(kcal./mole)
10–40	11.0	15.7	12.3	10.3
		ΔS_1(cal./mole-deg.)	ΔS_2(cal./mole-deg.)	ΔS_3(cal./mole-deg.)
10	9	32	0	2
20	9	32	0	2
30	9	32	1	2
40	9	32	0	2

cis-1,2-Cyclohexanediamine

		log K_1				log K_2			
10	10.19 ±0.02	11.20 ±0.06	7.50 ±0.06	6.00 ±0.02	5.87 ±0.06	5.43 ±0.06	9.99 ±0.04	6.10 ±0.06	5.55 ±0.04	4.87 ±0.06
20	9.93 ±0.06	10.91 ±0.06	7.28 ±0.04	5.89 ±0.04	5.73 ±0.08	6.13 ±0.02	9.69 ±0.04	5.94 ±0.04	5.48 ±0.05	4.74 ±0.09
30	9.66 ±0.05	10.72 ±0.09	7.12 ±0.02	5.74 ±0.08	5.65 ±0.04	5.94 ±0.09	9.40 ±0.05	5.80 ±0.13	5.38 ±0.03	4.64 ±0.04
40	9.39 ±0.02	10.33 ±0.02	6.91 ±0.05	5.62 ±0.09	5.42 ±0.04	5.68 ±0.06	9.10 ±0.07	5.65 ±0.13	5.25 ±0.09	4.45 ±0.05
		$-\Delta F_1$(kcal./mole)				$-\Delta F_2$(kcal./mole)				
10	13.2	14.5	9.7	7.8	7.6	8.3	13.0	7.9	7.2	6.3
20	13.3	14.7	9.8	7.9	7.7	8.2	13.0	8.0	7.3	6.4
30	13.4	14.8	9.8	7.9	7.8	8.2	13.0	8.0	7.5	6.4
40	13.5	14.8	9.9	8.1	7.8	8.1	13.0	8.1	7.5	6.4
		$-\Delta H_1$(kcal./mole)				$-H_2$(kcal./mole)				
10–40	11.5	11.6	7.7	5.2	5.7	10.1	12.0	6.3	4.2	5.6
		ΔS_1(cal./mole-deg.)				ΔS_2(cal./mole-deg.)				
10	6	10	7	9	7	−6	4	6	10	2
20	6	10	7	9	7	−6	3	6	10	2
30	6	10	7	9	7	−6	3	6	10	2
40	6	10	7	9	7	−6	3	6	10	2

TABLE I (*Continued*)

trans-1,2-Cyclohexanediamine

		log K_1					log K_2				log K_3
10	10.24 ±0.02	11.55 ±0.04	8.22 ±0.06	6.37 ±0.07	6.05 ±0.07	6.71 ±0.01	10.11 ±0.10	7.08 ±0.09	5.66 ±0.08	5.14 ±0.08	5.14 ±0.08
20	9.94 ±0.03	11.22 ±0.05	7.93 ±0.03	6.24 ±0.03	5.86 ±0.07	6.47 ±0.03	9.73 ±0.07	6.84 ±0.02	5.41 ±0.03	4.93 ±0.04	4.90 ±0.07
30	9.60 ±0.01	10.96 ±0.04	7.82 ±0.04	6.14 ±0.02	5.74 ±0.06	6.20 ±0.02	9.54 ±0.02	6.71 ±0.06	5.31 ±0.04	4.74 ±0.06	4.67 ±0.04
40	9.38 ±0.02	10.56 ±0.11	7.60 ±0.12	6.01 ±0.09	5.63 ±0.07	5.96 ±0.02	9.19 ±0.10	6.49 ±0.10	5.25 ±0.04	4.66 ±0.03	4.45 ±0.06
		$-\Delta F_1$(kcal./mole)					$-\Delta F_2$(kcal./mole)				$-\Delta F_3$(kcal./mole)
10	13.3	15.0	10.6	8.3	7.9	8.7	13.1	9.2	7.3	6.6	6.6
20	13.3	15.1	10.7	8.4	7.9	8.7	13.1	9.2	7.3	6.6	6.6
30	13.3	15.2	10.8	8.5	8.0	8.6	13.2	9.3	7.4	6.6	6.5
40	13.4	15.1	10.9	8.6	8.1	8.5	13.2	9.3	7.4	6.7	6.4
		$-H_1$(kcal./mole)					$-H_2$(kcal./mole)				$-\Delta H_3$(kcal./mole)
10–40	11.7	13.6	8.5	5.0	5.6	10.2	12.3	7.9	5.2	6.6	9.1
		ΔS_1(cal./mole-deg.)					ΔS_2(cal./mole-deg.)				ΔS_3(cal./mole-deg.)
10	6	5	7	12	8	−5	3	5	7	0	−9
20	5	5	8	12	8	−5	3	5	7	0	−9
30	5	5	8	12	8	−5	3	5	7	0	−9
40	5	5	8	12	8	−5	3	4	7	0	−9

trans(?)-1,2-Cycloheptanediamine

		log K_1					log K_2				log K_3
10	10.48 ±0.04	11.64 ±0.13	7.77 ±0.12	6.11 ±0.04	5.88 ±0.05	6.67 ±0.02	10.11 ±0.02	6.64 ±0.12	5.53 ±0.06	4.92 ±0.05	3.83 ±0.15

[a] Values for ethanediamine complexes are taken from McIntyre (ref. 24) except those for Cd^{++}, which are taken from Droll (ref. 27).

tive confirmation of this relationship is the failure of 1,3-propanediamine to form stable chelates with zinc and cadmium ion under the conditions used for these experiments, although chelates can be detected with 1,2-ethanediamine under similar conditions.[24,27] It is interesting to note that 1,3-propanediamine has been found to form stable complexes with cadmium ion in solutions of higher ionic strength than those used in these experiments.[5] A more quantitative comparison is possible for the chelation of both copper(II) and nickel ions with 1,3-propanediamine and 1,2-ethanediamine. The chelates with the former diamine are significantly less stable than those with the latter. The $-\Delta H_1$ values for the chelation with 1,3-propanediamine are the larger, however, in harmony with the greater basicity of this diamine as shown by its larger $-\Delta H$ values with H^+. Consequently, the large difference in stability of the chelates of these two diamines arises from a less favorable entropy change in the formation of the 6-membered ring. This is presumably associated with an increase in strain in the ring and with a greater loss of freedom of the ligand when the 1,3-propanediamine molecule is fixed in a ring system. Recently, calorimetric ΔH values[6] as well as some calculated from formation constants at two temperatures[5] have been reported for the chelation of copper(II) and nickel ions with both 1,2-ethanediamine and 1,3-propanediamine in the presence of neutral electrolyte.

Similar 7-membered ring systems are less stable than 6-membered rings and do not form in aqueous solution although chelates of copper(II), nickel and zinc with 1,4-butanediamine can be isolated from absolute alcohol.[28] In this connection it is interesting to note that the color changes during the titration of copper(II) with the diamines investigated also qualitatively indicate that 1,3-propanediamine does not chelate as extensively as the 1,2-diamines because the deep blue color characteristic of the 1:1 chelate does not change to the deep violet color characteristic of the 2:1 chelate with the former although it does with the latter.

The 1,2-cyclic diamines resemble 1,2-ethanediamine in that the amino groups are separated by two carbon atoms but differ in that the ring structures restrict the rotation of these groups. Therefore, it is possible that a metal ion with the correct radius may just fit between the donor atoms, resulting in the formation of an unusually stable chelate. The *cis* and *trans* isomers of 1,2-cyclohexanediamine have equal values for the first proton-amine formation constant, as might be expected. The slightly larger second constant for the *trans* isomer appears to be due to an entropy effect arising from the somewhat smaller repulsion of the second proton because of the greater separation of the two nitrogens in the *trans* isomer. The somewhat larger value for the second proton-amine formation constant for 1,2-ethanediamine as compared to the 1,2-cyclohexanediamine values appears to be the result of ΔH and ΔS effects.

Both the *cis* and *trans* isomers of 1,2-cyclohexanediamine resemble 1,2-ethanediamine in coördinating with silver, copper(II), nickel, zinc and cadmium. There are slight increases in stability in the copper chelates in going from 1,2-ethanediamine to *cis*- to *trans*-1,2-cyclohexanediamine. The data are not accurate enough to permit one to assign a reason to the first difference; the latter is the result of two opposing tendencies. The bonding is stronger with the *trans* isomers, but the entropy effect is less favorable. With nickel on the other hand, the stabilities of the chelates with the two isomeric diamines are notably different, the

(27) H. Droll, Ph.D. thesis, The Pennsylvania State University, 1955.

(28) P. Pfeiffer, *Naturwissenschaften*, **36**, 190 (1948).

trans isomer forming the more stable chelate. Although three molecules of the *trans* isomer coördinate per nickel ion as with 1,2-ethanediamine, only two molecules of the *cis* isomer coördinate under the conditions of these experiments. For the three-step processes the $-\Delta H$ values for each of the three steps are approximately equal so that the greater stability of the chelate with *trans*-1,2-cyclohexanediamine is an entropy effect. This effect is probably associated primarily with the greater loss of freedom of the 1,2-ethanediamine upon chelation compared to the cyclic diamine with its relatively fixed amino groups, although the formation of a more hydrophobic ion with the consequent release of more solvent molecules may also be a factor.

The relative weakness of chelation with *cis*-1,2-cyclohexanediamine compared to either the *trans* isomer or 1,2-ethanediamine is related to the low values of $-\Delta H$, an indication that the bond strengths are weaker. Apparently the restricted rotation in the ligand holds the two nitrogen atoms in positions unfavorable for chelation with nickel in the *cis* isomer and favorable in the *trans* isomer. It is interesting to note that the entropy effect is about the same for both the *cis* and *trans* isomers. Here, too, the color changes during titration are indicative of the products forming. The solution goes through a yellowish green to a pink during the titration with the *trans* isomer but stays yellowish green with the *cis* isomer. Tris-(*trans*-1,2-cyclohexanediamine)-nickel(II) perchlorate is somewhat insoluble in water, for a pink solid deposits if the titrated solution is allowed to stand although no precipitation is apparent during the course of the titration.

Zinc and cadmium ions are similar to copper ions in that there is little difference between the formation constants for chelation with *cis*- and *trans*-1,2-cyclohexanediamine. The zinc and cadmium chelates with the cyclic diamines are more stable than the corresponding chelates with 1,2-ethanediamine. This is clearly an entropy effect with both metal ions.

The limited amount of 1,2-cycloheptanediamine available was sufficient for titration at only one temperature, and, therefore, the thermodynamic quantities could not be calculated. 1,2-Cycloheptanediamine forms a slightly more stable chelate with copper ion at 10° than does *trans*-1,2-cyclohexanediamine. The color of the solution of the copper chelate is similar to the deep violet color of the copper chelate with 1,2-ethanediamine, with a slightly reddish tinge. The nickel, zinc and cadmium chelates with 1,2-cycloheptanediamine are not as stable as the corresponding chelates with *trans*-1,2-cyclohexanediamine. The color of the solution of the nickel chelate with 1,2-cycloheptanediamine is faint pink.

The coördination of 2,2′,2″-triaminotriethylamine with copper ion was investigated because the geometry of this ligand is such as to force the copper ion to enter into a tetrahedral configuration.[29] The color of this complex in solution is light blue. The $-\Delta H_1$ value for the formation of the 2,2′,2″-triaminotriethylamine copper chelate is only slightly higher than for chelation with a bidentate ligand, whereas McIntyre[24] has shown that this value is usually quite a bit higher for a terdentate ligand. The low $-\Delta H$ value is probably a result of the copper being forced into the tetrahedral configuration.

The chelation of nickel ion with 1,3-diamino-2-propanol is weaker than with 1,3-propanediamine but the two amines are alike in that only two molecules chelate. The $-\Delta H$ values for the hydroxyamine are lower indicating that the bonding is weaker in this case. It is uncertain whether oxygen is taking part in the coördination. The chelation of copper with 1,3-diamino-2-propanol involves the displacement of the proton from the hydroxyl group and is discussed elsewhere.[30]

It was possible to obtain constants for the chelation of silver ion with 1,3-propanediamine, 1,4-butanediamine and 1,3-diamino-2-propanol by using the usual equations for the case $N = 1$. The formation curves have the shape of the theoretical formation curve for this type of chelation. Therefore, any species such as $AgHA^{++}$, Ag_2A^{++} or $Ag_2A_2^{++}$ (where A represents an amine and HA represents the monoprotonated amine), which have been reported by Schwarzenbach and co-workers[31] for various diamines at 20°, can be safely neglected in the calculation of K_1, the constant for the formation of the species AgA^+, under the conditions used in this investigation. If these species were not negligible, the formation curves would not follow the theoretical curve for the case of $N = 1$, and the calculated constants would vary with the data points used in the calculations. Droll[27] has found that the species reported by Schwarzenbach cannot be neglected in the silver–1,2-ethanediamine system under similar conditions.

The somewhat different order of stability with increasing ring size for the silver chelates with diamines probably is due, as suggested by Schwarzenbach,[32] to the fact that silver ion tends to form linear complexes, and, as a result, the ring structure becomes less strained as the ring becomes larger. Although the value of log K_1 for 1,4-butanediamine is less than that for 1,3-propanediamine, this is an enthalpy effect, due to the greater basicity of the latter, which completely offsets the more favorable entropy change for the formation of the 7-membered ring. In both cases a strained ring structure is indicated by the negative values of ΔS. It should be pointed out that Schwarzenbach, *et al.*,[31] found the formation constant for the 1,4-butanediamine–silver chelate to be slightly larger than that for the 1,3-propanediamine chelate. Since the values reported here are, in general, in agreement with Schwarzenbach's, the reason for this difference is not readily apparent.

Comparison of the values for the chelation of silver with 1,3-diamino-2-propanol and with 1,3-

(29) H. Ackermann, J. E. Prue and G. Schwarzenbach, *Nature*, **163**, 723 (1949).

(30) C. R. Bertsch, B. P. Block and W. C. Fernelius, THIS JOURNAL, **62**, 503 (1958).

(31) G. Schwarzenbach, B. Maissen and H. Ackermann, *Helv. Chim. Acta*, **35**, 2333 (1952); G. Schwarzenbach, H. Ackermann, B. Maissen and G. Anderegg, *ibid.*, **35**, 2337 (1952).

(32) G. Schwarzenbach, *ibid.*, **36**, 23 (1953).

propanediamine shows that the stronger chelation with the latter is primarily an enthalpy effect. This indicates that, if the hydroxy group is involved in the bonding, the hydroxy to silver bond is weaker than the water to silver bond which it replaces. If the hydroxy group is not bonded to the silver, then the presence of the hydroxy group on the amine must affect the silver-to-nitrogen bond strength.

Titrations were run in the presence of silver ion with both isomers of 1,2-cyclohexanediamine. The formation curves did not follow the theoretical curve for the case $N = 1$, and the values that were calculated for the constants were dependent on the data points used. It is probable that the formation of a dimerized species, such as was reported by Schwarzenbach for the silver ion–1,2-ethanediamine system, is taking place. Such a reaction would be expected because of the similarity of the 1,2-cyclic diamines and 1,2-ethanediamine. The formation curves were found to be identical for the *cis* and *trans* isomers, indicating that the actual reaction is independent of the distance between the donor atoms. This would be the case if the dimer $Ag_2A_2^{++}$ were formed.

Acknowledgment.—This investigation was carried out in part under Contract N6-onr26913 with the Office of Naval Research and in part under Contract AT(30-1)-907 with the United States Atomic Energy Commission.

A HITTORF TRANSFERENCE NUMBER APPARATUS EMPLOYING CONDUCTIMETRIC ANALYSIS OF THE SOLUTIONS

BY B. J. STEEL AND R. H. STOKES

Contribution from the Chemistry Department of the University of New England, Armidale, N.S.W., Australia

Received November 26, 1957

The design and operation of a Hittorf transference number apparatus are described. The necessary high precision in the analysis of the solutions is obtained by conductimetric analysis of the solution *in situ*. The method is used to determine transference numbers of potassium bromide in aqueous sucrose and glycerol solutions.

Introduction

In view of the difficulties encountered in the application of the moving-boundary method for determining transference numbers in non-aqueous solvents,[1] we are attempting to develop the classical Hittorf method for this purpose. While we have not yet been able to obtain quite the precision of the best moving-boundary work in aqueous solutions, the method described below has yielded useful results in mixed solvents, and we are describing its development to the present stage in order to permit the discussion of individual ion mobilities in mixed solvents.

The present form of the apparatus is shown in Fig. 1. The reversible electrodes used for the electrolysis are in the bulbs A and B which are connected by 1 cm. bore tubing and a wide-bore stopcock T. Connected to the bulb B by a graduated tube is a mixing bulb C of about 100-ml. capacity, which is sufficient to hold the entire contents of the rest of the apparatus. Another side-arm carries a conductance cell. The dimensions of the connecting-tubes are so chosen that the solution readily can be poured into and out of the mixing bulb and the conductance cell. The interior of the mixing bulb C and its calibrated stem is coated with a silicone layer[2] to ensure complete drainage—a most important point. The volume contained by the electrode vessel B, the S-shaped arm up as far as the stopcock, and the conductance cell D, is determined by weighing with water filling these parts and with the meniscus standing at a known position on the calibrated stem of bulb C, the bulb C itself being full of air. This volume is reproducible and measurable within 0.01 ml. and is about 50 ml. in the present apparatus. The reversible electrodes are fitted through ground-glass joints with Teflon sleeves. The stopcock T is lapped to a very accurate fit so that only a trace of grease at the key end is needed; thus in operation the solution scarcely makes contact with any grease.

During the run the vessel is immersed in an oil-bath controlled at 25 ± 0.001° and is mounted on a vibration-free support. The electrolysis current (of up to 6 ma.) is provided from dry batteries *via* a simple electronic current-stabilizer, and is measured by a precision potentiometer across a certified 100 ohm resistance in series with the apparatus. The stabilized current changes slowly (by not more than a few tenths of 1%) during the electrolysis period of a few hours; it is measured at frequent intervals and the number of coulombs passed is obtained by a tabular integration. This gives a precision of at least 0.01% in the quantity of electricity passed, *i.e.*, better than could be obtained by the use of a coulometer.

The procedure for a measurement is as follows, taking as an example a determination of the transference number of potassium bromide in 20% aqueous sucrose: the cathode, a helix of heavy silver wire, is coated electrolytically with silver bromide, employing two to three times the number of coulombs to be passed during the run. The anode is a similar silver helix, but requires no bromide coating. A 20% sucrose solution is prepared and its specific conductance checked. The potassium bromide solution is then made up in this solvent,

(1) J. R. Graham and A. R. Gordon, *J. Am. Chem. Soc.*, **79**, 2350 (1957).

(2) Silicone "Repelcote," Hopkins and Williams, Ltd., Essex, England.

and the apparatus, with one electrode in place, is rinsed several times with solution and then filled so that the level of the liquid is within the range of the graduated portion of the connecting-tube, the bulb C being full of air. The silicone film on the inner surface of this bulb permits complete drainage so that the volume (after thermostating to 25°) can be read within 0.01 ml. The other electrode is inserted and the apparatus is set up in the thermostat.

The conductance is measured (on a Leeds and Northrup bridge of Jones' design) and the apparatus is allowed to stand for some time; then the entire contents are tipped into the mixing-bulb, thoroughly mixed, and returned to the original position. This process is repeated until the conductance is constant within one part in 50,000, in order to ensure that adsorption changes are complete. The electrodes are then connected to a commutator-switch which is arranged to switch over to the electrolysis from a dummy load on which the constant-current device has been warmed up. Electrolysis is carried on until a reasonably large concentration change (say 10% of the initial concentration) has occurred in the electrode bulbs. The current is switched off at a known time, the stopcock T is closed, and the contents of the cathode compartment and conductance cell are mixed in the bulb and poured back repeatedly until quite uniform. The volume is checked by reading the level in the graduated connecting tube; unless there has been leakage or gassing at the electrodes it should be unchanged.

The final cathode concentration is now obtained from the conductance, and as a check on the reversibility of the electrolysis the tap T is opened, the whole contents of the apparatus thoroughly mixed, and the conductance—which should be identical with the original value—is again measured.

The data provided by such a run are related to the transference number in a frame of reference fixed in the apparatus by

$$(c_2 - c_1)V = t_{K^+}q/F \qquad (1)$$

where

c_1 is the initial concn.
c_2 is the final concn. in the cathode compartment
V is the vol. of the soln. in the cathode compartment (including the conductance cell arm and the bent tube up to the stopcock)
F is the faraday
q is the quantity of electricity passed
t_{K^+} is the transference no. of the potassium ion at concn. c_1

The conversion of this transference number into the conventional Hittorf number (with frame of reference fixed with respect to solvent) is made in the usual way using the densities of the solutions.

Transference numbers of potassium bromide in 20% aqueous glycerol and sucrose solutions obtained by this method are reported in Table I.

Accuracy of the Method.—Of the quantities needed in equation 1, the volume V can be measured with an accuracy of 0.01 ml. so that it contributes an uncertainty of no more than one unit in the fourth decimal place of the transference number. The quantity of electricity q depends on the current which can be measured with an accuracy of 0.01% and the time, error in which does not exceed a second in a run of two hours or more; thus uncertainty in q will not contribute more than one unit in the fourth decimal place. Evidently then the important quantity for the accuracy of the method is the concentration change $(c_2 - c_1)$. The resistances measured in the conductance cell are of the order of 10,000 ohms, and by calibrating the bridge coils against an internal standard a precision of 0.1 ohm can be obtained in the resistance readings. Since all resistance readings are taken in the same cell, without problems of evaporation and transfer arising, the accuracy of c_1 and c_2 relative to one another should be considerably better than 0.01%. In a typical run, the difference $(c_2 - c_1)$ is about 10% of c_1, and this difference should therefore be determinable within at worst 0.1%, corresponding to about 5 in the fourth

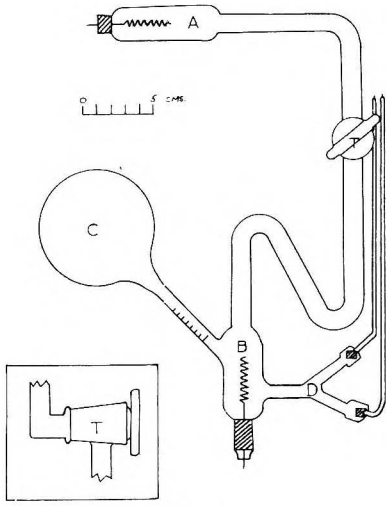

Fig. 1.

TABLE I

TRANSPORT NUMBERS OF K^+ FROM SOLUTIONS OF KBr IN (1) 20% SUCROSE, (2) 20% GLYCEROL

Concn., moles/l. Initial[a]	Final	Coulombs[b]	Vol. cathode compartment, ml.	t_+ apparent	t_+ Hittorf
(1) 20% sucrose solutions					
0.0148004	0.0162874	14.824	50.39	0.4877	0.4880
.0249559	.0261471	11.995	50.67	.4855	.4860
.0260062	.0283424	23.211	50.14	.4870	.4875
.0322601	.0347958	25.239	50.31	.4877	.4884
.0324110	.0350899	26.594	50.13	.4873	.4879
.0428552	.0454201	25.381	50.20	.4895	.4903
.0437363	.0457994	20.438	50.07	.4876	.4886
.0513194	.0559803	54.742	59.30	.4872	.4882
.0602548	.0648356	53.700	59.21	.4873	.4886
(2) 20% glycerol solutions					
0.0200419	0.0213756	15.509	59.09	0.4903	0.4907
.0309610	.0330224	20.311	49.99	.4895	.4901
.0422582	.0446798	24.079	50.49	.4899	.4906
.0425143	.0444024	22.030	59.20	.4895	.4902
.0506821	.0537804	30.821	50.44	.4893	.4902

[a] In cases where the conductivity obtained after remixing the whole solution at the completion of the run did not agree exactly with that obtained before the run, the "initial" concentration is obtained from the *final* conductivity after this remixing. [b] Corrected for the solvent conductivity as described in text.

decimal place of the transference number. By directly calibrating the conductance cell of the apparatus with solutions of the salt being studied, made up very exactly by weight-dilution of a common stock solution, about twice this precision might reasonably be expected; this was in fact done for the data quoted in Table I. It will be appreciated that very precise temperature control at the time of the conductance measurements is necessary to give this precision. In fact, the movement of the mercury in the thermometer was less than 0.001°. It is also necessary to employ an extremely sensitive graph of the conductance *versus* concentration relationship for the electrolyte studied. This is plotted in the form $(\Lambda + a\sqrt{c})$ *versus* c, the constant a being so chosen that $(\Lambda + a\sqrt{c})$ varies by only a few tenths of an equivalent conductance unit in the concentration range of interest. By a rapidly-converging series of successive approximations using this graph the measured specific conductances can be converted to concentrations with an accuracy better than 0.01%; the precision of the two concentrations relative to each other is even better, so that a concentration *change* of 10% can be obtained with an accuracy considerably better than 0.1% of its value.

A real difficulty arises over the solvent correction, however. This was relatively large, about 2×10^{-6} ohm^{-1}cm.$^{-1}$ for the solvents used; subsequently to the measurements reported we have found that a fivefold reduction in this figure can be obtained by passing the solvent through a mixed-bed ion-exchange resin. With this reduced figure we expect no difficulty in future measurements, but the present ones do raise some interesting points. If the impurity is a trace of salt it will probably have little effect on the result, but if it is an acid its anion and cation will migrate in considerably different proportions to those of potassium bromide, and will give an apparently high concentration to the cathode compartment. Such an error, if present, will of course be most serious in dilute solutions. We have adopted the following course in dealing with the solvent correction: in determining the concentrations from the conductances, it is subtracted from the measured conductance in the usual way; and in calculating the number of coulombs, a fraction equal to the ratio of the solvent conductance to the solution conductance is subtracted, on the grounds that this fraction of the current is used in transporting something other than potassium bromide. In a 0.02 N solution with a solvent conductance of 2×10^{-6} this amounts to reducing both q and $(c_2 - c_1)$ by 0.1%, and thus has a negligible effect. It is however far from clear that this course is the correct one, and it will clearly be better to reduce the solvent conductance to the lower level which now seems practicable.

The present form of the apparatus, being without the "middle compartment" of the conventional Hittorf apparatus, provides no *direct* evidence that convection and diffusion are not contributing to the transport in the region of the stopcock. It does not seem practicable to introduce such a compartment and another conductance cell without raising a number of manipulative problems: at least two more stopcocks would be needed, and the dimensions of the apparatus would become inconvenient. Convective mixing is certainly absent in the case of the potassium bromide solutions, which have a high density increment per unit concentration; this is sufficiently established by the independence of the transference number on the duration of the run (in the range 1 to 5 hours). It possibly occurs however in the case of potassium chloride, with which salt appreciably more scatter was found than could be explained by the estimated errors of measurement. We have also made a number of measurements with silver electrodes in silver nitrate solution, both in water and in 20% glycerol. In water, the scatter was about ±0.001 in the transport number, but the averages agreed well with the moving boundary results. In the glycerol solution, the results again scatter by about the same amount, but the results led to individual ion mobilities in fair agreement with those obtained from the potassium bromide data. These ion mobilities, and the conductance data from which they are derived, will be dealt with in another paper. The scatter obtained in the silver nitrate solutions possibly is connected with the presence of dissolved oxygen; this point is being examined further.

We plan to extend the tests of this method to non-aqueous solvents in the near future, being satisfied that it has distinct possibilities for such work, although its inherent precision is somewhat lower than that of the moving-boundary method.

VAPOR PRESSURES AND MOLECULAR COMPOSITION OF VAPORS OF THE SODIUM FLUORIDE–BERYLLIUM FLUORIDE SYSTEM[1]

BY KARL A. SENSE[1a] AND RICHARD W. STONE

Battelle Memorial Institute, Columbus, Ohio

Received December 3, 1957

A new study made on the vapor pressure of BeF_2 over the temperature interval 802 to 1025° showed good agreement with previous data taken over the 802–968° range. Excessive scatter of the vapor pressure data in the lower temperature region prevented a melting point determination of BeF_2 by the transpiration method alone. Thermal analysis showed the melting point to be about 545°. Vapor pressures of the NaF–BeF_2 system were measured over the range 509 to 1061°. On the basis of previously developed theory, it was concluded that the complex $NaBeF_3$ exists in the vapor phase in addition to NaF and BeF_2. Resolution of the vapor phase on this basis indicated that another complex might exist in the vapor phase. A plot is presented showing the change of total pressure with composition for various temperatures.

Introduction

This work is a continuation of the physical properties of fused-salt systems which was started with the investigation of the NaF–ZrF_4 system.[2]

Experimental

The method and apparatus used have been adequately described previously.[2-4] The only change from previous procedure was in improved oxygen removal from the argon which was used as a carrier gas. This was accomplished by passing the argon over heated uranium chips after most of the oxygen had been removed by heated copper turnings.

The fused-salt mixtures were supplied by the Mound Laboratory at Miamisburg, Ohio, and the Oak Ridge National Laboratory at Oak Ridge, Tennessee.

In most cases, the composition of the salt mixtures changed somewhat during the runs because of the preferential vaporization of the more volatile component. Corrections were made for this effect, and the average compositions are listed in the various plots with the proper curves.

Results and Discussion

The Vapor Pressure of BeF_2.—The vapor pressure of BeF_2 had been measured some time ago.[3] Because the apparatus and techniques in measuring vapor pressures have been improved since publication of that paper, another set of measurements was made. For temperatures greater than about 800°, relatively little difficulty was experienced in obtaining reasonably consistent data (see Table I). The results compare favorably with those given in the previous paper.[3] Figure 1 is a plot of the recent measurements and the best curve[5] obtained, as well as the best curve obtained for the previous set of data. The new vapor pressure curve has a somewhat flatter slope, resulting in a heat of vaporization value of

$$\Delta H_{\text{vaporization}} = 50.1 \text{ kcal./g. mole} \qquad (1)$$

as compared with the old value of 50.9 kcal./g. mole. At $1/T(°K.) = 7.8 \times 10^{-4}$, the new vapor pressure curve yields a value about 10 per cent. lower than the previous one, while at $1/T(°K.) = 9.3 \times 10^{-4}$, it is only about 4 per cent. lower. The revised vapor pressure equation which holds for the temperature interval 802 to 1025° is

TABLE I

VAPOR PRESSURES OF BeF_2

Temp., °C.	Pressure,[a] mm. Obsd.	Calcd.	Deviation, %	Flow rate of carrier gas, cm.[3]/min.
1025	106.2a	108.6	− 2.2	8.5
1010	88.9	86.3	+ 3.0	11.5
989.6	70.4a	63.1	+11.6	9.0
974.8	50.7b	49.8	+1.8	11.2
960.5	40.4b	39.4	+2.4	10.0
945.9	31.6a	30.9	+2.4	14.9
932.0	24.4a	24.3	−1.1	18.9
932.0	22.1b	24.3	−9.0	21.2
917.4	18.2b	18.8	−3.1	19.9
917.4	18.4a	18.8	−2.1	20.9
900.7	13.86a	13.93	−0.5	23.3
889.7	11.25a	11.37	−1.1	23.6
889.1	10.85	11.17	−2.8	23.0
877.6	8.59b	9.06	−5.2	20.2
863.0	6.94a	6.83	+1 6	20.9
850.3	5.48	5.32	+3.1	31.1
839.5	4.05a	4 28	−5.3	31.2
838.0	4.27b	4 15	+2.9	30.8
825.4	3.47	3.20	+8.5	32.4
813.9	2.70	2.51	+7.4	40.1
802.2	2.05	1.95	+5.2	41.1

[a] a, pressure based upon average of two analyses; b, pressure based upon average of three analyses.

$$\log p \text{ (mm.)} = 10.466 - \frac{10943}{T, °K.} \qquad (2)$$

$$\text{extrapolated boiling point} = 1170° \qquad (3)$$

Because of increasing scatter of the vapor-pressure data below 800° the melting point of BeF_2 could not be redetermined. Thermal analysis showed the melting point of BeF_2 to be about 545°. This is considerably lower than the melting point derived from previous vapor pressure data,[3] and is in agreement with the results obtained by Roy, Roy and Osborn.[6]

Since the scatter of the vapor pressure data of BeF_2 increased for lower temperatures an attempt was made to obtain data at lower temperatures for the 26 mole % NaF–74 mole % BeF_2 composition. The results obtained over the 509 to 977° range are given in Table II. When these data are plotted, some scatter is evident below 635°, although excessive scatter starts only below 535°. A break in the curve is not evident above that temperature. Why the data scatter for pure BeF_2 and not for

(1) Work performed under AEC Contract W-7405-eng-92.

(1a) Atomics International, Canoga Park, California.

(2) K. A. Sense, C. A. Alexander, R. E. Bowman and R. B. Filbert, Jr., THIS JOURNAL, **61**, 337 (1957).

(3) K. A. Sense, M. J. Snyder and J. W. Clegg, *ibid.*, **58**, 223 (1954).

(4) K. A. Sense, M. J. Snyder and R. B. Filbert, Jr., *ibid.*, **58**, 995 (1954).

(5) In the least-squares treatment, the data were weighted, since in some instances two or more analyses were made for a single run.

(6) D. M. Roy, R. Roy and E. F. Osborn, *J. Am. Ceram Soc*, **36**, 185 (1953).

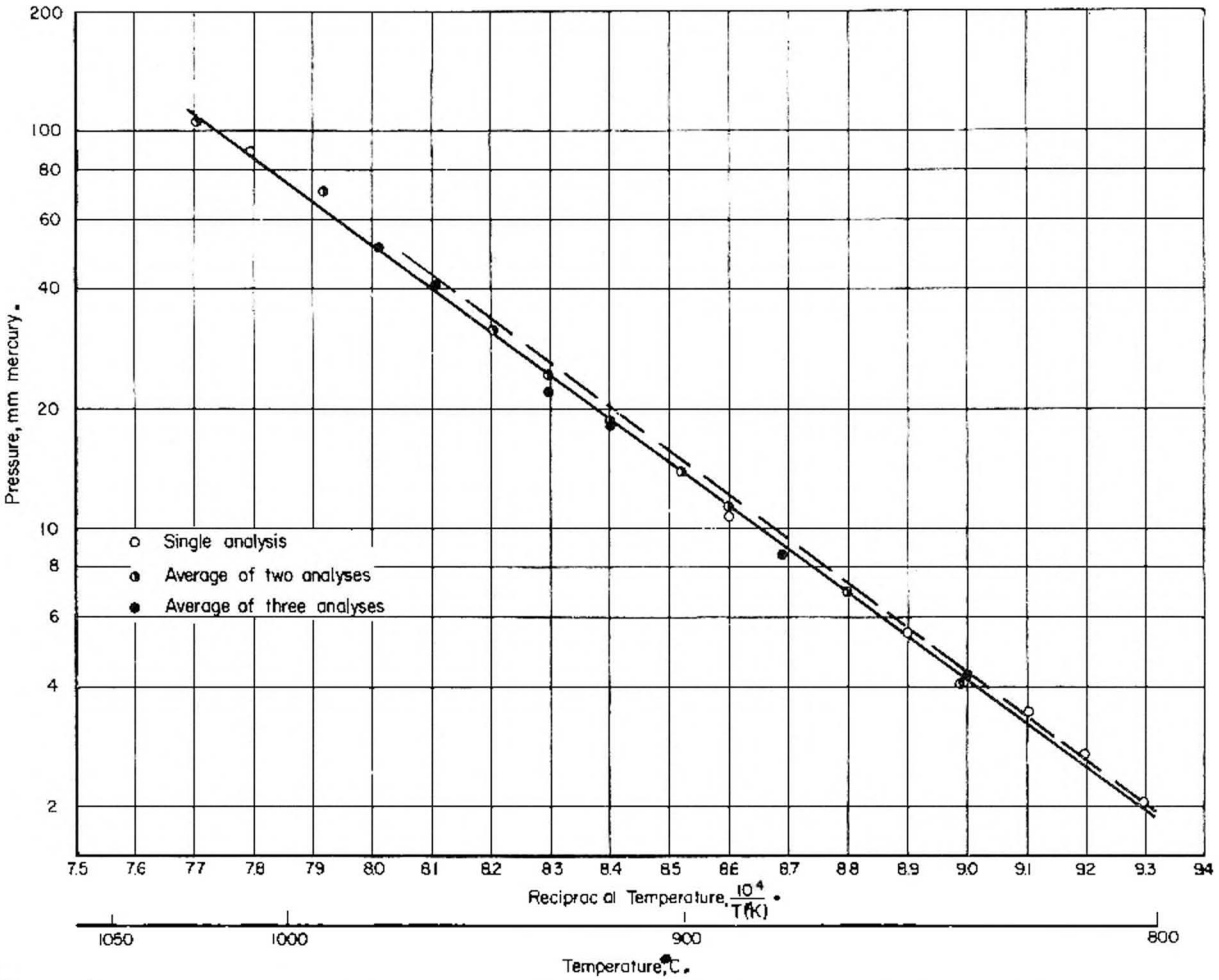

Fig. 1.—Vapor pressures of pure BeF_2 over the range 802 to 1025°. Solid curve is result of weighted least-square treatment of data. Dashed curve is result of previous study.

the NaF–BeF_2 mixture has not been determined. However, this behavior is believed to be related to the differences in viscosity of the two liquids. Below 800° BeF_2 becomes increasingly viscous while the NaF–BeF_2 melt remains quite fluid at lower temperatures.

The Vapor Pressures of the NaF–BeF_2 System. Molecular Composition of Vapor Phase.—Results of vapor pressure runs for the NaF–BeF_2 system are given in Table II. A plot of the partial pressures of BeF_2 is given in Fig. 2. The data are presented on the basis that only NaF and BeF_2 exist in the vapor phase. Figure 3 is a partial pressure plot of NaF and BeF_2 as a function of composition at 890°, assuming that only NaF and BeF_2 exist in the vapor phase. Previously presented theory,[2] based on the Duhem–Margules equation

$$x_1 \left(\frac{\partial \ln p_1}{\partial x_1}\right)_T = x_2 \left(\frac{\partial \ln p_2}{\partial x_2}\right)_T \qquad (4)$$

discloses that the peak of a partial pressure curve indicates the presence of a molecular complex in the vapor phase, the composition of the complex being given by the location of the peak of the partial pressure curve. In Fig. 3 the peak of the p'_{NaF}[7] curve is located at 50 mole % BeF_2. Hence, the complex is immediately determined as being $NaBeF_3$. In accordance with the procedure worked out previously,[2] the partial pressures of NaF, BeF_2 and $NaBeF_3$ were determined for 890° and plotted in Fig. 4. From this plot the composition which melts at 890° is determined as being about 17 mole % BeF_2. This is in slight disagreement with the phase diagram by Thilo and Schröder,[8] which indicates that this is the melting point for a 15 mole % BeF_2 composition. Since the solid phase is NaF, p_{NaF} remains constant over that composition region. The dashed line above it represents the vapor pressure of the supercooled solution. From the shape of the p_{NaF} curve, it appears that another p_{NaF} peak must occur in the NaF–$NaBeF_3$ system. This peak would have to occur in the 31.5-50 mpc[9] region and according to our theory would indicate the presence of an additional vapor phase complex. The simplest complex which could have its partial pressure peak in that composition range is Na_2BeF_4.

Construction of partial pressure plots, similar to that of Fig. 4 but at higher temperatures, indicates that this p_{NaF} peak becomes less prominent as the

(7) Partial pressures calculated on the basis that only NaF and BeF_2 exist in the vapor phase will be denoted by a prime (′); for a system based on the existence of NaF, BeF_2 and $NaBeF_3$ in the vapor phase, the partial pressures will be given without any primes.

(8) E. Thilo and H. Schröder, *Z. physik. Chem.*, **197**, 41 (1951).

(9) The phrase "mole per cent. BeF_2 composition" is abbreviated to "mpc."

TABLE II

VAPOR PRESSURE DATA OF THE NaF-BeF_2 SYSTEM[10]

Temp., °C.	Obsd. p_{NaF}, mm.	Obsd. p_{BeF_2}, mm.	Flow rate of carrier gas, cm.³/min.
	15.0 mole % BeF_2		
1061	1.082	0.43	40.1
1060	1.039	.23	40.2
1043	0.742	.29	40.0
1034	.656	.15	37.9
1023	.563	.22	37.3
1009	.499	.16	41.6
1008	.485	.13	35.7
993.8	.345	.092	39.3
991.4	.353	.14	39.3
985.2	.314	.14	51.4
978.7	.277	.082	49.4
961.8	.229	.066	47.4
961.8	.189	.078	49.5
960.4	.169	.074	52.8
942.6	.140	.040	50.1
939.0	.128	.044	51.3
938.9	.130	.026	50.9
929.9	.112	.029	45.4
917.3	.0906	.029	50.4
917.3	.0797	.029	49.2
903.8	.0609	.018	51.6
896.6	.0567	.018	50.7
887.0	.0540	.013	50.8
	19.2 mole % BeF_2		
1060	1.189	0.472	44.4
1051	1.018	.334	39.8
1043	0.848	.291	47.0
1026	.619	.205	47.1
1009	.459	.152	51.7
992.6	.345	.136	47.8
977.1	.246	.0640	50.6
961.4	.208	.0647	50.0
947.4	.142	.0404	51.2
931.6	.0971	.0278	50.2
917.6	.0824	.0227	50.2
903.3	.0848	.0168	49.8
896.4	.0530	.0148	49.6
890.7	.0449	.0142	51.4
	24.5 mole % BeF_2		
1035	0.915	0.453	47.5
1025	.736	.467	49.9
1021	.636	.372	47.9
996.4	.437	.260	49.1
992.6	.414	.286	49.2
976.7	.292	.179	43.5
963.3	.247	...	47.3
961.4	.220	.145	47.8
947.0	.171	.102	48.7
946.4	.181	...	47.2
932.9	.133	...	49.3
932.0	.129	.0755	48.9
926.7	.114	.0550	49.6
921.8	.103	.0438	51.3
916.7	.0981	.0527	48.8
910.0	.0747	.0356	47.2
909.5	.0912	...	15.2
897.8	.0620	.0327	49.2
893.1	.0607	.0289	51.0
882.9	.0486	.0194	48.5
876.2	.0431	...	48.9
867.1	.0381	.0202	48.4
856.8	.0280	.0128	50.8
836.0	.0188	...	48.0
825.6	.0125	.00635	51.2
	31.5 mole % BeF_2		
1060	2.91	2.40	23.7
1060	2.41	2.19	22.6
1043	1.64	2.09	25.4
1043	1.67	1.99	25.7
1026	1.72	1.50	31.1
1026	1.30	1.72	25.1
1009	0.851	0.891	50.3
992.6	.671	.612	43.4
992.5	.739	.654	48.2
979.0	.539	.497	49.7
977.5	.485	.450	49.3
969.0	.459	.229	50.3
961.4	.401	.279	49.5
961.3	.366	.159	49.7
946.1	.292	.228	48.7
931.7	.226	.0667	48.2
931.6	.224	.190	53.8
917.5	.165	.117	51.0
916.9	.160	.0984	50.7
903.3	.114	.0577	49.2
903.3	.115	.0735	49.0
889.8	.0907	.0685	50.7
876.2	.0689	.0555	49.4
876.2	.0698	.0117	43.7
	39.5 mole % BeF_2		
1026	2.52	3.56	21.0
1010	2.05	3.35	21.8
994.2	1.52	2.28	21.5
978.5	1.15	1.99	21.9
961.4	0.950	1.34	26.5
946.9	.672	1.02	33.5
917.3	.399	0.616	47.3
896.3	.257	.409	48.5
876.2	.166	.240	49.0
855.4	.113	.189	48.1
	50.0 mole % BeF_2		
1012	3.35	16.0	19.5
996.8	2.73	14.1	16.3
987.0	2.70	13.6	14.2
983.2	2.20	12.3	15.4
975.6	1.82	8.53	44.6
970.7	2.01	9.68	13.4
961.4	1.61	8.85	15.4
956.6	1.23	6.57	29.8
932.0	0.952	5.71	24.2
918.3	.677	3.89	30.4
916.1	.727	3.71	18.9
895.3	.450	2.72	26.8
877.9	.312	1.90	34.1
854.4	.191	1.27	41.0
833.5	.130	0.804	47.5
815.1	.0779	0.548	50.0
796.5	.0547	0.367	49.7

(10) The original data have been deposited as Document number 5491 with the ADI Auxiliary Publications Project, Photoduplication Service, Library of Congress, Washington 25, D. C. A copy may be secured by citing the Document number and by remitting $1.25 for photoprints, or $1.25 for 35 mm. microfilm in advance by check or money order payable to: Chief, Photoduplication Service, Library of Congress.

TABLE II (*Continued*)

	58.8 mole % BeF_2		
988.6	2.26	30.3	15.8
963.1	1.505	20.5	12.2
938.8	0.993	14.25	15.0
919.4	.674	9.61	22.4
896.4	.477	6.03	26.4
877.7	.292	4.71	31.1
856.8	.198	3.07	33.3
840.3	.131	2.24	50.8
819.8	.0855	1.43	50.5
802.2	.0556	0.980	50.4
	73.9 mole % BeF_2		
976.9	1.36	48.5	13.7
956.0	0.851	37.2	13.9
937.0	.684	23.6	19.7
910.3	.372	15.0	21.9
890.2	.248	10.1	22.3
871.0	.170	7.67	26.5
850.4	.108	4.63	30.2
833.4	.0712	3.62	37.8
813.7	.0512	2.32	37.2
800.6	.0324	1.74	43.3
784.9	.0234	1.18	50.3
768.5	.0104	0.785	50.8
752.5	.00817	.482	50.6
736.8	.00415	.357	50.6
726.7	.00422	.288	49.4
717.9	.00602	.232	49.9
688.3	.00158	.110	50.0
670.2	.00106	.0635	49.8
657.4	.00167	.0483	49.4
635.7	.....	.0196	51.0
625.8	.....	.0101	50.2
604.0	.....	.00801	50.1
595.7	.....	.00526	50.4
574.3	.....	.00183	51.1
566.5	.....	.00192	51.0
539.8	.....	.000794	50.2
534.5	.....	.000823	51.0
514.3	.....	.00132	50.4
509.2	.....	.000555	50.6
490.2	.....	< .000536	50.6
488.1	.....	< .000564	50.2

TABLE III

DERIVED VAPOR PRESSURE CONSTANTS FOR THE NaF-BeF_2 SYSTEM ON THE BASIS THAT THE VAPOR PHASE IS COMPOSED OF NaF, BeF_2 AND $NaBeF_3$

$$\log p\,(\text{mm.}) = A - \frac{B \times 10^3}{T,\ ^\circ\text{K.}}$$

Compn. mole % BeF_2	p_{NaF} A	p_{NaF} B	p_{NaBeF_3} A	p_{NaBeF_3} B	p_{BeF_2} A	p_{BeF_2} B
73.9	...	....	9.808	12.113	10.506	11.051
58.8	...	....	9.804	11.891	10.038	10.825
50.0	...	....	9.868	11.934	9.580	10.785
39.5	...	....	9.747	12.099	8.719	11.150
31.5	3.038	5.198	11.361	14.694	11.037	15.490
24.5	7.316	10.278	10.496	14.068	....	....
19.2	8.753	11.907	9.948	13.797	....	....
15.0	8.946	12.039	8.830	12.593	....	....

temperature is increased until it finally disappears. One could explain this behavior on the basis that a complex such as Na_2BeF_4 is rather unstable and

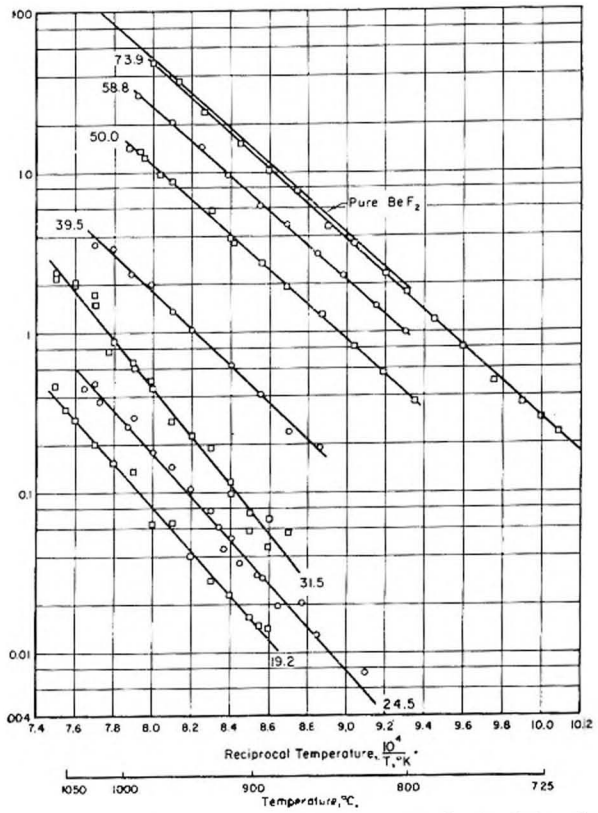

Fig. 2.—Partial pressures of BeF_2 on the basis that only NaF and BeF_2 exist in the vapor phase. Figures on plot denote mole % BeF_2.

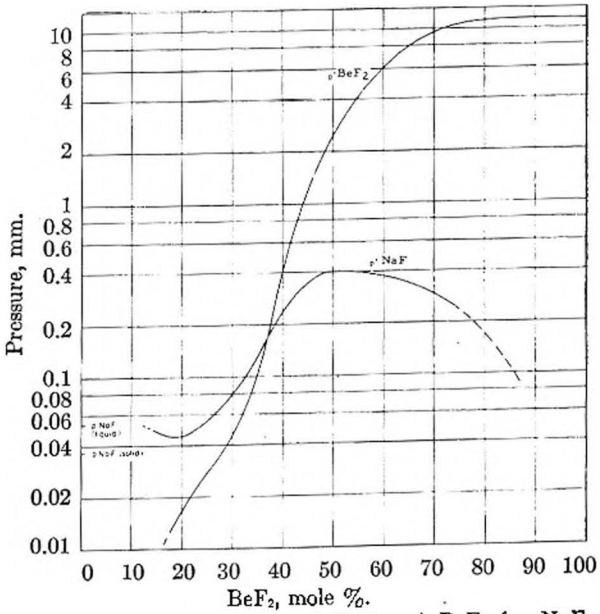

Fig. 3.—Partial pressures of NaF and BeF_2 for NaF-BeF_2 system at 890° on the basis that only NaF and BeF_2 exist in vapor phase.

dissociates readily into NaF and $NaBeF_3$ as the temperature is increased.

Though the existence of gaseous Na_2BeF_4 seems quite possible, it seems that further work is indicated to establish its presence unambiguously. Perhaps either more data over a greater temperature range for 31.5 mpc. or data for compositions between 31.5 and 39.5 mpc. might have been helpful

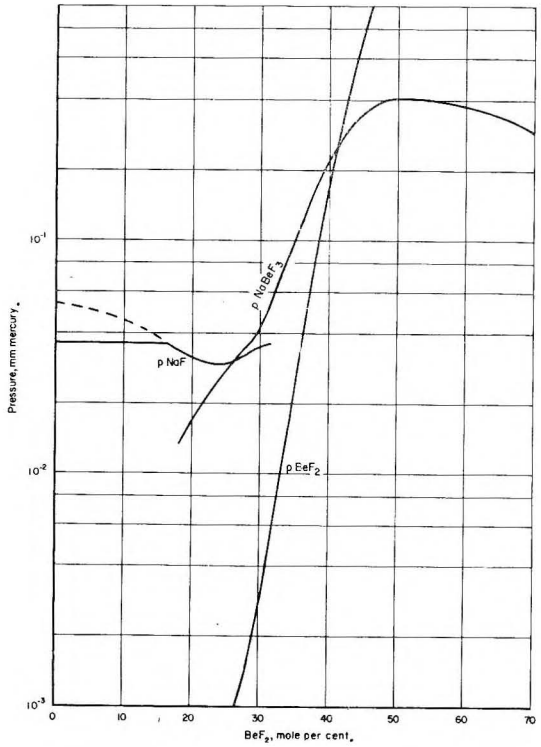

Fig. 4.—Partial pressures at 890° on the basis that NaF, BeF_2 and $NaBeF_3$ exist in the vapor phase.

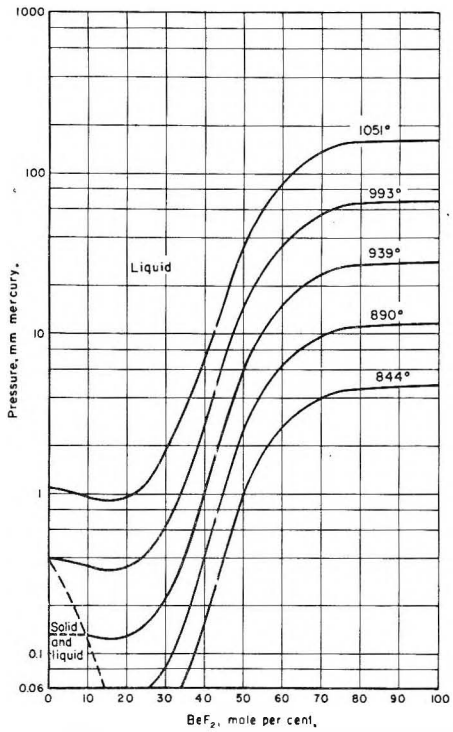

Fig. 5.—Total vapor pressures of the NaF–BeF_2 system on the basis that NaF, BeF_2 and $NaBeF_3$ exist in the vapor phase.

in establishing definitely the existence of such a vapor phase complex.

In the absence of firm evidence of the existence of gaseous Na_2BeF_4, the vapor phase of the NaF–BeF_2 system was treated as consisting only of the NaF, BeF_2 and $NaBeF_3$ molecular species. A tabulation of all the derived constants of the partial pressure equations for NaF, BeF_2, and $NaBeF_3$ is given in Table III.

Total Vapor Pressures of the NaF–BeF_2 System.—Figure 5 shows how the total pressure of the NaF–BeF_2 system changes with composition for various temperatures. Previously obtained vapor pressure data for pure NaF[11] were used in the construction of this plot. The phase diagram by Thilo and Schröder[8] was used to determine the compositions which melt at the various temperatures.

Acknowledgments.—The authors express their sincere thanks to Dr. J. W. Droege for many helpful discussions. They also thank the analytical department at Battelle Memorial Institute, as well as Tom Culbertson for his assistance in carrying out the experimental work.

(11) K. A. Sense, C. A. Alexander, R. E. Bowman, R. W. Stone and R. B. Filbert, Jr., THIS JOURNAL, **61**, 384 (1957).

THERMAL TRANSPIRATION OF GASES AT LOW PRESSURES[1]

BY A. J. ROSENBERG AND C. S. MARTEL, JR.

Lincoln Laboratory, Massachusetts Institute of Technology, Lexington, Massachusetts

Received December 5, 1957

Measurements of the thermal transpiration of krypton have been extended to low pressures. The functional dependence of p_1/p_2 on p_2D has been verified, but Liang's equation does not represent the data when $p_2D < 75\ \mu$ mm. A general empirical correction to Liang's equation, applicable to gases which obey the equation at higher pressures, is proposed for the region $\phi_g p_2 D \lesssim 300\ \mu$ mm.

In recent years the thermal transpiration[2] of gases has received considerable attention by workers in the field of low pressure gas adsorption.[3-9] In the conventional apparatus for adsorption measurements[10] the sample chamber is separated by

(1) The research reported in this document was supported jointly by the Army, Navy and Air Force under contract with the Massachusetts Institute of Technology.

(2) M. H. C. Knudsen, "Kinetic Theory of Gases," Methuen and Co., Ltd., London, 1934; *Ann. Physik*, **31**, 205, 633 (1910).

(3) S. C. Liang, *J. Appl. Phys.*, **22**, 148 (1951).

(4) S. C. Liang, THIS JOURNAL, **56**, 660 (1952).

(5) S. C. Liang, *ibid.*, **57**, 910 (1953).

(6) S. C. Liang, *Can. J. Chem.*, **33**, 279 (1955).

(7) J. M. Los and R. R. Ferguson, *Trans. Faraday Soc.*, **48**, 730 (1952).

(8) G. L. Kington and J. M. Holmes, *ibid.*, **49**, 417, 425 (1953).

(9) A. J. Rosenberg, *J. Am. Chem. Soc.*, **78**, 2929 (1956).

(10) S. Brunauer, "Adsorption of Gases and Vapors on Solids," Princeton University Press, Princeton, N. J., 1943.

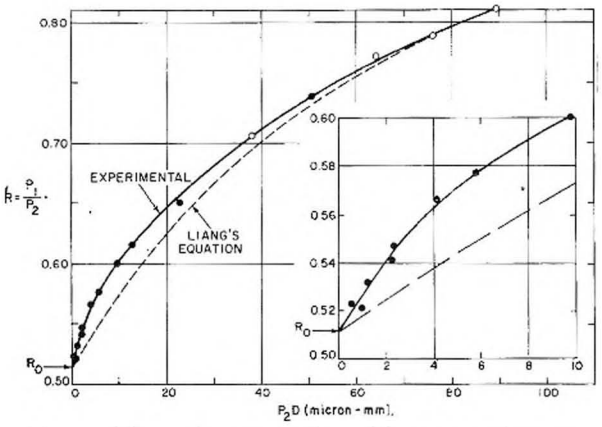

Fig. 1.—Thermal transpiration of krypton at low pressures: $T_1 = 77.8°K.$, $T_2 = 297.1°K.$ The experimental values of p_1/p_2 are compared with those obtained by eq. 3 using $\phi_{Kr} = 3.84$. Solid circles show present results; open circles, previous results.[9]

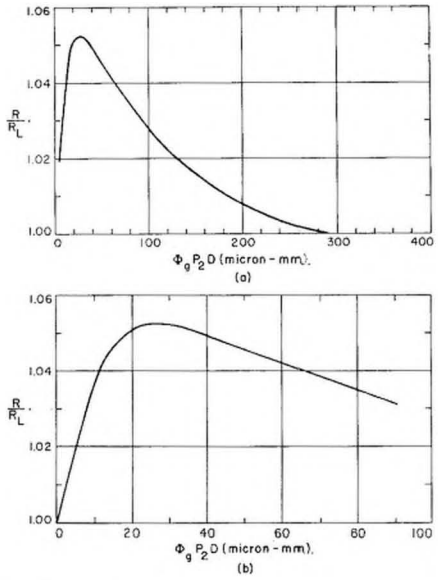

Fig. 2.—Deviation of the thermal transpiration ratio $R = p_1/p_2$ from Liang's equation. These curves may be used for the necessary correction of eq. 3 when $\phi_g p_2 D \lesssim 300\ \mu$ mm. Values of ϕ_g for several common gases are given by Liang.[6]

small-bore tubing from the remainder of the system, which includes the manometer. When the sample chamber is maintained at a temperature differing from that in the rest of the gas enclosure, the equilibrium pressure is lower in the colder section. While the deviation is negligible at high pressures, it becomes appreciable when the mean free path (λ) of the gas approaches the diameter (D) of the connection. In the limit of very low pressures, when $\lambda >> D$, the ratio of pressure in the colder part of the system (p_1) to that in the warmer part (p_2) is given by the Knudsen equation for thermal transpiration[2]

$$(p_1/p_2)_{\lambda >> D} = (T_1/T_2)^{1/2} \equiv R_0 \qquad (1)$$

where T_1 and T_2 are the lower and higher absolute temperatures, respectively. At intermediate pressures, Liang[3-6] has assumed that, for a given gas, p_1/p_2 can be expressed as a function of R_0 and the product p_2D alone, *i.e.*

$$R \equiv p_1/p_2 = f(p_2D, R_0) \qquad (2)$$

He has also proposed a general empirical formula for R, *viz.*

$$R_L = \frac{R_0 - 1}{\alpha_{He}\phi_g^2(p_2D)^2 + \beta_{He}\phi_g(p_2D) + 1} + 1 \qquad (3)$$

where

$$\alpha_{He} = 2.52 \times 10^{-6}\ \mu^{-2}\ \text{mm.}^{-2}$$
$$\beta_{He} = 7.68 \times 10^{-3}(1 - R_0)\mu^{-1}\ \text{mm.}^{-1}$$

and ϕ_g is a constant characteristic of the gas in question (*e.g.*, $\phi_{He} = 1$, $\phi_{Kr} = 3.84$). Equation 3 accurately describes existing data on thermal transpiration.[3,5,9] Suitable test data have been lacking, however, in the region $0 < p_2D \lesssim 100\ \mu$ mm.

Thermal transpiration is conventionally measured by connecting separate manometers to the ends of a U-tube made by joining two tubes of large and small diameters, immersing the lower half of the U-tube at the temperature of interest, admitting various charges of gas to the system and making simultaneous pressure readings.[3] The diameter of the large tube is so chosen that, in the range of pressures measured, thermal transpiration within it is negligible, and the measured pressure difference can be ascribed wholly to the smaller tube. Even if this condition is not observed, however, the data can be corrected by a simple mathematical procedure based on eq. 2.[9]

The thermal transpiration of krypton was recently determined[9] with high precision by utilizing an apparatus of the kind just described which was equipped with thermistor manometers. The average deviation of the measured values of R from the values calculated from eq. 3, utilizing $\phi_{Kr} = 3.84$, was less than 0.001 in the range $75\ \mu$ mm. $< p_2D <$ $1900\ \mu$ mm. At $p_2D < 75\ \mu$ mm., however, positive deviations from eq. 3 were evident.

With the apparatus employed, precise determinations of R were difficult when $p_2D \lesssim 50\ \mu$ mm. The present paper describes results obtained by another technique which confirms the applicability of eq. 2 for all values of p_2D, but reveals a pronounced deviation from eq. 3 as p_2D approaches zero.

Experimental

A length of tubing consisting of successive 7 cm. sections of 10.1, 3.98, 2.10 and 0.904 mm. Pyrex tubing was used to connect a 5-cc. sample chamber containing 50 mg. of TiO_2 powder to a gas adsorption apparatus which has been described elsewhere.[9] The total dead-space in the apparatus was 11 cc. The sample chamber was immersed in liquid nitrogen and sufficient krypton was added to give an equilibrium adsorption pressure of $\approx 4\ \mu$ in the sample chamber. The liquid nitrogen level was lowered successively to positions midway on each capillary section and the pressure in the warm side of the system (p_2) was determined with a thermistor gage. The conditions were such that, when the nitrogen level was changed, the maximum quantity of krypton adsorbed or desorbed ($\Delta N_s \approx 40\ \mu$ cc.) was very small compared to the total quantity adsorbed ($N_s \approx 40{,}000\ \mu$ cc.). Since p_1 is approximately proportional to N_s at the low surface coverages involved ($\theta < 0.5$), the variation in p_1 was negligible and the observed variation in p_2 was due only to the changes in D.

When the nitrogen level was centered on the 10.1 mm. tubing, p_2 was $5.00 \pm 0.02\ \mu$, hence, p_2D was $50.5\ \mu$ mm. The validity of eq. 2 was assumed, permitting the use of the data obtained previously[9] to give $R(p_2D = 50.5\ \mu\text{ mm.}) = 0.740$. Accordingly p_1 was $3.70 \pm 0.01\ \mu$, which, divided by the values of p_2 observed at the smaller D, gave R at

smaller p_2D. By repeating the entire procedure with successively smaller charges of krypton, a sufficient overlapping of data was obtained to describe the entire range of R *vs.* p_2D.

Results and Conclusion

The results are summarized in Fig. 1. The applicability of eq. 2—the basis of the experimental procedure—is confirmed by the approach of R to the Knudsen value, R_0, as p_2D approaches zero. Equation 3, on the other hand, fails to describe the results when $0 < p_2D < 75\ \mu$ mm.

The ratio of R to R_L, where R is the real value of p_1/p_2, and R_L is the value calculated from eq. 3 using $\phi_{Kr} = 3.84$, is plotted *vs.* $\phi_{Kr}p_2D$ in Fig. 2. Since eq. 3 is general,[3-6] it is not unreasonable to conclude that the deviations from eq. 3 are also general, depending likewise on the variable, $\phi_g p_2 D$. For a given value of $\phi_g p_2 D$, therefore, the product of the corresponding values of R_L, calculated from eq. 3, and R/R_L, obtained from Fig. 2, should give the correct value of the pressure ratio, p_1/p_2, arising from the thermal transpiration of simple gases in tubing made of Pyrex glass.

THE ROLE OF CROSS-LINKAGES IN THE SOLUBILIZATION OF INSOLUBLE COLLAGEN

By Arthur Veis and Jerome Cohen

Research Division, Armour and Company, Chicago, Illinois

Received December 6, 1957

To determine the relative contributions of interchain hydrogen bonds and covalent cross-linkages to the stability of collagen, the solubilization process was compared with the thermal shrinkage in a variety of solvents, some of which compete with internal protein hydrogen bonds (*e.g.*, 2.0 *M* KCNS, 6.0 *M* urea). The solubilization process in all solvents clearly occurred in two stages showing the existence of at least two species of molecules in the intact structure. This was confirmed by coacervation–fractionation of the soluble gelatins. The thermodynamics of the activation step in solubilization were determined by rate studies. In water, at $T_{Extraction} < T_{Shrinkage}$, $\Delta F_{50}^{\ddagger} = 27.7$ kcal., $\Delta H_{50}^{\ddagger} = 42.5$ kcal., $\Delta S_{50}^{\ddagger} = 45.6$ e.u.; at $T_E > T_S$, $\Delta F_{70}^{\ddagger} = 27.5$, $\Delta H_{70}^{\ddagger} = 5.9$, $\Delta S_{70}^{\ddagger} = -63$. In 2.0 *M* KCNS $\Delta F_{50}^{\ddagger} = 25.9$, $\Delta H_{50}^{\ddagger} = 13.3$, $\Delta S_{50}^{\ddagger} = -38.9$ while $\Delta F_{70}^{\ddagger} = 27.0$, $\Delta H_{70}^{\ddagger} = 6.7$, $\Delta S_{70}^{\ddagger} = -59.2$. Since $\Delta S_{50}^{\ddagger} = +361$ e.u. and $\Delta H_{50}^{\ddagger}$ 141 for shrinkage, it is evident that imbibition of solvent rather than thermal shrinkage is essential for extraction. The discontinuity in $\Delta S^{\ddagger}$ occurred when the molecular species being extracted was changed rather than at T_S as would have been expected if H-bonds were the primary cause of the insolubility of collagen. The origin and distribution of the cross-linkages is discussed.

Introduction

The native fibrous proteins are particularly interesting polymeric systems since, in contrast to the synthetic cross-linked random-chain high polymers, any interchain cross-linkages which are present are "superimposed on, or in, a previously ordered system."[1] By studying the disaggregation process, and characterizing the molecular species involved, one may approach the question of the nature and distribution of the cross-linkages and the influence of these linkages on solubility, thermal stability and biological properties. Collagen fibers are especially suited to such an investigation since it is well recognized that their stability is a function of the fiber source.[2] Consequently, a number of different initial cross-linkage distributions or structures must be available for study. Further, it is our belief that a knowledge of these distributions lies at the very heart of the understanding of the collagen–gelatin transition as well as of a variety of problems concerned with the aging of connective tissue.

On the basis of our recent investigations[3,4] of the collagen–gelatin transition, we may tentatively write the following steps as being crucial in the solubilization process (but not necessarily in this order): (a) irreversible melting of the polypeptide helical coil, (b) irreversible severance of interpeptide chain bonds and (c) irreversible hydrolysis of peptide linkages. The interchain stabilizing forces have been ascribed to salt links,[2] interchain hydrogen bonds,[2] covalent cross-linkages[3] and small amounts of cementing mucopolysaccharides.[5] In view of the fact that acid-swelling and high salt concentrations do not necessarily disrupt the collagen structure, and since thermal shrinkage does not involve salt-links,[6,7] we prefer to disregard these links in our subsequent considerations. We shall also assume, with perhaps less justification, that collagen–mucopolysaccharide interactions are unlikely to be of importance in the systems we have studied.[8,9]

It remains, then, to differentiate between the effects of hydrogen-bond and interchain-covalent-bond rupture on the solubility of collagen and on the resulting molecular species distributions. We have, therefore, examined the solubilization of native steer hide collagen in water, H-bond competing solvents, and in 1–1 salt of equivalent ionic strength.

Procedure

A. Experimental.—Small cubes of native steer hide collagen (N = 18.4%, ash <0.01%) were prepared as de-

(1) P. J. Flory, *J. Am. Chem. Soc.*, **78**, 5222 (1956).

(2) K. H. Gustavson, "Chemistry and Reactivity of Collagen," Academic Press, Inc., New York, N. Y., 1956, pp. 202–243.

(3) A. Veis and J. Cohen, *J. Am. Chem. Soc.*, **78**, 6238 (1956).

(4) A. Veis, J. Anesey and J. Cohen, "Recent Adv. in Gelatine and Glue Research," 1957.

(5) See F. Wasserman and A. Lindenbaum, *J. Biophys. Biochem. Cytology Supp.*, **2**, 299 (1956), for a brief summary of evidence on this point.

(6) C. W. Weir and J. Carter, *J. Research Natl. Bur. Standards*, **44** 599 (1950).

(7) K. H. Gustavson, *Biochem. J.*, **311**, 347 (1942); *Acta Chem. Scand.*, **1**, 581 (1947); *J. Am. Leather Chem. Assn.*, **41**, 47 (1946).

(8) Dr. Martin Mathews kindly analyzed a sample of our collagen preparation for polysaccharide and reported that only a trace of hexosamine was present.

(9) F. O. Schmitt, J. Gross and J. A. Highberger, *Exp. Cell Research*, **3**, Supp. 326 (1955).

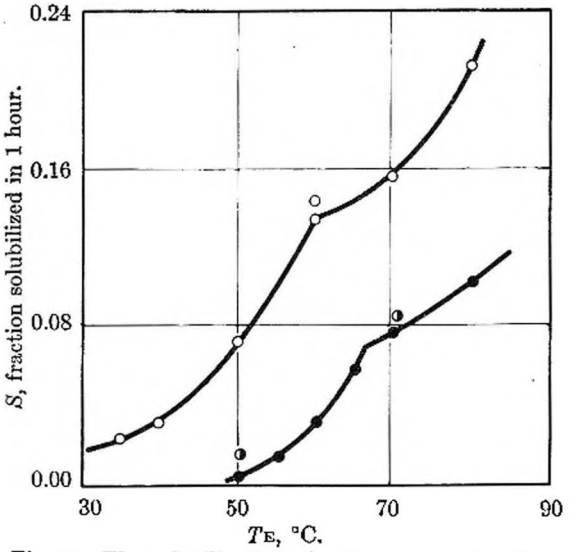

Fig. 1.—The solubilization of collagen as a function of extraction temperature, T_E, in various solvent systems: ●, H_2O; ○, 2.0 *M* KCNS; ◑, 2.0 *M* NaCl.

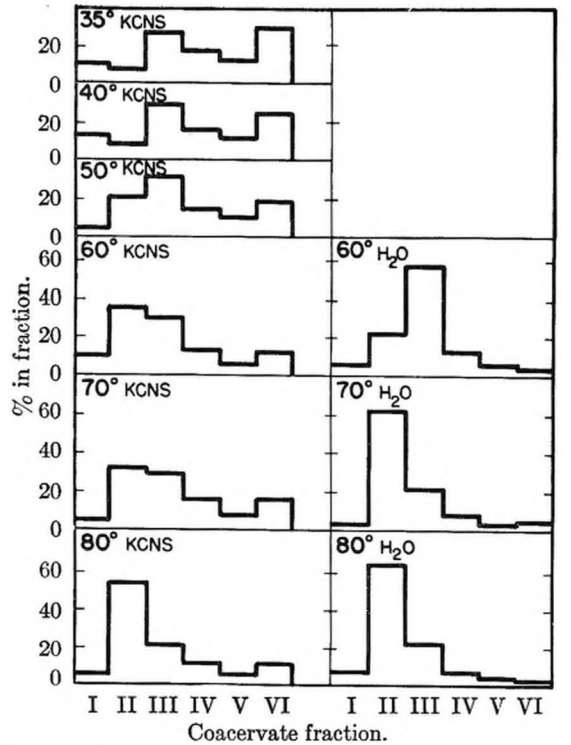

Fig. 2.—Alcohol-coacervation fractionation distribution of solubilized collagen.

scribed previously.[3] For an extraction, 10 g. of the collagen was equilibrated with 100 cc. of a 2.0 *M* KCNS solution, 2.0 *M* NaCl solution or distilled water at room temperature. Extractions were also made in 6.0 *M* urea, dimethylformamide and 90% phenol. The mixture was deaerated, placed in a constant-temperature-bath at the desired temperature, and stirred for one hour. At the end of this period, the mixture was immediately poured through a coarse sintered glass filter. Both filtrate and residue were cooled, dialyzed at 5 to 10° against distilled water until free of salt, then lyophilized. The dry protein was weighed and the results, based on the weight of the soluble portion, were recorded in terms of the fraction solubilized, *S*. As before[3] we assumed that all weight losses occur in the insoluble portion. Total recovery averaged 95%. The results are given in Fig. 1. The data obtained for urea, dimethylformamide and 90% phenol are all intermediate between the thiocyanate and water curves. The direct ionic strength effect is small (see NaCl points, [◑], in Fig. 1); thus the increase in solubilization in KCNS is due to other properties. These data cannot be particularly well correlated with the instantaneous contraction temperatures, Table I. The contraction temperatures were determined by observations of single fibers in sealed glass capillary tubes heated in an aluminum block on a microscope hot stage.[10]

TABLE I

INSTANTANEOUS SHRINKAGE TEMPERATURES OF COLLAGEN PREPARATION IN EXTRACTION SOLVENT SYSTEMS

Solvent	T_S range, °
Water	55.8–60.6
2.0 *M* NaCl	52.3–55.6
2.0 *M* KCNS	39.8–43.2
6.0 *M* Urea	36.5 42.8

A portion of each thiocyanate and each water extract was fractionated by an ethanol-NaCl coacervation technique, the details of which have been described elsewhere.[3] Six fractions were obtained. The fractionation-distribution data, characteristic of the molecular weight or molecular-configuration distributions, are shown in Fig. 2.

B. Treatment of the Data.—The fraction of protein solubilized in one hour, *S*, is a rate term and our earlier solubilization rate studies indicate that this is very close to the initial rate.[11] Further, since the initial rate of solubilization, in terms of *S*, is independent of the amount of insoluble protein present, *S* is proportional to the rate constant, *k*, if we include in *k* all of the solvent effects. One can, therefore, use the transition state theory and calculate the free energies, enthalpies and entropies of activation according to equation I.

$$k'S = \frac{kT}{h} e^{-\Delta F^{\ddagger}/RT} = \frac{kT}{h} e^{-\Delta H^{\ddagger}/RT} e^{+\Delta S^{\ddagger}/R} \quad (1)$$

Thus, if the statement that *S* is proportional to the specific rate is valid, a plot of ln S/T *vs.* $1/T$ should be a straight line. Such plots of both the 2.0 *M* KCNS and H_2O extraction data, Fig. 3, show two linear portions, which is not surprising in view of the two stages evident in the plots of *S vs. T*, Fig. 1. Values of $\Delta F^{\ddagger}$ calculated from equation 1 of $\Delta H^{\ddagger}$ from the slopes of the lines of Fig. 3, and of $\Delta S^{\ddagger}$ from

$$\Delta F^{\ddagger} = \Delta H - T\Delta S^{\ddagger} \quad (2)$$

are given in Table II.

TABLE II

THERMODYNAMICS OF THE ACTIVATION STEP IN THE SOLUBILIZATION OF INTACT COLLAGEN

	Water extraction			2.0 *M* KCNS extraction		
T_E, °C.	$\Delta F_T^{\ddagger}$, kcal.	$\Delta H_T^{\ddagger}$, kcal.	$\Delta S_T^{\ddagger}$, e.u.	$\Delta F_T^{\ddagger}$, kcal.	$\Delta H_T^{\ddagger}$, kcal.	$\Delta S_T^{\ddagger}$, e.u.
35				25.4		
40				25.6		
50	27.7	42.5	45.6	25.9	13.3	−38.9
55	27.6					
60	27.3					
				26.3		
70	27.5	5.9	−62.9	27.0	6.7	−59.2
80	28.1			27.6		

Interpretation and Discussion

1. Are hydrogen bonds primarily responsible for the insolubility of collagen?

The experiments which have been described were designed specifically to contrast the situations:

(10) R. Borasky and G. C. Nutting, *J. Am. Leather Chem. Assn.*, **44**, 830 (1949).

(11) A. Veis and J. Cohen, *J. Am. Chem. Soc.*, **77**, 2364 (1955).

Case A.—Intact, organized structure + solvent ----→ Soluble, disorganized fragments solvated

and

Case B.—Intact, disorganized structure, solvated ----→ Soluble, disorganized fragments solvated

the terms "organized" and "disorganized" referring to the presence or absence of both inter- and intrachain H-bonds. It was presumed that an extraction of native collagen in water at a temperature below the contraction temperature, T_S, would be equivalent to case A, while case B would be exemplified by extraction either in water or in 2.0 M KCNS at $T > T_S$. It also was presumed that a case B extraction particularly in 2.0 M KCNS would be characterized by a *positive* $\Delta S^{\ddagger}$ somewhat smaller than the entropy of denaturation of globular proteins, while $\Delta S^{\ddagger}$ for case A would be a larger positive term.

The plots of $\Delta F^{\ddagger}$ *vs.* T (dashed lines in Fig. 4) show that there are in fact two solubilization processes, differing in temperature dependence, for the two types of experimental situations described above. However the entropy values, also shown, are of particular interest for three reasons. First, there is a distinct discontinuity in $\Delta S^{\ddagger}$ (and $\Delta H^{\ddagger}$) in the 2.0 M KCNS; second, $\Delta S^{\ddagger}$ for each case B extraction is a rather large negative quantity; while finally, there does not appear to be any obvious connection between the discontinuities in $\Delta S^{\ddagger}$ and the T_S ranges.

Even though the solid collagen fibers are hydrated and the internal H-bonds are severed in 2.0 M KCNS, it is obvious that an increased immobilization of solvent must account for the negative entropies of solubilization. This solvent immobilization could be achieved if the solubilized molecules are random coils, partially stiffened coils, or very swollen networks of chains held together by a few widely separated cross-linkages. The value of +45 e.u. for the solubilization in H_2O at $T \leqslant 65°$ must then include a large positive contribution related to the disordering of the native fiber. Weir[6] found $\Delta S_{60}^{\ddagger}$ for the thermal shrinkage of tendon collagen to be +361 e.u. The difference, −316 e.u./mole, may relate to the hydration accompanying the solubilization, indicating that the accumulation of solvent in the structure is an essential part of the activation step in the solubilization process. Some such step must be added to the three given in the introduction.

On this basis the discrepancy between the T_S range and the $\Delta S^{\ddagger}$ discontinuity is easier to rationalize. Shrinkage, thermal or mediated by H-bond competing molecules or ions, must be a coöperative phenomenon in which an entire segment of the fiber changes configuration while retaining the relative lateral peptide chain alignments. Solubilization on the other hand requires high hydration and chain or chain-segment separation. Thus, while shrinkage makes hydration easier, it is not the key process in solubilization. It becomes clear that some forces other than H-bonds must interlock the collagen fiber structure.

2. Do discrete cross-linkage distributions exist?

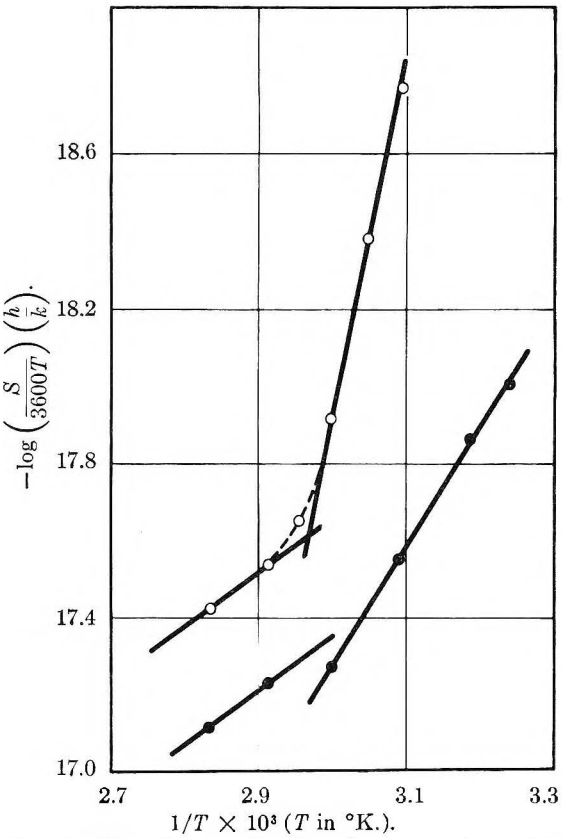

Fig. 3.—Plot of extraction data in terms of transition-state-theory parameters for calculation of $\Delta H^{\ddagger}$: ○, H_2O; ●, 2.0 M KCNS.

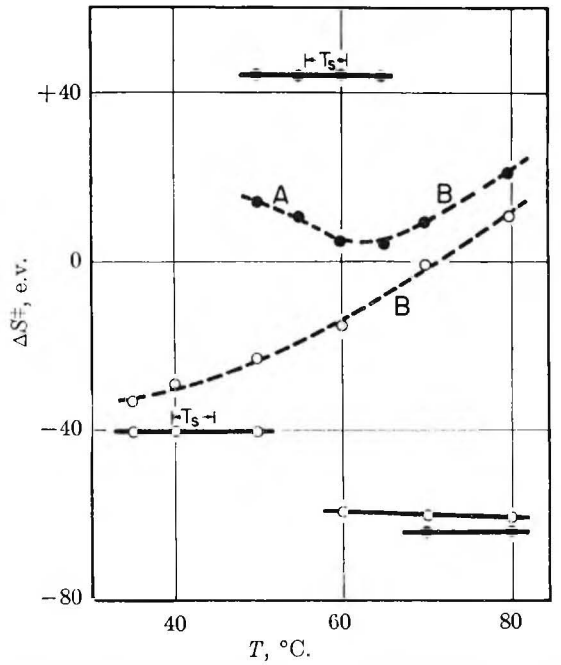

Fig. 4.—Change in free energy and entropy of activation as a function of extraction temperature. Solid lines refer to $\Delta S^{\ddagger}$, dashed lines to $\Delta F^{\ddagger}$. ●, H_2O extraction; ○, 2.0 M KCNS. The notations A and B refer to the situations described in the interpretation section.

In our study of the solubilization process as a function of the order in which extraction conditions were changed,[3] we showed that fragments of differ-

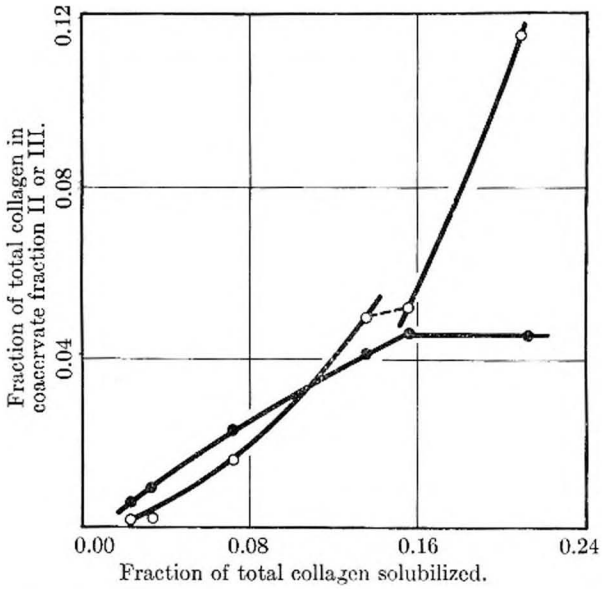

Fig. 5.— Distribution of coacervate fractions as a function of total amount of collagen solubilized in 2.0 *M* KCNS: ○, fraction II; ●, fraction III.

ent molecular weight could be solubilized selectively, the heaviest particles being obtained under the more drastic conditions. The fractionation data illustrated in Fig. 2 show that we have again achieved this selective type of extraction but in even a more clear-cut fashion. When the data for extraction in 2.0 *M* KCNS are replotted as in Fig. 5, relating the amount of the total protein in a given fraction to the total quantity of protein dissolved, two points are seen. First, the discontinuity in $\Delta S^{\ddagger}$ coincides with the sharply increased solubilization of higher-molecular-weight structure fragments. Second, the amount of more readily extracted smaller molecules increases up to the point of the $\Delta S^{\ddagger}$ discontinuity, then remains constant. (A comparison of these data with Fig. 2 of reference 3 shows that peptide-bond hydrolysis does not play any significant role in the solubilization of collagen in KCNS under these conditions.) From these observations we are led to the conclusion that collagen "molecules" of different size exist in the intact structure. Since H-bonds do not appear to be primarily responsible for the insolubility of these molecules it is likely that these species are characterized by being integrated into the collagen fiber structure with different cross-linkages or different cross-linkage densities.

3. Is there a unique protofibrillar unit in collagen?

Current theories of the biogenesis of collagen fibrils or fibrogenesis *in vitro* assume that protofibrillar elements of characteristic structure, stabilized by intramolecular hydrogen bonds, aggregate into the more gross fibrillar forms or are incorporated into the existing fiber structure in a high degree of order.[12] The over-all structure of the fibers, as revealed by X-ray diffraction and electron-microscopic investigations, is remarkably similar for collagens from different sources. Yet, Eastoe has shown[13] that collagens and gelatins from different sources do have detectably different amino acid compositions and, if the composition is widely enough at variance from the average mammalian collagen values, structure differences are observed (*e.g.*, Singleton points out that earthworm cuticle, a very abnormal collagen in terms of amino acid content, has a typical X-ray diffraction pattern but does not show banded fibers in the electron microscope[14]). Burton, *et al.*,[15] have concluded, without complete proof, that partial solubilization of collagen leads to products of varying amino acid contents. Further, Boedtker and Doty[16] have concluded that a protofibrillar element, tropocollagen, is composed of three peptide chains of unequal weight, and Cowan, McGavin and North[17] have indicated that if the basic collagen structure is a three-chain unit, the chains cannot have the same amino acid composition.

On considering this varied information, one is led to conclude that there is no single, homogeneous protofibrillar element. Apparently, within certain broad limits, considerable variation in amino acid composition does not alter the organization of the collagen helix. Thus polypeptide strands of slightly different chemical composition may be readily accommodated within a given tissue. Such compositional variations allow for variations in the extent of interaction between chains and provide the opportunity for the formation of varying distributions of interchain cross linkages. One is tempted to speculate that the neutral-salt-soluble collagen described by Jackson[12] and Slack[18] as the precursor of insoluble collagen may be a slightly heterogeneous mixture of single peptide chains.

Conclusions

1. The entropy of activation for the solubilization, $\Delta S^{\ddagger}$, of the native, intact structure (45.6 e.u.) is much smaller than the $\Delta S^{\ddagger}$ for thermal shrinkage (361 e.u.), while $\Delta S^{\ddagger}$ for the solubilization of the disorganized structure is a large negative number, −62.9 e.u. Thus, the imbibition of solvent is very important in the activation step. 2. There is no direct relationship between T's and the rate of solubilization, though in solvents for which T's is lowered the rate of solubilization is increased, even at $T < T$'s. 3. Units of varying solubility exist in what is normally termed "insoluble collagen." 4. On the basis of these data, interchain linkages other than hydrogen bonds are primarily responsible for the insolubility of collagen; different distributions of these cross-linkages occur; and these different distributions probably arise from the fact that the peptide chains in collagen are not identical in amino acid composition (or sequence).

(12) D. S. Jackson, *Biochem. J.*, **65**, 277 (1957).

(13) J. E. Eastoe, *ibid.*, **65**, 363 (1957).

(14) L. Singleton, *Biochem. et Biophys. Acta*, **24**, 67 (1957).

(15) D. Burton, D. A. Hall, M. K. Keech, R. Reed, H. Saxl, R. E. Tunbridge and M. J. Wood, *Nature*, **176**, 966 (1955).

(16) H. Boedtker and P. Doty, *J. Am. Chem. Soc.*, **78**, 4267 (1956).

(17) P. M. Cowan, S. McGavin and A. C. T. North, *Nature*, **176**, 1062 (1955).

(18) H. G. B. Slack, *Biochem. J.*, **65**, 459 (1957).

THE VAPOR PRESSURES OF $BiCl_3$ OVER LIQUID Bi–$BiCl_3$ SOLUTIONS[1]

BY DANIEL CUBICCIOTTI, F. J. KENESHEA, R., AND C. M. KELLEY

Stanford Research Institute, Menlo Park, California

Received December 6, 1957

A study of the pressure of $BiCl_3$ vapor in equilibrium with Bi–$BiCl_3$ liquid mixtures was made by the transpiration method. The study covered the range of temperature of 230 to 410° and of composition from pure $BiCl_3$ to about 0.4 in Bi mole fraction. The vapor was found to be essentially $BiCl_3$ over the entire range studied. Activities of $BiCl_3$ calculated from the vapor pressures reflected positive deviations from Raoult's law for the solution. The relative partial molal enthalpies and entropies of $BiCl_3$ in the Bi–$BiCl_3$ solutions were slightly positive for low concentrations of Bi and somewhat negative for higher Bi concentrations.

Introduction

The solution of metals in their molten salts is a facet of high temperature chemistry that is still inadequately understood. Recent studies have shown the limits of miscibility in a number of metal metal halide systems.[2] In order to probe more deeply into the nature of these intriguing systems, we have undertaken in this Laboratory a study of the thermodynamics of these solutions. The present paper is a report of our first results.

The Bi–$BiCl_3$ system is particularly interesting among those systems that show metal–salt solubility. Below a certain temperature a compound is known to precipitate from compositions which exhibit liquid immiscibility at higher temperatures.[3] We chose this system to study in the hope of explaining this behavior and also because the low melting points of the phases in the system and the high vapor pressure of $BiCl_3$ allowed the materials easily to be handled in Pyrex glass.

The vapor pressure of $BiCl_3$ provided a conveniently measurable property from which thermodynamic information could be derived. From the change of the partial pressure of $BiCl_3$ with temperature and composition the partial molal thermodynamic functions for $BiCl_3$ in the solution can be obtained. That was the approach employed for this study as reported below.

Experimental

Method.—After some unsuccessful attempts to use other techniques to measure the vapor pressure of $BiCl_3$ above its melt, we found that we could obtain satisfactory results with the transpiration (or transportation) method. In this procedure inert gas is passed over the condensed phase slowly enough to be saturated, the saturated gas then being subjected to analysis. Kubaschewski and Evans[4] discuss the method and Sense and co-workers[5] have recently applied it to some fused salt systems.

Our adaptation of the transpiration method is described as follows. The system was made of Pyrex glass, which had been found to be unattacked by molten Bi–$BiCl_3$ mixtures. During operation pure, dry nitrogen, metered by a needle valve and flowmeter, was passed through a preheating spiral, bubbled through the liquid sample and out through a standard ball joint and a $BiCl_3$ receiver into an N_2 collector. The exit line was wrapped with heater wire and a layer of asbestos and maintained a few degrees (10–15°) above the temperature of the furnace so that no condensation of vapor could occur before the ball joint. At the end of a run the volume of N_2 was measured, the exit line flushed with N_2, and the receiver disconnected, cooled and weighed. From the weight of material condensed in the $BiCl_3$ receiver, the amount of gas collected, and the pressure in cell (measured by an oil manometer), a vapor pressure was calculated on the assumption that in the vapor the bismuth chloride had a molecular weight of 315.

Bismuth chloride was purified and introduced into the cell by double distillation in a stream of dry N_2. This procedure purified the salt of the involatile BiOCl and the volatile H_2O, which are the important impurities in the reagent grade material. After a series of transpiration determinations on pure $BiCl_3$, the composition was changed by addition of Bi through a large stopcock, with a stream of dry nitrogen passing through the cell, and a new set of determinations was made. After several Bi additions the series of runs was terminated and the cell removed from the furnace. The final weight of the material in the cell together with a mass balance of Bi added and $BiCl_3$ removed in the individual determinations allowed the calculation of the composition of the sample for each pressure determination. A sample of about 80 g. of $BiCl_3$ was used for each series of determinations.

Furnace.—The furnace shell was a stainless steel kettle (15 in. high × 15 in. diam.). Inside the shell was about 2″ of fire brick insulation and a set of Hevi-duty heating elements on all walls (sides, top and bottom), the heating elements exposed to the air space of the furnace. A window consisting of a double layer of Pyrex glass separated by a 1 in. air gap was built into the lid of the furnace. This window was very useful in allowing us to analyze the operation of the apparatus while the system was at temperature. A coil of auxiliary heater wire was placed near the top of the cell to keep it about 3–6° warmer than the bottom. This was necessary so that the liquid sample in the bottom of the cell was the coolest part of the cell and thus determined the vapor pressure of the $BiCl_3$.

The temperature of the furnace was controlled by a chromel–alumel thermocouple and a Brown proportioning controller so arranged that full scale corresponded to 150° (*i.e.*, the zero of the instrument was adjustable in 125° steps). The temperature of the liquid was measured with a Pt–10% Rh thermocouple which had been calibrated at the melting points of Bureau of Standards samples of Pb, Sn and Zn. It read about one degree higher than tabulated values at those three temperatures and corrections for intermediate temperatures were interpolated. The junction of this thermocouple was placed inside the 3-mm. (o.d.) thermocouple well so that it was centered in the volume of the liquid. It was felt that the temperature of the liquid was uniform because starting and stopping stirring of the liquid by the bubbling N_2 stream did not change the temperature reading by so much as 0.1°.

Collection System. The N_2 collecting and measuring system consisted of a graduated cylinder (or 100-ml. buret for small volumes) inverted in a beaker and filled with water. The N_2 bubbled in through a medicine dropper tube at the mouth of the graduated cylinder, and the water displaced

(1) This work was made possible by the financial support of the Research Division of the United States Atomic Energy Commission.

(2) (a) M. A. Bredig, J. W. Johnson and W. T. Smith, Jr., *J. Am. Chem. Soc.*, **77**, 307 (1955); (b) M. A. Bredig, H. R. Bronstein and W. T. Smith, Jr., *ibid.*, **77**, 1454 (1955); (c) D. Cubicciotti and C. D. Thurmond, *ibid.*, **71**, 2149 (1949); (d) D. Cubicciotti, *ibid.*, **71**, 4119 (1949); (e) J. D. Corbett and S. von Winbush, *ibid.*, **77**, 3964 (1955).

(3) (a) B. Eggink, *Z. physik. Chem.*, **64**, 449 (1908); (b) L. Marino and R. Becarelli, *Atti accad. nazl. Lincei*, **24**, 625 (1915); **25**, 221 (1916); **25**, 326 (1916); (c) M. A. Sokolova, G. G. Urazov and V. G. Kuznetsov, *Akad. Nauk, S.S.S.R., Inst. Gen. Inorg. Chem.*, **1**, 102 (1954).

(4) O. Kubaschewski and E. Ll. Evans, "Metallurgical Thermochemistry," 2nd ed., John Wiley and Sons, Inc., New York, N. Y., 1956, p. 151 ff.

(5) (a) K. A. Sense, M. J. Snyder and J. W. Clegg, THIS JOURNAL, **58**, 223 (1954); (b) K. A. Sense, M. J. Snyder and R. B. Filbert, Jr., *ibid.*, **58**, 995 (1954).

dripped over the lip of the beaker. In this way the pressure in the cell was maintained constant at a few cm. of oil above atmospheric throughout a determination.

The temperature of the gas was measured by an Hg in glass thermometer inverted in the graduated cylinder so that the bulb was exposed to the gas. The pressure of the collected gas was taken as the ambient atmospheric pressure minus a correction for water head and water vapor pressure. The graduated cylinders were calibrated by weighing with water filled to various levels. The volumes measured ranged from 50 to 4000 ml. By suitable use of an assortment of graduated cylinders the accuracy of the volume measurement was about ±0.5%.

The condensable gas (essentially $BiCl_3$) was collected in the receiver which was simply a glass bulb with one side arm terminating in a standard ball joint and another leading to the gas collector. At the end of a determination the bulb was disconnected from the system, both ends capped, the bulb allowed to cool to room temperature, and weighed. Then the condensate was washed out of the bulb with concentrated HCl, the bulb dried and reweighed. Since the reweighing of the bulb usually was done at a different ambient temperature from the first weighing, it was necessary to apply a buoyancy correction to those weights. The apparent weight of the 25-g. bulbs changed by about 0.06 mg. per °C. This correction amounted to as much as a per cent. of the 0.1 to 0.15 g. of sample collected.

Diffusion Error.—One of the errors inherent in a transpiration experiment is the so-called diffusion error which arises from the diffusion of the condensable vapor into the collector in addition to that carried by the inert gas stream. The importance of that factor was evaluated for our system by determining the amount of material collected when no N_2 was flowing.

The results of the diffusion error studies are given in Table I. The last column of that table gives the per cent. of the amount of material collected due to diffusion in a typical experiment.

TABLE I

DIFFUSION ERROR STUDIES

Temp. (°C.)	Time of diffusion (min.)	Amount collected (mg.)	% of av. run due to diffusion
300	120	0.1	0.1
300	260	0.3	
360	130	1.5	0.3
360	240	2.1	
400	60	5.0	0.3

Effect of Flow Rate.—In a transpiration experiment one expects the apparent pressure of the transported material to increase as the flow rate is decreased (see Kubaschewski and Evans[4] for discussion); and so in practice one either extrapolates the apparent pressure to zero flow, or if the pressure appears independent of flow rate, he takes the constant value. In our system we found that over a range of flow rates the calculated pressure was independent of flow rate. For the smallest flow rates examined there was a repeated tendency to obtain low values of the pressure. No detailed investigation of this effect was made. Results of flows in the range giving constant pressures were considered to give reliable pressure values.

Materials.—The $BiCl_3$ was J. T. Baker Analyzed Reagent Grade material. It was quoted to contain less than 0.1% impurity. This material was purified of BiOCl and H_2O by double distillation in a stream of dry N_2, as mentioned above. Analysis for Cl of a doubly distilled sample gave 33.74% Cl as compared with 33.73% as theoretical.

The Bi was "spectroscopically standardized" metal obtained from Johnson, Matthey and Co. Their spectroscopic analysis indicated a total of about 15 p.p.m. assorted metal impurities. Our experience showed that the first pressure determination made on the sample after the addition of a piece of Bi gave high results. That effect indicated a volatile impurity (or an impurity forming a volatile material when mixed with $BiCl_3$) corresponding to 0.2 to 0.3% of the Bi added. For that reason the results of the first determination after a Bi addition were always discarded.

The N_2 was Stuart Oxygen Co. high purity N_2. It was dried before admission into the system by passing it through a U-tube containing dry silica gel, maintained at Dry Ice–acetone temperature. A rough calculation indicates that such treatment should reduce the H_2O vapor pressure to about 10^{-5} mm. The only experimental evaluation of the dryness of the gas was the fact that in one series of determinations 12 liters of gas was bubbled through a sample of $BiCl_3$, with no precipitation of BiOCl.

Analysis of Transported Vapor.—In order to calculate a pressure from the amount of material transported by a given amount of N_2 it is necessary to know the average molecular weight of the vapor. Because the vapor pressures calculated for pure $BiCl_3$ using 315 for the molecular weight agreed with literature vapor pressures measured by manometric methods, it was assumed that the vapor over liquid $BiCl_3$ is monomeric $BiCl_3$.

The vapor in equilibrium with Bi and $BiCl_3$ mixtures must contain some species richer in Bi than $BiCl_3$ because Bi can be transported through the vapor by $BiCl_3$. This has been observed by us as follows. The liquid condensing from the vapor on a cool spot in a closed evacuated bulb containing a liquid Bi + $BiCl_3$ mixture is dark colored and exhibits a Bi:Cl ratio greater than 1:3 on analysis. Corbett[6] has reported a similar transport of Bi by the vapor of $BiCl_3$.

Thus to determine the average molecular weight of the vapor we analyzed the material transported into our receivers. Two analytical methods were used. In one series of determinations the per cent. chloride in the transported material was determined by gravimetric analysis as AgCl. The precision of our analyses was poor because at the time we were not aware of the large effect of buoyancy on the sample weights. The results of the chloride determinations fell in the range 33.5 to 33.9% Cl (theoretical for $BiCl_3$ = 33.73%) for a whole series of vapor pressure determinations in which the Bi mole fraction reached 0.35. There was no detectable trend of per cent. chloride with Bi concentration in the liquid.

The second method of analysis determined the reducing power of the transported material. In this method the material was dissolved in a solution 0.3 *M* in HCl and 0.1 *M* in $FeCl_3$, and the solution titrated with 0.005 *N* $Ce_2(SO_4)_3$ using Ferroin indicator. This method was tested in two ways. In one, weighed samples of powdered Bi metal were subjected to the procedure. The titers of several samples were found to be no more than 2% below that calculated from the Bi weights. In the other test a few milligrams of Bi were melted with about 3 g. of $BiCl_3$, the melt cooled and subjected to the procedure. The resultant titer was 5% lower than that calculated from the weight of Bi. It was concluded from these tests that the method would reflect the amount of Bi in the sample with sufficient accuracy.

This analytical method was used in a second series of pressure determinations. In all the samples collected from Bi + $BiCl_3$ mixtures with Bi mole fraction 0.16 or less the titer was the same as the blank (about 0.1 ml. of 0.005 *N* Ce^{+4}). The samples from mixtures 0.26 and 0.34 in Bi mole fraction gave titers of 0.01 to 0.02 ml. (in excess of the blank), corresponding to a Bi metal content in the transpired material of less than 0.1 mole %.[7]

The vapor pressures calculated should have been reduced by the per cent. of Bi found in the sample. Since that percentage was so small, the vapor was considered to be essentially pure $BiCl_3$ and in all the calculations a molecular weight of 315 was used for the vapor.

Results

The results of three series of determinations are reported below. In one series the $BiCl_3$ pressures were measured over a temperature range from 230 to 420° for pure $BiCl_3$ and three mixtures of Bi + $BiCl_3$ made by three successive Bi additions. In the second series the pressure of pure $BiCl_3$ was determined over the same temperature range but the pressures over Bi + $BiCl_3$ mixtures made only

(6) J. D. Corbett, S. von Winbush and F. C. Albers, *J. Am. Chem. Soc.* **79**, 3020 (1957).

(7) It should be stated that the transported material was slightly colored when the concentration of Bi in the liquid was relatively high. This darkening was taken to indicate that some Bi had been transported with the $BiCl_3$ but in very small amounts.

at 301 and 356° so that a careful evaluation of the the composition effect could be made. In the third series the pressures were measured at 392° only.

Pure $BiCl_3$.—The results obtained for pure $BiCl_3$ on three different samples are shown in curve A of Fig. 1. The internal agreement of the data is such that all but one or two points fall within a band whose width corresponds to 5% of the pressure, centered on the line drawn. The vapor pressure of $BiCl_3$ has been measured by Evnevich and Sukhodskii[8] by the dynamic method of measuring the temperature of condensing vapor at controlled pressure. Maier[9] used a static method with a buffer of N_2 between his Hg manometer and the $BiCl_3$ vapor. Our data fall between these two sets of data in the range 340 to 400°[10] and may be said to agree with both; however, the agreement with Evnevich and Sukhodskii's data is better, especially in temperature coefficient.

As observed above we have used a value of 315 for the molecular weight of the vapor, *i.e.*, that of monomeric $BiCl_3$. The agreement of our pressures with the literature values obtained by manometric methods shows that the vapor over pure $BiCl_3$ liquid is monomeric $BiCl_3$ (with less than 2–3% dimer), at least over the range of overlap of the measurements (340 to 420°). We have assumed further that in lower vapor concentrations of $BiCl_3$ no polymer is formed.

The change in enthalpy of $BiCl_3$ liquid on vaporization was calculated in the usual manner from the slope of the vapor pressure curve. Above about 300° our data give a constant ΔH of 18.9 ± 0.2 kcal. per mole. Below that temperature the ΔH increases somewhat with decreasing temperature so that at about 260° ΔH is 20.4 ± 0.5 kcal. per mole.

Mixtures of Bi with $BiCl_3$.—Three series of determinations were made on Bi + $BiCl_3$ mixtures as mentioned at the beginning of this section. The results of the first series are given in Fig. 1. They show that the heat of vaporization of $BiCl_3$ from the solutions was not much different from that of pure $BiCl_3$. From the slopes of the curves there appeared to be a slight increase in the ΔH of vaporization of a few hundred calories as the Bi concentration increased; however, the data were not considered sufficiently precise to give reliable information concerning the change in ΔH, and so the second and third series of determinations were made to evaluate these effects.

The results of the second and third series of determinations are given in Fig. 2. The lengths of the I's in these figures give the range of pressures determined at each composition and indicate the experimental error. In Fig. 2A each I represents six to eight determinations with the curve drawn through the average at almost every I. In Fig. 2B and C each I represents three and occasionally four

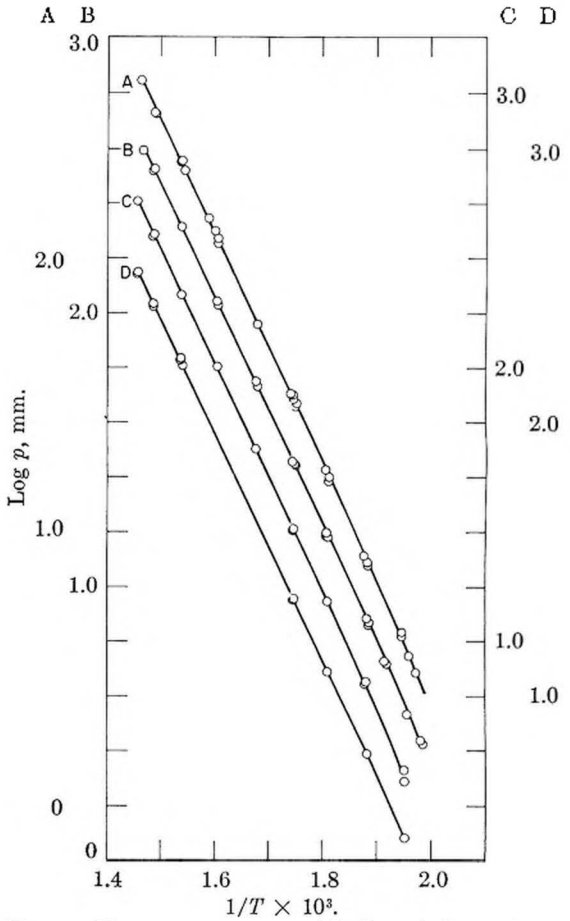

Fig. 1.—The vapor pressures of $BiCl_3$ and three mixtures with Bi: curve A, pure $BiCl_3$; curves B, C and D are the vapor pressure of $BiCl_3$ over mixtures 0.12, 0.24 and 0.33, respectively, in Bi mole fraction. (The ordinates have been displaced for clarity, and values from any curve must be read on the properly labeled ordinate.)

pressure determinations, the curve being drawn through the averages as closely as possible.

In Fig. 2 the horizontal parts of the curves to the right indicate that the two phase regions had been reached. This was determined at 356 and 392° by the fact that addition of Bi did not change the pressure. At 301° it was found that at mole fraction 0.38 Bi there was a tendency for a plug to form in the N_2 inlet (a 2-mm. bore capillary), and the plug melted above 320°, in agreement with phase diagram information.[11] In these figures the section of the curve before the horizontal is dotted to indicate that the composition at which the second phase first appeared was unknown. The dashed straight lines represent Raoult's law pressures. (It should be noted that the compositions used in this paper are mole fractions of Bi in $BiCl_3$, *i.e.*, g. Bi/209/(g. Bi/209 + g. $BiCl_3$/315).)

Discussion

The pressures measured in this work have been taken to be the partial pressures of the species $BiCl_3$. The justifications for this assumption are (1) for pure $BiCl_3$ the vapor pressures measured by manometric methods agreed with the calculation of

(8) E. V. Evnevich and V. A. Sukhodskii, *J. Russ. Phys.-Chem. Soc.*, **61**, 1503 (1929).

(9) C. G. Maier, U. S. Bur. Mines Tech. Paper No. 360, 1925.

(10) Maier's low temperature data were not considered because they are too high; see K. K. Kelley, U. S. Bur. Mines Bull. No. 383, 1935.

(11) Phase diagram studies have shown that a solid precipitates below 320° from the two liquid mixtures in the Bi–$BiCl_3$ system. See ref. 2.

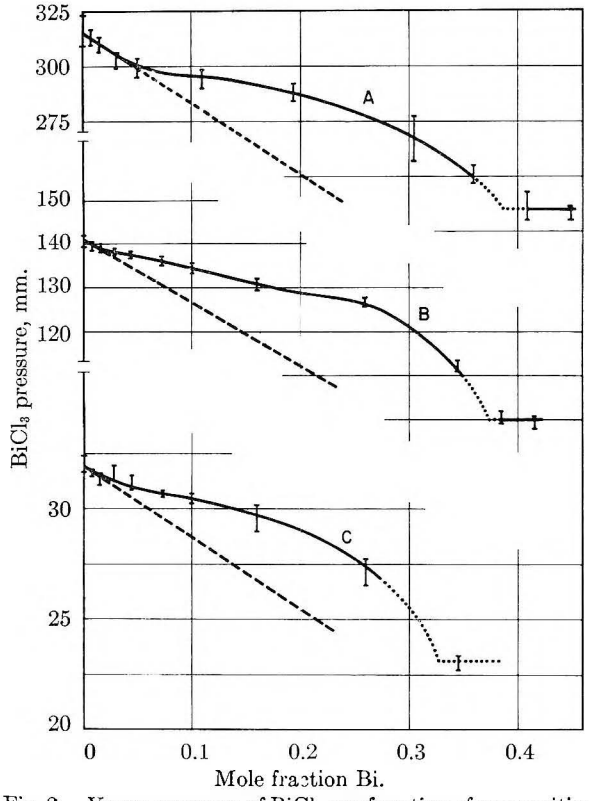

Fig. 2.—Vapor pressures of $BiCl_3$ as a function of composition at: A, 392.0°; B, 356.3°; C, 301.0°.

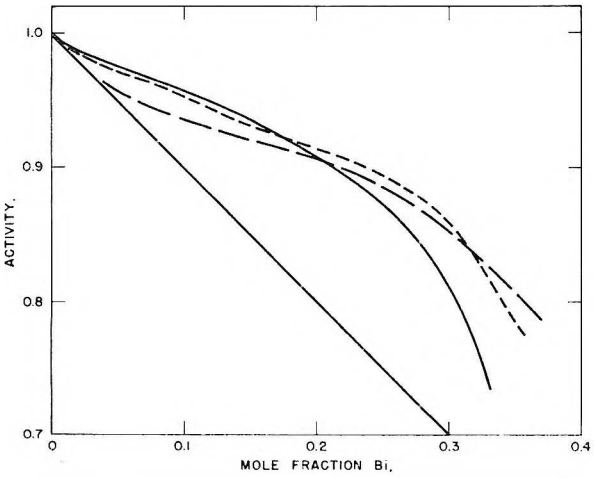

Fig. 3.—Activity of $BiCl_3$ as a function of added Bi at 392° (dashed curve), 356° (dotted curve) and 301° (full curve). The straight line represents Raoult's law.

the transpiration results for monomer; (2) analysis of transported material showed only a negligible fraction of lower-valent species.

The activity of $BiCl_3$ in the solutions has been calculated as the ratio of the $BiCl_3$ partial pressure over the solution to that over pure liquid $BiCl_3$ at the temperature in question. The activities at 301, 356 and 392° as a function of composition are shown in Fig. 3. At low Bi concentrations the solutions show a tendency to obey Raoult's law, the tendency increasing with temperature. The major trend of the system, however, is to exhibit marked positive deviations.

From the activities we calculated the partial molal free energies of $BiCl_3$ in solution relative to pure $BiCl_3$ at the three temperatures ($\overline{\Delta F} = RT \ln a$). The temperature coefficient of the partial molal free energy can be used to calculate the partial molal enthalpy and entropy of $BiCl_3$ in solution relative to pure $BiCl_3$. The temperature coefficients of $\overline{\Delta F}$ at the two median temperatures (328 and 374°) were taken to be the differences in $\overline{\Delta F}$ from 301 to 356° and from 356 to 392° divided by the temperature differences. These temperature coefficients of $\overline{\Delta F}$ were taken as equal to the negative of the relative partial molal entropy [$(\partial\overline{\Delta F}/\partial T) = -\overline{\Delta S}$]. The relative partial molal enthalpies were calculated for the two median temperatures from the free energies and entropies ($\overline{\Delta H} = \overline{\Delta F} + T\overline{\Delta S}$).

The values calculated for the enthalpies and entropies are shown in Figs. 4 and 5. In each case the curves represent the values calculated from the data. The shaded areas indicate our estimate of the probable error associated with the values, based on the experimental spread of the original pressure measurements. The dotted curves in the entropy figures represent the ideal partial molal entropy [$-R \ln$ (mole fraction)].

The probable error associated with the partial molal functions of $BiCl_3$ in these solutions is relatively large so that it is not worthwhile attempting to interpret the details of their variation with composition. A general view of the results obtained on the thermodynamic functions of $BiCl_3$ in Bi + $BiCl_3$ solutions is as follows. $BiCl_3$ shows a marked tendency toward positive deviations from Raoult's law, in accord with the existence of a miscibility gap in the phase diagram. In the range 0 to 0.2 in Bi mole fraction the partial molal enthalpy and entropy of $BiCl_3$ are somewhat positive. In the range 0.2 to about 0.35 in Bi mole fraction the enthalpy and entropy of $BiCl_3$ decrease to negative values with increase in Bi concentration. This behavior is rather unusual in a system with liquid immiscibility; however, it reflects the fact that a compound does form in the system at sufficiently low temperatures.

Although thermodynamic data do not specify the nature of the species that constitute a solution, still they can be used to give evidence in favor of or against certain postulated species. For example, the positive deviations from Raoult's law for $BiCl_3$ speak against the existence of lower valent ions formed by a reaction of Bi^{+3} ions with Bi atoms. Ions such as Bi^{+1} and Bi^{+2} would be expected to give rise to strong negative deviations since each atom of Bi dissolving would produce more than one such ion by the reactions

$$2Bi + Bi^{+3} = 3Bi^{+1}$$
$$Bi + 2Bi^{+3} = 3Bi^{+2}$$

It is possible to fit the activity curve on the basis of these lower valent ions by assuming them to be polymerized, as

$$nBi^{+1} = Bi_n^{+n}$$
$$mBi^{+2} = Bi_m^{+2m}$$

perhaps with intermediate stages of polymerization. However, one hesitates seriously to propose such complex ions as specific entities.

Alternately, one may consider the solution as composed of neutral atoms of Bi dissolved in the ionic melt. In the regions where Bi is dilute and the $BiCl_3$ obeys Raoult's law, the dissolved Bi is dissolved monomerically, and polymeric species such as Bi_2 need not be considered. There is, however, a range of Bi mole fractions (from just beyond the region where Raoult's law applies to about 0.15 in Bi mole fraction) in which the $BiCl_3$ activity approximates the curve calculated for it on the assumptions that the Bi is dissolved as Bi_2 and Raoult's law is obeyed for the $BiCl_3$, while from 0.15 to 0.3 Bi mole fraction it is necessary to include some higher polymer. Thus it is possible to calculate equilibrium constants at each temperature for the reactions

$$2Bi = Bi_2$$
$$3/2Bi_2 = Bi_3$$

such that in the dilute Bi range the predominant species is Bi and in the more concentrated range it is Bi_2 (always on the assumption that the $BiCl_3$ in the melt obeys Raoult's law, *i.e.*

$$\text{activity of } BiCl_3 = \left(\frac{\text{moles } BiCl_3}{\text{moles } BiCl_3 + \text{moles Bi} + \text{moles } Bi_x}\right)$$

However, it is not necessary to propose complex polymeric species to explain the observed properties of the solution. From the viewpoint of modern solution theory[12] positive deviations are to be expected from a pair of liquids with different solubility parameter. So there is no need to propose association of components just because positive deviations are observed.

The solubility parameters for liquid Bi and $BiCl_3$ in the temperatures of interest are ≤5 and 14.5.[13] From these values one would predict marked immiscibility of the components (with the concomitant positive deviations and positive enthalpies). In fact, one would approximate the relative partial molal enthalpy of $BiCl_3$ by

$$\overline{\Delta H}_{BiCl_3} = V_{BiCl_3} x^2_{Bi} (\delta_{Bi} - \delta_{BiCl_3})^2$$
$$= 8 \times 10^4 \, x^2_{Bi}$$

where

V = molal volume
x = mole fraction
δ = solubility parameter

Values from this equation are much in excess of those measured. A possible reason is that the value assigned to the solubility parameter of Bi is too high because the cohesive energy of the metal is in part due to "metallic binding" or long range electronic interaction, and that part of the cohesive energy is not applicable when the Bi finds itself in these salt solutions.

Another facet of the behavior of this system that needs explanation is the decrease of the enthalpy and entropy of the $BiCl_3$ as the mole fraction of Bi increases beyond about 0.2. This trend is quite noticeable, and indicates, to the authors at least, that some process is simultaneously tending to bind the $BiCl_3$ in the solution and increase its degree of order as the Bi concentration is increased. This binding may possibly indicate a restoration of the metallic binding of the Bi atoms coupled with Bi^{+3} ions.

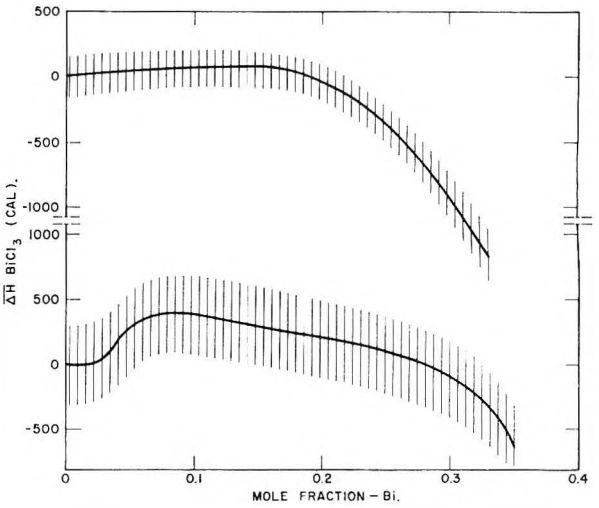

Fig. 4.—The relative partial molal enthalpy of $BiCl_3$ at 328° (upper curve) and 374° (lower curve). The shading indicates the estimated error.

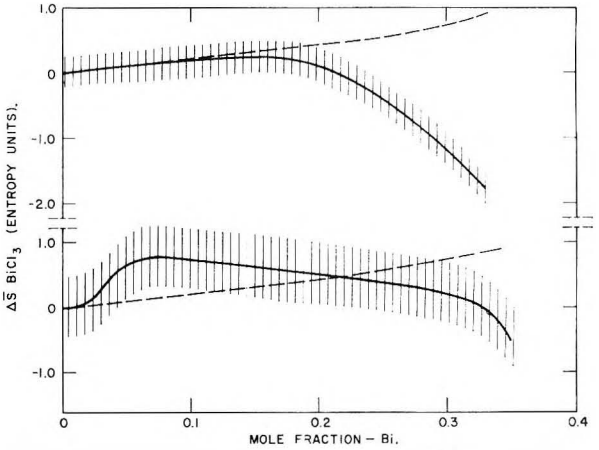

Fig. 5.—The relative partial molal entropy of $BiCl_3$ at 328° (upper curve) and 374° (lower curve). The shading indicates the estimated error. The dotted curves are values calculated for ideal solution.

Acknowledgment.—The authors are indebted to Mr. William E. Robbins, who performed a major part of the experimental work reported.

(12) For a discussion of this point see J. H. Hildebrand and R. L. Scott, "The Solubility of Nonelectrolytes," 3rd ed., Reinhold Publ. Corp., New York, N. Y., 1950, especially Chap. XI.

(13) The solubility parameter for liquid Bi was estimated from the data of reference (12), p. 324. The value for $BiCl_3$ liquid was estimated from the heat of vaporization and unpublished density measurements made in this Laboratory.

THE MAGNETIC SUSCEPTIBILITY OF COPPER(II) ACETATE IN VARIOUS SOLVENTS[1]

BY MICHIO KONDO AND MASAJI KUBO

Chemical Department, Nagoya University, Chikusa, Nagoya, Japan

Received December 10, 1957

The magnetic susceptibility of copper(II) acetate in solutions of various solvents was determined by means of a Gouy magnetic balance at room temperature. The values of effective magnetic moments in ethanol and dioxane solutions were practically identical with that in the solid state, indicating the presence of the solute in dimer molecules as in crystals. On the other hand, the moments in aqueous and pyridine solutions were slightly greater than the theoretical spin-only value 1.73 Bohr magnetons for a single unpaired electron, leading to the conclusion that copper(II) acetate dissociates into single molecules in these solvents. In methanol solution, the magnetic moment assumed an intermediate value between those in water and ethanol. The conclusion is in good agreement with the presumption advanced by Tsuchida and Yamada from the consideration of absorption spectra.

Introduction

Since van Niekerk and Schoening[2] showed by X-ray crystal analysis that copper(II) acetate monohydrate formed dimer molecules in crystals and that the distance 2.64 Å. between two copper atoms in the dimer molecule suggested the formation of a copper–copper bond, the nature of which was open to speculation, the problem has stimulated considerable interest among workers in other fields of physical chemistry. The results of earlier work by Bleaney and Bowers[3] on the paramagnetic resonance absorption could be explained by presuming that in a pair of copper atoms strong interaction acts through exchange forces, each pair forming a lower diamagnetic singlet state and an upper paramagnetic triplet state. Thus, the decreasing intensity of the resonance absorption with lowering temperature could be correlated with the static magnetic susceptibility of the same compound in the solid state. In fact, Figgis and Martin[4] have measured the temperature variation of the magnetic susceptibilities of anhydrous and hydrated copper(II) acetates. As the temperature is lowered below room temperature, the magnetic susceptibility, instead of obeying Curie–Weiss law, slightly increases at first, passes through a maximum at 270 and 255°K. for the anhydrous and hydrated compounds, respectively, and then abruptly decreases, tending to an almost vanishing value at the absolute zero of temperature. The observed magnetic susceptibility has indicated the existence of weak covalent copper–copper bonds in which the exchange contribution to the total bond energy is approximately 1 kcal. mole^{-1}. A suggestion was advanced that a δ-bond is formed between adjacent copper atoms by lateral overlap of $3d_{x^2-y^2}$ orbitals, the z-axis being taken as along the line joining the copper atoms. This hypothesis is promising, because it gives a clue to an adequate explanation of the subnormal magnetic moments of some copper(II) complexes recently studied.[5]

As has been pointed out by Figgis and Martin,[4] copper(II) acetate is the first case in which a δ-bond is the sole direct link between two atoms. The present magnetostatic investigation has been undertaken in order to see whether or not this bond persists in solutions of copper(II) acetate in various solvents.

Preparation of Materials.—Copper(II) Acetate Monohydrate.—Commercial preparation was twice recrystallized from dilute acetic acid solutions.

Solvents.—Water was twice distilled. Methanol was distilled three times. Ethanol preparation was subjected to oxidation in order to remove possible contamination with aldehydes, dehydrated over anhydrous cupric sulfate and distilled. Pyridine was dehydrated over caustic potash pellets and was twice distilled. Dioxane was distilled after being dehydrated over metallic sodium.

Apparatus and Experimental Results.—For the determination of magnetic susceptibility, a Gouy magnetic balance[6] was employed at room temperature. The sample tube made of hard glass was 20 cm. long and had a partition in the middle forming two compartments. One of them was filled with a solution under investigation, and the other with the pure solvent. The internal diameter of the tube amounted to 6 mm. The cell was suspended between the poles of an electromagnet from a semi-microbalance capable of determining weight changes as small as 0.01 mg. The electromagnet could be supplied with a direct current of up to 17 amp. taken from selenium rectifiers, ripples having been removed by means of a series of condensers. The rectifiers were fed from a 200 volt, three phase alternating current source, which was stabilized with an appropriate voltage stabilizer and was led through suitable transformers before it was applied to the rectifiers. The total resistance of the coil of the electromagnet was less than 3 ohms. Each tip of the pole pieces, which were separated from each other by about 1 cm., had a circular surface plane of 3 cm. in diameter. The resulting magnetic field could be raised up to about 24,000 oersteds. The magnetic balance was calibrated with distilled water, its magnetic susceptibility per gram being set equal to -0.720×10^{-6}.[7]

In each solvent, the magnetic susceptibility χ per gram of solution showed a linear dependence upon the concentration w of the solute in weight per cent. over the whole range investigated. From the slope of the straight line in the plots of χ against w, the magnetic susceptibility per gram of copper(II) acetate in each solvent was evaluated. The diamagnetic correction χ_{dia} for the hydrated salt was taken from Mookerjee[8] as -85×10^{-6}. The temperature-independent paramagnetism $N\alpha$ of a mole of copper atoms was assumed to be equal to 60×10^{-6} as Figgis and Martin also did. Allowing for these corrections and assuming the validity of the Curie–Langevins law, the effective magnetic moment μ per one copper atom was calculated from the molar susceptibility χ_M as

$$\mu = 2.84[(\chi_M - \chi_{dia} - N\alpha)T]^{1/2}$$

(1) This work was reported in part at a meeting of the Chemical Society of Japan held in Tokyo on October 14, 1957.

(2) J. N. van Niekerk and F. R. L. Schoening, *Nature*, **171**, 36 (1953); *Acta Cryst.*, **6**, 227 (1953).

(3) B. Bleaney and K. D. Bowers, *Proc. Roy. Soc. (London)*, **214A**, 451 (1952).

(4) B. N. Figgis and R. L. Martin, *J. Chem. Soc.*, 3837 (1956); R. L. Martin and H. Waterman, *ibid.*, 2545 (1957).

(5) M. Kishita, Y. Muto and M. Kubo, *Naturwiss.*, **44**, 372, 614 (1957); *Australian J. Chem.*, **10**, 386 (1957).

(6) M. Kondo and M. Kubo, THIS JOURNAL, **61**, 1648 (1957).

(7) Throughout this article, the data of magnetic susceptibility are given in c.g.s. e.m.u.

(8) A. Mookerjee, *Indian J. Phys.*, **19**, 63 (1945), *cf.* reference 4.

The results are shown in Table I.

TABLE I

THE MOLAR MAGNETIC SUSCEPTIBILITIES AND THE EFFECTIVE MAGNETIC MOMENTS IN BOHR MAGNETONS OF COPPER(II) ACETATE IN VARIOUS SOLVENTS

Solvents	t, °C.	w(%)	$\chi_M \times 10^6$	μ(B.M.)	Color
Water	23.5	0.3–1.4	1491	1.93	Blue
Pyridine	23	.2– .5	1330	1.80	Blue
Methanol	28	.1– .3	1019	1.58	Green
Ethanol	22	.1– .6	826.5	1.43	Green
Dioxane	26	.1– .3	749.6	1.37	Green
(Solid)	22	.....	807.5	1.41	Green

Discussion

The molar magnetic susceptibility of copper(II) acetate depends to a considerable extent upon the kind of solvents in which it is dissolved. The values of effective magnetic moments in ethanol and dioxane are practically identical with that in the solid state, indicating the presence of the solute in dimer molecules as in crystals. On the other hand, the moments in aqueous and pyridine solutions are slightly greater than the spin-only value 1.73 Bohr magnetons for a single odd electron. Since a cupric ion has a more than half filled 3d shell, the orbital contribution to the effective moment adds to rather than subtracts from the spin moment and the differences between the observed moments and the theoretical spin-only moment are presumed to be adequate for orbital contributions. From these normal moments, one can conclude that copper(II) acetate dissociates into single molecules in water and pyridine. The molecules of water and pyridine capable of being readily coordinated on metal atoms as ligands are considered to occupy appropriate positions about copper atoms, thereby breaking the weak copper–copper bonds in the dimer molecules. In methanol solution, the magnetic moment assumes an intermediate value between those in water and ethanol.

The color of the solutions of copper(II) acetate in those solvents in which the copper salt shows a normal magnetic moment was blue, while the solutions in which subnormal magnetic moments were observed assumed a green color. Tsuchida and Yamada[9] have found that copper(II) acetate and propionate in ethanol or chloroform showed a new absorption band at 80×10^{13} sec.$^{-1}$ in addition to that at 43×10^{13} sec.$^{-1}$ commonly observed for copper salts. They attributed the new band to the presence of a copper–copper link in such entities as $Cu_2(CH_3COO)_4X_2$ or $Cu_2(C_2H_5COO)_4X_2$, where X denotes H_2O, C_2H_5OH or $CHCl_3$. The present magnetic measurements provide a more direct and definite evidence in support of their conclusion.

(9) R. Tsuchida and S. Yamada, *Nature*, **176**, 1171 (1955); R. Tsuchida, S. Yamada and H. Nakamura, *ibid.*, **178**, 1192 (1956); *Bull. Chem. Soc. Japan*, **30**, 953 (1957).

KINETICS OF THE REACTION BETWEEN GASEOUS AMMONIA AND SULFURIC ACID DROPLETS IN AN AEROSOL[1]

BY R. C. ROBBINS AND R. D. CADLE

Contribution from Stanford Research Institute, Menlo Park, California

Received December 10, 1957

The rates of reaction in the system nitrogen, gaseous ammonia and sulfuric acid droplets have been studied at 28 and 8°. Initial rates are first order with respect to ammonia and droplet surface. The over-all reaction appears to be limited by the diffusion of product into the droplets, and an empirical rate equation for the over-all reaction has been obtained. The results are discussed in terms of collision and absolute rate theory.

Introduction

In spite of the large body of literature concerned with heterogeneous reactions, little information is available concerning chemical reactions in aerosol systems. Perhaps the most pertinent studies are those by Lewis and co-workers on reactions in fluidized beds[2,3] and studies of aerosol growth, such as those by La Mer and Cotson[4] and La Mer and Gruen.[5] This paper reports a study of the reaction between gaseous ammonia and sulfuric acid droplets in an aerosol. This system was chosen because the reaction would be expected to be rapid and the system can be prepared readily and reproducibly.

Experimental

The aerosols were prepared from 98.3% sulfuric acid, using a condensation-type generator; particle sizes were determined with an "owl."[6] Particle concentrations were monitored with a Sinclair–Phoenix forward-scattering Tyndallometer. The nitrogen was dried by passing it through a tube containing phosphorus pentoxide. Nitrogen–ammonia mixtures were prepared in a conventional gas-handling system.

Reaction rates were measured using a flow system. The reaction cells were vertical glass U-tubes, 20 mm. inside diameter, and varying in length from a few centimeters to approximately two meters. The aerosol and the nitrogen–ammonia mixture were introduced into the bottom of one arm of the cell from opposite directions so that turbulent mixing occurred. The Reynolds number in the cell was about 250 and the flow became laminar immediately above the mixing zone. The mixture flowing from the other end

(1) This work was supported by Grant S-30 of the Public Health Service.

(2) W. K. Lewis, E. R. Gilliland and W. A. Reed, *Ind. Eng. Chem.*, **41**, 1227 (1949).

(3) W. K. Lewis, E. R. Gilliland and G. T. McBride, Jr., *ibid.*, **41**, 1213 (1949).

(4) V. K. La Mer and Sidney Cotson, *Science*, **118**, 516 (1953).

(5) V. K. La Mer and R. Gruen, *Trans. Faraday Soc.*, **48**, 410 (1952).

(6) V. K. La Mer, E. C. Y. Inn and I. B. Wilson, *J. Coll. Sci.*, **5**, 471 (1950).

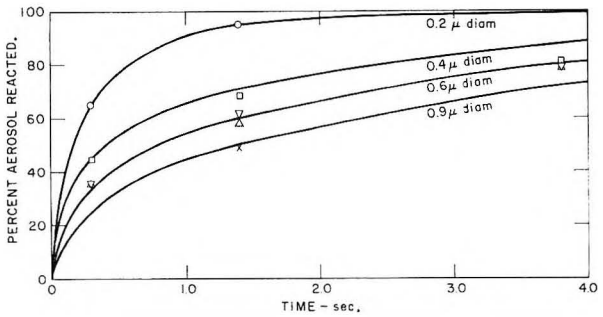

Fig. 1.—Reaction between ammonia (394 μmoles/m.³) and sulfuric acid droplets of various diameters (19.7 μmoles/m.³) at 28°. All reactions were in nitrogen except for the reaction of 0.6 μ diameter droplets, which was studied in nitrogen (Δ) and in the nitrogen–helium mixture (∇). Additional points, which are not shown, were obtained for later times.

of the cell passed through a bed of pelleted molecular sieve material,[7] about 5 cm. deep, which removed the ammonia without removing the aerosol. The particulate material was then collected from the aerosol with a Mine Safety Appliance electrostatic precipitator and analyzed for ammonium ion by titration with a dilute aqueous solution of methyl purple. The analytical method was corroborated by the colorimetric Nessler method for ammonia.[8] The gas velocity in the reaction cells was 19 cm./sec. The variation of fraction completion of the reaction with time was investigated by using several cells of different lengths for each set of conditions.

A few experiments were made in which most of the nitrogen (all except that used for generating the aerosol) was replaced with helium. The resulting concentration of helium in the reaction cells was 62.5 mole %.

Particle diameters of the sulfuric acid droplets ranged from 0.2 to 0.9 μ. Concentrations were of the order of micromoles of sulfuric acid and ammonia per mole of total aerosol.

Most of the experiments were undertaken at 28 ± 1°. A few experiments were made at 8 ± 0.1° by placing the entire apparatus in a large thermostated refrigerator equipped with blowers.

Results

Two sets of runs were made to determine the order of the reaction. One set involved maintaining the initial concentration of acid in the aerosol constant at 19.7 μmoles/m.³, and the droplet size constant at 0.6 μ while varying the initial stoichiometric ratio (equiv. H_2SO_4/equiv. NH_3) between 0.48 and 0.1. The other set involved maintaining the acid concentration at 19.7 μmoles/m.³ and the initial stoichiometric ratio at 0.1 while varying the particle diameter between 0.2 and 0.9 μ. Typical results are shown in Fig. 1 as % aerosol reacted plotted against time. The slopes of these curves were measured at several points and plotted on log paper against corresponding concentrations of sulfuric acid. Curved rather than straight lines were obtained, which showed that the over-all reaction had no particular order. The order of the initial reaction was estimated by plotting log initial rates against log initial concentrations of one reactant when the initial concentration of the other reactant was held constant. The slopes of the straight lines fitted to the points by the method of least squares were the orders with respect to the variable reactant. These were 0.96 with respect to ammonia and 0.99 with respect to droplet surface. Thus the order of the initial reaction was essentially two, and one with respect to each reactant. Initial rates can be represented by the equation

$$-\frac{da}{dt} = k\frac{3a_0}{r}[NH_3]_0$$

where a is the concentration of acid in the aerosol expressed in weight or volume units, r is the droplet radius, and the subscript 0 refers to initial conditions. The average second-order velocity constant, k, was 7.6×10^4 cm.⁴ mole^{-1} sec.$^{-1}$ with a standard deviation of 0.92×10^4.

Changing from an all-nitrogen atmosphere to one containing 62.5 mole % of helium had no measurable effect on the reaction rates (Fig. 1).

Decreasing the temperature from 28 to 8° slightly decreased the velocity constant. The usual Arrhenius-type plot led to an activation energy of about 3 kcal. mole^{-1}.

Discussion

Two facts suggest that gas-phase diffusion of ammonia did not control the over-all rates. These are (1) that even when a large excess of ammonia was present the rates were not constant over an appreciable period of time, and (2) that substituting helium for nitrogen had no appreciable effect on the rates. The fact that the over-all rates had no particular order suggests that these rates were controlled by diffusion of reaction product in the droplets. The over-all reaction rate can be represented by the equation

$$-\frac{da}{dt} = k\frac{3a_0}{r}(1 - Fx)[NH_3]$$

where x is the fraction of acid reacted and F is a dimensionless multiplier which allows for the rate of diffusion of products and for the surface area represented by each unit of product concentration. F was calculated from the rate data for various values of x and various initial conditions, and was found to be a single-valued function of x within the range of conditions studied. By substituting this function of x in the above equation, the empirical rate equation representing the over-all reaction was found to be

$$-\frac{da}{dt} = k\frac{3a_0}{r}\left(0.18\frac{1-x}{0.18+0.82x}\right)[NH_3]$$

It is of interest to consider the results for the initial reaction in terms of collision and absolute rate theory. Calculations based on the kinetic theory of gases and the empirical value of k at 28° indicate that the fraction of collisions between ammonia molecules and acid surface resulting in reaction is about 0.1. If the velocity constant is written as $k = PZ\exp(-E/RT)$, the steric factor P is 0.1 for $E = 0$, and has a maximum value of 1 for $E = 1.4$ kcal. mole^{-1}. The empirical value of E (3 kcal. mole^{-1}) is in fair agreement with these results, considering uncertainties in the calculation of the collision number Z and the experimental determination of E. Order of magnitude values for the pre-exponential factor PZ were calculated by using absolute rate theory. Partition functions for gaseous ammonia, liquid sulfuric acid, and an

(7) An artificial zeolite manufactured by the Linde Company.

(8) M. B. Jacobs, "Analytical Chemistry of Industrial Poisons, Hazards, and Solvents," Interscience Publishers, New York, N. Y., 1941, pp. 289–291.

activated complex of skeleton structure S—O$^{H\text{--}N}$ were calculated, using the method of Wilson and Johnston[9] for estimating the parameters of the activated complex. The resulting value of 10^2 cm.^{4} mole^{-1} sec.$^{-1}$ is too low by at least two orders of magnitude. This suggests the interesting possibility that the ammonia is physically dissolved in or adsorbed on the sulfuric acid droplet before reaction occurs, restricting the rotational and translational motion of the ammonia molecule, thus reducing the magnitude of the partition function and increasing the value of PZ. Present knowledge of the theory of liquids is inadequate to permit calculation of the magnitude of the partition function of ammonia in such states.

(9) D. J. Wilson and H. S. Johnston, *J. Am. Chem. Soc.*, **79**, 29 (1957).

THE ADSORPTION OF HYDROGEN ON NICKEL–KIESELGUHR

BY L. LEIBOWITZ,[1] M. J. D. LOW[1] AND H. AUSTIN TAYLOR

Nichols Laboratory, New York University, New York 53, N. Y.

Received December 11, 1957

The rates of chemisorption of hydrogen on a nickel–kieselguhr surface have been studied over a pressure range from about 1 cm. to 1 atm. in the temperature range 160 to 325°. The parameters α and $-\log t_0$ of the Elovich equation are approximately linearly proportional to the initial pressure and linear in the reciprocal temperature. New techniques are described which demonstrate the existence of site production and of site decay, proving the latter to be independent of the prevailing pressure during adsorption. The results are interpreted on the basis of the Taylor–Thon mechanism of chemisorption.

The generality of the applicability of the Elovich equation to chemisorption rates[2] and its interpretation from several different and mutually exclusive points of view,[2,3] require an investigation not only of the dependence of the parameters in the equation on the prevailing conditions but, what is even more important, a departure from the classical chemisorption procedures to discover factors of significance previously overlooked.

The system hydrogen on nickel–kieselguhr was chosen since there are no data in the literature reporting rate measurements at high temperatures. Sadek and Taylor[4] have measured some adsorption rates in the temperature interval −126 to −78°. The adsorption isobar shows a very rapid decrease with increasing temperature between −195 and −126° where the adsorption is reversible. Between −126 and −78° the volume adsorbed increases slightly, by less than 20%, reaching a flat maximum around 0°, decreasing steadily thereafter. Previous determinations of the energy of activation of adsorption have usually been made in the region where the isobar for the particular system is increasing with increasing temperature. The measurements reported here cover the temperature range 160 to 325° wherein the isobar is markedly decreasing. To investigate the dependence of the Elovich parameters on pressure, a pressure range from about 1 cm. to one atmosphere has been studied. Subsequently in the paper, a number of departures from the usual procedure are described which must cast doubt on the classical interpretations of chemisorption.

(1) Abstracts from dissertations in the Department of Chemistry submitted to the faculty of the Graduate School of Arts and Science in partial fulfillment of the requirements for the degree of Doctor of Philosophy at New York University, 1956.

(2) H. A. Taylor and N. Thon, *J. Am. Chem. Soc.*, **74**, 4169 (1952).

(3) G. S. Porter and F. C. Tompkins, *Proc. Roy. Soc. (London)*, **217A**, 529, 544 (1953); H. J. Engell and K. Hauffe, *Z. Elektrochem.*, **57**, 762, 733, 776 (1953); P. T. Landsberg, *J. Chem. Phys.* **23**, 1079 (1955); T. J. Jennings and F. S. Stone, paper presented at The International Congress on Catalysis, Sept. 1956.

(4) H. Sadek and H. S. Taylor, *J. Am. Chem. Soc.*, **72**, 1168 (1950).

Experimental

The measurements of rates of adsorption were carried out by admitting a known amount of hydrogen to a sample of the catalyst which had been suitably evacuated and measuring the rate of change of pressure in the system.

Catalyst.—To 75 g. of kieselguhr in 500 ml. of boiling water was added slowly a solution containing 60 g. of $Ni(NO_3)_2 \cdot 6H_2O$ in 300 ml. of water. The solution was boiled for 30 min. and $(NH_4)_2CO_3$ solution was added in excess to precipitate $NiCO_3$. The mixture was boiled for 2 hr. and then filtered by suction through sintered glass. The precipitate, washed ten times with 200-ml. portions of water, was sucked dry, heated overnight at 110°, crushed and sieved, the material between 10 and 100 mesh being retained for use. Duplicate analyses showed 11.5% Ni.

A 10.17-g. portion of the carbonate preparation was reduced in a 5–10 l./min. stream of tank hydrogen, which had been passed over copper at 400°, a liquid nitrogen trap, Ascarite and Drierite, at a pressure of 70 cm. for about 20 hours at 350°. The pressure of the hydrogen stream was reduced to 10 cm. and reduction continued for 45 hr. A Drierite tube attached to the exit of the catalyst vessel showed no gain in weight in 44 hr. The hydrogen was flushed out with helium and the exit tube sealed off.

The catalyst chamber was connected to a source of hydrogen and to two manometers, one containing dibutyl phthalate (D.B.P.), the other, mercury, in such a way that the D.B.P. manometer could be used for measuring the pressure changes in the system at any total pressure measured on the mercury manometer. A conventional pumping system of a mercury diffusion pump backed by a Megavac pump was used.

Procedure.—The catalyst was exhausted prior to a run by evacuation at 375°. After an initial evacuation for 15 or 20 min., helium was introduced to a pressure of 60 cm. and allowed to remain in contact with the catalyst for about 10 min. Evacuation was then resumed and continued for about 10 hr., when the remaining pressure was less than 10^{-6} mm. The flushing with helium was found to reduce the time required for evacuation from 25 to 10 hr. The furnace temperature was reduced to the desired value and hydrogen admitted to a pressure exerted on the two arms of the DBP manometer. A stopcock then isolated these two arms and the pressure changes were read from the change in the levels in the two arms.

All the data reported were carried out on the same sample of catalyst. However, mechanical failures on three occasions permitted the catalyst to be exposed to air. The catalyst was restored by allowing it to stand for about 24 hr. in contact with hydrogen at 1 atm. and 375°. After such a treatment the catalyst surface was somewhat changed and the adsorption rates were not identical with those obtained

before the exposure to air. The different surfaces are referred to as S_I, S_{II}, S_{III} and S_{IV}. Reproducibility of adsorption rates on a given surface was good but the surfaces are not quantitatively comparable. The volumes of the various parts of the system, as also of the dead space in the catalyst chamber, were measured by the expansion of a known volume of helium at both 215 and 273°. The temperature of measurement was without effect on these values.

Results and Discussion

From the pressure–time data obtained in the runs, q, the number of ml. STP adsorbed was calculated assuming ideality of the gas. In Table I are listed these data for two typical runs with time in minutes. The catalyst temperature is denoted T_c and the initial pressure P_0 is in cm. Hg or cm. DBP as indicated. Included are values of q calculated from the appropriate integrated Elovich equations.

TABLE I

RATES OF CHEMISORPTION

Run 18: P_0 = 3.39 cm., T_c = 325°, q_{calcd} = 0.674 log t + 5.93. Run 29: P_0 = 7.25 cm., T_c = 215°, q_{calcd} = 0.559 log t + 11.75.

	Run 18				Run 29	
Time (min.)	P, cm. DBP	$q_{obsd.}$, ml.	$q_{calcd.}$, ml.	P, cm.	$q_{obsd.}$, ml.	$q_{calcd.}$, ml.
0.5	14.89	5.69	5.73	3.37	11.49	11.57
1.0	13.62	5.93	5.93	3.28	11.73	11.75
1.5	12.98	6.06	6.06	3.24	11.83	11.85
2.0	12.51	6.14	6.13	3.23	11.94	11.92
2.5	12.19	6.21	6.20	3.20	11.98	11.97
3.5	11.69	6.30	6.30	3.17	12.06	12.05
4.0	11.50	6.34	6.34	3.15	12.09	12.09
4.5	11.34	6.37	6.37	3.14	12.11	12.11
5.0	11.18	6.40	6.40	3.14	12.14	12.14
7.5	10.55	6.52	6.52	3.10	12.26	12.24
10.0	10.14	6.60	6.60	3.09	12.31	12.31
12.5	9.81	6.66	6.67	..	...	...
15	9.55	6.71	6.72	3.02	12.40	12.41
20	9.08	6.80	6.81	3.00	12.46	12.48
25	8.74	6.87	6.87	2.97	12.54	12.53
30	8.43	6.93	6.93	2.96	12.57	12.58
35	8.18	6.97	6.97	2.95	12.61	12.61
40	7.95	7.02	7.01	2.94	12.65	12.65
45	7.78	7.05	7.04	2.92	12.68	12.67
50	7.65	7.07	7.08	2.91	12.70	12.70
60	7.39	7.16	7.13	2.89	12.75	12.75
75	6.97	7.20	7.19	2.86	12.82	12.80
100	6.57	7.28	7.28	2.83	12.91	12.87

Taylor and Thon[2] found that for the data of the adsorption of hydrogen on $ZnO{\cdot}Cr_2O_3$ a plot of q was linear in log t indicating that t_0 was extremely small, that is, the product $a\,\alpha$ was very large. The initial rapid adsorption goes over continuously into the subsequent "slow" process which consequently is still quite rapid. Any technique of plotting must fail to give values to t_0. Sarmousakis and Low[5] have described an algebraic procedure for the determination of the Elovich parameters. For systems such as those studied here, where t_0 is very small, the integrated Elovich equation takes the form

$$q = (2.3/\alpha) \log (a\alpha t)$$

If q_{nt} and q_{mt} are the amounts of gas adsorbed at times nt and mt, then

$$q_{nt} - q_{mt} = (2.3/\alpha) \log (n/m)$$

The constancy of $(q_{nt} - q_{mt})$ for a given ratio n/m throughout the course of the reaction provides a test of the applicability of the Elovich equation which is much more sensitive then the apparent rectilinear nature of a plot. The value of α follows at once from these differences. Values of a are calculable from α, q_{nt} and nt for the various readings made. The values of a and α obtained in this way from the data in one run show only small random deviations from the average reflecting a high degree of internal consistency and a reliability of a and t_0, in spite of their seeming extreme values. Furthermore, since the determination of α depends on a difference of two measurements any error in the zero time is minimized. In addition, what would appear as a break in the q − log t plots, corresponding to a change in α, evidences itself at once as a change in the q differences. In four of the forty runs made, no. 12, 19, 31 and 32 such a break appears after about 20 min. corresponding to a marked decrease in the rate of adsorption. These runs were made at the lowest initial pressures, around 2 cm., and undoubtedly indicate that adsorption was substantially complete. In these cases the initial linear portion of the q − log t data was used to determine α and a. Breaks in the opposite direction were also observed in other runs as shown later. Since an Elovich plot should be linear throughout, such breaks present anomalies to be accounted for by complexities in the process being studied, as Taylor and Thon have already indicated.

Table II gives a resume of the determinations made, in terms of the parameters α and − log t_0 of the Elovich equation. The state of the surface as indicated as S_I, S_{II}, S_{III} or S_{IV} and the catalyst temperature as T_c.

Evidence of Surface Heterogeneity.—It is seen that α decreases as the initial pressure increases, regardless of the particular surface studied and of its temperature. From a plot of α as a function of the initial pressure it can be seen that no single curve will satisfy all the points. In the higher pressure range, from about 10 to 60 cm., α appears to vary linearly and relatively slowly with the pressure. In the pressure range below about 10 cm., α decreases rapidly as the pressure increases. Such a change in the dependence of α on the initial pressure, from a rapid decrease to a slow one, implies a change in the adsorption process that is occurring, possibly involving a new type of site. Similar changes in the pressure dependence of α have been observed in this Laboratory with several different catalysts and will be reported subsequently. Interest, therefore, has become focussed on this change from a rapid to a slow dependence on initial pressure. Despite the fact that an expanded plot of such data as set (C) shows evidence of a definite curvature, the data are too meager to warrant its detailed analysis in relation to the catalyst and the temperature. Instead, the best straight lines, calculated by the least square method, for the low and the high pressure regions have been taken as emphasizing the change in the pressure dependence of α approximately quantitatively. These straight

(5) J. N. Sarmousakis and M. J. D. Low, *J. Chem. Phys.*, **25**, 178 (1956).

TABLE II

ELOVICH PARAMETERS AS FUNCTION OF TEMPERATURE AND PRESSURES

	(A) S_I T_c = 215°						(B) S_I T_c = 273°						
Run no.	11	8	13	12	10	9	6	1	2	3	4	7	5
P_0, cm.	3.02	6.10	13.71	31.30	53.85	56.44	6.00	6.51	12.25	21.88	38.48	47.35	58.36
α, ml.$^{-1}$	9.02	3.69	3.34	2.73	2.07	2.58	3.34	3.08	2.42	1.96	1.92	1.92	1.92
$-\log t_0$	27.7	17.7	15.5	14.9	13.0	16.8	12.0	13.6	11.7	10.7	11.1	10.3	11.3

	S_I T_c = 325°			S_{II} T_c = 325°				S_{III} T_c = 160°	S_{III} T_c = 215°		S_{III} T_c = 273°
Run no.	14	16	15	19	18	20	17	26	27	23	24
P_0, cm.	7.21	13.31	63.11	1.71	3.39	25.28	28.53	64.31	5.89	63.94	65.16
α, ml.$^{-1}$	2.37	2.44	1.76	7.30	3.41	2.19	2.14	3.43	5.7	2.95	2.50
$-\log t_0$	7.9	9.3	8.6	11.5	8.8	10.0	10.0	23.2	25.0	18.4	14.1

	S_{III} T_c = 325°		(C) S_{IV} T_c = 215°									
Run no.	21	22	32	31	33	34	30	29	36	37	35	38	39
P_0, cm.	25.30	65.31	2.19	2.71	4.06	4.20	5.80	7.25	15.52	27.36	38.59	49.89	64.30
α, ml.$^{-1}$	2.39	2.09	11.80	9.96	6.57	5.52	4.62	4.11	3.95	3.50	3.27	3.11	3.30
$-\log t_0$	11.4	11.5	27.7	28.9	26.1	23.7	21.8	21.0	21.3	19.9	20.5	19.7	21.0

TABLE III

ELOVICH PARAMETERS AND PRESSURE

	a	b	c	d	a'	b'	c'	d'
Set (A)	8.69	−0.439	37.2	−2 22	3.17	−0.0151	14.75	0.0128
Set (B)	4.03	− .134	−17.82	3.26	1.98	− .0011	10.5	.0092
Set (C)	9.36	− .456	27.36	−0.503	3.54	− .0056	19.40	.0200

lines expressed as $\alpha = a + bP_0$ for the low pressure range and $\alpha = a' + b'P_0$ for the high pressure range are listed in Table III. The change in the slope from b to b' is significant, indicating chemisorption processes which are pressure dependent. A similar treatment of the values of $-\log t_0$ has been made by expressing them as $-\log t_0 = c + dP_0$ or $c' + d'P_0$ for the low and high pressure ranges, respectively, and the values of the parameters are included in Table III. In view of the inherent uncertainties in the values of t_0, the scatter of these points is not surprising but qualitatively the same conclusion must be drawn as that from the α-P_0 results.

Sadek and Taylor[4] found evidence of two types of adsorption on a nickel–kieselguhr catalyst, using the method of Taylor and Liang.[6] Benton and White,[7] from isotherm determinations also found evidence that more than one type of adsorption occurred on a nickel catalyst. Further, if the adsorption rate data of Sadek and Taylor are plotted, q against $\log t$ following the Elovich procedure, a straight line is obtained which changes slope abruptly. The whole plot shows the type of discontinuity which Taylor and Thon[2] suggested to be due to two different types of chemisorption sites. Further evidence is afforded in the present work as shown later, wherein $q - \log t$ plots show the same type of discontinuity directly. It is suggested that these discontinuities have the same origin as that which is responsible for the abrupt change in slope of the α-P_0 plots around 10 cm. Finally in Fig. 1 are plotted the values of q, the total amount adsorbed after 1, 10 and 100 min. as functions of the initial pressure for the series of runs S_{IV} at 215° shown in Table II. The pressures in the system after 1, 10 and 100 min. for runs 33 and 39 were, respectively, 0.591, 0.463, 0.334 and 60.03, 59.79, 59.59 cm. The parallelism of the plots is striking. That the breaks occur at the same pressures in each case must have significance. It is suggested that the cause of all these variations is a change from one type of adsorption site to another, each functioning within a different pressure range. Such an idea is novel in that surface heterogeneity previously has been considered only temperature dependent. The result, nevertheless, is not unexpected on the basis of the Taylor–Thon mechanism which calls for site production by the initial reaction on contact of the gas with the surface. The initial pressure of the gas should, therefore, be significant.

Influence of Temperature.—The temperature dependence of α and of $-\log t_0$ can best be judged from the set of four runs 22, 23, 24 and 26 on surface S_{III} shown in Table II. The initial pressures in these runs varied only from 63.94 to 65.31 cm. From the slow variation in α with pressure in this range already demonstrated, it is clear that these four runs are at essentially the same pressure. The variation in α must be attributed to the change in temperature over the range 160 to 325°. It is found that α is inversely proportional to the absolute temperature and a least square analysis yields

$$\alpha = \frac{2.09 \times 10^3}{T} - 1.36$$

In a similar way it is found that

$$-\log t_0 = \frac{1.84 \times 10^4}{T} - 19.5$$

Comparison of these equations with the original data shows that the average deviation is quite small. A further set, but of only three runs, 9, 5 and 15, on surface S_I and in which the initial pres-

(6) H. S. Taylor and S. C. Liang, *J. Am. Chem. Soc.*, **69**, 1306 (1947).

(7) A. F. Benton and T. A. White, *ibid.*, **52**, 2325 (1930).

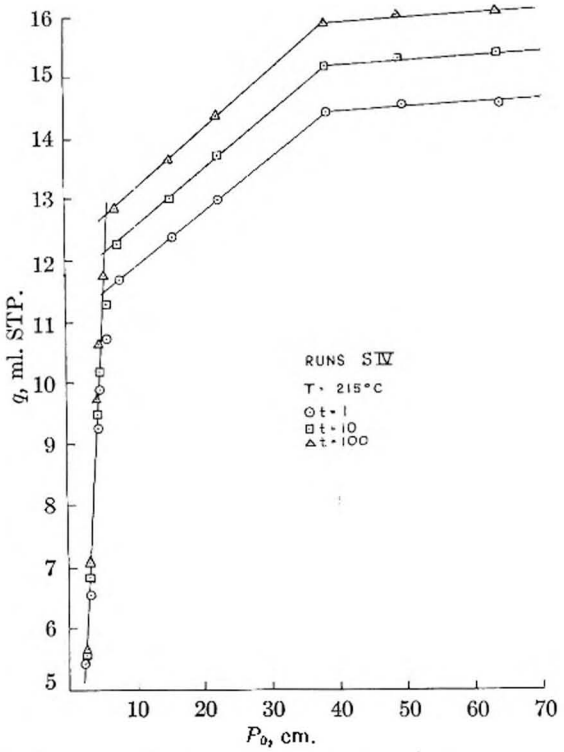

Fig. 1.—Amount adsorbed after 1, 10 and 100 min. as a function of the initial pressure.

sures are not as constant as in the former set, may be chosen as offering qualitative confirmation of the inverse proportionality to the absolute temperature.

The effect of temperature on the rate of adsorption usually has been interpreted as indicating an energy of activation of adsorption. The variation of the value of this energy of activation with the amount of gas adsorbed is considered a potent argument for "surface heterogeneity" which assumes a distribution of sites over activation energies following some definite analytical law. One of us[8] has already discussed this question using the meager data then available. A more searching analysis is possible with the above relations. To calculate the energy of activation of adsorption, use is made of the Arrhenius equation in the form: $\mathrm{d} \ln v/\mathrm{d}T = E/RT^2$ where v is the velocity of adsorption at comparable stages of adsorption at various temperatures. The necessity of using this form stems from the impossibility, as yet, of calculating a specific rate of adsorption. It has been assumed[9] that comparable stages of adsorption are achieved by using for the velocities "the times required for activated adsorption of equal volumes of gas on a clean surface." This is tantamount to writing: $\mathrm{d} \ln t/\mathrm{d}T = -E/RT^2$. From the integrated Elovich equation it follows that: $t = t_0 (e^{\alpha q} - 1)$ whence

$$\frac{\mathrm{d} \ln t}{\mathrm{d}T} = -\frac{E}{RT^2} = \frac{\mathrm{d} \ln t_0}{\mathrm{d}T} + q \frac{\mathrm{d}\alpha}{\mathrm{d}T} \frac{e^{\alpha q}}{e^{\alpha q} - 1}$$

It has been shown that the temperature dependence of $-\log t_0$ may be expressed by

$$-\ln t_0 = r/T - s$$

and of α by

$$\alpha = \frac{h}{T} - j$$

whence

$$E = Rhq \frac{e^{\alpha q}}{e^{\alpha q} - 1} - Rr$$

indicating that E must increase as q increases. If $e^{\alpha q} >> 1$ this reduces to $E = Rhq - Rr$. From the values of h and r found earlier the value of E is given by $4.14\ q - 83.8$ kcal, when q is in ml.

The surprising feature of this result is that E, though still linear in q, has a negative value for q values less than about 20 ml. a value larger than any achieved in the present study. If the Arrhenius equation in the form: $\mathrm{d} \ln(\mathrm{d}q/\mathrm{d}t)/\mathrm{d}T = E/RT^2$ is used, it is shown easily that the value of E is increased by an additional term whose value is only about 2 kcal. and with, therefore, relatively no effect on the negativity of E. From the classical point of view it might be suggested that the negative value of E results from a more rapid increase in desorption with increase in temperature, than the increase in adsorption. This also, however, cannot be true since the negativity of E decreases as q increases, while desorption, if it occurs spontaneously and appreciably at all, should increase and thus become more important as q increases. Since a negative value of E is without physical significance it must be concluded that the choice of the times required for the adsorption of equal volumes of gas at various temperatures, or, of the slopes of the volume–time plots for a constant amount adsorbed at various temperatures, does not correspond to comparable stages in the chemisorption process. The Elovich equation shows adsorption to be a decelerating process, to an extent dependent on the value of α which is itself temperature dependent. To apply the Arrhenius equation to rates at a constant amount adsorbed disregards whatever is responsible for the parameter α. In the Taylor-Thon view the deceleration is the result of spontaneous site decay. Hence, for the adsorption of a constant amount of gas, a different proportion of the surface sites has decayed at different temperatures. The density of remaining sites, one of the reactants, is different at different temperatures even though the adsorption is the same. The stages of reaction are thus not comparable. The conventional method of calculating energies of activation of adsorption is unjustifiable, the values so calculated are without meaning and the concept of "surface heterogeneity" loses a powerful argument.

Influence of Prevailing Pressure.—It is inherent in the Taylor–Thon mechanism that chemisorption involves the reaction of two species, the gas and the surface. From the classical point of view, the rate should be proportional to the product of the mass actions of each species. For the gas, this will be the concentration; for the surface, the site density, or the number of sites per unit area exposed. In the Taylor-Thon view sites decay spontaneously even in the absence of a gas phase. Since the rate of site decay is taken as rate con-

(8) H. A. Taylor, *Ann. N. Y. Acad. Sci.*, **58**, 798 (1954).

(9) Schwab–Taylor–Spence, "Sec Catalysis," D. Van Nostrand Co., New York, N. Y., 1937, p. 207.

trolling for adsorption, the rate of adsorption should be uninfluenced by changes in pressure during slow adsorption so long as the mass action of the gas is relatively much greater than that of the surface. Tests of such features require procedures not so far described in the literature. A large number of runs were made using the catalyst already described but which had not been used for several months and showed signs of further change beyond the condition described as S_{IV}. Only a resume of the principal features of these runs can be given here. Full details may be found elsewhere.[10]

In one such series, adsorption was permitted to proceed for 5 minutes, at which time the catalyst chamber was isolated from the rest of the system by closing a stopcock in the entrance tube of the chamber. After 40 minutes the chamber was rejoined and further measurements made. Figure 2 shows a comparison of such a run with an almost parallel run made without interruption. It should be noted in the first place that the "normal" uninterrupted run shows a break in the Elovich plot. Such breaks, referred to previously, were not observed in the earlier described studies but were always found in this later series and reflect progressive change in the catalyst during the intervening months. Similar breaks are to be found in plots of the data of Sadek and Taylor[4] and may indicate oxygen contamination such as that studied by Schuit and de Boer.[11] What is especially significant is the fact that the slopes of both parts of the plots are comparable, before and after the break, in each case. In the interrupted run the gas pressure fell steadily due to adsorption. During the interruption, the isolated catalyst chamber being now of smaller volume and yet the adsorption proceeding, the pressure must have fallen more rapidly. It was not possible to measure this actual pressure change in the catalyst chamber during the interruption but the total pressure change on reconnecting the chamber and manometer system, amounting to about 15%, is comparable with that in the uninterrupted run. The rate of the slow adsorption is obviously unaltered by the interruption and must be independent of the prevailing pressure.

In another type of experiment, adsorption was permitted to proceed for a short time. A known volume of gas then was removed rapidly from the system, keeping the volume of the latter constant, the pressure consequently falling. No appreciable change was observed in the rate of adsorption, indicated by a constant α, as a result of the gas removal. In one such experiment the pressure fell from 29.50 to 21.47 cm. DBP on gas withdrawal. Accompanying this pressure change there was observed a small desorption from 8.27 to 7.94 ml. adsorbed. A similar small desorption was observed whenever a sudden pressure change was induced in the system. A similar small adsorption was observed whenever a sudden pressure increase was induced in the system. Table IV presents a résumé of many such pressure changes imposed on different systems at different temperatures and pressures and

(10) M. J. D. Low, Doctoral Thesis, New York University, 1956.

(11) C. C. A. Schuit and N. H. de Boer, *Rec. trav. chim.*, **70**, 1067 (1951).

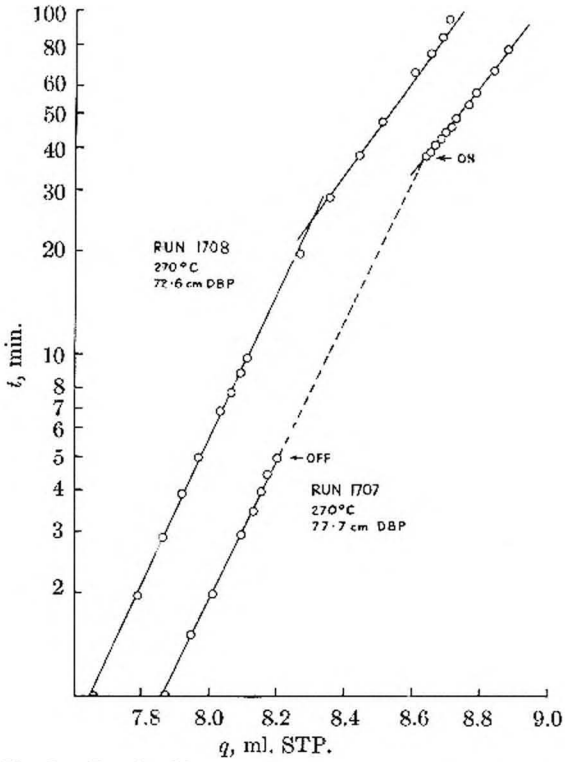

Fig. 2.—Result of interruption during adsorption showing the absence of any effect of a change in the prevailing gas pressure.

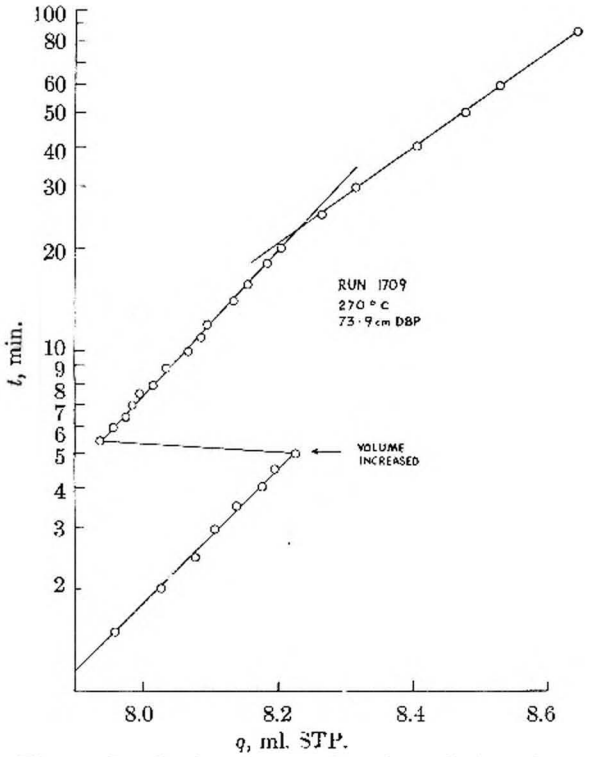

Fig. 3.—Result of an increase in volume during adsorption. Accompanying the volume increase the pressure fell from 31.63 to 22.70 cm. DBP and after 85 min. was 20.15 cm. DBP.

after different times for adsorption. The values before and after the rapid pressure changes are given as α_1 and α_2 for those runs where a sufficient number of points justify the calculation. In ad-

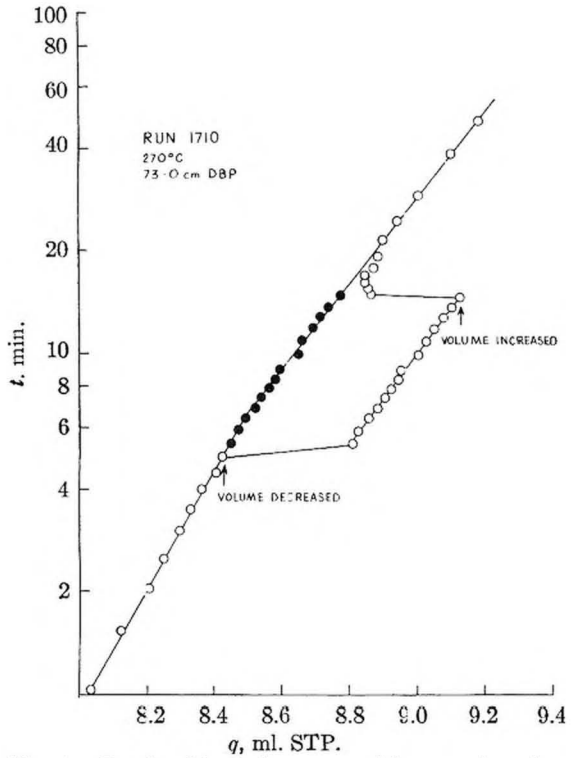

Fig. 4.—Result of both decrease and increase in volume during adsorption. The pressure change on decreasing the volume was from 43.01 to 60.18; on increasing the volume the pressure fell from 58.54 to 41.50 and after 50 min. the final pressure was 40.34 cm. DBP.

TABLE IV

Run	T, °C.	P_0, cm. DBP	P_1	P_2	t	qt	Δq	α_1	α_2
1705	270	71.2	31.80	23.05	10	8.31	−0.25	4.5	4.8
1706	270	72.7	29.50	21.47	5	8.27	− .33	4.5	4.5
1709	270	73.9	31.63	22.70	5	8.23	− .29	4.9	4.9
1710	270	73.0	43.01	60.18	5	8.43	+ .39	3.9	3.9
1710	270	73.0	58.54	41.50	15	9.14	− .29	2.9	2.9
1713	313	75.5	53.30	37.67	100	14	− .28	2.4	2.6
1721	310	68.5	18.60	13.49	1200	9.46	− .23	..	..
1722	−78	57.3	24.00	20.93	100	9.20	− .06	..	..
1729	−78	52.0	47.73	30.85	200	10.48	− .14	..	..

dition to the temperature and initial pressure in the system, the table includes P_1 and P_2, which refer, respectively, to the pressure before and after the change in condition, made at time t when the catalyst had adsorbed a volume q_t, the volume adsorbed changing by the amount Δq. An explanation of the phenomenon is not available. There appears to be no systematic variation in the amount of the change with either the temperature, the pressure or the amount adsorbed. The results at low temperature thus would appear to rule out a physical adsorption. It must be pointed out that the phenomenon is not caused by any detected experimental procedure since no such behavior could be observed when using helium under similar conditions. Although the amount of the change Δq may represent a considerable fraction of the total change for the slow adsorption it is a rapid and reversible adsorption amounting to about 3% at most of that already adsorbed. It is distinctly different in properties from the slow adsorption and although it may affect the total amount adsorbed to a very small extent, there is every indication that it does not affect the *rate* of the slow chemisorption which therefore remains independent of the prevailing pressure.

Figure 3 illustrates still another way in which the pressure in the system was changed during adsorption. After 5 minutes the volume of the system was increased from 145 to 245 ml. by opening the system to an evacuated bulb. Inspection of the q *vs.* log t plot shows an agreement of the α's before and after the 5 minute change and up to the break around 20 minutes. The small desorption accompanying the pressure decrease is evident.

Figure 4 describes a run in which the volume was decreased after 5 minutes and then increased back to the initial volume after 15 minutes. The reversibility of the small rapid adsorption and desorption is apparent. The continuity of the q–log t plot has been made more evident by subtracting 0.38 ml. from each of the readings taken during the 10 minute exposure to the increased volume. These reduced values are indicated by the full circles to contrast with the open circles which are the experimental points. The agreement of α in the early part of the 10-minute interval with that of the initial slope of the plot and of the later part of the 10-minute interval with that of the plot after 15 minutes shows the independence of the rates of both types of slow adsorption of the volume and therefore of the prevailing pressure in the system.

Finally the adsorption system was modified by the addition of a series of bulbs of measured volume so that the volume of the adsorption system could be changed at will. Various experiments were made at −78° using adsorption systems of varying size V_s. Owing to the impossibility of exactly reproducing the same initial pressure for each of these runs, the actual initial pressures used lay in the range 46.7 and 56.2 cm. DBP as the lowest and highest pressures. The average initial pressure for all these runs was 53 cm. DBP. Using the pressure dependencies found earlier for the Elovich parameters, those deduced from the linear q –log t plots were corrected from their actual initial pressure to 53 cm. DBP. The corrections in any case are small. Table V presents these results.

TABLE V

Temp., −78°, P_0 = 53 cm. DBP.

V_s	a	α	$q_t = 1$	$P_t = 1$	P_{Final}
242	7×10^8	2.5	6.9	31	22
290	7×10^7	2.4	7.6	32	24
340	3×10^7	2.5	7.6	35	28
884	2×10^6	2.2	7.6	46	45
3980	6×10^5	2	7.9	50	48
5600	2×10^5	2	9.6	52	50

Inspection of Table V shows that the volume of the system was changed by a factor of 20. The value of a seems to vary by as much as a factor of 100. However, as an extrapolated initial rate of a very rapid process this is not unexpected and the absence of any trend in the a values with variation in V_s suggests that the values are effectively constant. The constancy of α is more obvious. The apparent decrease at large V_s simply reflects the very slow pressure change occurring. Within experimental error α also is constant. This con-

stancy is achieved despite the fact that the pressure after 100 minutes, shown in the table as P_{Final} when the adsorption rate was very slow, changed by over 100%. For the system of largest volume the pressure change is so small that effectively the system is also at constant pressure. It appears therefore that the Elovich analysis of adsorption rates for a given initial pressure will yield the same parameters whether runs are made at constant volume or at constant pressure.

It is most important to note, however, that this independence of the prevailing conditions of constancy of volume or of pressure does not mean that the same absolute amounts will be adsorbed under the two conditions. The Elovich equation deals with the rate of adsorption. Taylor and Thon pointed this out earlier, suggesting a means whereby the well-known initial massive adsorption could be valuated as q_{t_0}. In those cases where t_0 was very small it was suggested that as an approximation the value $q_t = 1$ could be used. Table V lists these values for the various runs and the observed pressures at the same time. There is a definite increase in these values from 6.9 to 9.6 ml. as V_s increases. Lest it be suspected that this increase is connected with the change in q previously shown to accompany a rapid pressure change it may be noted that in Table V for a pressure change of 17 cm. DBP the maximum change in q was less than 0.4 ml. In Table V for a pressure difference at $t = 1$ of 21 cm. DBP between the runs for the smallest and largest system the difference in q is 2.7 ml. The effect of the secondary adsorption due to the pressure difference can only be a small fraction of this and leaves an amount of a higher order of magnitude to be accounted for. Taylor and Thon have suggested that q_{t_0}, here approximated as $q_t = 1$ represents the initial adsorption occurring during the site creation processes prior to the onset of the "slow" measurable adsorption. During this short time interval, a stationary rate is set up between site creation, site occupancy and site decay. In a constant volume system, the larger the volume, the less will be the pressure change accompanying creation and occupancy. Therefore, the higher will be the momentary pressure, thus favoring a larger occupancy. With an increased initial adsorption in systems of larger volume, the total adsorption at all succeeding stages must also be larger even though a, which is the initial rate of adsorption and α, which is the relative rate of site decay, are constant.

On the basis of these experiments including isolation of the catalyst during adsorption, withdrawal of gas at constant volume, volume decrease or volume increase, including a 20-fold volume increase of the system, there is cumulative evidence that the rate of adsorption is unaffected and is consequently independent of the prevailing gas pressure. When, in a homogeneous reaction between two species, the observed rate is found to be unaffected by the changes in concentration which are known to be occurring in one of the species, it can usually be shown that that species is present at a much higher concentration than the other and its concentration is thus effectively constant. It was this independence by the rate of adsorption of the prevailing gas pressure, inferred by Taylor and Thon from several slow adsorptions and now more fully substantiated in a case showing very high initial adsorption, which implied that the rate controlling species was the surface. The observed deceleration of adsorption rates demands a spontaneous site decay over and above occupancy and the form of the Elovich equation demands a bimolecular site decay process. It is this process, then, that is rate controlling for adsorption.

When a second-order homogeneous reaction becomes apparently first order due to the presence of an excess of one reactant, the velocity constant of the apparent first-order rate is, nevertheless, a function of the pressure of the reactant in excess, which pressure is taken as its initial pressure. To say that the rate of adsorption is dependent on the mass action of the surface, or to write: rate $= k[V]$ where $[V]$ represents the mass action of the surface, that is, the site density, does not preclude the possibility that k is a function of the gas pressure, which however being always present in excess can be measured effectively by its initial pressure. It is in this sense that α, the relative rate of site decay, while constant throughout a run and thus independent of the changing pressure during the run can still be a function of the initial pressure as found earlier. Whether the approximately linear relationship of α and P_0 assumed earlier is specific of the present system or is more general can only be ascertained by study of other systems. Such studies are under way.

Evidence of Site Creation and Decay.—In an attempt to obtain direct evidence for the concept of site creation and decay, two experiments were performed in an attempt to preactivate the catalyst by exposure to a high pressure of gas for a short time and then rapidly study a low pressure adsorption on the same surface. In the first experiment the catalyst at 310° was exposed to an initial pressure of 6.46 cm. and adsorption was followed for 5 minutes. At this time the system was opened to the pumps for 3 minutes. The pressure fell to 5×10^{-3} mm. thus removing most of the gas phase. At $t = 8$ minutes the catalyst chamber was isolated from the rest of the adsorption system which was prepared for Part B of the run. At $t = 10$ minutes, designated $t = 0$ for Part B, gas was let into the catalyst at an initial pressure of 71.9 cm. DBP and adsorption followed as usual. In the second experiment which was at the same temperature but at an initial pressure of 61.3 cm. at $t = 1.25$ minutes the system was evacuated for 3 minutes the pressure falling to 5×10^{-3} mm. At $t = 6.25$ minutes, designated as $t = 0$ for Part B, 75.5 cm. DBP of gas was introduced and adsorption followed. Table VI contains the experimental data for these two runs and, in addition, a third run on a freshly evacuated surface at the same temperature and comparable initial pressure of 68.5 cm. DBP.

In illustration, Fig. 5 shows a q *vs.* log t plot of run 1712. The adequate accounting of the data of both Parts A and B by the Elovich equation is evident from the linearity of the plots. From the data in the usual manner, the parameters a and α of the

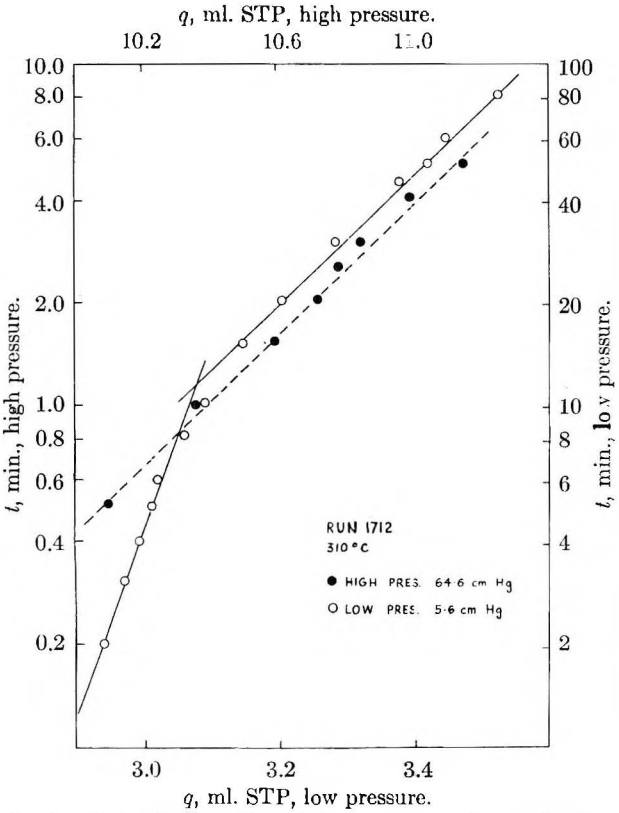

Fig. 5.—Rate of adsorption at low pressure after activation of the catalyst at high pressure.

TABLE VI

Temp., 310°

Run 1712 A, P_0 = 64.6 cm.			Run 1713 A, P_0 = 61.3 cm.			Run 1721 P_0 = 68.5 cm. DBP		
t	P	q	t	P	q	t	P	q
0.5	61.50	10.10	0.25	58.32	10.21	1.0	32.95	6.84
1.0	61.42	10.35	0.5	58.19	10.70	2.0	31.75	7.07
1.5	61.34	10.60	0.75	58.15	10.82	3.0	31.05	7.20
2.0	61.30	10.73	1.0	58.14	10.86	4.0	30.57	7.29
2.5	61.28	10.79	1.25	58.11	10.95	5.0	30.17	7.36
3.0	61.26	10.86				6.0	29.85	7.42
4.0	61.21	11.01				8.0	29.33	7.52
5.0	61.16	11.17	B, P_0 = 75.5 cm. DBP			10	28.85	7.61
B, P_0 = 71.9 cm. DBP						15		
0.5	57.00	2.85	0.5	59.00	3.20	21	27.35	7.89
1.0	56.79	2.89	1.0	58.79	3.24	30	26.44	8.06
2.0	56.56	2.94	2.0	58.37	3.32	50	25.55	8.22
3.0	56.41	2.97	3.0	58.15	3.37	460	20.05	9.10
4.0	56.30	2.99	4.0	57.96	3.40	1200	18.60	9.46
5.0	56.20	3.01	5.0	57.80	3.43			
6.0	56.13	3.02	6.0	57.62	3.46			
8.0	55.92	3.06	8.0	57.40	3.51			
10	55.75	3.09	10	57.19	3.55			
15	55.43	3.15	15	56.81	3.62			
20	55.13	3.21	20	56.47	3.70			
30	54.72	3.29	30	55.85	3.82			
45	54.20	3.39	40	55.38	3.91			
50	53.95	3.43	50	54.84	4.01			
60	53.80	3.46	60	54.40	4.10			
80	53.37	3.54	80	53.85	4.21			

equation were evaluated and are listed in Table VII as a_A, α_A and a_B, α_B for the two parts of each run, respectively. The duration of the high pressure activation is denoted t_{act}.

Inspection of the actual q–t data in Table VI shows that the unactivated run 1721 appears to be faster than either of the activated low pressure runs. Thus in the 8 to 10 minute interval the rates for 1712, 1713 and 1721 are, respectively, 0.015, 0.02 and 0.045 ml. per min. According to the Taylor–Thon theory this means that, at this stage, the site density in 1721 is higher than in either 1712 or 1713. To generalize that, on this account, no preactivation has occurred is equivalent to the error classically made in the determination of the energy of activation of adsorption. Adsorption is a decelerating process to an extent dependent on the value of α. It is precisely because preactivation did occur that the relative rate of site decay, α, is higher for 1712 and 1713 than it is for 1721. At a given time relatively late in the course of the run this rapid site decay in the preactivated runs has already reduced the site density to such an extent that fewer sites are present than in the normal run and hence the rate of adsorption is slower. Taylor and Thon showed earlier that site decay is a second-order process. Evidence for preactivation leading to a higher site density must be sought early in adsorption before the rapid site decay has taken its toll. This is precisely the advantage of the Elovich treatment wherein the analysis of the experimental data yields an "extrapolated" initial rate, a, which thereby measures the maximum adsorption rate reflecting the maximum site density for the slow adsorption. From Table VII it can be seen that a_B is many times larger for 1712 and 1713 than for 1721. Although, as pointed out earlier, the precision of the value of a may not be high, a factor of 10^2 or even 10^3 would still leave the initial rate of the preactivated runs considerably higher than that of the unactivated run. Preactivation must, therefore, have occurred.

TABLE VII

PREACTIVATION OF CATALYST

Run no.	P_0, cm.	a_A	α_A	t_{act}	P_0, cm. DBP	a_B	α_B
1712	64.6	4.4×10^{18}	4.3	5.0	71.9	1.6×10^{16}	13.8
1713	61.3	6.3×10^{24}	5.8	1.25	75.5	1.7×10^{21}	8.7
1721	..	.....	..	..	68.5	5.8×10^{7}	2.8

Such a result is to be expected from the Taylor–Thon mechanism of adsorption. Site creation occurs on contact of the gas with the surface. The extent of site creation, that is, the density of sites produced, increases with increasing pressure. In the pretreatment runs, the initial high pressure of hydrogen produces a large number of sites. Some of these are occupied by gas; others decay during the high pressure–adsorption. In such high pressure runs adsorption is known to continue considerably longer than 100 minutes. The 5 or 1.25 minute intervals in runs 1712 and 1713 are long enough for only some of the sites to decay. On evacuation adsorption must cease since the gas phase has been largely removed but site decay will continue. The site density remaining after the evacuation period will probably still be much larger than it ever is in the case of a normal low pressure run. However, at the moment more gas is introduced for the low pressure run further site creation can occur, aggravating the existing site density to a still higher maximum. It is this which is responsible for the high initial adsorption rate, a, and also for the high value of α. It is apparent that blind adherence to the classical procedure for the study of chemisorption rates can overlook factors which are most significant to their interpretation.

KINETICS OF THE REACTION BETWEEN SODIUM FLUORIDE AND URANIUM HEXAFLUORIDE. I. SODIUM FLUORIDE POWDER[1]

BY F. E. MASSOTH AND W. E. HENSEL, JR.[2]

Goodyear Atomic Corporation, Portsmouth, Ohio

Received December 11, 1957

Introduction

The reaction of uranium hexafluoride with sodium fluoride has been found to give a solid addition compound of the formula $UF_6 \cdot 3NaF$.[3,4] Since this reaction results in an increase in weight due to the solid product formed, the kinetics may be studied conveniently by a weight-change method at constant pressure. Although the reaction is reversible at higher temperatures,[4] dissociation can be ignored safely below 100°.

Farrar and Smith[5] have discussed the kinetics of solid–gas reactions in considerable detail. The two laws which are most often followed in these reactions are the linear and parabolic laws. Thus

Linear law:

$$\frac{dx}{dt} = a \qquad (1)$$

Parabolic law:

$$\frac{dx}{dt} = \frac{a}{x} \qquad (2)$$

where x is the film thickness of product at time t and a is a proportionality constant.

Assuming spherical particles, the final integrated rate expressions as given by Farrar and Smith are

Linear law:

$$\frac{k_1 V_0}{r_i} t = 1 - (1 - F)^{1/3} = f(A) \qquad (3)$$

Parabolic law:

$$\frac{k_2}{r_i^2} t = {}^1/_2 + {}^1/_2(1 - F)^{2/3} - (1 - F)^{1/3} = f(B) \qquad (4)$$

where

k_1 is the linear rate constant
k_2 is the parabolic rate constant
r_i is the initial particle radius
F is the fraction converted to product
V_0 is the molar volume of the solid reactant

Light microphotographs of the sodium fluoride powder show that the basic particles are cubic. Integration of the fundamental rate equations for cubic particles following the method of Farrar and Smith yields expressions similar to (3) and (4) with r_i replaced by $l_i/2$, where l_i is the edge of a cube. For convenience, the quantity $(4k_2/l_i^2) - (k_2/r_i^2)$ will be defined as k, the rate constant for the parabolic law. The fraction converted can be obtained by the relationship

$$F = \frac{W_t - W_0}{W_0(M_c/3M_0 - 1)} \qquad (5)$$

where

W_t is the weight of sample at time t
W_0 is the initial weight of sodium fluoride
M_0 is the molecular weight of sodium fluoride
M_c is the molecular weight of the complex, $UF_6 \cdot 3NaF$

Hence, the functions $f(A)$ and $f(B)$ can be calculated from the F values obtained experimentally by weight gain measurements. A plot of $f(A)$ or $f(B)$ *versus* t should give a straight line if the rate of reaction follows the linear or parabolic laws, respectively.

Variation of the rate constant with temperature is usually treated by the Arrhenius equation. In most cases when a diffusion mechanism prevails, the activation energy is that for the diffusion process. Pressure over a reasonably wide range is generally not a variable in solid–gas reactions. In this investigation, the uranium hexafluoride pressure was maintained at about 90 mm.

Experimental

Materials.—Reagent grade sodium fluoride powder (J. T. Baker Chemical Company) of 99.9% purity was used. This material was passed through a 100-mesh screen, heated overnight at 275° to remove surface moisture, and stored in a desiccator until used; it had a surface area of 0.33 sq. m./g. by nitrogen adsorption measurements. Uranium hexafluoride was purified by several liquefaction and flashing cycles until the theoretical vapor pressure was attained.

Apparatus.—Two types of reactors were used: *viz.*, a nickel reactor and a helix spring reactor. The nickel reactor was fabricated from one-inch tubing and was equipped with a small valve and connector. Sodium fluoride was introduced by unsoldering a coupling between the body and the valve. The total reactor weight was kept below 200 g. so that an analytical balance could be used for the weight measurements.

The helix reactor, constructed of nickel and Pyrex tubing joined by a Kovar seal, had over-all dimensions of 1.5 by 30 inches. A ground glass joint sealed with Halocarbon grease permitted disassembly. A quartz helix spring, having a maximum load capacity of five grams, was employed for weight change measurements. Spring displacement was measured with a 10 cm. cathetometer. A small Pyrex bucket held the sample. One-half and one gram analytical weights were used for calibration of the spring extension *versus* load, linear displacement being assumed over the range measured. No change in spring constant was observed upon recalibration after the run. A nickel manifold system provided for introduction and removal of gases. Pressure was measured by means of a Booth–Cromer pressure transmitter[6] used in conjunction with a mercury manometer. A thermostated water-bath maintained reactor temperature to ±0.1°.

Procedure. The nickel reactor was loaded with approximately one-half gram of sodium fluoride, heated under vacuum and exposed to fluorine to minimize subsequent reaction of uranium hexafluoride with the metal surface. The sample was then allowed to react with uranium hexafluoride at the bath temperature. At desired time intervals, the reactor was removed and weighed. In the procedure

(1) This work was performed under contract AT-(33-2)-1, with the United States Atomic Energy Commission.

(2) Presented before the Division of Physical and Inorganic Chemistry of the American Chemical Society at the 132nd National Meeting in New York, N. Y., September, 1957.

(3) H. Martin, A. Albers and H. P. Dust, *Z. anorg. allgem. Chem.*, **265**, 128 (1951).

(4) G. I. Cathers and R. L. Jolley, "Formation and Decomposition Reactions of the Complex $UF_6 \cdot 3NaF$," paper presented at the American Chemical Society Meeting, Spring, 1957.

(5) R. L. Farrar, Jr., and H. A. Smith, THIS JOURNAL, **59**, 703 (1955).

(6) S. Cromer, "The Electronic Pressure Transmitter and Self Balancing Relay," Columbia University, June 30, 1944, (MDDC-803) Declassified March 20, 1947.

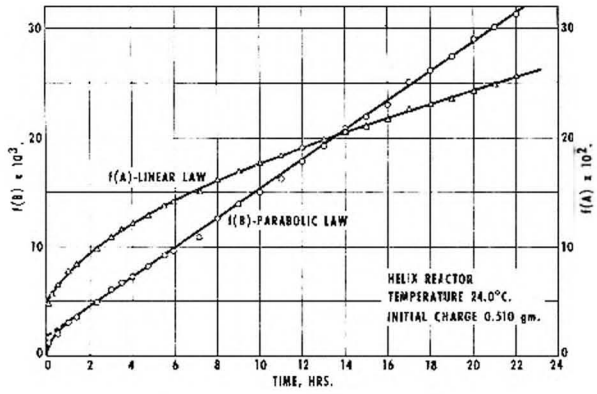

Fig. 1.—$f(A)$ and $f(B)$ *versus* time.

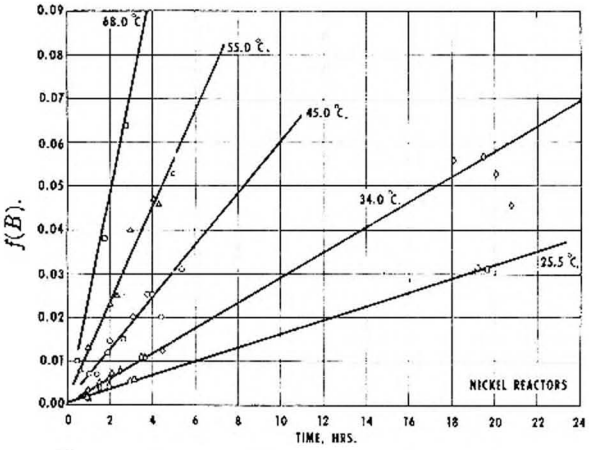

Fig. 2.—$f(B)$ *versus* time at several temperatures.

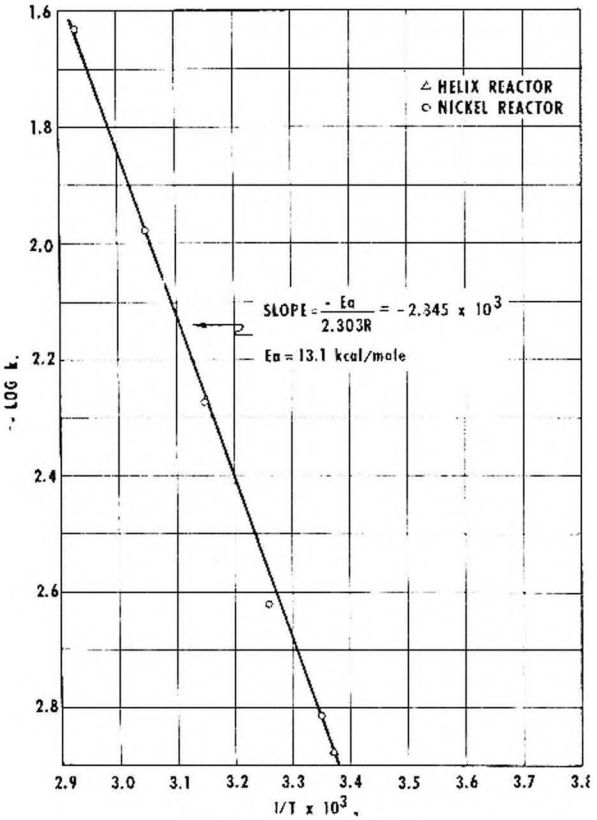

Fig. 3.—Arrhenius plot.

for the helix reactor, about one-half gram of sodium fluoride was weighed into the sample bucket on an analytical balance and the apparatus was assembled. The system was evacuated overnight to remove adsorbed moisture. The sodium fluoride was then exposed to uranium hexafluoride and the spring extension was measured at various time intervals with the cathetometer. Five readings were taken at each interval and averaged; the deviation of the average was ±0.03 mm. corresponding to a weight deviation of ±3 mg. A blank run with uranium hexafluoride resulted in no weight change, thus indicating negligible reaction of uranium hexafluoride with the Pyrex bucket.

Results

The helix reactor was employed to establish the rate dependency of the reaction since measurements with this reactor were continuous, while the nickel reactor was more conveniently utilized in studying the reaction rate variation with temperature. The results of the run with the helix reactor are shown in Fig. 1. The curves of $f(A)$ and $f(B)$ *versus* time clearly show the parabolic dependence of the reaction. The data obtained with the nickel reactor at several temperatures are presented in Fig. 2. Rate constants were calculated from the values of the least squares slopes of the curves in Fig. 2. These are presented in Table I together with the constant calculated from the helix reactor run.

TABLE I

REACTION RATE CONSTANT AT VARIOUS TEMPERATURES

Temp., °C.	$k \times 10^5$ hr.$^{-1}$	Temp., °C.	$k \times 10^3$ hr.$^{-1}$
68.0	23.4	34.0	2.38
55.0	10.5	25.5	1.54
45.0	5.34	24.0[a]	1.335[a]

[a] Helix reactor run.

An Arrhenius plot of log k *versus* $1/T$ is given in Fig. 3. From the least squares slope, the activation energy of the reaction is 13.1 ± 0.2 kcal./mole of uranium hexafluoride and the frequency factor, 5.0×10^6 hr.$^{-1}$. Thus the rate constant is given by the expression

$$k = 5.0 \times 10^6 e^{-13,100/RT} \text{ hr.}^{-1} \qquad (6)$$

Discussion

In the Arrhenius plot, Fig. 3, the value represented by the helix reactor run is in line with those obtained with the nickel reactors. This good agreement indicates that prefluorination of the sodium fluoride in the nickel reactor runs apparently has no effect upon the reaction rate, since prefluorination was not employed when the helix reactor was used.

Comparison of the curves of $f(A)$ and $f(B)$ *versus* time, Fig. 1, shows that the reaction follows the parabolic rate law very closely. However, the straight line in the $f(B)$ plot does not pass through the origin. The same behavior is shown with the nickel reactor data (Fig. 2). The $f(B)$ function exhibits a large initial slope followed by a gradual reduction to a constant value. Examination of the basic differential form of the parabolic equation shows that as x approaches zero, the rate, dx/dt, approaches infinity, which is impossible. Thus, deviations from the parabolic equation are to be expected at very low values of x. Correction for this, by use of a modified expression, *viz.*, dx/dt =

$a/(1 + bx)$, as suggested by Mott,[7] still does not account for the large initial slope which is obtained experimentally. Hence, the results imply a faster initial rate of attack. It is probable that rapid chemical reaction or physical sorption occurs on the initial surface by a different mechanism, which prevails until a sufficient amount of surface is covered by the complex. Diffusion through the film layer then becomes rate-determining with parabolic dependency. The parabolic law does not take into account the initial surface reaction, and therefore cannot be expected to account for the early stages of reaction.[8]

Additional evidence for a dual mechanism was obtained in a separate experiment. Sodium fluoride was allowed to react for three hours in the helix reactor at room temperature, the excess uranium hexafluoride was removed, nitrogen admitted to a pressure of 5 p.s.i.g., and the system allowed to remain intact overnight. Upon re-exposure to uranium hexafluoride, a marked increase in initial rate was observed above that which would be expected by the parabolic rate law and similar to that observed in the beginning of a run. After continued reaction, the data again followed the parabolic law, with the slope of the $f(B)$ *versus* time plot exactly equal to that obtained in the first three-hour reaction period. This renewed activity of the sodium fluoride shows that the diffusion of uranium hexafluoride to the interior of the particle is the rate-determining step which kinetically follows the parabolic law. Since diffusion is the rate-determining process, the uranium hexafluoride surface concentration is higher than that in the particle itself. Under this concentration gradient, uranium hexafluoride apparently migrated to the particle interior during the overnight standing. This process partially renewed the surface for subsequent rapid reaction with uranium hexafluoride. A similar occurrence has been observed for the oxidation of copper.[9]

(7) N. F. Mott, *Trans. Faraday Soc.*, **36**, 1 (1940).

(8) S. J. Gregg, "Surface Chemistry of Solids," Reinhold Publ. Corp., Inc., New York, N. Y., 1951, Chapter XIV.

(9) J. B. Brown, M. Dole and G. A. Lane, *J. Chem. Phys.*, **27**, 251 (1957).

LIQUID–LIQUID SOLUBILITY OF PENTAERYTHRITOL TETRAPERFLUOROBUTYRATE WITH CHLOROFORM, CARBON TETRACHLORIDE AND OCTAMETHYLCYCLOTETRASILOXANE

BY KŌZŌ SHINODA[1] AND J. H. HILDEBRAND

Contribution from the Department of Chemistry of the University of California, Berkeley, California

Received December 23, 1957

We have determined liquid–liquid solubility curves for mixtures of (a) $CHCl_3$, (b) CCl_4, and (c) c-$(CH_3)_8Si_4O_4$ with $(C_3F_7COOCH_2)_4C$ in order to show the effects of great disparity in molal volumes. The molal volume of the pentaerythritol ester at 25° is 542 cc., the others are (a) 81 cc., (b) 97 cc., (c) 312 cc. The critical temperatures and compositions, the latter expressed as mole % of $(C_3F_7COOCH_2)_4C$, are, respectively, (a) 43.5°, 7.3; (b) 72.1°, 9.1; (c) 123.5°, 30.7. The critical compositions in the very unsymmetrical systems (a) and (b) agree well with an expression derived from a regular solution equation in which the entropy term is based upon mole fraction, not volume fraction.

The extraordinarily large molal volume of pentaerythritol tetraperfluorobutyrate, 542 cc. at 25°, together with its compact structure, lends it unique value for studying the extent to which the thermodynamic properties of solutions are affected by disparity of the components in molal volume alone in the absence of pronounced configurational factors. We have found already that the solutions of iodine in this liquid[1a] as well as in octamethylcyclotetrasiloxane,[2] molal volume 312 cc., show no additional entropy of solution attributable to this disparity. The present investigation was undertaken in order to learn whether this conclusion would be confirmed in the case of highly unsymmetrical liquid–liquid mixtures.

Experimental

The pentaerythritol tetraperfluorobutyrate, $(C_3F_7COOCH_2)_4C$, was obtained from Minnesota Mining and Manufacturing Company through the kindness of Dr. N. W. Taylor. It had been vacuum distilled at *ca.* 0.5–2 mm. and 160°. Its refractive index was 1.3340 at 25°. Its density has been determined to be: 20°, 1.703; 25°, 1.699; 44.4°, 1.6620; 59.2°, 1.6357.

The octamethylcyclotetrasiloxane, $(CH_3)_8Si_4O_4$, was pure material furnished by the General Electric Company through the kindness of Dr. R. C. Osthoff. It was dried over $CaCl_2$ and vacuum distilled shortly before use in order to remove small amounts of polymer b.p. 66° at 14 mm.

The carbon tetrachloride, obtained from Eastman Organic Chemicals, "Spectro Grade," was dried over silica gel and distilled; b.p. 76.52° at 760 mm.

The chloroform, "Baker Analyzed" Reagent, was shaken with mercury, washed successively with dilute sulfuric acid, aqueous potassium carbonate and water and then dried over $CaCl_2$ with protection from light and distilled; b.p. 61.2° at 755 mm.

Various amounts of the degassed ester were weighed into tubes 6 mm. in diameter and 12 cm. long. The second liquid was then added, the contents frozen, evacuated, sealed and reweighed. Consolute temperatures were observed by repeated heating and cooling while shaking the tubes. Successive observations agreed within 0.05° near the top of the liquid–liquid curves, and within 0.2° on the sides.

The values at 25° for the mixture with CCl_4 were obtained by evaporating the volatile CCl_4 at 90° from weighed portions of each phase.

Results

The results are shown in Table I and plotted in

(1) Department of Chemistry, Yokohama National University, Minamiku Yokohama, Japan.

(1a) Kōzō Shinoda and J. H. Hildebrand, THIS JOURNAL, **62**, 295 (1958).

(2) Kōzō Shinoda and J. H. Hildebrand, *ibid.*, **61**, 789 (1957).

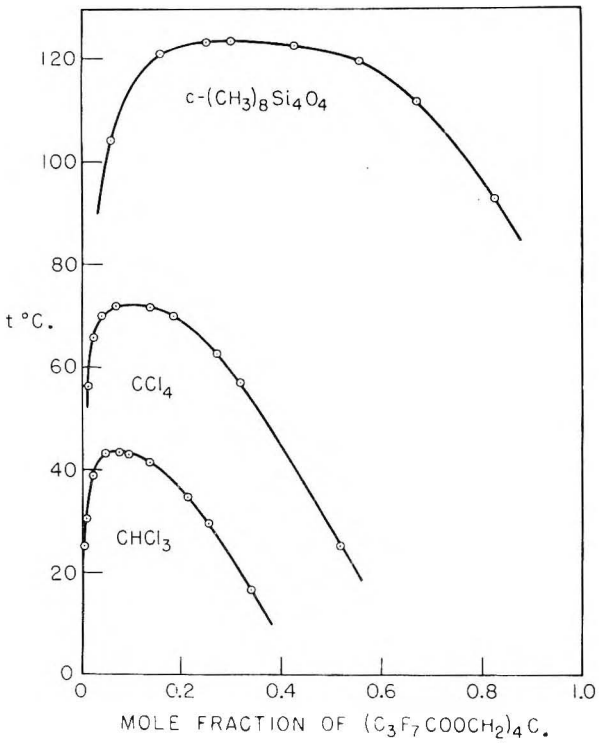

Fig. 1.

Fig. 1. The critical compositions and temperatures given in the table were obtained by plotting the data as volume fractions, ϕ, *vs.* temperature in order to get more symmetrical curves, more suitable for drawing rectilinear diameters.

The curves for $CHCl_3$ and CCl_4 are extraordinarily unsymmetrical and offer a stringent test of the equations we have used for calculating the critical composition. The one is derived from the expression

$$\ln a_2 = \ln x_2 + v_2\phi_1^2(\delta_2 - \delta_2)^2/RT' \qquad (1)$$

which is based upon the assumption that the partial molal entropy is ideal, $-R \ln x_2$; the other is derived by using in place of ideal entropy the "Flory–Huggins" entropy

$$-R\,[\ln \phi_2 - \phi_1(1 - v_2/v_1)] \qquad (2)$$

At the critical point, the derivatives $\partial \ln a_2/\partial x^2$ and $\partial^2 \ln a_2/\partial x_2^2$ are both zero. Equation 1 gives for the critical composition,[3]

$$x_2 = [(v_1^2 + v_2^2 - v_1v_2)^{1/2} - v_2]/(v_1 - v_2) \qquad (3)$$

Equation 2 gives $x_2/x_1 = (v_1/v_2)^{3/2}$ In the case of

$$x_2/x_1 = (v_1/v_2)^{4/2} \qquad (4)$$

systems that are only moderately unsymmetrical, equations 3 and 4 do not give very different results, and equation 4 gives satisfactory agreement.[4] However, the systems with $CHCl_3$ and CCl_4 here presented are so unsymmetrical as to distinguish between them, as seen in Table II. The good agreement with equation 3 adds one more impressive evidence to those we have recently presented, that large differences in molal volume are accompanied, in the case of compact molecules, by no appreciable increase in entropy of mixing. We have used for the calculation the molal volumes at the critical temperatures shown in Table III.

(3) J. H. Hildebrand and R. L. Scott, "Solubility of Nonelectrolytes," Reinhold Publ. Corp., New York, N. Y., 1950, Chapter XVI.

(4) J. H. Hildebrand, *Faraday Soc. Disc.*, No. 15, 9 (1953).

TABLE I

LIQUID–LIQUID SOLUBILITY OF $(C_3F_7COOCH_2)_4C$ IN MOLE PER CENT., $100x_2$

Component 1		$100x_2$	t, °C.
$CHCl_3$		0.692	19.55
		1.241	30.35
		2.327	38.60
		4.963	43.38
		8.028	43.49
		9.472	43.15
		13.57	41.7
		21.36	34.6
		25.41	29.5
		33.88	16.6
	crit.	7.3	43.5
CCl_4		0.23	25.0
		1.292	56.6
		2.524	65.8
		3.941	69.95
		7.094	71.82
		9.116	72.09
		13.70	71.68
		18.29	69.90
		27.06	62.7
		32.13	57.1
		52	25.00
	crit.	9.13	72.1
$c\text{-}(CH_3)_8Si_4O_4$		6.14	109.3
		15.71	121.5
		25.07	123.4
		33.54	123.47
		42.84	122.86
		54.48	119.6
		67.22	111.6
		82.46	91.8
	crit.	30.7	123.5

TABLE II

CRITICAL COMPOSITIONS, OBSERVED AND CALCULATED. MOLE PER CENT. OF $(C_3F_7COOCH_2)_4C$

Component 1	Obsd.	Calcd. Eq. 3	Calcd. Eq. 4
$CHCl_3$	7.3	7.7	5.5
CCl_4	9.1	9.4	7.1
$(CH_3)_8Si_4O_4$	30.7	31.3	30.9

TABLE III

MOLAL VOLUMES, CC.

Component 1	t_c	v_1	$(C_3F_7COOCH_2)_4C$ v_2
$CHCl_3$	43.5	82.6	553
CCl_4	72.1	103	571
$(CH_3)_8Si_4O_4$	123.5	354	606

We have no value for the heat of vaporization of $(C_3F_7COOCH_2)_4C$ from which to calculate a solubility parameter, and can ask only whether a reasonably consistent value can be obtained from its solubility relations. Using the equation[3]

$$RT_c(x_1v_1 + x_2v_2)^3 = 2x_1x_2v_1^2v_2^2(\delta_1 - \delta_2)^2 \qquad (5)$$

and the values of critical temperatures and mole fractions from Table I, we obtain the values of $\delta_1 - \delta_2$ given in Table IV. Although δ-values are temperature dependent, their differences are much less so; therefore, if we use δ_1-values at 25°, the mean of the δ_2-values in the last column of the table may be interpreted as a fairly approximate parameter for this substance. Because of the high critical temperature of the mixture with c-$(CH_3)_8Si_4O_4$ we do not include the figure for δ_2 calculated for this system.

TABLE IV

SOLUBILITY PARAMETER OF $(C_3H_7COOCH_2)_4C$

Other component	$\delta_1 - \delta_2$	$\delta_1(25°)$	δ_2
$CHCl_3$	1.9	9.0	7.1
CCl_4	1.8	8.6	6.8
I_2	7.4	14.1	6.7

The fact that t_c is so much higher for its mixture with $(CH_3)_8Si_4O_4$ than with CCl_4, in spite of the nearness of the δ-values of these liquids, 8.2 and 8.6, respectively, is consistent with the large molal volume of the former, and accords with equation 5. The effect is seen more easily in the equation

$$4RT_c = (v_1 + v_2)(\delta_1 - \delta_2)^2$$

which, although less accurate, more clearly illustrates the effect of substituting a component having the same δ-value but larger molal volume.

We express our gratitude to Drs. N. W. Taylor and R. C. Osthoff for materials, and to the National Science Foundation for support of the work.

NUCLEAR QUADRUPOLE SPECTRA OF THE CHLOROACETONITRILES

BY J. D. GRAYBEAL AND C. D. CORNWELL

Department of Chemistry, University of Wisconsin, Madison, Wisconsin

Received January 6, 1958

Resonance frequencies for Cl^{35} in polycrystalline samples of the three chloroacetonitriles are reported. The line shapes obtained with a coherently operated super-regenerative spectrometer are discussed. A technique for making frequency measurements is described which involves the injection into the spectrometer oscillator of a synchronizing voltage from a second oscillator. The coupling constants for the solids at 77°K. are −76.25, −79.60 and −83.29 Mc. for mono-, di- and tri-chloroacetonitriles, respectively, averaged over small splittings due to crystal effects. The deviations from the value expected for a purely covalent C–Cl bond are probably due more to the influence of ionic character than to that of π-bonding. The effect of the –CN substitution on the Cl^{35} coupling constant, a 6–8 Mc. increase, is unusually large compared with corresponding shifts observed for other substituted chloromethanes, and confirms the strong electron withdrawal power of this substituent.

Introduction

Nuclear quadrupole spectra in solids arise from an interaction of the electric quadrupole moment of the nucleus, eQ, and the electrostatic field gradient tensor $q_{ij} = (\partial^2 V/\partial x_i\, \partial x_j)$ at that nucleus produced by all other charges in the crystal.[1] Coupling to a radiation field is through the nuclear magnetic dipole moment, with the selection rule $\Delta m = \pm 1$. Since the spin of the Cl^{35} nucleus is $^3/_2$, only a single transition, $m = \pm\, ^3/_2 \longleftrightarrow \pm\, ^1/_2$, is observed. The frequency[2] is

$$\nu = \frac{1}{2}\,|eQq/h|\left(1 + \frac{\eta^2}{3}\right)^{1/2}$$

where $q = q_{zz}$, and $\eta = (q_{xx} - q_{yy})/q_{zz}$ is an asymmetry parameter. The measurement of the quadrupole coupling constants, eQq/h, for the three chloroacetonitriles will be described and the results discussed.

Experimental

Samples.—The monochloroacetonitrile was purchased from the Eastman Kodak Company and distilled on a concentric tube fractionating column. Di- and tri-chloroacetonitrile were prepared from the corresponding chloroacetic acids.[3] The samples were allowed to age at Dry Ice temperature for several days before use because this procedure led to an improvement in signal-to-noise ratio.

Spectrometer.—The radio-frequency spectrometer includes an externally quenched super-regenerative oscillator, provision for Zeeman modulation, a narrow-band audio amplifier tuned to the modulation frequency, a phase-sensitive detector, and a chart recorder. The oscillator (15–60 Mc.) and the associated quenching circuit (20–110 Kc.) follow the design of Dean.[4] The sample coil, immersed in a dewar containing the coolant liquid, is thermally isolated by a pair of ceramic capacitors or short pieces of small diameter wire, mechanical support being provided by a Lucite block. The modulation coil is large enough to surround the dewar and shield. The modulating current is approximately a square wave, at 85 c./sec., with a peak value of two amperes, and is provided by four 6AS7's which are alternately conducting and cut off. The current is monitored by observation of the voltage wave form developed across a resistor in series with the modulation coil. The twin-T in the narrow-band amplifier[5] is adjusted for a band width of approximately 3 c./sec. The phase-sensitive detector circuit of Schuster[6] is used with only slight modification. Frequency measurements were made with a BC-221 heterodyne frequency meter, the crystal calibration oscillator of which was adjusted to agree with station WWV

Analysis of Line Shapes.—In the super-regenerative circuit, the oscillations may or may not be permitted to decay below the level of noise voltages in the circuit before the next build-up begins, and the corresponding modes of operation are called *incoherent* and *coherent*.[7] The quenching voltage is a pulse of controllable width and amplitude, and can be adjusted for either mode of operation. Adjustment for coherent operation is relatively critical, because for optimum sensitivity the oscillations must be permitted to decay to as low an amplitude as possible, consistent with the requirement that the minimum amplitude still be large enough to

(1) H. G. Dehmelt and H. Krüger, *Z. Physik*, **129**, 401 (1951).

(2) H. Krüger, *ibid.*, **130**, 371 (1951).

(3) L. F. Fieser and M. Fieser, "Organic Chemistry," D. C. Heath and Co., Boston, Mass., 1950, pp. 176, 180, 238.

(4) See H. C. Allen, Jr., THIS JOURNAL, **57**, 501 (1953).

(5) G. E. Valley, Jr., and H. Wallman, "Vacuum Tube Amplifiers," M. I. T. Radiation Laboratory Series, Vol. 18, McGraw-Hill Book Co., Inc., New York, N. Y., 1948, p. 403.

(6) N. A. Schuster, *Rev. Sci. Instr.*, **22**, 254 (1951).

(7) J. R. Whitehead, "Super-regenerative Receivers," Cambridge Press, London, 1950.

ensure phase coherence of oscillations in successive quench cycles, despite the presence of noise voltages in the circuit. Nevertheless, this mode has been employed almost exclusively in the present work, because the oscillator spectrum in this case consists of a series of discrete frequencies rather than a series of broad bands; only in this mode do the sample resonances exhibit their proper shapes and widths. The resulting oscillator spectral pattern is depicted in Fig. 1.

As the oscillator frequency is slowly changed by a synchronous motor, the pattern of Figure 1 is shifted along the frequency axis, and a resonance effect is observed as each component in turn interacts with the sample. Since the quench frequency is several times larger than the line width, one need consider only the radio frequency field of a single component of the oscillator current spectrum, say the nth, of complex amplitude I_n, close to a sample resonance frequency. The response of the sample to a monochromatic field may be described in terms of a complex magnetic susceptibility, $\chi' - i\chi''$, the real and imaginary parts of which correspond, respectively, to the phenomena of dispersion and absorption.[8] This change in susceptibility modifies the impedance which the tuned circuit presents to the current I_n. In the approximation of constant current, the result is equivalent to the introduction of a signal voltage v, having a prescribed relationship to I_n, and hence also to $V_n \exp(i\vartheta_n)$, the complex amplitude of the corresponding component of the oscillator voltage. If the phase of I_n be measured relative to that of V_{min}, the voltage present when the oscillations are at their lowest level, the complex form of v is

$$v = 4\pi Q(i\chi' + \chi'')V_n \cos\beta \exp i(\vartheta_n - \beta)$$
$$\beta = \tan^{-1}(2Qu) \qquad -\pi/2 < \beta < \pi/2$$
$$u = (\omega - \omega_0)/\omega_0 \qquad \omega_0^2 = 1/LC$$

where ω_0 and Q are parameters of the tank circuit. The factor $\cos\beta \exp(-i\beta)$ is associated with the frequency dependence of the tank circuit impedance. Hence β takes on a different value for each component of the oscillator spectrum, but does not vary significantly over the width of a sample resonance line.

This signal alters V_{min}. The effect is amplified through super-regenerative action, in that the average level of oscillation is determined by the amplitude of V_{min}.[7,8] If v is small compared with V_{min}, the output of an amplitude modulation detector arises from the real part of v

$$\mathcal{R}e(v) = 4\pi Q V_n \cos\beta[\chi'' \cos(\vartheta_n - \beta) - \chi' \sin(\vartheta_n - \beta)]$$

while a frequency modulation detector responds to the imaginary part. The observed line shape will then represent a mixture of absorption and dispersion effects, the relative proportions being determined by the phase angle, $\vartheta_n - \beta$.

Oscillator Synchronization.—Some difficulty arises in the measurement of resonance frequencies in deciding which of the components of the oscillator spectrum at a given oscillator setting, is actually the one producing the signal. A technique depending on synchronization of the spectrometer oscillator with an external oscillator has been developed by the authors. This has proved to be unambiguous and relatively rapid compared with other procedures tried.

It is found that by coupling a sufficiently strong signal into the spectrometer oscillator from an external oscillator, the former can be synchronized with the latter. A number of tests served to establish that not merely the central component (Fig. 1), but any of the stronger sidebands can be locked with the external signal, and remain synchronized in spite of relatively large variations in quench frequency. Thus, if a particular component is synchronized with the external oscillator, and the quench frequency is then changed, the single locked component remains fixed and the others draw in or spread out, the interval between successive components being determined by the quench frequency. Even with one of the outer sidebands synchronized, the quench frequency can be changed over a large fraction of the usable range without loss of synchronization. Alternatively, with the quench frequency held constant, the external oscillator frequency may be varied by at least several tens of kilocycles with the spectrometer oscillator remaining locked, the entire set of oscillator components shifting together in this case.

Several aspects of the mechanism of this process are pertinent. The voltage from the external oscillator increases the signal level in the oscillator tank circuit and thereby depresses the gain enough to control V_{min}, which then becomes coherent with the injected signal. Since the quench frequency is fixed and the form of the oscillation envelope is not much altered, the relative phases, ϑ_n, are not appreciably changed. Thus the line shape detected remains the same when the oscillator is synchronized as when the observation is made in the normal fashion. The occurrence of locking with the external oscillator tuned to sidebands can be understood from the fact that the sensitive period is a small fraction of the entire quench cycle, so that the external signal and the oscillator voltage, V_{min}, can remain essentially in phase during this period; between one sensitive period and the next, the relative phase difference amounts to an integral number of cycles, so these voltages regularly come into the proper phase relationship during each sensitive period.

The actual procedure for frequency measurement is then as follows. The spectrometer oscillator (without frequency sweep) is set initially so that any one of its spectral components produces a sample resonance signal, and this setting need not be precise. A sufficiently strong signal from the external oscillator is coupled into the spectrometer oscillator to lock with successive components, and at each such setting the quench frequency is varied. In most cases a change of several Kc., of the order of the sample resonance line width or less, is sufficient to result in the disappearance of the resonance signal. The component in resonance with the sample can be selected unambiguously by the fact that when this component is locked, the sample resonance signal remains strong in spite of changes in quench frequency of 40 Kc. or more. After the correct component has been identified, the measurement is made by adjusting the external oscillator to maximize the sample resonance signal. The most convenient procedure, if sufficient power is available, is to use the frequency meter oscillator directly as the external oscillator, since the result is then known immediately. In other cases, a signal generator may be used to effect synchronization; after it has been set properly to the sample resonance, the frequency is measured with the frequency meter.

If the line is an absorption curve a single frequency is measured; in the case of a dispersion curve both peaks are measured and the average taken as the line center. Measurements obtained with a given sample resonance being produced successively by several different oscillator components agree within experimental error. The chief errors in frequency measurements arise from uncertainty in setting the BC-221 oscillator to the line peak, and in the calibration of the BC-221. These amount to ±1.5 and ±0.8 Kc., respectively. The maximum uncertainty in frequencies reported is believed to be ±3.0 Kc.

Results and Discussion

Frequencies of the Cl^{35} nuclear quadrupole resonances for the three chloroacetonitriles are given in Table I.

TABLE I

QUADRUPOLE RESONANCE FREQUENCIES AND LINE WIDTHS FOR SOLID CHLOROACETONITRILES

Compound	Observed frequency,[a] Mc.	Line width,[a] Kc.
CH_2ClCN	38.1251 ± 0.0030	6.5 ± 0.7
$CHCl_2CN$	40.0840 ± .0030	4.3 ± .5
	39.9233 ± .0030	5.2 ± .6
	39.7537 ± .0030	7.4 ± .8
	39.4434 ± .0030	5.2 ± .6
CCl_3CN	41.7296 ± .0030	2.9 ± .4
	41.6660 ± .0030	3.5 ± .4
	41.5340 ± .0030	3.2 ± .4

[a] Measured at liquid nitrogen temperature, 77 ± 1°K.

The small splittings of the lines for the di- and tri-chloroacetonitriles are due to slight differences in crystallographic environment. Averages of these values may be used for a discussion of chemi-

(8) An expression for χ is given by H. G. Dehmelt, *Z. Physik*, **130**, 356 (1951). The equation for v obtained above differs from the corresponding result of Dehmelt in the inclusion of a factor, $\cos\beta \exp(-i\beta)$, which affects the shapes of sideband lines.

cal bonding. For a singly-bonded chlorine atom, η is small, and the quadrupole coupling constants can be obtained from the average frequencies with negligible error in the present case by assuming $\eta = 0$. The resulting values appear in Table II.

TABLE II

EFFECT OF CN SUBSTITUTION ON QUADRUPOLE COUPLING CONSTANTS FOR CHLOROMETHANES

Compound[a]	eQq/h, Mc.	Compound	eQq/h, Mc.	Difference, Mc.
CH_3Cl	−68.40	ClH_2CCN	−76.25	7.8
CH_2Cl_2	−72.47	HCl_2CCN	−79.60	7.1
$CHCl_3$	−76.98	Cl_3CCN	−83.29	6.3

[a] R. Livingston, THIS JOURNAL, 57, 496 (1953); 20°K.

It has been shown by Townes and Dailey[9] that the principal contribution to the quadrupole coupling constant arises from valence p electrons, and that accordingly eQq/h is a measure of bond type. In order to interpret data in these terms, we may describe each chloroacetonitrile molecule as a superposition of several resonating structures. The most important of these has a covalent C–Cl bond, which may be considered to involve an sp hybrid orbital of chlorine with 15% s character, as suggested by Townes and Schawlow[9]; for this structure, the estimated quadrupole coupling constant is −93 Mc. The differences between this and the observed values, which range from −76 to −83 Mc., may be due to any of three effects: intermolecular forces occurring in the solid, ionic character of the bond, and π-bonding. For common molecular solids, the first rarely causes a difference in eQq/h between solid and gas of more than 10%; therefore part of the difference must presumably be attributed to the latter two factors.

Quadrupole coupling constants alone, without actual measurement of η, cannot serve to distinguish between ionic character and π-bonding, but we may note one indication that the former factor is dominant in the substituted methanes. Attachment of substituents which are recognized from other lines of evidence as having increasingly large electron withdrawal power leads to a consistent increase in the coupling constant of chlorine attached to the same carbon.[10] The direction of this effect is that expected from a variation in ionic character, and opposite to that expected from a variation in amount of π-bonding. This result suggests that the coupling constants are being affected more by variation in population of the p_σ-orbital than by that of the p_π-orbital.

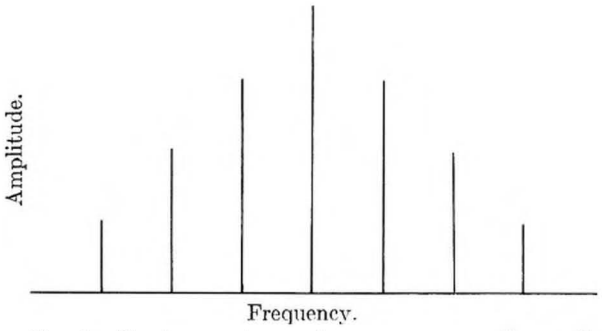

Fig. 1.—Fourier spectrum of a super-regenerative oscillator operated in the coherent mode. The spectral components are separated by the quench frequency.

The –CN substituent, as shown by group moment[11,12a] and chemical evidence,[12b,13] exhibits unusually strong electron withdrawal power, and hence replacement of H by CN might be expected to produce a particularly large *increase* in the magnitude of eQq/h if the dominant effect is that indicated above. The present results, when compared with the data of Livingston for substituted methanes, also included in Table II, do indeed show this behavior. Replacement of H by CN results in increases of 7.8, 7.1 and 6.3 Mc. in the chlorine coupling constants. By comparison, the corresponding substituent effects observed in the series studied by Allen[10] range from 1.7 to 4.8 Mc.

These conclusions may be summarized as follows. The direction of the change in eQq/h produced by CN substitution shows that the principal effect is that of variation in population of the p_σ-orbital of chlorine. The magnitude of the change in eQq/h confirms the relatively large electron withdrawal power of the –CN substituent in aliphatic compounds.

Acknowledgment.—The authors are indebted to Dr. Harry C. Allen and Dr. Harlan C. Meal for supplying details regarding the design and operation of their super-regenerative spectrometer.

(9) For a general description of the Townes–Dailey procedure see C. H. Townes and A. L. Schawlow, "Microwave Spectroscopy," McGraw–Hill Book Co., Inc., New York, N. Y., 1955, Chap. 9.

(10) H. C. Allen, Jr., *J. Am. Chem. Soc.*, **74**, 6074 (1952).

(11) C. P. Smyth, "Dielectric Behavior and Structure," McGraw–Hill Book Co., Inc., New York, N. Y., 1955, p. 253.

(12) (a) C. K. Ingold, "Structure and Mechanism in Organic Chemistry," Cornell University Press, Ithaca, N. Y., 1953, pp. 101–103; (b) pp. 260–262.

(13) R. W. Taft, Jr., *J. Chem. Phys.*, **26**, 93 (1957); L. P. Hammett, "Physical Organic Chemistry," McGraw–Hill Book Co., Inc., New York, N. Y., 1940, p. 188.

GASEOUS SPECIES IN THE NaOH–KOH SYSTEM[1]

BY RICHARD F. PORTER AND RICHARD C. SCHOONMAKER

Department of Chemistry, Cornell University, Ithaca, New York

Received January 9, 1958

Mass spectrometric studies of the gaseous species evaporating from NaOH–KOH mixtures show that in the temperature range 600 to 700°K. the vapor consists of $NaK(OH)_2$ molecules in addition to monomers and dimers of NaOH and KOH. Thermodynamic treatment of ion current data yields for the reactions $2KOH(g) = K_2(OH)_2(g)$, $\Delta H^0_{650°K} = -46.5 \pm 5$ kcal./mole of dimer; $KOH(s) = KOH(g)$, $\Delta H^0_{298} = 44.6 \pm 3$ kcal./mole and for $Na_2(OH)_2(g) + K_2(OH)_2(g) = 2NaK(OH)_2(g)$, $\Delta H^0 \simeq 0$.

Introduction

In previous work on the pure KOH[2a] and pure NaOH[2b] systems it was shown that the dimer is the predominant gaseous species in equilibrium with the condensed phase in the temperature range 600–700°K. However, it was only possible to determine a lower limit for the energy of dimerization of KOH because dissociative ionization of a dimer molecule could not be positively eliminated as the primary process for the formation of KOH^+. The present investigation was undertaken with the intention of obtaining a value for the energy of dimerization of KOH(g) and information on the vaporization processes of NaOH–KOH mixtures.

Experimental

The apparatus and experimental procedure employed in this research involved a combination of effusion and mass spectrometric techniques. Detailed discussion of the apparatus and procedure have been presented previously.[3,4]

Essential features of the apparatus include a 60 degree direction-focusing mass spectrometer with a furnace assembly mounted directly below the ion source. The furnace assembly includes an effusion cell, resistance heating element, several layers of radiation shielding, thermocouple and movable shutter plate. Neutral gaseous species which are in equilibrium with a condensed phase effuse from the orifice of the Knudsen cell and pass through the shutter plate and into the ion source of the mass spectrometer where they are ionized by electron bombardment with electrons of selected energy in the range 5–150 volts. The ions thus produced are accelerated in an electrostatic field, mass-analyzed in a variable magnetic field, and subsequently detected on the collector plate of a 9 stage electron multiplier. The output from the multiplier is fed through a vibrating reed amplifier utilizing a 100 megohm resistor and is recorded. The purpose of the shutter plate is to allow one to distinguish between ions produced from neutral species effusing from the Knudsen cell and ions produced from residual background at the same mass. Identification of and thermochemical data for the neutral species leaving the effusion cell may be obtained from a systematic study of ions produced, appearance potentials and dependence of ion current intensity on temperature.

During all runs platinum effusion cells were used, and the ratio of orifice area to evaporating area of the condensed phase was less than 0.002. The effusion cell was heated by radiation from a tungsten filament. Radiation shielding consisted of concentric cylinders of tantalum and molybdenum. With this arrangement the temperature of the effusion cell could be maintained constant for several minutes. Temperatures were measured with a Chromel–Alumel thermocouple which had been calibrated against the melting point of a sample of pure zinc obtained from the National Bureau of Standards. Commercial, reagent grade KOH and NaOH were employed throughout. Several runs were made with arbitrary NaOH–KOH ratios in the condensed phase. Generally, the initial molar ratio of KOH to NaOH was greater than 1. Since KOH is the more volatile component, the ratio KOH to NaOH decreases in the course of an experiment; and it is not possible to specify the actual condensed phase composition corresponding to a single measurement of ion intensity.

Results

The major ion species for which shutter effects were observed were: Na^+, K^+, $NaOH^+$, KOH^+, Na_2OH^+, $NaKOH^+$ and K_2OH^+. No shutter effects were observed during scans for higher species such as $NaK(OH)_2^+$, $Na_2K(OH)_2^+$, $K_2Na(OH)_2^+$, $Na_2K(OH)_3^+$ or $K_2Na(OH)_3^+$. If any of these higher species were present they would represent less than 2% of the intensity of the $NaKOH^+$. Identification of ion species was made initially by counting from known background peaks and confirmed by noting the isotopic mass shift when a mixed sample of NaOD–KOD was loaded into the effusion cell. A typical mass spectrum of NaOH–KOH vapor at 666°K. is shown in Table I.

TABLE I

TYPICAL MASS SPECTRUM OF NaOH–KOH VAPOR (T = 666°K., ELECTRON ENERGY = 50 VOLTS)

Ion	Mass no.	Intensity (relative units)
Na^+	23	71
K^+	39	97
$NaOH^+$	40	14
KOH^+	56	65
Na_2OH^+	63	86
$NaKOH^+$	79	100
K_2OH^+	95	39

Na^+, K^+, $NaOH^+$, KOH^+.—Over the entire range of experimental conditions, Na^+ and K^+ were among the most intense ion species observed. Appearance potentials for these ions were in good agreement with the ionization potentials of the free elements which implies that they were formed by simple ionization of neutral, gaseous Na or K atoms. Two processes may be considered for the formation of KOH^+ and $NaOH^+$: (1) dissociative ionization of a parent, parent + $e^- \rightarrow MOH^+ + 2e^-$ + other fragments; (2) simple ionization of a neutral species, $MOH(g) + e^- \rightarrow MOH^+ + 2e^-$ where M represents either Na or K. In previous work[2] with pure NaOH it has been shown that no appreciable amount of $NaOH^+$ is produced by dissociative ionization of a parent. Thus, the formation of $NaOH^+$ is attributed primarily to simple ionization of neutral NaOH molecules. In earlier work[2a] on the pure KOH system it was not possible

(1) This research was supported by the United States Air Force through the Air Force Office of Scientific Research of the Air Research and Development Command under Contract No. AF18(603)-1.

(2) (a) R. F. Porter and R. C. Schoonmaker, THIS JOURNAL, **62**, 234 (1958); (b) R. C. Schoonmaker and R. F. Porter, *J. Chem. Phys.*, in press.

(3) W. A. Chupka and M. G. Inghram, THIS JOURNAL, **59**, 100 (1955).

(4) M. G. Inghram, W. A. Chupka and R. F. Porter, *J. Chem. Phys.*, **23**, 2159 (1955).

to present evidence which was sufficiently conclusive to allow ruling out either process (1) or (2) as the primary source of KOH^+. If KOH^+ is formed by dissociative ionization of a parent, the ratio I_{KOH^+}/I_{parent^+} should be essentially independent of both temperature and composition of the condensed phase. The data presented in Tables II and III show that $I_{KOH^+}/I_{K_2OH^+}$ and I_{KOH^+}/I_{NaKOH^+} are dependent upon composition of the condensed phase and therefore KOH^+ cannot be formed mainly by dissociative ionization of either the parent molecule of $NaKOH^+$ or $K_2(OH)_2$.[5] If KOH^+ is formed by simple ionization of the neutral species, KOH, the following equilibria may be considered: (a) 2KOH(s or l) = $K_2(OH)_2$(g), (b) KOH(s or l) = KOH(g), (c) $K_2(OH)_2$(g) = 2KOH(g). The equilibria for the vaporization reactions (a) and (b) imply that if the activity of KOH(s,l) is altered at fixed temperature, there must be a change in the partial pressures of both KOH(g) and $K_2(OH)_2$(g) with a consequent change in the ratio $P_{KOH}/P_{K_2(OH)_2}$ if the equilibrium constant, $K = P^2_{KOH}/P_{K_2(OH)_2}$, for reaction (c) is to remain invariant. However, $P_x(g) = cTT_x^{-4}$ and a change in the ratio $P_{KOH}/P_{K_2(OH)_2}$ at fixed temperature should be manifested as a change in the ratio $I_{KOH^+}/I_{K_2OH^+}$. The data presented in Tables II and III show that this behavior is realized. Furthermore, the data in Tables II and III indicate that at most only 10% of the KOH^+ could be attributed to fragmentization of $K_2(OH)_2$ and 25% to fragmentization of the parent molecule of $NaKOH^+$. These percentages represent upper limits and the true values may be much smaller. Thus, the primary source of KOH^+ must be simple ionization of neutral KOH molecules.

TABLE II

VARIATION OF $I_{KOH^+}/I_{K_2OH^+}$ WITH EXPERIMENTAL CONDITIONS

Condensed phase	T °K.	$I_{KOH^+}/I_{K_2OH^+}$[a]
Pure KOH	661	0.53
	728	0.49
NaOH–KOH mixture	703	5.5

[a] Ionizing electron energy = 10 volts.

TABLE III

VARIATION OF I_{KOH^+}/I_{NaKOH^+} AND $I_{KOH^+}/K_{K_2OH^+}$ WITH EXPERIMENTAL CONDITIONS

Condensed[a] phase	T, °K.	I_{KOH^+}/I_{NaKOH^+}[b]	$I_{KOH^+}/I_{K_2OH^+}$[b]
(NaOH KOH)(liq.) Mixture (1)	664	2.5	2.7
(NaOH KOH)(liq.) Mixture (2)	666	0.64	1.6

[a] Mole fraction of KOH in mixture (2) greater than that in mixture (1). [b] Ionizing electron energy = 50 volts.

Na_2OH^+, $NaKOH^+$, K_2OH^+.—Three processes may be considered for the formation of each of the ion species Na_2OH^+, $NaKOH^+$ and K_2OH^+

(3) ion–molecule combination

$$M^+ + MOH \longrightarrow M_2OH^+$$
$$\text{or } M + MOH^+ \dashrightarrow M_2OH^+$$

(4) simple ionization of a neutral species

$$e^- + M_2OH \longrightarrow M_2OH^+ + 2e^-$$

(5) dissociative ionization of a parent

$$e^- + \text{parent} \longrightarrow M_2OH^+ + 2e^- + \text{other fragments}$$

where M represents either Na or K. Mechanism 3 is considered to be highly improbable under the experimental conditions employed. Such a process would involve an ion–molecule collision in the mass spectrometer ion source. Since the total pressure in the ion source region is less than 10^{-4} mm. the mean free path of ions and neutral molecules in this region is large in comparison to the dimensions of the ion source. Moreover, the period of time that an ion remains in the ion source after formation from a neutral molecule is small. These two factors tend to make an ion–molecule collision improbable. In earlier work[1,2] with pure samples of NaOH and KOH it was shown by thermodynamic argument that neither K_2OH^+ nor Na_2OH^+ was formed by simple ionization of neutral K_2OH or Na_2OH molecules, but that they were most probably formed by dissociative ionization of a parent dimer. The appearance potential for $NaKOH^+$ was found to be approximately 8.5 volts. This value is intermediate between those for K_2OH^+ and Na_2OH^+, approximately 8 and 9 volts, respectively. This fact together with the apparently analogous nature of $NaKOH^+$ to Na_2OH^+ and K_2OH^+ leads to the conclusion that all three ions probably are formed by a similar process, namely, dissociative ionization of a parent. The absence of detectable fragments of mass higher than that of $NaKOH^+$ containing Na indicates that the most probable parent of $NaKOH^+$ is the neutral $NaK(OH)_2$ molecule. The presence of OH^- was indeterminate due to masking at mass 17 by high residual background ion intensities.

The data presented in Table IV show that within the limits of experimental error the equilibrium constant, K_{eq}, for the reaction (d) $Na_2(OH)_2$(g) + $K_2(OH)_2$(g) = 2$NaK(OH)_2$(g) is essentially independent of temperature and condensed phase composition. Since K_{eq} is independent of temperature, $\Delta H^0_T \simeq 0$ for this reaction. It should be noted that except for electron multiplier efficiency and ionization cross-section corrections the ratio $I^2_{NaKOH^+}/(I_{Na_2OH^+})(I_{K_2OH^+})$ represents the true equilibrium constant for reaction (d). We would expect that the relative ionization cross-sections for $Na_2(OH)_2$, $NaK(OH)_2$ and $K_2(OH)_2$ would be nearly equal. The over-all correction for electron multiplier efficiency[6] is considerably smaller than the experimental error in the determination of K_{eq}. During a run with ionizing electron energy of 20 volts it was found that the experimental determined values of K were still included in the range 2.8–3.3. This indicates that K_{eq} is also independent of ionizing electron energy as one might predict for this reaction.

Dimerization Energy of KOH(g).—Since KOH^+ has been shown to be produced principally by simple ionization of KOH(g) under the conditions of these experiments, we may calculate ΔH^0 for the

(5) The formation of K_2OH^+ is attributed to dissociative ionization of $K_2(OH)_2$(g); see reference 2a.

(6) M. G. Inghram, R. Hayden and D. Hess, "Mass Spectroscopy in Physics Research," Nat. Bur. Standards, Circular 522, 1952.

TABLE IV

ION CURRENT INTENSITY DATA RELATED TO THE REACTION
$Na_2(OH)_2(g) + K_2(OH)_2(g) = 2NaK(OH)_2(g)$

Condensed[a] phase	T °K.	$I_{Na_2OH^+}$[b]	I_{NaKOH^+}[b]	$I_{K_2OH^+}$[b]	$K = \frac{I^2_{NaKOH^+}}{(I_{Na_2OH^+})(I_{K_2OH^+})}$
(NaOH–KOH)	631	1.0	2.3	1.7	3.1
(liq.) mixture (1)	647	1.3	3.0	2.2	3.1
	658	2.2	5.2	4.0	3.1
	672	4.3	8.5	6.0	2.8
	683	4.3	10.3	7.7	3.2
(NaOH–KOH)	641	1.0	1.4	0.6	3.3
(liq.) mixture (2)	666	2.4	2.8	1.1	3.0

[a] Mole fraction KOH greater in mixture (1) than in mixture (2). [b] Ionizing electron energy = 50 volts. Ion current intensity units are relative.

reaction $K_2(OH)_2(g) = 2KOH(g)$ by the "Third Law" method. The equilibrium constant $P_{KOH}^2/P_{K_2(OH)_2}$, is obtained from the partial pressures of KOH(g) and $K_2(OH)_2(g)$ calculated with the aid of the equation[4] $P_{x(g)} = cTI_{x^+}$ where c incorporates a sensitivity calibration of the mass spectrometer, electron multiplier efficiencies as a function of ion mass, and the relative ionization cross sections for x(g) and the calibrating agent. Generally the calibrating substance is added to the effusion cell and the calibration is made at the beginning of each experiment. Since most metals which can be used for this purpose react with the molten hydroxides, it was necessary to make separate calibrations before and after an experiment. Potassium metal was selected since it has a high vapor pressure near the temperature range of interest. The effusion cell was loaded with a large quantity of potassium and after waiting for equilibration of the vapor with the condensed phase, the ion intensity of K^{39+} was recorded together with the cell temperature. Since the vapor pressure of potassium is quite accurately known at the cell temperature,[7] the sensitivity of the mass spectrometer could be determined. Results of the pressure calibration are given in Table V. For each species listed it is assumed that the ionization cross section to form the ion from its parent molecule, relative to that to form K^+ from K(g), is approximately cancelled by the relative multiplier efficiencies. The pressures indicated are therefore only the product of temperature, ion intensity and the sensitivity constant. The values of ΔF^0 for each reaction listed in Table V were combined with a value of $\Delta S^0 = 40 \pm 5$ e.u. to obtain ΔH^0. The value of ΔS^0 was obtained by combining the terms

ΔS^0 (translation) 660°K. = +40.7 e.u.
ΔS^0 (rotation) 660°K. = +4.9 (assuming a K–O distance of 2.27 Å.[8] and a square planar configuration analogous to that proposed for the alkali halide dimers[9] with a symmetry number of four.)
ΔS^0 (vibration) 660°K. = 0 to −11.6 e.u. (assuming cancellation by all but four modes of vibration with frequencies of 300 cm.$^{-1}$ on higher.)

The major uncertainty in the values of ΔS^0 used is in the vibration term since vibration frequencies have not been reported for either the monomer or dimer. The uncertainty in ΔH^0 values listed in Table V is estimated to be within ± 5 kcal./mole of dimer and results from both the uncertainty in ΔS^0 and the estimation of ionization cross sections. The equilibrium constants for calculation of ΔF^0 are based on these cross sections and probably are good to within a factor of five. A value of $\Delta H^0 = 54 \pm 5$ kcal. for the reaction $Na_2(OH)_2(g) = 2NaOH(g)$ has been obtained earlier[2] by a method requiring neither estimates of cross sections nor entropies. This value is in reasonable agreement with that given in Table V and establishes a basis for justification of the other values listed.

Combining an averaged value of $\Delta H^0_{650°K.} = 46.5 \pm 5$ kcal./mole of dimer for the reaction $K_2(OH)_2(g) = 2KOH(g)$ from Table V with the heat of sublimation of $K_2(OH)_2(g)$ ($\Delta H^0_{626°K} = 36 \pm 2$ kcal./mole of dimer[1]) we obtain as the heat of sublimation of KOH(g), $\Delta H^0_{626°K} = 41.3 \pm 3$ kcal./mole. Using an estimated[7] ΔC_p of −10 cal./deg./mole for the sublimation process, we find for KOH(s) = KOH(g), $\Delta H^0_{298} = 44.6 \pm 3$ kcal./mole. Assuming the monomer to be the principal gaseous species near the boiling point of KOH liquid, Kelley[7] has calculated a value of $\Delta H^0_{298} = 43.9$ kcal./mole for the reaction KOH(l) = KOH(g) from the vapor pressure measurement of von Wartenberg and Albrecht.[10] Combining this value with a heat of fusion of KOH(s) of 1.8 kcal./mole[11] gives $\Delta H^0_{298} = 45.7$ kcal./mole for the heat of sublimation. Although the dimer is the principal species evaporating from pure KOH at low temperatures, the monomer will increase more rapidly with temperature than the dimer. This is seen by comparing the temperature coefficients (or ΔH of vaporization values) for the two species and noting that $\overline{\Delta C_p}$ of dimerization should be small. A rough calculation taking ΔH (dimerization) = 46.5 kcal., ΔS(dimerization) = 40 e.u. and $\overline{\Delta C_p} = 0$, gives a pressure ratio of monomer to dimer of approximately 250 at the reported boiling point of 1600°K.[7] Using a value of ΔS as low as 30 e.u. gives a ratio of about 2. Thus the assumption that KOH(g) is the species observed in von Wartenberg and Albrecht's experiment in the 1400–1600°K. range is justified and it is unlikely that the agreement between the value calculated by Kelley and that obtained in the present work is accidental.

Discussion

The analogy between the vaporization processes

(7) K. K. Kelley, Bur. of Mines Bulletin 383.

(8) L. Brewer and D. F. Mastick, *J. Am. Chem. Soc.* **73**, 2045 (1951).

(9) B. H. Zimm and J. E. Mayer, *J. Chem. Phys.*, **12**, 362 (1944).

(10) H. Von Wartenberg and P. A. Albrecht, *Z. Electrochem.*, **27**, 162 (1921).

(11) R. Seward and K. Martin, *J. Am. Chem. Soc.*, **71**, 3564 (1949).

TABLE V

SUMMARY OF DATA FOR DIMER DISSOCIATION REACTIONS

Reaction	T(°K.)	I_{KOH^+}[a]	$I_{K_2OH^+}$[a]	P_{KOH} (atm.)	$P_{K_2(OH)_2}$ (atm.)	ΔF_T^0 (kcal.)	ΔH_T^0 (kcal.)[b]
$K_2(OH)_2(g) = 2KOH(g)$	641	5.7	2.8	6.2×10^{-3}	3.1×10^{-5}	20.3	45.9
	666	8.6	4.8	9.7×10^{-3}	5.4×10^{-5}	20.6	47.2
	T (°K.)	I_{NaOH^+}[a]	$I_{Na_2OH^+}$[a]	P_{NaOH} (atm.)	$P_{Na_2(OH)_2}$ (atm.	ΔF_T^0 (kcal.)	ΔH_T^0 (kcal.)[b]
$Na_2(OH)_2(g) = 2NaOH(g)$	666	1.9	11.5	2.2×10^{-3}	13×10^{-3}	25.7	51.4
	T (°K.)	I_{NaOH^+}[a]	I_{KOH^+}[a]	I_{NaKOH^+}[a]	P_{NaOH} (atm.)	P_{KOH} (atm.)	$P_{NaK(OH)_2}$ (atm.)	ΔF_T^0 (kcal.)	ΔH_T^0 (kcal.)[b]
$NaK(OH)_2(g) = NaOH(g) + KOH(g)$	666	1.9	8.6	13.4	2.2×10^{-3}	9.7×10^{-3}	1.5×10^{-3}	24.0	49.6

[a] Ion current units are relative to $K^{39+} = 100$ corresponding to the vapor pressure of potassium of 7.3×10^{-7} atm. at 429°K., the calibration temperature. Sensitivity constant for mass spectrometer = 1.7×10^{-11} atm./unit °K. [b] Assuming $\Delta S^0 = 40$ e.u.

of alkali halide and sodium and potassium hydroxide should be noted. Evidence for gaseous dimers of the alkali halides has been obtained in molecular beam studies by Miller and Kusch[12] and in mass spectrometric studies on LiI by Friedman.[13] In the latter study the major ion peak observed is Li_2I^+ which is analogous to the Na_2OH^+ or K_2OH^+ peaks. In neither the LiI study nor in the present experiments were the parent dimer ions of appreciable intensity. The existence of the substituted dimer $NaK(OH)_2$ in the vapor of NaOH-KOH mixtures suggests that substituted species might also occur in mixed alkali halides. It is interesting to speculate whether a quadratomic molecule with different alkali metal and halide groups would be stable and whether a hydroxyl group could be substituted for a halide. It is noteworthy that the present results indicate the stability of $NaK(OH)_2$ to be intermediate between $Na_2(OH)_2$ and $K_2(OH)_2$.

(12) R. C. Miller and P. Kusch, *J. Chem. Phys.*, **25**, 860 (1956).
(13) L. Friedman, *ibid.*, **23**, 477 (1955).

NOTES

ESTIMATIONS OF THE SURFACE POLARITY OF SOLIDS FROM HEAT OF WETTING MEASUREMENTS

BY A. C. ZETTLEMOYER, J. J. CHESSICK AND C. M. HOLLABAUGH

Contribution from the Surface Chemistry Laboratory, Lehigh University, Bethlehem, Pennsylvania

Received August 21, 1957

Few efforts have been made to differentiate quantitatively between various solids in terms of their surface polarity. An effective method is to determine the heats of immersion of these solids in selected organic liquids from which an estimation of the average electrostatic field strength of the polar solids can be made. Differentiation can also be made between non-polar solids.

Such measurements have been made for rutile (TiO_2), Graphon[1] and Teflon[2] immersed in straight chain butyl compounds which differ in functional groups. These measurements have been extended to include CaF_2 and Aerosil, the former an example of a strongly polar solid with a weakly polarizable anion and the latter a predominantly hydrophobic silica.

(1) J. J. Chessick, A. C. Zettlemoyer, F. H. Healey and G. J. Young, *Canadian J. Chem.*, **33**, 251 (1955).
(2) J. J. Chessick, F. H. Healey and A. C. Zettlemoyer, THIS JOURNAL, **60**, 1345 (1956).

Experimental

The calorimeter, associated equipment and general techniques have been described.[3,4] Baker C.P. grade CaF_2 was used. This sample was washed with absolute ethyl alcohol and distilled water, then activated at 150° and 10^{-5} mm. pressure for two hours before use. The surface area as measured by nitrogen adsorption measurements was 12.7 m.²/g. Aerosil (Cab-O-Sil) is finely divided SiO_2 prepared from $SiCl_4$ by hydrolysis in a hydrogen flame and contains at least 99% SiO_2. This material was supplied by Godfrey L. Cabot, Inc. The surface area was 120 m.²/g.

Heats of immersion were determined in heptane, butyl alcohol, butyl chloride and nitropropane. These are designated RH, ROH, RCl and RNO_2, respectively, in Fig. 1.

Results and Discussion

For a heteropolar surface interacting with a polar molecule, the polar van der Waals forces make a significant contribution to the interaction energy. A major energy term, E_μ, arises from the interaction of the dipole moment of the adsorbate, μ, and the electrostatic field of the surface, F, and is given by the equation

$$E_\mu = -\mu F \qquad (1)$$

The heats of immersional wetting for rutile in a series of straight chain butyl compounds were measured previously and were found to be a linear

(3) F. H. Healey, J. J. Chessick, A. C. Zettlemoyer and G. J. Young, *ibid.*, **58**, 887 (1954).
(4) A. C. Zettlemoyer, G. J. Young, J. J. Chessick and F. H. Healey, *ibid.*, **57**, 649 (1953).

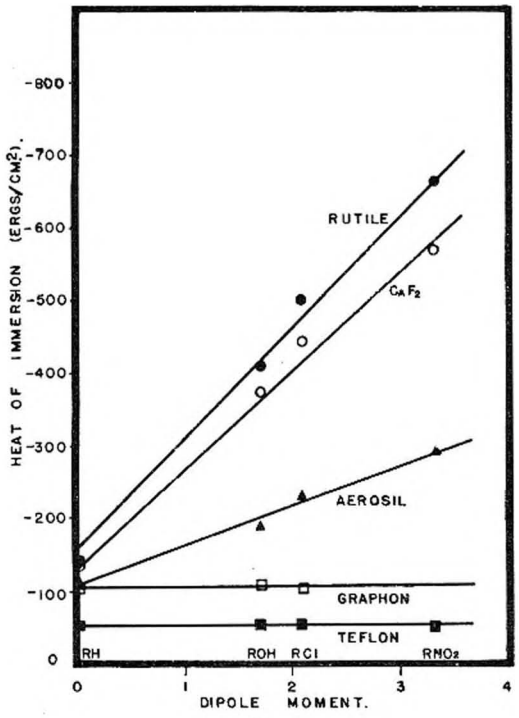

Fig. 1.

function of the dipole moment[5] of the wetting liquid.[3] Assuming that the differences in the heat values were due primarily to E_μ, the slope of the linear curve was taken as a measure of the average electrostatic field strength of the rutile surface. Similar determinations are possible for other solids.

Heat of wetting values for rutile, CaF_2, Aerosil, Graphon and Teflon immersed in hexane, butyl alcohol, butyl chloride and nitropropane are shown plotted in Fig. 1 as a function of the dipole moment of the wetting liquid. The average electrostatic field strength calculated from the slopes of the curves in Fig. 1 using equation 1 are shown in Table I, assuming a surface concentration of adsorbed liquid molecules of 5×10^{14} molecules per cm.[2,3] and neglecting any differences in the packing of polar molecules in the surface of the solid.

It is probably proper to place the lines for the rutile, calcium fluoride and Aerosil so that the intercepts fall above the points for the hydrocarbon as was done previously.[1] The other wetting liquids contain polar groups so that the contributions of the induced dipole moments are no doubt more important in the latter cases.

TABLE I

CALCULATED AVERAGE FIELD STRENGTHS FOR SOLID ADSORBENTS

Solid	$F \times 10^{-6}$ e.s.u.
Rutile	2.7
CaF_2	2.5
Aerosil	1.1
Graphon	0
Teflon	0

(5) R. J. W. Le Fevre, "Dipole Moments," John Wiley and Sons, Inc., New York, N. Y., 1953, p. 133.

De Boer[6] has calculated the field at a distance of 2.7 Å. from the surface of NaCl to be 2.15×10^5 e.s.u. so the agreement in magnitude is excellent. In addition, De Boer has calculated from completely different experiments values for the fields on rutile of 4.1×10^5 e.s.u. and 0.9×10^5 e.s.u. at sparse and approximately monolayer coverage, respectively.

The values listed in Table I do not include the contributions due to dispersion forces. The heats of immersion in heptane clearly indicate a large difference in this contribution between Graphon and Teflon. Smaller differences occur between the polar solids.

The positive slope found for Aerosil suggests that this material is weakly polar. However, water and nitrogen adsorption measurements show that the surface of this solid is predominantly hydrophobic; only about 25% of the surface will adsorb water up to about 0.3 relative pressure. The hydrophilic portion consists of silanol groups. Aerosil was included in this study to show that judgment of the nature and the over-all polarity of a solid on the basis of heat of immersion measurements can be misleading if other information is not available. Graphon and Teflon are both hydrophobic solids. It is noteworthy that Teflon has more polar sites per unit area than Graphon.[2] These polar sites amount to 0.75 and 0.15% of the surfaces of Teflon and Graphon, respectively. The data in Table I suggest an absence of a field at the Graphon and Teflon surface. This certainly is not so. Apparently, the experimental approach is not sensitive enough to detect the small electrostatic fields at the surface of these solids.[7]

Acknowledgment.—The authors greatly appreciate the support provided by the Office of Ordnance Research, U. S. Army.

(6) J. H. De Boer, "Advances in Colloid Science," Vol. III, Interscience Publishers Inc., New York, N. Y., 1950, Vol. VIII, p. 102, 1956.

(7) J. H. De Boer, "Advances in Catalysis," Vol. VIII, Academic Press Inc., New York, N. Y., 1956, p. 36.

THE MOLECULAR WEIGHT AND VAPOR PRESSURE OF GASEOUS BORON SUBOXIDE

BY MILTON D. SCHEER

Applied Research Operation, Flight Propulsion Laboratory Department, General Electric Company, Cincinnati, Ohio

Received September 9, 1957

The stability of a suboxide of boron has been known for some time.[1,2] A polymer of composition $(BO)_x$ has been prepared[3] by the dehydration of sub-boric acid ($H_4B_2O_4$). The preparation of this same suboxide from a $B(s)$–$B_2O_3(l)$ mixture has been accomplished by Kanda and his co-workers.[4] These investigators heated such a mixture *in vacuo* in a tantalum crucible covered by a perforated lid. Condensation of macroscopic quantities of the polymeric $(BO)_x$ upon a glass target was observed with the crucible at temperatures as low as 1320°K.

(1) H. Kahlenberg, *Trans. Am. Electrochem. Soc.*, **47**, 23 (1925).

(2) E. Zintl, W. Morawietz and E. Gastinger, *Z. anorg. allgem. Chem.*, **246**, 8 (1940).

(3) T. Wartik and E. Apple, *J. Am. Chem. Soc.*, **77**, 6490 (1955).

(4) F. A. Kanda, A. J. King, V. A. Russell and W. Katz, *ibid.*, **78**, 1509 (1956).

Inghram, Porter and Chupka[5] recently have made a mass spectrometric study, in the temperature range 1300 to 1500°K., of the gaseous species effusing from an alumina Knudsen cell containing a B(s)–B_2O_3(l) mixture. The major ion peaks observed were $B_2O_2^+$, $B_2O_3^+$, B^+ and BO^+. The presence of B^+ and BO^- was attributed to the dissociative ionization of B_2O_2(g) and B_2O_3(g), while $B_2O_2^+$ and $B_2O_3^+$ seemed to be formed by the simple ionization processes

$$B_2O_2(g) + e^- \longrightarrow B_2O_2^+ + 2e^- \text{ and}$$

$$B_2O_3(g) + e^- \longrightarrow B_2O_3^+ + 2e^-$$

Assuming that the relative ionization cross sections for Ag(g):B_2O_2(g):B_2O_3(g) were as 1:2:2, Inghram, *et al.*, calculated the partial pressures of B_2O_3(g) and B_2O_2(g) from the known vapor pressure of Ag and the measured ion current ratios $B_2O_3^+/Ag^+$ and $B_2O_2^+/Ag^+$ at an ionizing energy of about 120 e.v. The B_2O_2:B_2O_3 pressure ratio, calculated in this fashion, was found to be about 7 to 1 in this temperature range. The pressure of B_2O_3 from the B(s)–B_2O_3(l) mixture was found to be about one-fifth that measured by Speiser, Naiditch and Johnston[6] and about one-half that observed in this Laboratory[7] for pure B_2O_3. Inghram, *et al.*, tentatively attributed this decreased thermodynamic activity of the B_2O_3(l) to its depletion in a reaction with B(s) forming another unidentified condensed phase. From the slope of a log $p_{B_2O_2}$ *versus* $1/T$ plot, a value of 94 kcal./mole was obtained for the heat of sublimation of B_2O_2(g) from the B(s)–B_2O_3(l) mixture.

This present investigation is concerned with an independent method of measuring the pressure and gas phase constitution of the species evaporating from a B(s)–B_2O_3(l) mixture. The apparatus used is described in detail in a previous communication.[7] In brief, it consists of a device which can measure both the weight of, and force exerted by, the vapor evaporating from a condensed phase and effusing through two small circular orifices. From kinetic theory considerations, such measurements yield both the molecular weight and pressure of the effusing species.

Experimental

The only modification of the apparatus described previously[7] is the substitution of a tantalum cell for the one made of platinum. The reason for this is the formation of a low-melting (<1000°) Pt–B alloy. Tantalum also forms a boride, but it is highly refractory.

Boric oxide was prepared by the dehydration of C.P. boric acid. Elemental boron (about 99% pure) was obtained from Cooper Metallurgical Associates. The major impurity was found to be boric oxide. Except for about 12 hr. of outgassing at 800° and 10^{-6} mm. pressure, no further purification of the boron was attempted. A mixture of this boron and boric oxide, in a 3 to 1 boron to oxygen atom ratio, was placed in the torsion cell and thoroughly degassed before the torsion and weight loss measurements were made.

Results

It has been shown previously[7] that the pressure p and the molecular weight M of the vapor effusing out of the cell at some temperature T is given by the expressions

$$p = \frac{2k\beta}{afq}\left(\frac{2qW_B + \sum_n q_nW_{nB}}{\sum_n q_nW_{nB}}\right) \quad (1)$$

$$M = 2\pi RT\left(\frac{2qW_B + \sum_n q_nW_{nB}}{2qW_B \sum_n q_nW_{nB}}\right)^2 \frac{w^2}{p^2} \quad (2)$$

β is the angle through which the cell rotates as a result of the effusing gas, k is the torsion constant of a quartz fiber from which the cell is suspended, a is the perpendicular distance between the effusion holes in the cell, q is the area of one of these two equal cell holes, q_n is the area of one of the twelve holes in the platinum radiation furnace which surrounds the cell, f, W_B, and W_{nB} are factors correcting for the departure of the holes from ideal orifices, w is the rate of weight loss of the cell, and R is the molar gas constant.

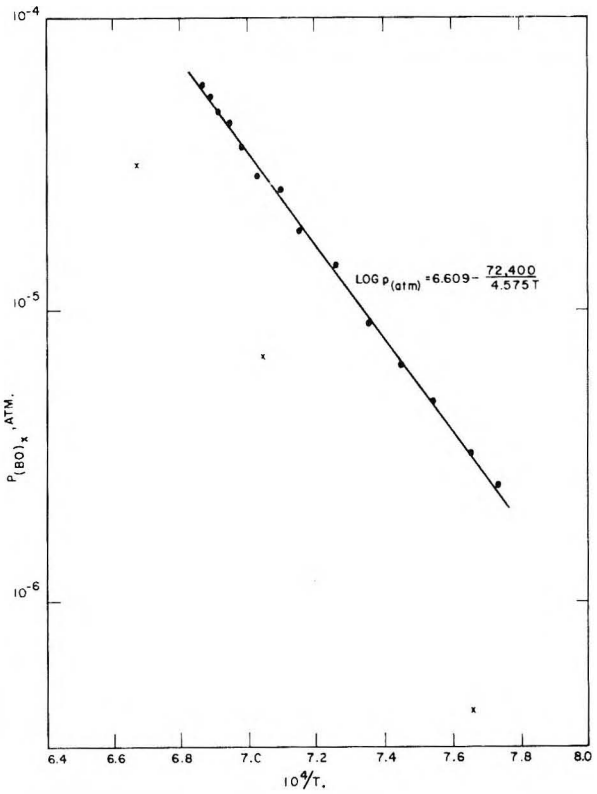

Fig. 1.—Pressure of gas evaporating from a B(s)–B_2O_3(l) mixture: x, mass spectrometric data of Inghram, *et al.*[5]; ●, torsion data obtained in this investigation for a mixture with a 3 to 1 B/O atom ratio.

A summary of the data obtained from 14 torsion measurements in the temperature range 1294 to 1457°K. is given in the first two columns of Table I. The pressure p given in the third column is calculated from β by means of eq. 1. The last column of Table I gives the pressure exerted by the suboxide species, and hence is corrected for the partial pressure of B_2O_3(g) as obtained from measurements reported previously.[7] This correction assumes that the thermodynamic activity of B_2O_3(l) does not decrease in the presence of B(s),

(5) M. G. Inghram, R. F. Porter and W. A. Chupka, *J. Chem. Phys.*, **25**, 498 (1956).

(6) R. Speiser, S. Naiditch and H. L. Johnston, *J. Am. Chem. Soc.*, **72**, 2578 (1950).

(7) M. D. Scheer, THIS JOURNAL, **61**, 1184 (1957).

so that p and $p_{(BO)_x}$ given in the last two columns of Table I are in effect upper and lower limits for the gaseous suboxide pressure. Figure 1 is a plot of log $p_{(BO)_x}$ *versus* $1/T$ for the data obtained here as compared with the mass spectrometric measurements by Inghram, *et al.*[5] A least mean square representation of the torsion data is given by

$$\log p_{(BO)_x} = 6.609 - (72{,}400/4.575T) \qquad (3)$$

when $1294° \leq T \leq 1457°K.$

Table II contains the results of four rate of weight loss measurements carried out with the same apparatus used for the torsion measurements. The quantity given in the second column has been corrected for the maximum possible amount of $B_2O_3(g)$ in the effusing vapor (less than one-tenth of the suboxide in this temperature range). The suboxide pressures at these temperatures are calculated from the torsion data represented by eq. 3 and are given in the third column. The last column of Table II gives the molecular weight of the effusing species as obtained from these data and eq. 2. The average of these four determinations is 55 ± 3 g./mole, while 53.6 is the formula weight of B_2O_2.

Discussion

The measurements reported here show that, in the 1300° to 1500°K. temperature range, the major gaseous suboxide formed in a reaction between B(s) and $B_2O_3(l)$ is $B_2O_2(g)$. The presence of BO(g) was not detected in these experiments. Even using the smallest experimentally determined molecular weight (51), the calculated BO(g) concentration is found to be considerably less than one-tenth of the $B_2O_2(g)$. These conclusions are in complete agreement with the mass spectrometric observations of Inghram, Porter and Chupka.[5]

The pressures measured here, however, are six to eight times larger than those measured in the same temperature interval by Inghram, *et al.* Also, the temperature dependence of the present results yields a ΔH of 72 kcal./mole compared to the 94 ± 8 found by Inghram. These differences are greater than any experimental uncertainty in either set of measurements. It is necessary, therefore, to look elsewhere for an explanation.

A possible explanation is suggested by the effusion experiments of Kanda and co-workers[4] who reported that the yield of sublimed $(BO)_x$ polymer depends upon the B/O atom ratio of the mixture used. They found that maximum suboxide yields were obtained with mixtures having a B/O ratio between 3 and 4. *It is therefore suggested that equilibration between the condensed phases [B(s), $B_2O_3(l)$, and possibly $(BO)_x$] and gaseous B_2O_2 is not readily achieved in such effusion experiments.* The difference between the two sets of measurements can then be understood, if it is assumed that complete equilibrium was not achieved in either set of experiments. Hence, both values for the heat of vaporization are probably in considerable error.

Gaseous B_2O_2 can be formed by at least two paths —one directly from B(s) and $B_2O_3(l)$, namely

$$\frac{2}{3}\,B(s) + \frac{2}{3}\,B_2O_3(l) \longrightarrow B_2O_2(g)$$

TABLE I

TORSION MEASUREMENTS FOR THE B–B_2O_3 SYSTEM[a]

T, °K.	$\beta \times 10^{-4}$, rad.	$p \times 10^{-6}$, atm.	$P_{(BO)_x} \times 10^{6}$ atm.
1294	3.3	2.5	2.5
1307	4.4	3.3	3.2
1326	6.7	5.0	4.8
1342	9.1	6.8	6.4
1361	12.7	9.5	8.9
1379	17.8	13.3	12.4
1399	26.4	19.8	18.7
1410	36.3	27.2	25.7
1424	41.4	30.9	28.4
1432	51.1	38.2	34.9
1441	62.8	46.9	42.8
1448	69.6	52.0	47.3
2453	79.0	59.1	53.3
1457	87.7	65.6	59.3

$$\log p_{(atm.)} = 6.609 - \frac{72{,}400}{4.575T}$$

[a] p was calculated from eq. 1, where $k = 8.948$ dyne cm./rad., $a = 1.55$ cm., $f = 0.850$, $W_B = 0.805$, $q = 0.019$ cm.^{2}, $\Sigma\, q_n W_{nB} = 0.523$ cm.^{2}. The quantities f, W_B, q and $\Sigma q_n W_{nB}$ are obtained from measurements at 298°K. Small corrections for the thermal expansion of tantalum and platinum at the high temperatures were made from the data of Edwards, Speiser and Johnston.[8]

TABLE II

WEIGHT LOSS MEASUREMENTS FOR THE B–B_2O_3 SYSTEM[a]

$$\left(\frac{2qW_B + \sum_n q_n W_{nB}}{2qW_B \sum_n q_n W_{nB}}\right) w$$

T, °K.	g./cm.^{2} sec.	$P_{(BO)_x}$, dynes/cm.^{2}	M, g./mole
1340	54.2×10^{-6}	6.32	51
1355	74.0	8.54	53
1370	107.3	11.5	62
1410	209.0	24.4	54
		Av.	55 ± 3

[a] $p_{(BO)_x}$ is calculated from the least squares fit of the torsion measurements given in Table I. M is calculated from eq. 2.

and the other *via* the intermediate formation of a condensed $(BO)_x$ polymer

$$\frac{X}{3}\,B(s) + \frac{X}{3}\,B_2O_3(l) \longrightarrow (BO)_x$$

$$(BO)_x \longrightarrow \frac{X}{2}\,B_2O_2(g)$$

Evidence for the occurrence of an appreciable condensed phase reaction is provided by (1) the decreased $B_2O_3(g)$ pressure in the presence of B(s), observed by Inghram, *et al.*, and (2) some X-ray diffraction data taken in this Laboratory of the B–B_2O_3 mixtures used for the above measurements. Separate samples from various regions of the tantalum torsion cell were taken. A thin shiny film of the refractory Ta_3B_4 was found to be formed wherever the mixture came in contact with the cell wall. Dark brown globules, appearing sporadically throughout the mixture, gave patterns showing the amorphous structure of B_2O_3 only. There was no trace of the distinct boron structure shown by either pure boron or those portions of the mixture not formed into dark brown globules.

(8) J. W. Edwards, R. Speiser and H. L. Johnston, *J. Appl. Phys.*, **22**, 424 (1951).

Since pure boric oxide is white, these dark brown globules must contain additional boron in some form other than B_2O_3 and B [probably as $(BO)_x$]. Quantitative measurements of the condensed phase reactions between B and B_2O_3 at temperatures in excess of 1000° would be of great value for further elucidating the origin and energetics of the gaseous suboxide of boron.

Acknowledgment.—The author wishes to express his thanks to J. A. Homan for assisting with the experimental work. The X-ray diffraction data were supplied by W. M. Spurgeon and O. Isaacs of the chemical engineering group in this Laboratory.

THE STABILITY OF ORGANIC SULFONIC ACIDS IN DILUTE AQUEOUS HYDROGEN PEROXIDE

BY H. T. HOOKWAY AND B. SELTON

Chemical Research Laboratory, Department of Scientific and Industrial Research, Teddington, England

Received September 12, 1957

In a recent communication,[1] Wood has drawn attention to the degradation of sulfonated cross-linked ion-exchange resins with hydrogen peroxide. Some years ago we commenced a study of the stability of sulfonic acids toward hydrogen peroxide[2] but the work was not completed. The results obtained are however of interest in confirming and extending Wood's observations.

The reactions of the following acids with hydrogen peroxide were studied: methanesulfonic-, benzenesulfonic-, *m*-nitrobenzenesulfonic-, toluene-*p*-sulfonic-, polyvinyl sulfonic-, polystyrene sulfonic-, and two sulfonated styrenedivinylbenzene copolymers. In all cases extensive decomposition of the sulfonic acids occurred at 60° with 2.94 molar aqueous hydrogen peroxide solutions. Sulfuric acid, carboxylic acids and carbon dioxide were produced. The results are summarized in Table I and Figs. 1, 2 and 3.

Experimental

Since oxidations involving hydrogen peroxide are catalyzed to varying extents by metallic ions, care was taken in purifying the sulfonic acids. The water soluble materials were freed from traces of copper and iron by passing 0.1 *N* aqueous solutions slowly through a column of sulfonated cross-linked polystyrene (10% divinylbenzene; resin in the hydrogen form). Spectrographic examination of materials treated in this way showed that copper and iron were no longer present. The cross-linked materials were laboratory prepared samples and it is unlikely that they contained even trace amounts of copper or iron.

The oxidations were carried out in the presence of a large excess of hydrogen peroxide. Small samples of the reaction mixtures were withdrawn from time to time and titrated against 0.05 *N* sodium hydroxide. Hydrogen peroxide was estimated in other small samples by titration with 0.1 *N* potassium permanganate. Sulfuric acid was determined as barium sulfate; consistent results were obtained by following Rudy's procedure.[3]

The reaction flasks were connected to absorption trains consisting of two traps containing sulfuric acid, a calcium chloride–soda lime tube and, finally, another trap containing sulfuric acid. In all experiments a slow stream of nitrogen was bubbled first through a hydrogen peroxide "saturator" and then through reaction flask and absorption train. It was found that under these conditions all the carbon dioxide formed during the reactions was swept into the absorption train and that changes in volume of the reaction mixtures due to evaporation were negligible. The weight of carbon dioxide evolved was determined by weighing the soda lime trap. Corrections were applied to allow for changes in volume of the reaction mixtures due to removal of samples for titration.

(1) W. Wood, THIS JOURNAL, **61**, 832 (1957).

(2) Chemistry Research 1952, Her Majesty's Stationery Office, London, 1953.

(3) R. B. Rudy, *J. Res. Natl. Bur. Standards*, **16**, 555 (1936).

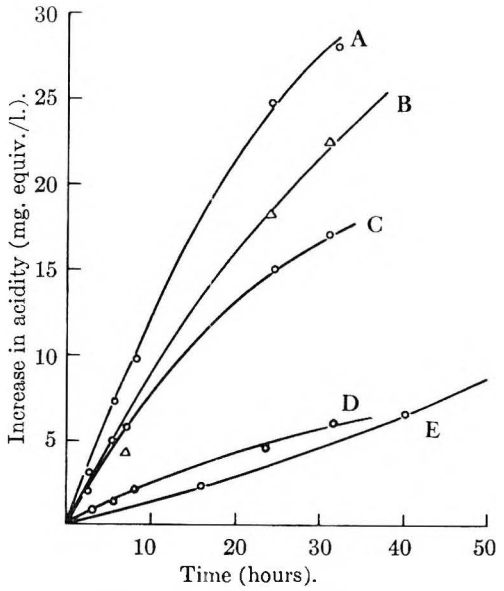

Fig. 1.—Oxidation of sulfonic acids with hydrogen peroxide at 60°: A, 5×10^{-2} *M* toluene-*p*-sulfonic acid + 2.94 *M* H_2O_2; B, 5×10^{-2} *M* *m*-nitrobenzenesulfonic acid + 2.94 *M* H_2O_2; C, 5×10^{-2} *M* benzenesulfonic acid + 2.94 *M* H_2O_2; D, 5×10^{-2} toluene-*p*-sulfonic acid + 0.29 *M* H_2O_2; E, 5×10^{-2} *M* methanesulfonic acid + 2.94 *M* H_2O_2.

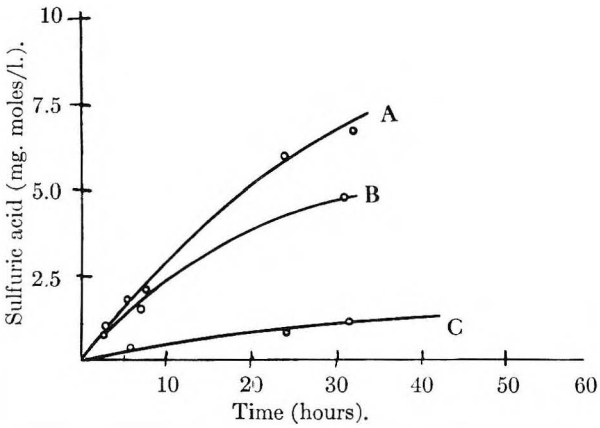

Fig. 2.—Sulfuric acid produced during oxidation of sulfonic acids: A, conditions as for Fig. 1, curve A; B, conditions as for Fig. 1, curve C; C, conditions as for Fig. 1, curve D.

TABLE I

OXIDATION OF POLYVINYL SULFONIC ACID AT 60°

2.94 *M* H_2O_2, 4.2×10^{-2} *M* Acid

Time (hr.)	10.5	24.5	31.5	48.0	55.0	72.0	80.0
Increase in acidity (mg. equiv./l.)	14.0	18.5	19.5	24.0	28.0	38.0	42.5
H_2SO_4 (mg. moles/l.)	16.5	18.5	20.0	..	25.5	..	29.5
CO_2 (mg. moles/l.)	0.5	1.5	1.5	6.5	9.0	16.0	17.5

Discussion

It is evident that even in the absence of catalytic

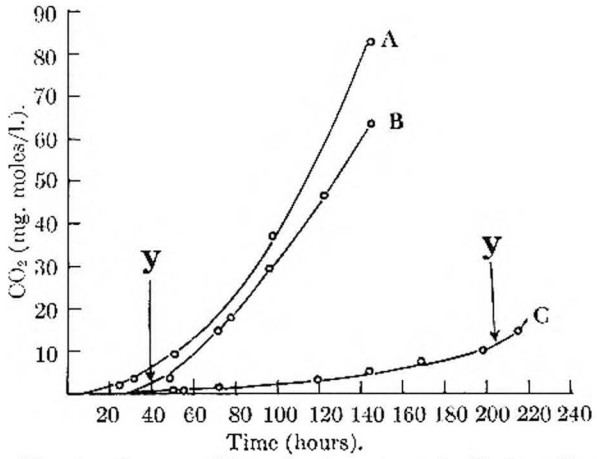

Fig. 3.—Decomposition of polymeric arylsulfonic acids: A, polystyrenesulfonic acid (sulfonated styrene–divinylbenzene copolymer); B, 0.5% divinylbenzene; C, 10% divinylbenzene; all 5×10^{-2} *M* with respect to reaction mixture; Y, polymer in solution.

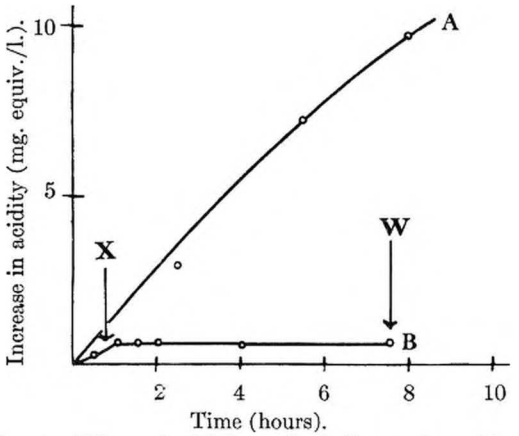

Fig. 4.—Effect of added acrylonitrile on the oxidation: A, 2.94 *M* H_2O_2, 5×10^{-2} *M* $C_7H_7SO_3H$; B, as above but 1 *M* with respect to acrylonitrile; X, polymer pptd.; W, 90% yield of polymer.

amounts of copper or iron, extensive decomposition of both aliphatic and aromatic sulfonic acids occurs under the reaction conditions described. The course of the breakdown of the aromatic sulfonic acids is undoubtedly complex, and the marked increases in total acidity and sulfuric acid in the reaction mixtures support the view that ring-breaking must be an early consequence of the oxidation. The rates of decomposition of benzenesulfonic, *m*-nitrobenzenesulfonic and toluene-*p*-sulfonic acids are remarkably similar (Fig. 1, curves A, B and C), and it is tempting to suggest that the first step at least of their decomposition involves a radical, rather than an ionic mechanism. Some support for this view has been obtained by observing the effect of adding a 1 molar aqueous solution of acrylonitrile to a toluene-*p*-sulfonic acid–hydrogen peroxide substrate at 60°. The results are shown in Fig. 4. It will be seen that the oxidation reaction is virtually completely suppressed, but that rapid polymerization of the acrylonitrile takes place. Experiments with methanesulfonic acid and benzenesulfonic acid gave similar results.

Polystyrenesulfonic acid and its cross-linked analogs may be attacked both in the polymer chain and the aromatic ring system. Figure 3 shows the carbon dioxide evolution from typical reaction mixtures. The material containing 0.5% divinylbenzene as cross-linking agent behaved very similarly to polystyrenesulfonic acid. The rate of evolution of carbon dioxide with both the 0.5% and 10% cross-linked materials increased markedly when complete solution was achieved. This increase in rate of decomposition might be expected as a result of the transition from a heterogeneous to a homogeneous reaction.

It will be observed from Table I that the oxidation of polyvinylsulfonic acid showed features which had not previously been encountered. Until rather less than half the sulfonic acid groupings had disappeared virtually no carbon dioxide was evolved and the increase in acidity of the reaction mixture was due entirely to the presence of sulfuric acid. There was a marked increase in the total acidity of the reaction mixture after half the sulfonic groups had formed sulfuric acid. This increase in acidity was greater than the increase in sulfuric acid and was accompanied by a sharp rise in the amount of carbon dioxide evolved. Thus, in contrast to the other sulfonic acids, polyvinylsulfonic acid does not undergo appreciable degradation of the molecule until roughly half the sulfonic acid groupings have disappeared.

Acknowledgment. This note is published with the approval of the Director, Chemical Research Laboratory.

THE SUBLIMATION PRESSURE OF KRYPTON BELOW 80°K.

BY B. B. FISHER AND W. G. MCMILLAN

Department of Chemistry, University of California, Los Angeles, Calif.

Received September 19, 1957

In connection with a study[1] of transitions in absorbed monolayers of krypton it became necessary to know the vapor pressure of solid krytpon in a range considerably below those previously recorded in the literature. In the absorption apparatus employed[2] the vapor pressure of the krypton could be measured directly by condensation of a large excess into the adsorption chamber. Temperatures were measured with an argon vapor pressure thermometer, using the tables of Hoge[3] for conversion to degrees Kelvin. Krypton, of spectroscopic grade (Linde Air Products Company), was used directly without further purification. The argon employed in the vapor pressure thermometer, originally "99.5%" grade (Ohio Chemical and Manufacturing Company), was passed through a charcoal trap at liquid nitrogen temperature to remove adsorbable impurities.

The solid triangles of Fig. 1 show how our data overlap and extend those of previous investigators.[4-7] (The experimental points above 80°K. of

(1) B. B. Fisher and W. G. McMillan, *J. Am. Chem. Soc.*, **79**, 2969 (1957); *J. Chem. Phys.*, to be published.

(2) Ref. 1, Part I.

(3) H. J. Hoge, Table 19.50, NBS-NACA, Tables of Thermal Properties of Gases, July, 1950.

(4) K. Peters and K. Weil, *Z. physik. Chem.* **A148**, 27 (1930).

(5) E. Justi, *Physik. Z.*, **36**, 573 (1935).

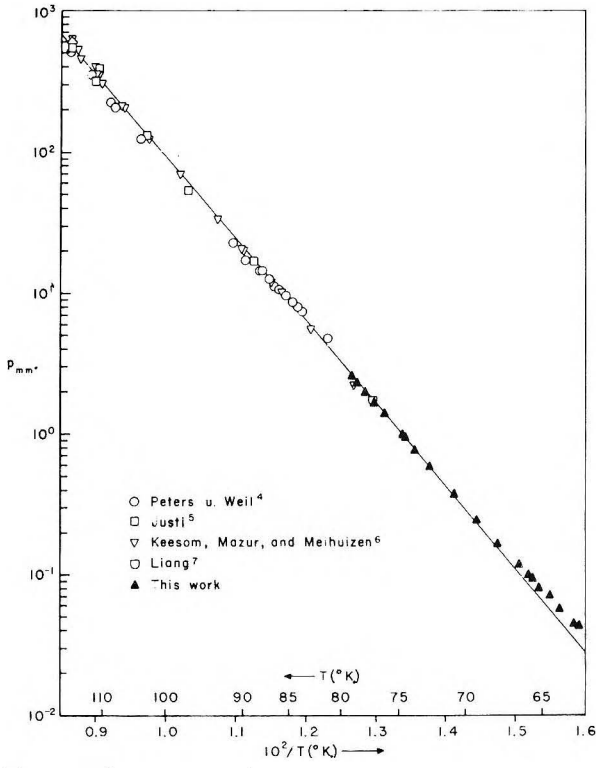

Fig. 1.—Comparison of experimental vapor pressure of krypton with theoretical curve.

several other investigators[8,9] are in essential agreement, but have been omitted for clarity.) The curve in Fig. 1 was derived from the theoretical formula[6]

$$\ln p_{mm} = -\frac{\lambda_0}{RT} + \frac{1}{R}\left\{\frac{1}{T}\int_0^T C_s\,dT - \int_0^T \frac{C_s}{T}\,dT\right\} + \frac{5}{2}\ln kT - B'P - \frac{3}{2}\ln(2\pi\hbar^2/m) - \ln(1.013.10^6/760)$$

in which the data of Clusius[10] for the heat capacity C_s at saturation were used in the integration. Values for the second virial coefficient were calculated from the results of Mason and Rice[11] with the aid of the tabulation given by Rice and Hirshfelder.[12] This correction for gas imperfection amounts to only 1% at the triple point, and rapidly declines in importance with decreasing temperature. Since there apparently exists no direct calorimetric measurement of the heat of sublimation, the quantity λ_0 has been selected so as to give the best fit to the composite vapor pressure data. The resulting choice of 2.6575 kcal./mole is to be compared with the values 2.660 and later 2.6526 recommended by Clusius,[10] *et al.*,[9] and 2.633 by Keesom[6] and co-workers.

Below about 70°K., as indicated in Table I, our data exhibit significant departures from the theoretical curve, which we believe to be more trustworthy in this range. Although in the appropriate direction, it is doubtful that deviations of the magnitude indicated can be due to thermal transpiration, since even at the lowest pressure (~0.05 mm.) the ratio of the critical tubing diameter (8 mm. i.d.) to the mean free path is ~30. This qualitative conclusion is reinforced by the analysis of Bennett and Tompkins,[13] from which we estimate only ~5% deviation at our lowest pressure of ~0.05 mm. A subsequent mass spectrographic analysis of the krypton, however, showed traces of nitrogen. An examination of the expected effect of a small amount of nitrogen shows that if an ideal solid solution were formed with krypton, a nitrogen mole fraction of 10^{-4} would raise the measured vapor pressure at 65°K. by 15%, at 75° by 5% and at 110° by 0.4%. Fortunately such a small impurity, if indeed present, would have a completely negligible effect on monolayer adsorption measurements, which were our primary interest.

Table I

Comparison between Theoretical and Experimental Krypton Vapor Pressure Below 80°K.

T(°K.)	p_{Kr} (mm.) Exp.	Theory	T(°K.)	p_{Kr} (mm.) Exp.	Theory
80	3.17	3.18	71	0.386	0 370
79	2.55	2.56	70	.298	.284
78	2.04	2.05	69	.229	.215
77	1.62	1.63	68	.174	.161
76	1.29	1.30	67	.132	.120
75	1.020	1.031	66	.1005	.0885
74	0.805	0.810	65	.0765	.0640
73	635	.630	64	.0577	.0455
72	.498	.485	63	.0428	.0324

We wish to thank Miss Elizabeth Force for assistance with the numerical calculations.

(6) W. H. Keesom, J. Mazur and J. J. Meihuizen, *Physica*, **2**, 669 (1935).
(7) S. Chu Liang, *J. Appl. Phys.*, **22**, 148 (1951).
(8) F. J. Allen and R. B. Moore, *J. Am. Chem. Soc.*, **53**, 2522 (1931).
(9) K. Clusius, A. Kruis and F. Konnertz, *Ann. Phys.*, **33**, 642 (1938).
(10) K. Clusius, *Z. physik. Chem.*, **B31**, 459 (1936).
(11) E. A. Mason and W. E. Rice, *J. Chem. Phys.*, **22**, 843 (1954).
(12) W. E. Rice and J. O. Hirshfelder, *ibid.*, **22**, 187 (1954).
(13) M. J. Bennett and F. C. Tompkins, *Trans. Faraday Soc.*, **53**, 185 (1957).

THE RATE OF REACTIONS AS A FUNCTION OF TIME

By Alexander Meller and John E. Bright

Research Division, Australian Paper Manufacturers Limited, Melbourne Australia

Received October 3, 1957

In a recent paper[1] a method was described for determining rate equations for reactions in which the initial concentration of the reacting species or the total amount of product at infinite time is not known.

For reactions in which the rate is proportional to a power of the concentration of a single reactant the expression is

$$\frac{dx}{dt} = k(a - x)^n \qquad (1)$$

where k and a are constants, and n is defined as the order of the reaction.

It was shown[1] that for $n \neq 1$

$$\left(\frac{dx}{dt}\right)^{(1-n)/n} = (n - 1)\,k^{1/n}\,t + k^{(1-n)/n}\,a^{1-n} \qquad (2)$$

and therefore the rate of advancement of the reaction in terms of the rate of formation of a product can be determined as a function of time.

(1) J. H. Flynn, This Journal, **60**, 1332 (1956).

This method necessitates the computation of dx/dt values by graphical or mathematical approximations from experimentally measured x and t values. An alternative method to obtain an expression for the rate in terms of time consists of a rearrangement of the integrated form of equation 1 giving

$$x = a - [a^{1-n} - (1 - n)kt]^{1/(1-n)} \quad (3)^2$$
$$\text{for } n \neq 1$$

This equation, when applied to experimental data, obviates the computation of dx/dt values by approximation methods, and is suitable to establish the kinetic order and to determine the concentration of the reacting species for reactions the rate of which is represented by equation 1.

Examples will show that a straight line relationship exists between functions of both x and t, *i.e.*, these functions do not involve the concentration of the reacting species.

For $n = 2$, equation 3 gives

$$x = a - \frac{a}{1 + ak_2t} = \frac{a^2k_2t}{1 + ak_2t}$$

or

$$\frac{t}{x} = \frac{1}{a^2k_2} + \frac{1}{a}t$$

where k_2 is the second-order rate constant. Thus a plot of t/x against t gives a straight line and evaluation of its gradient and intercept with the ordinate gives the values for the rate constant and for the amount of reactant which reacts according to second-order kinetics.

For $n = -1$, equation 3 results in

$$x = a - a(1 - 2a^{-2}k_{-1}t)^{1/2}$$

or

$$x = 2a - 2k_{-1}\frac{t}{x}$$

where k_{-1} is the "negative first-order" rate constant. Thus a plot of x against t/x gives a straight line; its intercept with the ordinate and its gradient yield the values for the amount of reactant which reacts according to "negative first-order" kinetics and for the rate constant.

The "negative first-order" equation may represent the rate of a zero-order retarded reaction, *viz.*

$$\frac{dx}{dt} = k_{-1}(a - x)^{-1} = \frac{1}{k_{-1}(a - x)} = \frac{c}{1 + bx}$$

where c and b are constants.[1,3]

In other instances where n has values different to those discussed above, except unity, the order of the reaction and the values for k and a can be found by substituting experimental values of x and t in equation 3 and using algebraic elimination procedures.

For $n = 1$, it can be shown that a linear relationship exists between the logarithm of the rate and time of reaction, since

$$\frac{dx}{dt} = ak_1e^{-k_1t}$$

(which on integration gives $x = a(1 - e^{-k_1t})$). Thus

$$\log dx/dt = \log ak_1 - k_1t \quad (4)$$

where k_1 is the first-order rate constant.

While the application of equation 4 involves the computation of dx/dt values by approximation methods, exact algebraic techniques were devised by Guggenheim[4] and by Roseveare[5] for establishing whether experimental data conform to first-order kinetics and for determining the concentration of the reacting species. Further discussion of the merits of these methods is outside the scope of this note.[6]

The rate of concurrent first and zero-order reactions also can be expressed in terms of time. The relationship between x and t, as shown below, permits the evaluation of both the zero- and first-order rate constants and the relative amounts of the reactant which react according to zero- and first-order kinetics, respectively.[7]

Total rate: $dx/dt = dx_0/dt + dx_1/dt$ for the same t values and $x = x_0 + x_1$ at any instant. dx_0/dt is the zero-order rate, dx_1/dt the concurrent first-order rate and x_0 and x_1 are the reacted amounts at time t.

$$\frac{dx}{dt} = k_0 + k_1a_1e^{-k_1t}$$

and

$$x = k_0t + a_1(1 - e^{-k_1t}) \quad (5)$$

where a_1 is the fraction of the reactant which reacts according to first-order kinetics. Substitution of experimental values of x and t in this equation and algebraic elimination procedures do not lead to the values of k_1, k_0 and a_1, because, for given x values a_1 not being known, the logarithm of the differences (log $(a_1 - x)$) itself constitutes an insoluble problem.

However it was shown[7] that the constants can be found by means of either of two expressions, *viz.*

1. Increm. $(dx/dt)_{\Delta t} = k_2$ Increm. $x_{\Delta t} + k_0k_1\Delta t$

where Increm. $x_{\Delta t}$ values are the differences between x-values for a chosen and constant time interval of Δt; and Increm. $(dx/dt)_{\Delta t}$ values are the differences between the rates for the successive and constant intervals of Δt.

2. $$\log_e \frac{x'''' - 2x''' + x''}{x''' - 2x'' + x'} = k_1\Delta t$$

where x'''', x''', x'' and x' denote the amounts reacted at successive time intervals of Δt. The other constants (k_0 and a_1) may be computed by simple algebraic substitution and elimination using equation 5.

A further attractive point in expressing rates of reactions only as a function of time is that such interpretations may contribute to a better understanding of the mechanism of complex heterogeneous reactions.

As an example it should be quoted that the

(2) The differentiated form of equation 3 is $\frac{dx}{dt} = a^nk[1 + (n - 1)a^{n-1}kt]^{n/(1-n)}$, which may be of interest when compared with equation 2.

(3) A. Meller, *J. Polymer Sci.*, **10**, 213 (1953).

(4) E. A. Guggenheim, *Phil. Mag.*, **2**, 538 (1926).

(5) W. E. Roseveare, *J. Am. Chem. Soc.*, **53**, 1651 (1931).

(6) See: "Kinetics and Mechanism," by A. E. Frost and R. G. Pearson, John Wiley and Sons, Inc., New York, N. Y., 1954.

(7) A. Meller, *Tappi*, **36**, 264 (1953); *Austral. J. Chem.*, **7**, 157 (1954).

constants in the logarithmic rate equation for chemisorption, $dq/dt = ae^{-\alpha q}$,[8] were interpreted in a recent paper[9] by identifying the integrated form of this equation

$$q = \frac{1}{\alpha} \ln\left(t + \frac{1}{\alpha a}\right) - \frac{1}{\alpha a} \ln \frac{1}{\alpha a}$$

with the integral of a rate equation which expresses the rate of chemisorption as a function of time, *viz.*

$$\frac{dq}{dt} = \frac{k_0}{1 + \frac{k_0}{k} t}$$

and

$$q = k \ln\left(t + \frac{k}{k_0}\right) - k \ln \frac{k}{k_0}$$

Thus $k = 1/\alpha$ and $a = k_0$.

(8) H. A. Taylor and N. Thon, *J. Am. Chem. Soc.*, **74**, 4169 (1952).
(9) A. Meller, *Monatsh.*, **87**, 491 (1956).

THE CONDUCTANCES OF SOME ELECTROLYTES IN AQUEOUS SUCROSE AND MANNITOL SOLUTIONS AT 25°

BY JEAN M. STOKES AND R. H. STOKES

Contribution from the Chemistry Department of the University of New England, Armidale, New South Wales, Australia

Received October 21, 1957

In a previous paper,[1] the limiting conductances of a number of 1:1 electrolytes in 10 and 20% aqueous sucrose solutions at 25° were reported; the present work is a continuation of the investigation to other salts, another non-electrolyte, (mannitol), and to higher concentrations of sucrose.

Experimental

Purification of Materials.—Conductance-water prepared by distillation of the laboratory distilled water was used, without exclusion of carbon dioxide; its specific conductance was 1–1.3 × 10^{-6} ohm^{-1} cm.$^{-1}$. The potassium salts, sodium chloride, lithium chloride and silver nitrate were purified as previously described.[1] Sodium bromide was prepared from analytical reagent quality hydrobromic acid and sodium hydroxide, as recrystallization of commercial sodium bromide does not yield a product free from chloride. Magnesium chloride was analytical reagent used without further purification. Calcium chloride was prepared from analytical reagent calcium carbonate and hydrochloric acid. Lanthanum chloride was prepared from commercial material by precipitation as oxalate, ignition to oxide at 800°, and dissolution of the oxide in pure hydrochloric acid followed by centrifuging to remove excess oxide. The lanthanum chloride stock solution was analyzed for chloride by potentiometric titration, and diluted by weight to 0.1 *N*; at this concentration its equivalent conductance agreed with the values given by Longsworth and MacInnes,[2] Jones and Bickford,[3] and Spedding,[4] (who however do not all agree at lower concentrations). Tetra-*n*-amylammonium iodide was kindly supplied by Professor A. E. Martell; its limited solubility in water (less than 0.002 *N* at room temperature) gave rise to some difficulty in preparing solutions of accurately known composition, but potentiometric titration with silver nitrate gave a composition leading to equivalent conductances (in water) which agreed within 0.1% with the known ionic mobilities.[5] Hydrochloric acid was analytical reagent material suitably diluted and analyzed by determination of its conductance at 0.05 to 0.1 *N* with reference to the data of Shedlovsky. Wherever possible the purity of the various dry salts or stock solutions was checked by measuring the conductance of 0.1 *N* or 0.05 *N* solutions in water at 25° and comparing with accepted data, usually those of Shedlovsky[6]; in most cases agreement was better than 0.05%.

Sucrose was either best commercial loaf sugar (specific conductance of 20% solution ~ 8 × 10^{-6} ohm^{-1}cm.$^{-1}$) or British Drug Houses "AnalaR" sucrose (specific conductance of 20% solution 1.5–2 × 10^{-6} ohm^{-1}cm.$^{-1}$); the latter was used for the work on the higher valence type salts and tetra-*n*-amylammonium iodide, as it made possible measurements at higher dilutions. Mannitol was prepared from the commercial material (Colonial Sugar Refining Co.) by three recrystallizations from conductance-water followed by thorough drying; at 25° the specific conductance of the 10% solution was 1.5–3 × 10^{-6}ohm^{-1}cm.$^{-1}$.

Measurement of Resistances.—A Leeds and Northrup conductivity-bridge of Grinnell Jones' design was used in all measurements. Pyrex cells of the usual pattern, with leads well separated from the solution tubes, were employed for most of the work. In the case of silver nitrate in 10% mannitol, even the lightest coating of platinum black on the electrodes caused rapid reaction between the mannitol and the silver nitrate with the formation of a precipitate (presumably silver, since it was soluble in nitric acid but not in ammonia). For this salt and for certain other measurements in solutions below 0.01 *N* in electrolyte a flask-cell with bright platinum electrodes was therefore used, the resistance being extrapolated to infinite frequency. Where black electrodes were used, frequency-dependence in the range 500–2000 c./sec. was less than 0.01%; however if dilute solutions were studied with black electrodes the solution in the cell was renewed until constant resistance was obtained, in order to eliminate errors arising from adsorption on the electrodes. This effect was not significant at electrolyte concentrations above 0.01 *N*. All cells were maintained in an oil-thermostat held at 25 ± 0.002°, and were calibrated by means of the Jones and Bradshaw[7] 0.1 D. and 0.01 D. standards. Since the object of the work is comparison of conductances with already known values in water, the obsolete International Ohm units in which the latter are expressed were retained in the cell calibrations. In the case of hydrochloric acid in sucrose the effects of inversion were eliminated by taking a series of resistance readings at known times from the addition of the sucrose to the acid solution, and extrapolating back to zero time. The corrections involved did not exceed 0.1%.

Results

In general the upper limit of electrolyte concentration employed was between 0.05 and 0.1 *N*; the lower limit was dictated in large measure by the relatively high solvent conductances. For the alkali halides, a lower limit of 0.005 *N* was sufficient to give a satisfactory extrapolation to zero concentration, using the extrapolation-function of the previous paper,[1] though in several cases measurements were made down to 0.001 *N*. The nitrates, which (as in water) do not show as simple a concentration-dependence as the alkali halides, required measurements down to 0.001 *N*. Magnesium, calcium and lanthanum chlorides do not conform well to a simple extrapolation-function, and the steepness of the Λ *vs.* $\sqrt{c}$ plots requires measurements at concentrations down to 10^{-4} *N* or less to give a good extrapolation. These concentrations are not accessible with solvents of the conductances used here, so the following alternative method was used: the equivalent conductance at the concentration c was measured and its ratio to that of the same electrolyte at concentra-

(1) J. M. Stokes and R. H. Stokes, THIS JOURNAL, **60**, 217 (1956).
(2) L. G. Longsworth and D. A. MacInnes, *J. Am. Chem. Soc.*, **60**, 3070 (1938).
(3) G. Jones and C. F. Bickford, *ibid.*, **56**, 602 (1934).
(4) F. H. Spedding, *ibid.*, **74**, 2055 (1952).
(5) R. A. Robinson and R. H. Stokes, "Electrolyte Solutions," Butterworth's, London, 1955, p. 452.
(6) T. Shedlovsky, *J. Am. Chem. Soc.*, **54**, 1411 (1932); T. Shedlovsky and A. S. Brown, *ibid.*, **56**, 1066 (1934).
(7) G. Jones and B. C. Bradshaw, *ibid.*, **55**, 1780 (1933).

TABLE I

LIMITING EQUIVALENT CONDUCTANCES (Λ^0) IN AQUEOUS SUCROSE SOLUTIONS AT 25°, AND RATIO TO VALUES IN WATER $R = \Lambda^0$ (SUCROSE)/Λ^0 (WATER) (SEE NOTE *a*)

Wt. % sucrose	10		20		40		60	
Viscosity, poise[b]	0.01179		0.01699		0.05171		0.4373	
Density, g. ml.$^{-1}$	1.03679		1.07940		1.17462		1.28413	
Dielectric constant	76.20		73.66		67.72		60.19	
	Λ^0	R	Λ^0	R	Λ^0	R	Λ^0	R
$MgCl_2$	103.96	0.8034	79.09	0.6112	....	....	...	....
$CaCl_2$	108.97	.8021	83.00	.6110	....	....	...	....
$LaCl_3$	116.36	.7967	87.72	.6006	....	....	...	....
$N(n\text{-Am})_4I$	74.5	.790	56 0	.594	....	....	...	....
HCl[c]	356.5	.8365	278.4	.6533	155.6	0.365	...	...
KCl[d]	121.87	.8135	94.26	.6292	44.02	.2937	10.48	0 0699
$KClO_4$	113 81	.8080	87.23	.6193	....	....		

[a] Λ^0 in International ohm^{-1} cm.^{2} equiv.$^{-1}$. [b] Viscosities from Bingham and Jackson, *Bull. Bur. Stands.*, **14**, 59 (1918-1919), but multiplied by 0.997 to convert to the new standard value of 0.01032 poise for water at 20° given by Swindells, Coe and Godfrey, *J. Research Natl. Bur. Standards*, **48**, 1 (1952). [c] Measurements by L. A. Woolf in this Laboratory. [d] 10 and 20% data from ref. 1; 40 and 60% by L. A. Woolf.

tion c in water was calculated. The resulting ratios for a series of concentrations were extrapolated linearly to zero concentration. This procedure is illustrated for magnesium chloride in 20% sucrose in Fig. 1, from which it is clear that the extrapolated ratio is not likely to be in error by as much as 0.1%. The same ratio-plotting procedure was used to confirm the Λ^0 values obtained by the extrapolation-function method for the 1:1 electrolytes.

Since the individual measurements are too numerous to report in full, only the limiting equivalent conductances and their ratios to the corresponding values in water are given in Tables I and II.

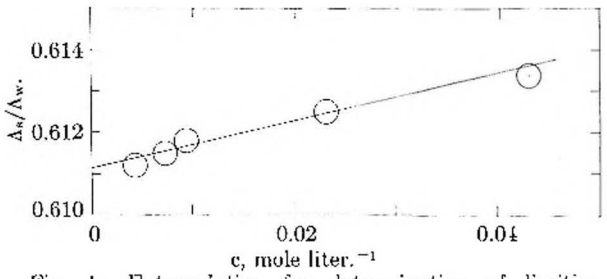

Fig. 1.—Extrapolation for determination of limiting conductance ratio of magnesium chloride in 20% sucrose and water at 25°. Λ_s = equivalent conductance in 20% sucrose at concentration *c*; Λ_w = equivalent conductance in water at concentration *c*. Diameter of circles = 0.1% in Λ.

Discussion

In the previous paper[1] it was noted that in a given solvent the ratio $R = \Lambda^0$(solvent)/Λ^0(water) is to a first approximation independent of the electrolyte. The new results reported here for 10 and 20% sucrose solutions make it clear that this is merely because all the electrolytes studied in the previous paper had simple and comparatively small ions; with the larger ions of magnesium, calcium, lanthanum and tetraamylammonium considerable variations are apparent. As the ion size increases, the R values move nearer to the ratio of the fluidities of the solvent and water which are 0.756 for 10% sucrose and 0.525 for 20% sucrose. This behavior is consistent with the expectation that large ions will encounter a resistance more nearly proportional to the solvent viscosity, as implied by Walden's rule. The results for hydrochloric acid in both sucrose and mannitol solutions show clearly that the hydrogen ion is considerably less affected by increased viscosity than are other ions. The results for the other 1:1 electrolytes in 10% mannitol are similar to those in 10% sucrose. The limiting conductance of a particular electrolyte is however not simply a function of the solvent viscosity, for a graph of Λ^0_{KCl} *versus* relative viscosity shows that the line through the 0, 10 and 20% sucrose data lies about 1% above the point for 10% mannitol. In the very concentrated sucrose solutions the departure from Walden's rule becomes several hundred per cent.; thus for KCl the relative values of the Walden product $\Lambda^0\eta$ in water, 10, 20, 40 and 60% sucrose are, respectively, 1, 1.076, 1.200, 1.705, 3.430. However, the corresponding values of the empirical function $\Lambda^0\eta^{0.7}$ are 1, 0.991, 0.988, 1.007 and 1.067, so that even at a viscosity 50 times that of water the latter function varies by only 7%.

In a forthcoming paper transport number measurements will be presented, making possible a more detailed discussion on the basis of individual ion mobilities.

TABLE II

LIMITING CONDUCTANCES OF ELECTROLYTES IN 10% AQUEOUS MANNITOL SOLUTIONS AT 25°

Solvent properties; d = 1.03256 g. ml.$^{-1}$[a]; ϵ = 77.12[b]; η = 0.01192 poise[c]

Electrolyte	Λ^0	$R = \frac{\Lambda^0 \text{ mannitol}}{\Lambda^0 \text{ water}}$
KCl	119 70	0.7988
KBr	120 90	.7973
KI	119.48	.7947
KNO_3	116.03	.800
NaCl	100.75	.7967
NaBr	102.05	.7958
LiCl	91.25	.7933
$AgNO_3$	105.70	.7926
HCl	353.9	.8304

[a] This research. [b] G. Åkerlöf, *J. Am. Chem. Soc.*, **54**, 4133 (1932). [c] This research. Viscosity of water at 25° taken as 0.00891 poise—see note *b* of Table I.

Acknowledgments.—We wish to thank Professor A. E. Martell for the sample of tetra-*n*-amylam-

monium iodide, and Mr. L. A. Woolf for the measurements in 40 and 60% sucrose solutions.

LOW TEMPERATURE HEAT CAPACITY, ENTROPY AT 298.15°K., AND HIGH TEMPERATURE HEAT CONTENT OF Mo_3Si

BY E. G. KING AND A. U. CHRISTENSEN, JR.

Minerals Thermodynamics Experiment Station, Region II, Bureau of Mines, United States Department of the Interior, Berkeley, California

Received November 2, 1957

Metallic silicides have received almost no attention as regards determinations of heat capacity, entropy and heat content. The literature contains no low temperature heat capacity values and no well-grounded entropies. The heat content above 298°K. of only one substance, a molybdenum silicide ($MoSi_2$), has been measured previously.[1-3] The present paper reports heat capacity measurements between 51 and 298°K., the entropy at 298.15°K., and high temperature heat content measurements to 1451°K. of another molybdenum silicide (Mo_3Si).

Material.—The molybdenum silicide for this work was furnished by Prof. A. W. Searcy, Division of Mineral Technology, University of California. It was prepared in several batches by direct reaction of powdered molybdenum and silicon at 1900° *in vacuo*, using molybdenum containers. The batches were ground to −100 mesh and thoroughly mixed; the composite sample was analyzed. The results were 91.25% molybdenum and 8.24% silicon, as compared with the theoretical 91.11 and 8.89%. The 0.51% difference between this analysis and 100% was assumed to be principally oxygen. The X-ray diffraction pattern indicated no impurity other than a very small amount of Mo_5Si_3 phase. For the purpose of this paper, the substance was treated as if it had the composition $Mo_3Si_{0.925}O_{0.075}$ (which conforms with the analyses for molybdenum and silicon and accounts for most of the deficit from 100%), and the molecular weight was taken accordingly as 315.03. (The molecular weight of the pure compound is 315.94.)

Low Temperature Heat Capacity.—The heat capacity from 51 to 298°K. was measured with previously described apparatus.[4] A 544.69-g. sample of the silicide was used. No correction of the heat capacity data for the oxygen content of the substance was attempted, other than the adjustment in molecular weight as indicated above. The experimental results, expressed in defined calories (1 cal. = 4.1840 abs. joules) per deg. mole, are listed in Table I. (The 298.15°K. value is an extrapolation.) The substance behaved normally at all temperatures and the heat capacity curve is entirely regular.

Entropy at 298.15°K.—The entropy increment for the interval 51–298.15°K. was calculated by Simpson-rule integration of a plot of C_p against log T; this gave 23.82 cal./deg. mole. The entropy increment for the interval 0–51°K. was obtained by extrapolation, using the empirical Debye and Einstein function sum, $D(222/T + 3E(364/T)$, which fits the experimental heat capacity data between 51 and 240°K., with a maximum deviation of 1.5%. The extrapolated portion of the entropy is 1.42 cal./deg. mole, making a total of 25.24 cal./deg. mole for 298.15°K. Latimer's[5] rule was used to correct the 298.15°K. value for the oxygen content of the silicide. The correction is $\Delta S = 3/2R \times 0.075$ in 28.09/16.00 = 0.13 cal./deg. mole. The entropy of pure Mo_3Si is $S^0_{298.15} = 25.4$ cal./deg. mole, in which the uncertainty is estimated as ± 0.2.

TABLE I

HEAT CAPACITY (CAL./DEG. MOLE)

T, °K.	C_p	T, °K.	C_p	T, °K.	C_p
53.67	3.844	114.88	13.06	216.19	20.03
57.86	4.440	124.50	14.13	226.32	20.34
62.71	5.253	136.08	15.28	236.15	20.70
67.50	6.084	145.57	16.13	245.62	20.97
72.18	6.882	155.87	16.92	256.35	21.27
76.97	7.678	165.64	17.57	266.64	21.54
80.38	8.243	175.81	18.17	276.14	21.73
84.57	8.903	186.45	18.76	286.38	21.95
94.56	10.42	195.83	19.17	295.99	22.19
104.93	11.85	206.06	19.66	298.15	(22.22)

Heat Content above 298.15°K.—The high temperature heat content measurements also were made with previously described apparatus,[4] using a 28.863-g. sample of the silicide. A platinum–rhodium capsule, the heat content of which was determined beforehand, was used to hold the substance during the measurements. The capsule was filled, the air evacuated and replaced by helium, and the neck sealed gas-tight by platinum welding. Measurements to 1451°K. were made with no apparent attack of the capsule by the silicide. At higher temperatures, however, the capsule was seriously attacked, and measurements were discontinued. The furnace thermocouple was calibrated five times and the calorimeter four times during the course of the measurements.

The experimental heat content results, expressed in defined calories per mole, are in Table II. No correction for the oxygen impurity has been applied other than the adjustment in molecular weight mentioned previously. These results plot to give a regular heat content temperature curve, which is quite similar to that obtained by Douglas and Logan[1] for $MoSi_2$, as may be shown by taking ratios of the heat contents of Mo_3Si and $MoSi_2$. The ratio is 1.415 at 600°K., 1.410 at 900°K., and 1.401 at 1200°K.

TABLE II

HEAT CONTENT (CAL./MOLE)

T, °K.	$H^0_T - H^0_{298.15}$	T, °K.	$H^0_T - H^0_{298.15}$	T, °K.	$H^0_T - H^0_{298.15}$
400.0	2,320	903.3	14,780	1203.5	22,680
501.8	4,730	1003.6	17,350	1252.5	24,060
597.6	7,040	1004.3	17,330	1303.2	25,480
601.9	7,140	1102.0	19,910	1350.7	26,810
648.2	8,280	1102.0	19,890	1401.6	28,240
700.8	9,610	1148.5	21,140	1450.7	29,740
798.6	12,090				

Table III gives smooth values of the heat con-

(1) T. B. Douglas and W. M. Logan, *J. Research Natl. Bur. Standards*, **53**, 31 (1954).

(2) C. T. Ewing and B. E. Baker, WADC Tech. Report 54-185, Part 1, 1954.

(3) B. E. Walker, J. A. Grand and R. R. Miller, THIS JOURNAL, **60**, 231 (1956).

(4) K. K. Kelley, B. F. Naylor and C. H. Shomate, U. S. Bur. Mines Tech. Paper 686, 1946.

(5) W. M. Latimer, *J. Am. Chem. Soc.*, **43**, 818 (1921); **73**, 1480 (1951).

tent and entropy increments above 298.15°K., for use in thermodynamic calculations.

TABLE III

SMOOTH VALUES OF HEAT CONTENT (CAL./MOLE) AND ENTROPY (CAL./DEG. MOLE) INCREMENTS ABOVE 298.15°K.

T, °K.	$H_T - H_{298.15}$	$S_T - S_{298.15}$	T, °K.	$H_T - H_{298.15}$	$S_T - S_{298.15}$
400	2,320	6.69	1000	17,250	29.29
500	4,670	11.93	1100	19,870	31.78
600	7,090	16.34	1200	22,580	34.14
700	9,580	20.17	1300	25,370	36.37
800	12,120	23.56	1400	28,240	38.50
900	14,680	26.58	1500	31,190	40.53

The heat content values in Table III are represented, with an average deviation of 0.2%, by the equation

$$H_T - H_{298.15} = 21.98T + 2.29 \times 10^{-3}T^2 + 1.00 \times 10^5 T^{-1} - 7092$$

THE EFFECT OF QUINOLINE AND ITS DERIVATIVES ON MALONIC ACID

BY LOUIS WATTS CLARK

Department of Chemistry, Saint Joseph College, Emmitsburg, Maryland

Received November 16, 1957

In studies by Fraenkel, *et al.*,[1] on the decarboxylation of malonic acid in quinoline–dioxane mixtures varying from 0.27 to 4.24 *M* quinoline concentration, a first-order dependence upon quinoline of the rate of reaction in dioxane was demonstrated. Furthermore, at least near 100°, Fraenkel's quinoline concentration–rate constant data extrapolate to a pure quinoline value not too different from that observed (allowance being made for the change in character of solvent in going from dioxane–quinoline mixtures to pure quinoline). On the basis of these results Fraenkel, *et al.*, formulated a possible mechanism for the reaction. The proposed mechanism involves the formation of a transition complex between the un-ionized diacid and the unshared pair of electrons on the nitrogen atom of the quinoline molecule, facilitating cleavage of the malonic acid. Evidence for the validity of this proposed mechanism has accrued from studies in this Laboratory on the decarboxylation of malonic acid in twenty-eight additional, non-ionizing, basic type solvents.[2] The enthalpy of activation of the reaction in different solvents has been shown to decrease with an increase in the effective negative charge on the nucleophilic atom of the solvent, a result to be expected from the principle that an increase in the attraction between two reagents causes a decrease in the activation energy.[2a,3] It was subsequently observed that the data for the decarboxylation of malonic acid in quinoline obtained by Fraenkel, *et al.*,[1] did not appear to be in harmony with the foregoing principle. The conclusion was that the principle was not valid in this case, or a discrepancy existed in the kinetic data.

(1) G. Fraenkel, R. L. Belford and P. E. Yankwich, *J. Am. Chem. Soc.*, **76**, 15 (1954).

(2) (a) L. W. Clark, THIS JOURNAL, **62**, 79 (1958); (b) **62**, 368 (1958).

(3) K. J. Laidler, "Chemical Kinetics," McGraw–Hill Book Co., Inc., 1950, New York, N. Y., p. 138.

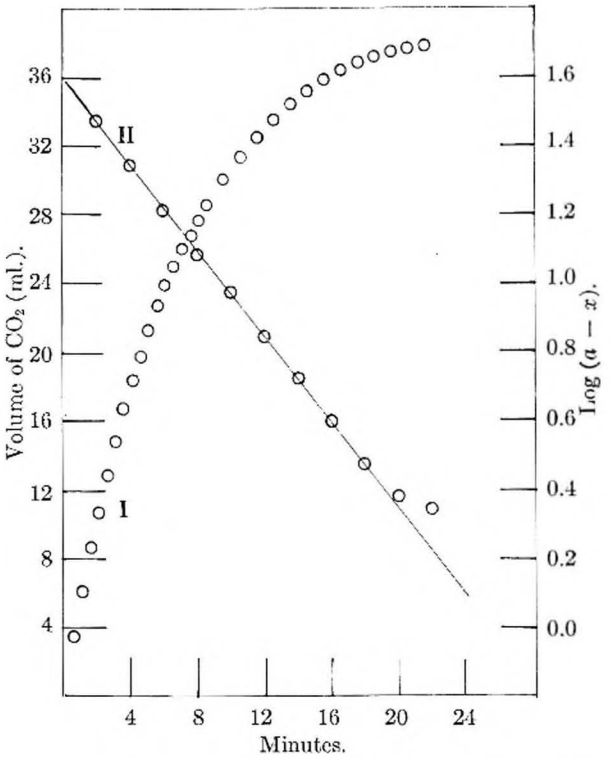

Fig. 1.—Decomposition of 0.1857 g. of malonic acid in 50 ml. of quinoline at 117.86° (cor.): I, volume of CO_2 (ml.); II, log $(a - x)$.

It was therefore decided to carry out further kinetic studies on the decarboxylation of malonic acid in quinoline in this Laboratory to determine whether or not the principle was valid for quinoline also. It was thought to be of interest also to study the reaction in several quinoline derivatives. Results of this investigation are reported herein.

Experimental

Reagents.—(1) Malonic acid, 100.0% assay, was used in these experiments. (2) Solvents: (a) quinoline, Reagent grade, b.p. 235–237°; (b) 6-methylquinoline, highest purity grade, b.p. 129–130° (15 mm.); (c) 8-methylquinoline, highest purity grade, b.p. 112–114° (8 mm.). Each sample of each solvent was distilled at atmospheric pressure directly into the dried reaction flask immediately before the beginning of each experiment.

Apparatus and Technique.—The kinetic experiments were conducted in a constant-temperature oil-bath (±0.1°) by the technique previously described.[4] Temperatures were determined by means of a thermometer calibrated by the

TABLE I

APPARENT FIRST-ORDER RATE CONSTANTS FOR THE DECOMPOSITION OF MALONIC ACID IN VARIOUS AMINES

Solvent	Temp. (°C. cor.)	$k \times 10^4$ (sec.$^{-1}$)
Quinoline	104.52	7.03
	107.70	9.50
	112.63	15.15
	117.86	24.55
6-Methylquinoline	100.34	5.71
	111.86	16.95
	115.60	24.16
8-Methylquinoline	109.68	4.10
	111.33	4.70
	121.58	11.18

(4) L. W. Clark, THIS JOURNAL, **60**, 1150 (1956).

TABLE II

KINETIC DATA FOR THE DECOMPOSITION OF MALONIC ACID IN VARIOUS AMINES

Solvent	E^* (cal.)	A (sec.$^{-1}$)	$\Delta H^{\ddagger}$ (cal.)	$\Delta S^{\ddagger}$ (e.u.)	$\Delta F^{\ddagger}_{140}$ (cal.)	$k_{140} \times 10^6$ (sec.$^{-1}$)
Aniline[2b]	28,100	4.16×10^{12}	26,900	− 4.45	28,750	500
Quinoline	27,360	5.42×10^{12}	26,740	− 2.37	27,720	1607
6-Methylquinoline	26,970	3.91×10^{12}	26,350	− 3.02	27,600	1871
8-Methylquinoline	25,180	1.08×10^{11}	24,440	−10.47	28,760	462

U. S. Bureau of Standards. In each experiment a 0.1857-g. sample of malonic acid (the amount required to produce 40.0 ml. of CO_2 at STP on complete reaction) was introduced in the usual manner into the reaction flask containing 50.0 ml. of solvent saturated with dry CO_2 gas.

Results and Discussion

The decomposition of malonic acid in the three solvents studied was quantitative and first order, as shown by a typical example in Fig. 1. In Table I the apparent first-order rate constants, obtained from the slope of line II in Fig. 1 in each case, are listed for the different solvents at the various temperatures studied. Straight lines were obtained when log k was plotted against $1/T$ in the case of each solvent as shown in Fig. 2. The parameters of the Arrhenius and the Eyring equations for the reaction in the three solvents studied are listed in Table II. The data for aniline are included for comparison.

Since quinoline is slightly more basic than aniline (the ionization constant for quinoline is 6.3×10^{10}, for aniline 3.8×10^{-10})[5] one would expect that the enthalpy of activation for the reaction in quinoline should be lower than that in aniline on the basis of the principle that an increase in the effective negative charge on the nucleophilic atom of the solvent should result in a lowering of $\Delta H^{\ddagger}$. The results shown in Table II, lines 1 and 2, are in good agreement with this expectation, and tend to substantiate the validity of the foregoing principle. The kinetic data for the decomposition of malonic acid in quinoline previously reported[1] appear, therefore, to be discrepant.

The effect of substituent groups on the reaction is demonstrated by the data in lines 3 and 4 of Table II. If a methyl group is placed on the 8-position in quinoline one would expect an increase in basicity, due to the positive inductive effect, and at the same time a large decrease in the entropy of activation due to the steric effect. These predictions are completely realized (line 4 of Table II). The increase in basicity is demonstrated by the decrease in the activation energy, and the steric hindrance is revealed by the large decrease in $\Delta S^{\ddagger}$. The rate at 140° in 8-methylquinoline is less than 1/3 as great as in quinoline.

If a methyl group is placed in the 6-position on quinoline one would expect very little added steric effect. Furthermore, with the methyl group so far removed from the nitrogen atom, one would not expect the positive inductive effect to be as pronounced as in the case of 8-methylquinoline. Both these predictions are borne out by the data (line 3 of Table II). The methyl group in the 6-position causes only a very slight decrease in the activation energy as well as in the entropy of activation. The rate at 140° is considerably faster in 6-methylquinoline than it is in quinoline.

(5) "Lange's Handbook of Chemistry," 9th edition, 1956, Handbook Publishers, Inc., Sandusky, Ohio, p. 1202.

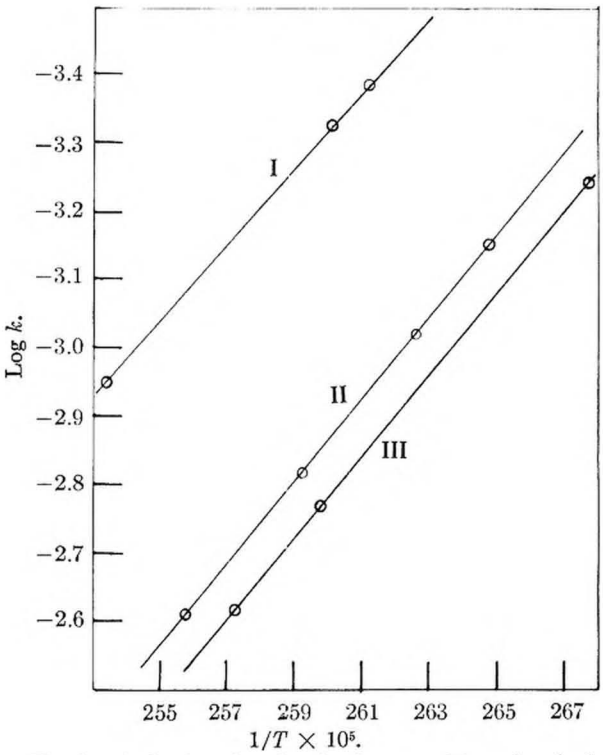

Fig. 2.—Arrhenius plots for the decomposition of malonic acid in: I, 8-methylquinoline; II, quinoline; III, 6-methylquinoline.

Acknowledgments.—The support of this research by the National Science Foundation, Washington, D. C., is gratefully acknowledged. Valuable assistance was rendered by Miss Dolores Sicilia in purification of the reagents and running the kinetics experiments.

REACTIONS OF METHYL RADICALS WITH WATER ON QUARTZ AND PYREX SURFACES[1]

BY P. AUSLOOS AND J. PACLSON

Department of Chemistry, University of Rochester, Rochester, N. Y.

Received November 20, 1957

The photolysis and radiolysis of acetone-d_6 have been investigated briefly in the presence of H_2O. The results of runs carried out under various conditions of temperature, intensity and concentration are given in Table I. The photolysis runs were

(1) This research was supported in part by the United States Air Force through the Air Force Office of Scientific Research of the Air Research and Development Command, under Contract No. AF18-(600)1528, and in part by the Atomic Energy Commission. Reproduction in whole or in part is permitted for any purpose of the United States Government.

TABLE I

Cell	Temp., °C.	CD_3COCD_3 molec./cc.	H_2O 10^{-18}	CO molec./cc./sec. 10^{-17}	C_2D_6	$(CD_3H)/(CD_4)$	$(CD_4)/(C_2D_6)^{1/2}(A)$ molec.$^{-1/2}$ cm.$^{3/2}$ sec.$^{-1/2}$ 10^{18}	$(CD_3H)/(C_2D_6)^{1/2}$ molec.$^{1/2}$ cm.$^{-1/2}$ sec.$^{-1/2}$ 10^{-3}
				Photolysis				
Quartz	30	6.3	0.095	1.85	2.05	0.206	1.88	2.44
Quartz	30	1.61	.095	0.84	0.99	.905	1.92	2.98
Quartz	63	1.58	.03	3.87	3.85	.535	7.35	6.38
Quartz	63	1.58	.095	4.02	3.95	.463	7.21	5.40
Quartz	63	1.58	.285	3.95	3.84	.550	7.40	6.60
Quartz	92	6.3	.095	317	317	.186	22.0	25.4
Quartz	92	0.95	.095	67	69	.955	23.0	23.4
Quartz	92	.95	.095	5.40	5.23	1.02	24.0	23.8
Pyrex	118	.95	.095	250	205	0.92	64.5	56.2
Pyrex	195	.95	.095	260	211	.58	528	295
Pyrex	92	.95	.000	66.0	67.0	.00	23.4	0.00
Pyrex[a]	63	1.58	.095	4.07	3.77	.04	7.3	0.46
Quartz[a]	63	1.58	.095	3.95	3.90	.07	7.36	0.81
				Radiolysis				
Pyrex	27	6.3	0.006	0.337	0.30	0.275	4.05	11.4
Pyrex	48	6.3	.006	.367	.22	0.90	10.1	91.0
Pyrex	110	6.3	.006	.42	.077	1.66	27.0	450
Pyrex	150	6.3	.006	.462	.042	0.00	128	0.00

[a] Cells flamed out.

done mainly in a cylindrical quartz cell (10 cm. long, 5 cm. diameter) which had been treated with nitric and chromic acids and washed with distilled water. The Pyrex cells (4 cm. long, 5 cm. diameter) used in the radiolyses and photolyses had not been treated with any reagents, including water. A few runs were made using cells which had been thoroughly flamed out before introducing the acetone and water.

The photolyses were carried out with a Hanovia (16A-13) SH type medium pressure lamp. A Pyrex filter was used to cut off short wave length radiation. The intensity was varied by means of copper screens. A cobalt-60 γ-ray source of about 485 curies was used for the radiolyses.

The cells were filled by expanding acetone-d_6 vapor into the cell to known pressure, closing off the cell, and then expanding water vapor to a known pressure into a known volume. This water vapor was condensed into the cell at $-195°$ and the cell sealed off.

Acetone-d_6 was obtained from Merck Co. of Canada and was found by mass spectrometric analysis to be 99.5% deuterated.

Analysis of the CD_4 and CD_3H products was performed using a Consolidated model 21-620 mass spectrometer. The rates of formation of CD_3H were corrected for CD_3H formed by abstraction of a hydrogen atom from incompletely deuterated acetone. This correction amounted to roughly 6% of the CD_4 formed.

The following observations summarize the data of Table I: 1. CD_3H is only formed when H_2O is present. Substantial amounts of CD_3H are formed even when H_2O is present in concentrations less than 0.1 mole %. 2. CD_3H/CD_4 is independent of the H_2O concentration. 3. $CD_3H/C_2D_6^{1/2}$ is practically independent of the acetone and H_2O concentrations and increases with temperature. 4. In the radiolysis experiments CD_3H/CD_4 falls off drastically at temperatures above 110°. No such decrease was observed in the photolysis runs at temperatures up to 195°. The H_2O concentrations were, however, appreciably higher in the latter case. 5. Flaming out the Pyrex and quartz cells results in a substantial decrease of CD_3H/CD_4.

These facts indicate that CD_3H is formed on the surface. Abstraction of an H-atom by CD_3 from an H_2O molecule absorbed on the wall is the most likely explanation. It is not clear however why practically no CD_3H is formed in cells which have been flamed out before introducing the acetone-d_6–water mixtures.

An alternative possibility, such as a reaction between an electronically excited acetone molecule

$$CD_3COCD_3^* + H_2O = CD_3H + CD_3COOH$$

and an H_2O molecule is unlikely in view of the fact that in the radiolysis experiments the decrease of CD_3H at high temperatures is not accompanied by an increase of the rate of formation of carbon monoxide.

The independence of $CD_3H/C_2D_6^{1/2}$ with acetone concentration and intensity indicates that under these experimental conditions all CD_3 radicals reach the wall and that abstraction on the surface and recombination are two competing reactions.

Values of log $CD_4/C_2D_6^{1/2}$ (A) for the runs done at 118 and 195° lie close to the Arrhenius plot given by Whittle and Steacie.[2] The low temperature runs however gave values which lie well above the extrapolated Arrhenius curve. It previously has been suggested[3] that the analogous curvature found in the photolysis of CH_3COCH_3 may be due to a reaction between methyl radicals and acetone molecules absorbed on the wall.

Acknowledgments.—The authors wish to thank Professor W. Albert Noyes, Jr., and Professor Edwin O. Wiig for discussion and criticism of this work.

(2) E. Whittle and E. W. R. Steacie, *J. Chem. Phys.* **21**, 993 (1953).

(3) P. Ausloos and E. W. R. Steacie, *Can. J. Chem.*, **33**, 47 (1955).

THE COÖRDINATION OF COPPER(II) WITH 1,3-DIAMINO-2-PROPANOL

BY CHARLES R. BERTSCH, B. P. BLOCK AND W. CONARD FERNELIUS

Department of Chemistry, the Pennsylvania State University, University Park, Pa.

Received November 22, 1957

The coördination of 1,3-diamino-2-propanol (BOH) with copper(II) ion is unique in that $\bar{n}$ (the average number of ligands bound per ion) appears to be 1:5.[1] Two possible explanations of such an anomalous value are indicated in the equations

$$2Cu^{++} + 3BOH \rightleftarrows Cu_2(BOH)_3^{4+} \quad (1)$$

$$2Cu^{++} + 3BOH \rightleftarrows 2Cu(BO)^{+} + H_2BOH^{2+} \quad (2)$$

The second is suggested by the isolation[2] of compounds containing a complex of the formula $Cu(BO)_2^{+}$. The system has been investigated in dilute solution by methods previously described and earlier findings confirmed. Calculations on the basis of the first equation did not yield constant values while those based on the second equation did.

Method of Calculation.—If V = volume of solution being titrated at any given point, V_i = the initial volume of solution, $C_{Cu^{++}}$ and C_{H^+} = concentration of Cu^{++} and H^+ in the initial solution, and C_A = concentration of the amine solution added, then the equation for the H^+ balance in the system $Cu^{++} + BOH \rightleftarrows Cu(BO)^{+} + H^+$ is

$$[H^+]V = V_iC_{H^+} + [OH^-]V - [HBOH^+]V - 2[H_2BOH^{++}]V + [CuBO^+]V \quad (3)$$

and

$$\bar{n} = \frac{(V - V_i)C_A - ([BOH] + [HBOH^+] + [H_2BOH^{++}])V}{V_iC_{Cu^{++}}} \quad (4)$$

The numerator of this expression is evaluated with the use of $\bar{n}_A$, the average number of protons bound per *uncoördinated* ligand

$$\bar{n}_A = \frac{([HBOH^+] + 2[H_2BOH^{++}])V}{([BOH] + [HBOH^+] + [H_2BOH^{++}])V} \quad (5)$$

Substitution of (3) into (5) and the result into (4) yields

$$\bar{n} = \frac{(V - V_i)C_A - \dfrac{V_iC_{H^+} + V([OH^-] - [H^+] + [CuBO^+])}{\bar{n}_A}}{V_iC_{Cu^{++}}} \quad (6)$$

This equation may be rearranged to the form

$$\bar{n} = \frac{(V - V_i)C_A - \dfrac{V_iC_{H^+} + V([OH^-] - [H^+])}{\bar{n}_A}}{V_iC_{Cu^{++}}} - \frac{V[CuBO^+]}{V_iC_{Cu^{++}}\bar{n}_A} \quad (7)$$

Equation 7 now contains the quantity originally used to calculate $\bar{n}$ on the assumption that a simple, step-wise process was occurring. If we call this quantity $\bar{n}_B$ and recognize that $\bar{n}_A = 2$ throughout the *p*H range of chelation, then equation 7 becomes

$$\bar{n} = \bar{n}_B - \frac{v[CuBO^+]}{2(V_iC_{Cu^{++}})} \quad (8)$$

However, if we assume that $CuBO^+$ is the only coördinated species present

$$\bar{n} = \frac{V[CuBO^+]}{V_iC_{Cu^{++}}}$$

and equation 8 can be converted to

$$\bar{n} = 2/3\bar{n}_B \quad (9)$$

This results in a maximum $\bar{n}$ of 1 rather than the anomalous value of 1.5 previously reported, a result which is consistent with the assumption that $CuBO^+$ is the only coördinated species present.

The calculation of [BOH] from equation 3 requires the elimination of $[CuBO^+]$. Since $\bar{n}_A$ remained at 2 throughout the chelation range, the concentrations of BOH and $HBOH^+$ are small, and all the 1,3-diamino-2-propanol is essentially present as either $CuBO^+$ or H_2BOH^{++}. Consequently

$$(V - V_i)C_A = ([CuBO^+] + [H_2BOH^{++}])V \quad (10)$$

and equation 3 becomes

$$[H^+]V = V_iC_{H^+} + [OH^-]V - 3[H_2BOH^{++}]V + (V - V_i)C_A \quad (11)$$

$[H_2BOH^{++}]$ is the only unknown in equation 11 and may therefore be calculated directly. From this concentration $[CuBO^+]$ follows from equation 10 and [BOH] and $[HBOH^+]$ from the proton-1,3-diamino-2-propanol constants reported elsewhere.[3] The values found are negligible with respect to $[CuBO^+]$ and $[H_2BOH^+]$ and validate the assumptions made. The remaining concentration, $[Cu^{++}]$, needed in order to calculate the equilibrium constant for

$$Cu^{++} + BOH \rightleftarrows CuBO^+ + H^+ \quad (12)$$

follows from $V_iC_{Cu^{++}} = ([Cu^{++}] + [CuBO^+])V$.

Results and Discussion

The values of this constant over the temperature range 10–40°, with 95%-confidence intervals based on at least three independent calculations, and the thermodynamic quantities derived from them are presented in Table I.

TABLE I

VALUES FOR THE EQUILIBRIUM CONSTANT AND THERMODYNAMIC QUANTITIES FOR EQUATION 12

	10°	20°	30°	40°
log K	3.72 ± 0.03	3.64 ± 0.03	3.57 ± 0.17	3.34 ± 0.07
ΔF	−4.9	−4.9	−5.0	−4.8
ΔH		−5.2		
ΔS	−1	−1	−1	−1

The ligand is apparently terdentate, and only one adds per Cu^{++} in the concentration range investigated. Since the activity of the hydrogen ion enters into the equilibrium constant (see equation 12), the values of the constant are not strictly comparable with formation constants for the usual step-wise processes. However, ΔH reflects energy changes in bond formation, by and large,[4] which permits some rough comparisons to be made. Generally in going from a bidentate to a terdentate ligand the value of $-\Delta H$ increases. In this case

(1) E. Gonick, W. C. Fernelius and B. E. Douglas, *J. Am. Chem. Soc.*, **77**, 6506 (1955).

(2) J. G. Breckenridge and J. W. Hodgins, *Can. J. Research*, **17**, 331 (1939).

(3) C. R. Bertsch, W. C. Fernelius and B. P. Block, THIS JOURNAL **62**, 444 (1958).

(4) C. G. Spike and R. W. Parry, *J. Am. Chem. Soc.*, **75**, 2726 (1953).

$-\Delta H$ for the addition of 1,3-propanediamine to Cu^{++} is much larger[3] than for the reaction indicated by (12). Lotz[5] has reported that polyamines containing oxygen are not bound as strongly as corresponding amines containing no hetero atom, and this effect would be reflected in the enthalpy change. Another factor influencing the value of ΔH, is the fact that if the 1,3-diamino-2-propanol is acting terdentate it cannot form a planar configuration, therefore the copper ion is present in a forced non-planar configuration and is not as strongly bound as it would be in a planar configuration. It has been found that the $-\Delta H$ value for the formation of the copper chelate with 2,2′,2″-triaminotriethylamine is only slightly greater than the usual $-\Delta H_1$ values for chelation of copper ion with bidentate ligands, although 2,2′,2″-triaminotriethylamine has four available donor atoms, and this is attributed to the copper ion being forced into a non-planar configuration.[3] Furthermore, the $-\Delta H$ value for $CuBO^+$ would be expected to be low because an oxygen–hydrogen bond is ruptured during its formation.

The ΔS value for the formation of the copper chelate with 1,3-diamino-2-propanol is of the same order of magnitude as the corresponding value for the formation of the copper chelate with 1,3-propanediamine. The fact that the oxygen atom of the 1,3-diamino-2-propanol takes part in the chelation would be expected to increase the entropy change, since the number of rings in the chelate structure is increased. This is probably offset by an entropy decrease caused by the forced non-planar configuration.

Acknowledgment.—The authors gratefully acknowledge financial support furnished for this work by the United States Atomic Energy Commission through Contract AT(30-1)-907.

(5) J. R. Lotz, Ph.D. Thesis, The Pennsylvania State University, 1954.

OUT-OF-PLANE HYDROGEN VIBRATIONS IN SOME HIGHLY SUBSTITUTED NAPHTHALENES

By Robert W. Bayer and Edward J. O'Reilly, Jr.

Department of Chemistry, University of North Dakota, Grand Forks, North Dakota

Received November 22, 1957

The infrared spectra of several naphthalenes substituted in the α-positions have been observed in this Laboratory. The spectra in the region 1000–650 cm.$^{-1}$ are listed in Table. I. Five of these compounds, 1,5-dibromo-4,8-diiodonaphthalene, 4-bromo-1,5-diiodonaphthalene, 1,4,5,8-naphthalene-d_4 and 1,4-naphthalene-d_2, have at least one set of two adjacent hydrogens and the 1,2,3,-4-tetra-substituted benzene structure. The intense absorption at 823 cm.$^{-1}$ in the spectra of the above halogen compounds is in agreement with the generally accepted range of 800–860 cm.$^{-1}$ for the absorption corresponding to the out-of-plane vibration of two adjacent hydrogen atoms on a benzene nucleus.[1] The intense absorption at 874 cm.$^{-1}$ in the spectra of the deuterium compounds is on the high side of this range. This behavior, however, seems fairly common in the spectra of deuteronaphthalenes.[2] An analysis of the spectra of naphthalene, naphthalene-d_8 and 1,4,5,8-naphthalene-d_4, shows that the 874 cm.$^{-1}$ absorption is in fact associated with the out-of-plane bending vibration of the hydrogen atoms.

In the 1,4-bromo- and 1,4-dideuteronaphthalene spectra, the frequencies associated with the out-of-plane vibrations of the four adjacent hydrogen atoms are 760 and 771 cm.$^{-1}$, respectively, in agreement with the accepted range of 735–770 cm.$^{-1}$. The three adjacent hydrogens in the 4-bromo-1,5-diiodonaphthalene and 1-bromo-5-iodonaphthalene spectra are undoubtedly the cause of the intense absorptions at 796 and 791 cm.$^{-1}$, in agreement with the accepted region of 750–810 cm.$^{-1}$. The second components in the region of 680–725 cm.$^{-1}$ are located at 694 and 692 cm.$^{-1}$.

Table I

Infrared Absorption Peaks of Some Substituted Naphthalenes in CS_2 Solution

1-Br-5-I	1,4-Br_2	4-Br-1,5-I_2	1,5-Br_2-4,8-I_2	1,4-I_2[a]	1,4,5,8-d_4[a]
	962vs	951vs	963vs	946m	
	927w	863m	926w	882m	874vs
	823vs	823vs	823vs	873vs	837s
791vs		796vs		856m	798s
	760vs	783w	780m	771vs	785s
704w		745vs	720s		730s
692m	660w	694s			712s

[a] Only the bands whose intensity is greater than medium are recorded.

(1) L. J. Bellamy, "The Infrared Spectra of Complex Molecules," John Wiley and Sons, Inc., New York, N. Y., 1954.

(2) H. Luther, G. Brandes and B. Hample, *Z. Elektrochem.*, **59**, 1012 (1955).

EFFECT OF *p*H ON THE CATALYTIC ACTIVITY OF HYDROGEN-PRODUCING REACTIONS ON α- AND β-PALLADIUM–HYDROGEN CATHODES

By Sigmund Schuldiner and James P. Hoare

U. S. Naval Research Laboratory, Washington 25, D. C.

Received December 4, 1957

The authors[1,2] have determined the rate constants of α- and β-Pd–H alloys for electrolytic hydrogen-producing reactions. For these alloys the rate-determining step in strongly acid solutions (*p*H 0 to 1.2) was shown to be the desorption of an adsorbed hydrogen atom by combination with a hydrogen ion on the solution side of the double layer and an electron from the metal. In less acid solutions (*p*H 1.6 to 1.8) the rate-determining step was shown to be the combination of adsorbed hydrogen atoms to molecules.

Since the rate constants were a measure of catalytic activity, a relationship between the catalytic activity of the α- and β- Pd–H alloys and their

(1) J. P. Hoare and S. Schuldiner, *J. Electrochem. Soc.*, **102**, 485 (1955).

(2) J. P. Hoare and S. Schuldiner, *ibid.*, **104**, 564 (1957).

electronic configuration was shown.[3,4] In the β-phase alloy all of the holes in the d-band of the metal were filled with electrons contributed by dissolved hydrogen and it could be concluded[5,6] that the heat of adsorption of hydrogen atoms on the metal surface would be less than on the surface of the α-phase alloy. It was shown[3,7] that, if the rate-determining step in the hydrogen-producing reaction was atomic desorption, the higher the heat of adsorption of hydrogen atoms on the surface the slower would be the rate of this step. On the other hand, it has been demonstrated[8,9] that, if the rate-controlling step was the slow discharge of hydrogen ions to atoms, the higher the the heat of adsorption of hydrogen atoms on the surface the faster would be the rate of this step.

An investigation of the hydrogen overvoltage on bright platinum[10] showed that in neutral and alkaline solutions the rate-determining step for the hydrogen-producing reaction was the slow discharge of water to hydrogen atoms. Assuming that the same mechanism would prevail on α- and β-Pd cathodes in alkaline solutions, an experimental test of the pH effect was possible. If the rate-determining step changed from an atomic desorption to a slow discharge as the pH of the solution was increased, then the catalytic activity of the α-alloy should overtake that of the β-alloy at the point where the rate-determining step changed.

Hydrogen overvoltage curves for α- and β-Pd are shown in Figs. 1 and 2. These curves are the average values for three runs and were obtained by previously described techniques.[1,2,10] The same piece of 0.005 inch thick with 0.14 cm.^{2} exposed area palladium foil was used in all measurements. The preliminary anodic and cathodic treatment of this foil roughened the surface to such an extent that, when overvoltage measurements were taken, virtually no further change in surface area occurred. Overvoltage values for both α- and β-Pd were taken on the same electrode surface. The Tafel, b = 0.12, slope demonstrates that in the hydrogen-stirred 10.2 and 12.0 pH solutions (mixtures of purified 0.1 N KOH and 2 N Na_2SO_4) the rate-controlling step was the slow discharge of water to hydrogen atoms.

In Fig. 3 are shown the effect of pH on the rate constants, $k = -di/d\eta$, for the hydrogen-producing reactions. These rate constants were determined[1,2,10] by taking the derivative of the reciprocal of the η *vs.* i slope at low current densities where there is a linear relationship between these quantities. Included are the values for acid solutions which were reported earlier.[1,2] These rate constants directly measure the relative catalytic activity.

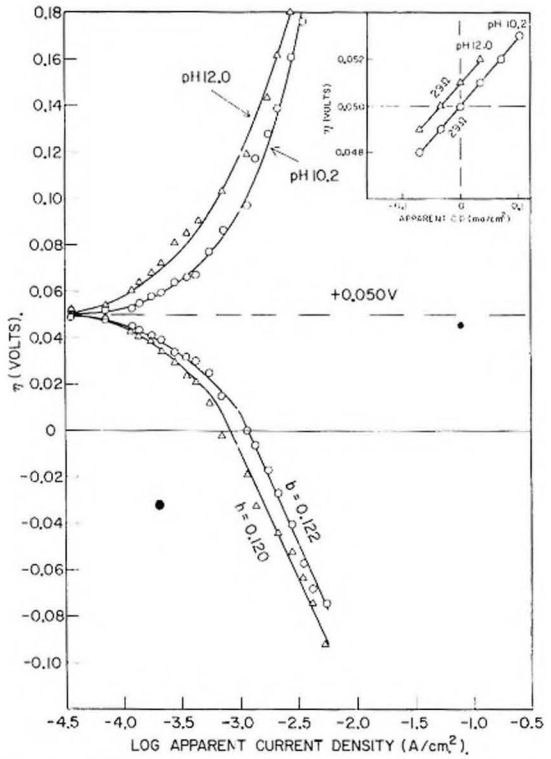

Fig. 1.—Hydrogen overvoltage on the anode and cathode sides of an α-Pd–H bielectrode. Inset shows values at low current densities; η *vs.* Pt/H_2 reference electrodes in the same solutions; $T = 27 \pm 1°$.

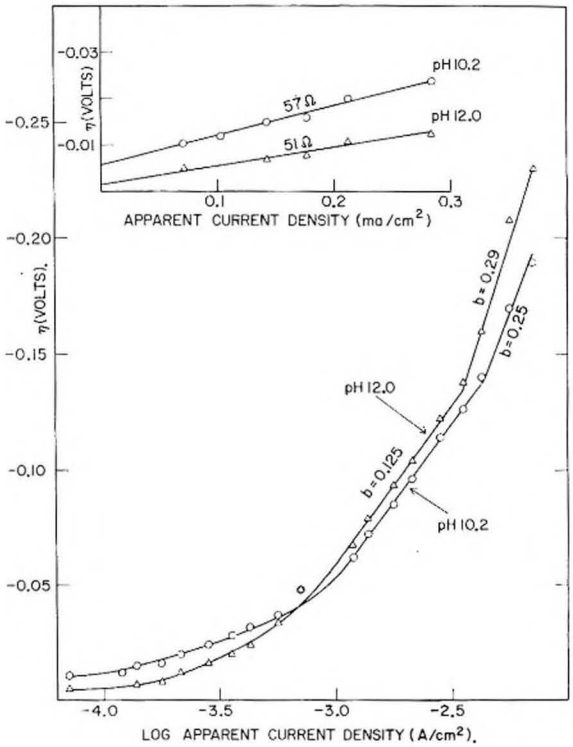

Fig. 2.—Hydrogen overvoltage on a β-Pd–H diaphragm cathode. Inset shows values at low current densities; η *vs.* Pt/H_2 reference electrodes in the same solutions; $T = 27 \pm 1°$.

Figure 3 shows that when the pH of the solution becomes sufficiently high the catalytic activity of the α-Pd becomes higher than that of the β-Pd.

(3) S. Schuldiner and J. P. Hoare, THIS JOURNAL, **51**, 705 (1957).

(4) S. Schuldiner and J. P. Hoare, "International Colloquium on Reference Electrodes and Structure of the Double Layer," Paris, October, 1956.

(5) O. Beeck, *Faraday Soc. Disc.*, **8**, 118 (1950).

(6) A. Couper and D. D. Eley, *ibid.*, **8**, 172 (1950).

(7) B. E. Conway and J. O'M. Bockris, *Naturwissenschaften*, **19**, 446 (1956); *J. Chem. Phys.*, **26**, 532 (1957).

(8) J. Horiuti and M. Polanyi, *Acta Physicochim. USSR*, **2**, 505 (1935).

(9) M. Oikawa, *Bull. Chem. Soc. Japan*, **28**, 626 (1955).

(10) S. Schuldiner, *J. Electrochem. Soc.*, **101**, 426 (1954).

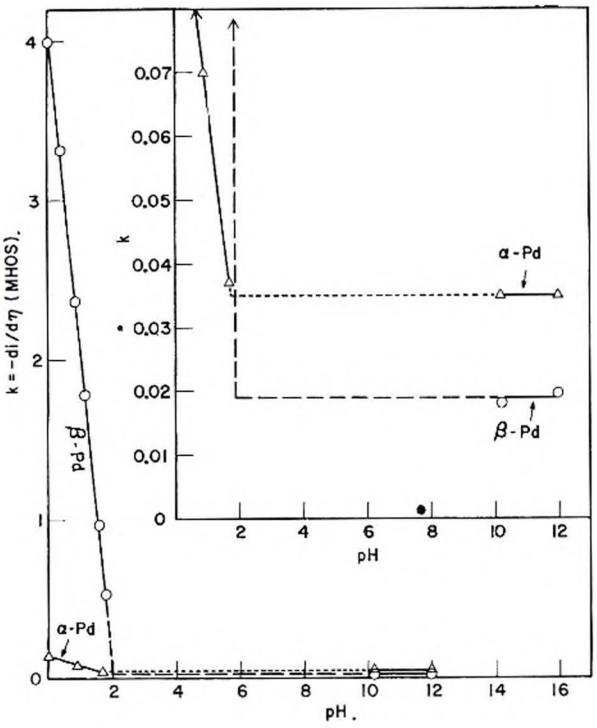

Fig. 3.—Effect of pH on the catalytic activity of α- and β-Pd–H cathodes. Inset shows an expanded scale for low values of the rate constant, k.

It is apparent that the crossover in catalytic activity occurs at the point where the rate-determining step changes from an atomic desorption to a slow discharge. These experimental results show the relationship between the electronic configuration (effect on the heat of adsorption of hydrogen atoms) and the rate-controlling step of the hydrogen-producing mechanism.

These results confirm previous results[10] which indicated that on platinum and palladium electrodes both hydronium ions and water are simultaneously reduced to hydrogen atoms on the cathode surface. As the hydronium ion concentration in the double layer is decreased, the primary source of hydrogen ions changes from hydronium ions to water.

THE EXTRACTION OF FERRIC CHLORIDE BY ISOPROPYL ETHER. PART II. A CONDUCTOMETRIC STUDY OF THE ETHER LAYER[1]

BY DONALD E. CAMPBELL, HERBERT M. CLARK AND WALTER H. BAUER

Department of Chemistry Rensselaer Polytechnic Institute, Troy, New York

Received December 7, 1957

It has been demonstrated,[2] in the extraction of ferric chloride from aqueous hydrochloric acid solutions, that five molecules of water must accompany each molecule of $HFeCl_4$ extracted in order to dissolve this complex in isopropyl ether. This is in accord with the results of previous investigators[3-5] who have indicated that water is directly associated with the iron complex which is dissolved in the ether layer during extraction of iron from strong hydrochloric acid solutions of ferric chloride. It has been proposed[2] that all of the water is associated with the hydrogen of the complex acid, $HFeCl_4$, possibly as $(H_3O^+ \cdot 4H_2O)FeCl_4^-$. Friedman and Taube[6] have shown by means of conductance measurements that an analogous salt, NH_4GaCl_4, dissolved in anhydrous ether exhibits the characteristic behavior of strong electrolytes dissolved in solvents of low dielectric constant. It was therefore of interest to examine the conductance behavior of ether layers from the iron extraction system.

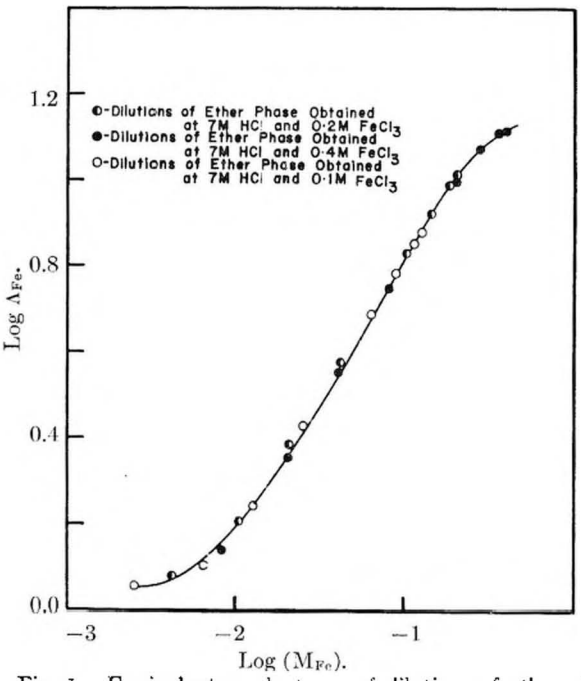

Fig. 1. –Equivalent conductance of dilutions of ethereal iron extraction phases prepared by extraction of 7 *M* hydrochloric acid solutions containing varying amounts of iron.

Experimental

Procedure.—Ethereal iron extraction phases were prepared by equilibration of aqueous solutions, containing varying concentrations of ferric chloride and hydrochloric acid, with equal volumes of isopropyl ether at 20° for 48 hours with frequent shaking. The ether layer was separated from the equilibrium aqueous phase by means of a siphon, and analyzed for chloride and iron as previously[2] described. Water in the ether layer was determined by a modified Karl Fischer titration, described by Laurene.[7] Dilutions of the ethereal iron extraction phases were made with isopropyl ether, which had been equilibrated over an equal volume of hydrochloric acid. The hydrochloric acid concentration in each case was the same as that used to prepare the given ethereal iron extraction phase. Other diluents, such as dry isopropyl ether, or isopropyl ether saturated with water, caused appearance of multiple ether layers. The iron concentrations in the diluted solutions were determined from the dilution ratio and the iron concentration of the original

(1) Abstracted from the Ph.D. Dissertation of Donald E. Campbell, Rensselaer Polytechnic Institute, Troy, N. Y., June, 1952.

(2) A. H. Laurene, D. E. Campbell, S. E. Wiberley and H. M. Clark, THIS JOURNAL, **60**, 901 (1956).

(3) S. Kato and R. Ishii, *Sci. Papers Inst. Phys. Chem. Research, Tokyo*, **36**, 82 (1939).

(4) J. Axelrod and E. L. Swift, *J. Am. Chem. Soc.*, **62**, 33 (1940).

(5) R. J. Myers, D. E. Metzler and E. H. Swift, *ibid.*, **72**, 3767 (1950).

(6) H. L. Friedman and H. Taube, *ibid.*, **72**, 3962 (1950).

(7) A. H. Laurene, *Anal. Chem.*, **24**, 1496 (1952).

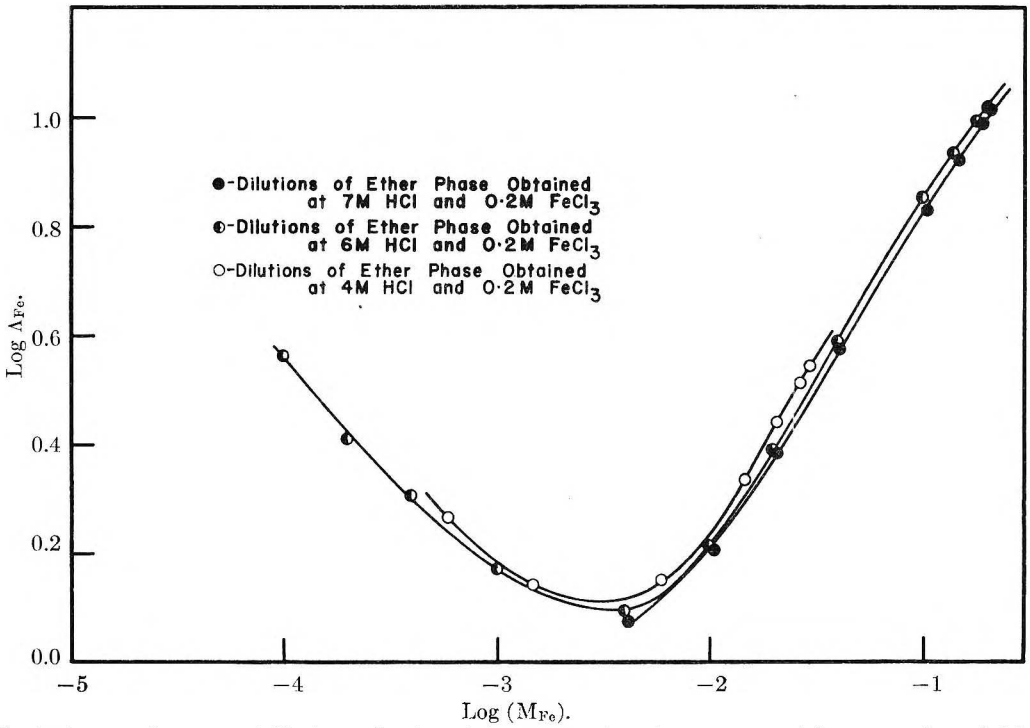

Fig. 2.—Equivalent conductance of dilutions of ethereal iron extraction phases prepared by extraction of 0.2 *M* ferric chloride solutions containing varying amounts of hydrochloric acid.

ethereal iron extraction phase. The water in the diluted solutions was determined either by direct analysis or from the water analyses of the equilibrated ether diluent and the ether extraction phase.

The specific conductances of the resulting series of diluted solutions were measured in a stoppered conductance cell constructed out of a standard taper 24/40 female joint. The lower end of the joint was blown into a bulb which enveloped the electrodes, and mercury wells were sealed to opposite sides of the bulb. A groove was ground in the stopper and a hole drilled in the side of the female joint so that there would be no pressure exerted on the solution in the cell when the stopper was put in place. Conductances were measured at 20.00 ± 0.01° with a General Radio 650-A impedance bridge equipped with 1000 cycle oscillator-amplifier. A Dumont 208-B cathode ray oscilloscope was employed as the null point detector.

Results

The dilution studies were carried out on two different groups of ether extraction phases. In the first group, three different ether phases were obtained by extraction of aqueous solutions which were initially 0.1, 0.2 and 0.4 *M* in iron, but which were all 7 *M* in hydrochloric acid. The results of the conductance measurements made on this first group are shown in Fig. 1. In the second group, three ether phases were prepared by extraction of aqueous solutions which were initially 7, 6 and 4 *M* in hydrochloric acid but were all 0.2 *M* in iron. The conductance data for diluted solutions of this group of ether extraction phases are plotted in Fig. 2. When the solvent conductance exceeded 1% of the specific conductance of the ethereal iron solutions, the specific conductance was corrected for the conductance of the solvent. The latter was was considered to be isopropyl ether equilibrated over an equal volume of hydrochloric acid at the same concentration used in the extraction.

Discussion

From the magnitude of the conductance per equivalent of iron and from its dependence upon the ethereal iron concentration shown in Figs. 1 and 2 it is evident that the iron complex which is extracted into the ether layer in the ether extraction of iron is ionic. Moreover, it is seen that the ionic nature of the extracted iron complex does not depend upon the initial conditions of extraction. The dilution curves shown in Figs. 1 and 2, which were obtained under widely differing initial conditions, are identical in shape and nearly coincident over the same range of iron concentration.

The conductance curves shown in Fig. 2, obtained for diluted extraction phases prepared at the lower initial hydrochloric acid concentrations, are slightly displaced in the direction of higher equivalent conductance. This effect is ascribed to the solution of water in the ether solvent. Such water is to be distinguished from the water which is known[2] to be associated with the iron complex. From work done on the ternary system, isopropyl ether–HCl–H_2O,[8] isopropyl ether equilibrated over an equal volume of hydrochloric acid below 9.5 *M* dissolves more water the lower the hydrochloric acid concentration.

When the dilutions were carried to low iron concentrations, minima in the conductance–dilution curves were found to occur, as shown in Fig. 2. Friedman and Taube[6] also observed conductance minima in their conductometric study of solutions of the analogous compound, NH_4GaCl_4, in ethyl ether. The occurrence of conductance minima has been shown by Fuoss and Kraus[9] to be characteristic for highly polar compounds dissolved in media of low dielectric constants, and has been as-

(8) D. E. Campbell, A. H. Laurene and H. M. Clark, *J. Am. Chem. Soc.*, **74**, 6193 (1952).

(9) C. A. Kraus and R. M. Fuoss, *ibid.*, **55**, 21, 2387 (1933).

cribed to the formation of electrostatically associated neutral ion pairs. At high concentrations in isopropyl ether, the tetrachloroferrate ion[2] may be largely associated in the form of triple ions such as $[H_3O^+\cdot 4H_2O\ FeCl_4^-H_3O^+\cdot 4H_2O]^-$ and $[FeCl_4^-H_3O^+\cdot 4H_2O\ FeCl_4^-]^-$, associated in neutral iron pairs as $[H_3O^+\cdot 4H_2O\ FeCl_4^-]$, and dissociated to a lesser extent as the ions $H_3O^+\cdot 4H_2O$ and $FeCl_4^-$. With dilution, the conductance would be expected to go through a minimum as the triple ions dissociated and the concentration of neutral ion pairs increased. The final increase in conductance would follow an increased dissociation of neutral ion pairs with high dilution. Thus, the appearance of such minima in the conductance–dilution curves of the ethereal phases of the iron extraction system provides supporting experimental evidence for the "polymerization" theory which Myers, Metzler and Swift[5] have proposed to account for the variation in the iron distribution coefficient with total iron concentration in ethereal extraction of iron from aqueous solution having constant initial hydrochloric acid concentrations.

Acknowledgment.—The authors are indebted to Lewis G. Bassett for his many suggestions during the course of this work. This work was partially supported by the U. S. Atomic Energy Commission under Contract No. At(30-1)-562.

GEOMETRIC CONSIDERATIONS OF TETRAZOLE DERIVATIVES FROM DIPOLE MOMENT DATA

MARTIN H. KAUFMAN AND ALAN L. WOODMAN

Physical Chemistry Branch, U. S. Naval Ordnance Test Station, China Lake, California

Received December 10, 1957

Hill and Sutton[1] in their study of electric dipole moments of some sydnones applied vector addition to the solution of geometric problems. From known moments and moments of aromatic compounds differing only by *para* substitution, they deduced various angles between substituted phenyl bonds and the direction of the dipole moments of the parent compound. A qualitative picture of the hybrid nature of tetrazoles was recently reported by Kaufman, *et al.*[2] The purpose of the present study was to investigate the geometry of tetrazoles by means similar to those of Hill and Sutton. With this idea in mind, chloro-, bromo- and nitrophenyltetrazoles were prepared and their dipole moments measured in benzene solution at 25°.

Experimental

Preparation and Purification of Materials.—Mallinckrodt analytical reagent grade benzene was purified by crystallizing twice, rejecting a small portion each time, and then fractionally distilling after standing several days over freshly cut and ribboned sodium. All was rejected but the center cut which was re-distilled in the same manner before use. The specific volume parameter for the solvent was obtained for each run from a least squares examination of the specific volume, weight fraction data and was found to be constant to ±0.02%.

Tetrazoles.—All were prepared from amide and hydrazoic acid by a method similar to that described by Harvill, *et al.*[3] Analytical data are presented in Table I. All tetrazoles were sublimed twice before making any physical measurements.

Amides.—These were prepared in the usual manner. In Table I, the melting points of the amides are listed; all were recrystallized twice from ethanol.

Physical Measurements and Calculations.—This experimental part is essentially that of Kaufman, *et al.* The apparatus was calibrated with benzene, the dielectric constant of which was taken to be 2.2750 at 25°.[4] The calculated data are presented in Table II, where ϵ_1 and V_1, the dielectric constant and the specific volume of the solvent, respectively, are the intercepts while α and β are the slopes of the straight lines obtained by plotting solution dielectric constant and specific volume, respectively, against weight fraction of solute.[5] P_∞ is the solute polarization at infinite dilution calculated from the Halverstadt and Kumler relationship[6] while R_2 is the molar refraction of the solute for the D-sodium line and μ is the dipole moment calculated from the approximate Debye equation

$$\mu = 0.01281 \times 10^{-18}\,[(P_\infty - R_2)T]^{1/2} \qquad (1)$$

Discussion

From the known moments of nitrobenzene (3.97 *D*), 1-phenyl-5-methyltetrazole (5.64 *D*) and 1-*p*-nitrophenyl-5-methyltetrazole (3.20 *D*) it follows that the angle between the phenyl–NO_2 bond and the moment of 1-phenyl-5-methyltetrazole is approximately 34°. Therefore, 34° is also the angle between the phenyl–N bond and the moment of 1-phenyl-5-methyltetrazole. In the following manner, Kofod, *et al.*,[7] obtained a value of 0.8 *D* for the Ph–N bond assuming a value of 1.3 *D* for the H–N bond. The experimental value for unsubstituted pyrrole is 1.80 *D* while that of N-phenylpyrrole is 1.32 *D*. Therefore, since the two rings are co-linear, the Ph–N bond must be 0.48 *D* less than the H–N bond or 0.8 *D*. Similarly the CH_3–N bond is 0.12 *D* more than the H–N bond or 1.42 *D*.

If the value of 0.8 *D* for the phenyl-N moment in 1-phenyl-5-methyltetrazole is utilized, a value of 5.00 *D* for the moment of 5-methyltetrazole and 39° for the angle between the phenyl–N bond and the moment of 5-methyltetrazole is obtained. From a similar treatment of 1-methyl-5-*p*-nitrophenyltetrazole (3.87 *D*) the following information was obtained. The angle between the phenyl–NO_2 bond and, therefore, the phenyl–C bond and the moment of 1-methyl-5-phenyltetrazole is approximately 43°. The angle between the phenyl–C bond and the moment of 1-methyltetrazole is approximately 45° while the dipole moment of 1-methyltetrazole is calculated to be 5.45 *D*. The experimental value of 5.38 *D* was reported for this compound by Jensen and Friediger.[8]

From the above data, predictions about the moments of phenyltetrazoles differing only by *para* substituents may be made: *e.g.*, from the known moments of chloro- (1.59) and bromobenzene

(1) R. A. W. Hill and L. E. Sutton, *J. Chem. Soc.*, 746 (1949).

(2) M. H. Kaufman, F. M. Ernsberger and W. S. McEwan, *J. Am. Chem. Soc.*, **78**, 4197 (1956).

(3) E. K. Harvill, R. M. Herbst, E. C. Schreiner and C. W. Roberts, *J. Org. Chem.*, **15**, 668 (1950).

(4) A. S. Brown, P. M. Levin and E. W. Abrahamson, *J. Chem. Phys.*, **19**, 1226 (1951).

(5) G. Hedestrand, *Z. physik. Chem.*, **B2**, 482 (1929).

(6) I. F. Halverstadt and W. D. Kumler, *J. Am. Chem. Soc.*, **64**, 2988 (1942).

(7) H. Kofod, L. E. Sutton and J. Jackson, *J. Chem. Soc.*, 1467 (1952).

(8) K. A. Jensen and A. Friediger, *Kgl. Danske Videnskab. Selskab. Math. fys. Medd.*, **20**, 1 (1943).

TABLE I

ANALYTICAL DATA

Tetrazole	Recrystallization	M.p., °C.	M.p., °C. lit			
				C	H	X
1-Ethyl-5-*p*-chlorophenyl-	Sublim.	82.7–83.8	....	Calcd. 51.80	4.35	16.99
				Found 51.33	4.24	17.1
1-*p*-Chlorophenyl-5-methyl-	ETOH-needles	88.5–89.4	....	Calcd. 49.37	3.62	18.21
				Found 49.47	3.59	18.1
1-*p*-Bromophenyl-5-methyl-	H_2O-needles, cyclohexane-plates	116.7–118	....	Calcd. 40.19	2.95	33.43
				Found 40.01	3.07	33.9
1-*p*-Bromophenyl-5-ethyl-	ETOH-plates	92.6–93.6	....	Calcd. 42.70	3.58	31.58
				Found 42.62	3.29	32.2
1-Methyl-5-*p*-nitrophenyl-	CH_2Cl_2–ETOH prisms	123.4–124.4	123–126[a]			
1-*p*-Nitrophenyl-5-methyl-	CH_2Cl_2-plates	132.3–132.7	130–135[a] 132–133[b]			
Amide						
p-Nitroacetanilide	(uncorr.)	214.8–215.6	215.9[c]			
p-Chloroacetanilide		179.6–179.8	178.4[c], 179.0[d]			
p-Bromoacetanilide		168.5–168.8	167[e]			
N-Ethyl-*p*-chlorobenzamide		109.0–110.2	....			
N-Ethylbenzamide		68.4–69.8	70–71[g], 67[h]			

[a] R. M. Herbst, *et al.*, *J. Org. Chem.*, **17**, 262 (1952). [b] Du-Yung Wu and R. M. Herbst, *ibid.*, **17**, 1216 (1952). [c] N. V. Sidgwick and H. E. Rubie, *J. Chem. Soc.*, 1014 (1921). [d] G. Owen, *ibid.*, 3395 (1923). [e] Buu-Hoï, *Ann.*, **556**, 1 (1944). F. D. Chattaway, *J. Chem. Soc.*, 817 (1902). [g] H. Meerwein, *et al.*, *J. prakt. Chem.*, **154**, 83 (1939). [h] J. von Braun, *Ber.*, **37**, 2815 (1904).

TABLE II

CALCULATED DATA

Tetrazole	ϵ	V_1	α	β	P_∞	R_2	μ
1-*p*-Nitrophenyl-5-methyl-	2.2805	1.14412	5.60	−0.38	261.9	52.0	3.20
1-Methyl-5-*p*-nitrophenyl-	2.2865	1.14543	8.19	− .49	354.7	47.9	3.87
1-Ethyl-5-*p*-chlorophenyl-	2.2920	1.14528	12.22	− .39	523.0	55.7	4.78
1-*p*-Bromophenyl-5-ethyl-	2.2748	1.14543	9.53	− .50	501.8	57.7	4.66
1-*p*-Chlorophenyl-5-methyl-	2.2874	1.14429	10.95	− .37	442.9	50.7	4.38
1-*p*-Bromophenyl-5-methyl-	2.2866	1.14512	9.25	− .54	456.9	51.9	4.45

(1.57),[9] the moments of 1-*p*-bromophenyl-5-methyl- and 1-*p*-chlorophenyl-5-methyltetrazole were calculated to be 4.43 and 4.41 *D*, respectively. The observed moments (Table II) are 4.45 and 4.38 *D*, respectively.

Assuming the simplest geometry for the tetrazole ring (a regular pentagon with all substituent bonds co-linear with a ring axis) the dipole moment of 5-methyltetrazole would have a direction somewhat as illustrated in Fig. 1. Figure 2 shows the

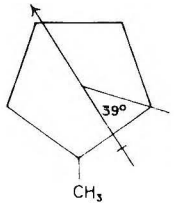

Fig. 1.

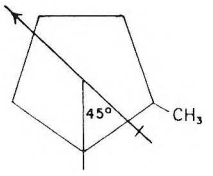

Fig. 2.

dipole moment of 1-methyltetrazole. Knowing the direction of the moment in 5-methyltetrazole, it is interesting to note that the direction of the 1-methyltetrazole could be predicted easily, qualitatively, by considering the addition of the $^+C–N^-$ dipole. It is also of interest to note that the information illustrated in Fig. 2 agrees very well with the resonance structures depicted for 2-ethyltetrazole by Kaufman, *et al.*[2]

(9) R. J. W. LeFevre, "Dipole Moments," John Wiley and Sons, Inc., New York, N. Y., ed. 3, 1953, p. 133.

Acknowledgment.—We wish to thank Dr. Richard Knipe for his interesting discussions and suggestions.

ALCOHOLIC FERRIC PERCHLORATE SOLUTIONS[1]

BY R. A. HORNE[2]

Department of Chemistry, Brookhaven National Laboratory, Upton Long Island, N. Y.

Received December 16, 1957

Solutions of ferric perchlorate in alcohol, acetone and many other organic solvents are much more intensely yellow colored than aqueous solutions of comparable concentration and acidity. Rabinowitch and Stockmayer[3] have suggested that, in the case of alcoholic solutions, this color intensification might be due to ferric perchlorate complex ion[4] or to alcoholysis. These same solvents also intensify the yellow color of ferric bromide and the red color of ferric thiocyanate solutions[5]; the latter has been utilized in the colorimetric determination of iron.[6]

(1) Research performed under the auspices of the U. S. Atomic Energy Commission.

(2) Radio Corporation of America, Needham Heights, Mass.

(3) E. Rabinowitch and W. H. Stockmayer, *J. Am. Chem. Soc.*, **64**, 335 (1942).

(4) *Cf.* J. Sutton, *Nature*, **169**, 71 (1952).

(5) J. Y. MacDonald and K. H. Mitchell, *J. Chem. Soc.*, 1310 (1951).

(6) *Vide* E. B. Sandell, "Colorimetric Determination of Traces of Metals," 2nd ed., Interscience Publishers, Inc., New York, N. Y., 1950.

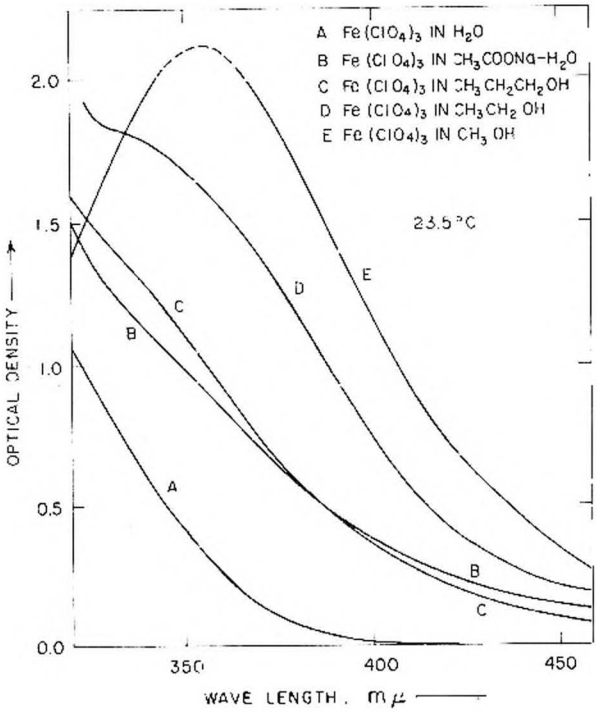

Fig. 1.

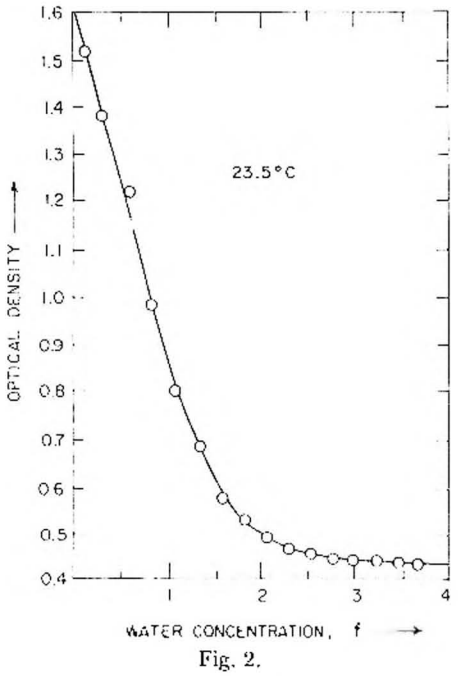

Fig. 2.

The absorption spectra of several ferric perchlorate solutions are shown in Fig. 1. A Beckman single beam spectrophotometer with "Corex" cells and a tungsten lamp source was used. Curve A is for an aqueous ferric perchlorate solution, B an aqueous solution made slightly alkaline by the addition of sodium acetate, C for ferric perchlorate in 1-propanol, D in ethanol and E in methanol. In each case the temperature is 23.5° and the ferric perchlorate complex is $7.9 \times 10^{-4} f$. In C, D and E the volume ratio of alcohol to water is 200:1. The similarity between curves B and C, the color intensification in acetone, the color intensification of ferric bromide and thiocyanate solutions, and the fact that alcoholic ferric perchlorate solutions decolorize gradually on the addition of water but very abruptly on the addition of perchloric acid all suggest that the colored species is a ferric hydrolysis product with its color intensified by the substitution of organic molecules for waters in the solvation sphere

$$(H_2O)_{5-n}(ROH)_nFeOH^{++} \qquad (1)$$

From steric considerations n might be expected to increase and the color intensity increase as the size of ROH decreases. Comparison of curves C, D and E in Fig. 1 show such to be the case.

Figure 2 shows the change in optical density of a $4.47 \times 10^{-4} f$ ferric perchlorate in ethanol solution upon the addition of one-ml. water–ethanol increments. The initial volume was 100 ml., the temperature 23.5°, and the measurements were made at a wave length of 420 mμ. Figures 1 and 2 are not quantitatively comparable because the solutions in the former are more acidic, the presence of a small amount of perchloric acid in the ferric perchlorate stock solutions being a consequence of the purification procedure. Figure 2 is not readily explained in terms of dilution or of changing macroscopic dielectric constant. The marked break in Fig. 2 probably is due to a reaction of the type

$$(H_2O)_{5-n}(ROH)_nFeOH^{++} + HOH \rightleftharpoons (H_2O)_{6-n}(ROH)_{n-1}FeOH^{++} + ROH \qquad (2)$$

Figure 2 indicates that the equilibrium constant for this process[7] is about 10. If the observed optical density is chiefly proportional to the concentration of $(H_2O)_{5-n}(ROH)_nFeOH^{++}$, presumably, then, an abrupt change in the concentration of this species is indicated by the abrupt change of slope in Fig. 2. In alcoholic media reactions such as (2) may be of greater importance in determining the rates of processes involving solvated species than changes in the macroscopic dielectric constant.

(7) For preferential solvation by the higher dielectric component of a mixed solvent see E. S. Amis, THIS JOURNAL, **60**, 428 (1956); *J. Chem. Phys.*, **26**, 880 (1957).

THE KINETIC BEHAVIOR OF SUBMICRON SIZE, POLYDISPERSED SODIUM CHLORIDE AND TITANIUM DIOXIDE AEROSOLS[1,2]

BY I. S. YAFFE AND R. D. CADLE

Stanford Research Institute, Menlo Park, California

Received December 16, 1957

Few experimental data exist in the literature concerning the interactions of submicron-size (<0.1 μ radius) polydispersed aerosol particles. Goldman[3] has developed an equation describing the behavior of such systems, but it has been solved only for simple cases such as an initially monodispersed aerosol. Recently a condensation-nuclei counter

(1) Work supported in part by a grant from the National Institutes of Health (S-30) and the Divisional Research Committee of Stanford Research Institute.

(2) Presented at 132nd meeting of American Chemical Society, New York (Sept. 1957).

(3) "Handbook on Aerosols," U. S. Atomic Energy Commission, Washington, 1950, Chap. 5, p. 69.

has been developed which makes possible the determination of the concentrations of submicron size aerosol particles in various size ranges.[4,5] This note describes the initial results of a program undertaken with this counter to investigate the interactions of such polydispersed aerosol particles.

Experimental

A commercially available model of the counter, General Electric "Small Particle Detector, Type C. N."[5] was used to determine the concentrations of the aerosol particles in various size ranges. The size information obtained from this instrument is based upon theory developed for water vapor condensing at various degrees of supersaturation upon spherical water droplets.[6] Hence, the assigned values are the radii of water droplets which have the same effectiveness as condensation nuclei for water vapor as the particles in question. "Equivalent" radii assigned by this instrument range from 8 to 1000 Å.

Aerosols were formed by the condensation of vapors produced by heating crystalline TiO_2 or NaCl supported on a bare, coiled Kanthal heating filament of 1 ohm resistance. No detectable condensation nuclei were emitted from the filament itself at the power level used (10 watts). The vapors were introduced into clean, filtered air at room temperature until a reproducible steady-state aerosol condition was attained as determined by repeated concentration measurements for the various expansion ratios of the counter. The aerosol was then allowed to age and concentration measurements were obtained at various times during the aging process by withdrawing aliquots into the previously evacuated viewing chamber of the counter.

The data were plotted as number concentration *versus* time for each expansion ratio of the counter. Smooth curves were drawn and these curves were averaged over several (3 to 6) replications for each expansion ratio. The average deviation of the experimental points from each smoothed curve was ±10%. Differences were taken between these averaged curves to obtain the concentrations within the size ranges. The significant features of each curve, *i.e.*, positions of maxima, inflection points and slopes, were quite reproducible from run to run.

Data and Discussion

A 5-liter glass flask was used as an aerosol container for the first two sets of experiments with NaCl and TiO_2. With the constant-volume container, the aerosol was diluted slightly each time an aliquot was removed for analysis; however, the total dilution after 15 minutes was less than 20% and should not have much influence upon the shape of the derived curves. The averaged curves illustrating the growth and decay of various size ranges between 8 and 1000 Å. in equivalent radii are shown in Fig. 1 for NaCl. The decay curves for TiO_2 were qualitatively similar.

For the most part, the shapes of the curves can be attributed to the growth of particles by coagulation into and out of the various size ranges as would be anticipated from normal aerosol theory. The linearity of the terminal slopes for each size range on the semi-log plots indicates that a first-order or pseudo-first-order reaction governs this portion of the decay. Thus for the linear portions of the decay, the rates may be controlled by the collision of the particles in the size range considered with much larger particles whose over-all concentration remains essentially constant, and with the walls. The fact that these slopes in general increase with decreasing particle size agrees with this interpretation.

The maxima in the curves for the 60–200 Å. particles of both NaCl and TiO_2 are more difficult to explain. The decrease in the number of particles

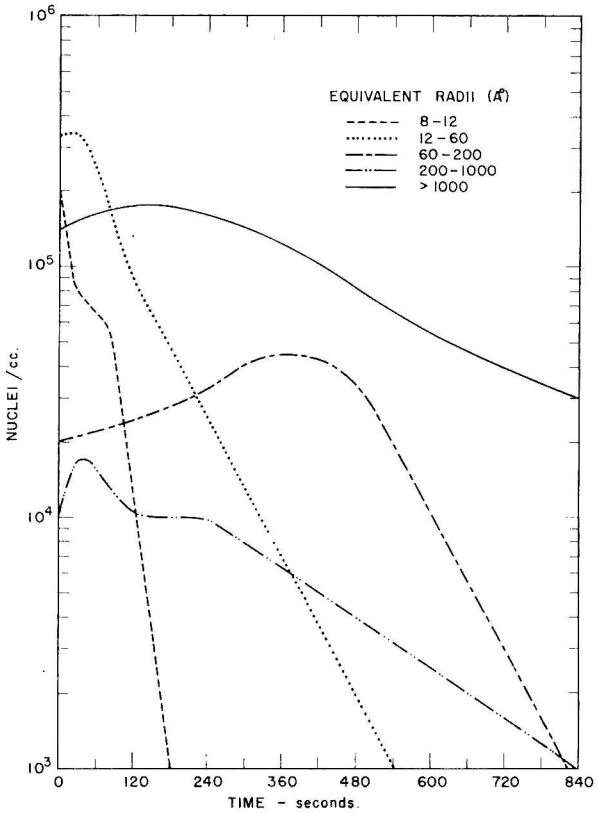

Fig. 1.—NaCl aerosol in 5-liter glass flask. Concentration of various size ranges as a function of time.

in the 8–60 Å. range is not sufficient to explain the late increase in the 60–200 Å. range. Possibly very large numbers of particles smaller than 8 Å. equivalent radius exist when the first measurement is made and these pass rapidly by coagulation through the 8–60 Å. range and much less rapidly through the 60–200 Å. range. However, it is difficult to account for the steep slopes of the curves for NaCl particles in the 8–12 Å. and 12–60 Å. range if this mechanism were correct. Possibly a phase change occurs which results in a decrease in effective radius when the particles have coagulated into the 60–200 Å. size range. Phase changes have been observed in other aerosol systems. For example, the particles in stearic acid aerosols prepared by condensation from the vapor phase first appear as droplets which later solidify.[7]

Another set of experiments was conducted in which the TiO_2 aerosol was contained in a flexible-walled 250-liter plastic bag, which eliminated the need for dilution as samples were withdrawn. Although the curves differ quantitatively from those of Fig. 1, which may be attributed to the smaller wall-to-volume ratio of the plastic bag, the same general behavior was observed.

(4) P. J. Nolan and L. W. Pollack, *Proc. Roy. Irish Acad.*, **51A**, 9 (1946).

(5) T. A. Rich, *Geofisica*, **31**, 60 (1955).

(6) N. N. Das Gupta and S. K. Ghosh, *Rev. Mod. Phys.*, **18**, 225 (1946).

(7) C. Schadt and R. D. Cadle, *Anal. Chem.*, **29**, 864 (1957).

SOME PHYSICAL PROPERTIES OF THE SYSTEM 2-ETHOXYETHANOL–BUTYL ACETATE

BY K. J. MILLER

Chemistry Department, Mount Union College, Alliance, Ohio

Received January 31, 1958

Particularly because of its excellent solvent properties 2-ethoxyethanol has been of interest to investigators. Little information has been available on binary mixtures of 2-ethoxyethanol–organic acetates. Consequently it seemed of interest to begin a study of these systems. This paper deals with the densities, refractive indices and viscosities at 25° and of the boiling point–composition diagram of the system 2-ethoxyethanol–butyl acetate.

Experimental

Materials.—2-Ethoxyethanol (Eastman Kodak No. 1697) was dried by refluxing over freshly ignited lime and carefully distilled using a Todd distillation column.

Butyl acetate (Eastman Kodak No. 710) was dried with anhydrous $MgSO_4$ and carefully distilled using a Todd distillation column.

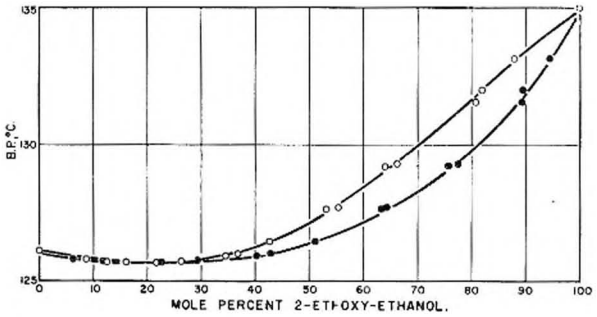

Fig. 1.—Boiling point–composition diagram for the system 2-ethoxyethanol–butyl acetate.

The center fractions in distillations were used for measurements.

Apparatus and Procedure.—The measurement of density, refractive index and viscosity and the preparation of solutions have been described previously.[1] In this study temperature of the refractometer was controlled at 25 ± 0.05° by circulating water through the refractometer cell with a small pump and a precision in refractive index of ± 0.0001 was obtained.

Boiling point–composition determinations were carried out in an Othmer equilibrium still[2] manufactured by the Emil Greiner Co. The pressure was maintained at 760 mm. by means of a manostat similar to that previously described.[3] Positive pressure on the still was provided by dry nitrogen. The boiling point was read to a precision of ±0.1°. Samples were analyzed by comparing their refractive indices with the refractive index–composition curve of the system.

Results

Refractive index values, listed in Table I, when plotted as a function of mole % show a curve bowed downward with maximum deviation from a linear relation at 50–50 mole %.

TABLE I

2-ETHOXYETHANOL–BUTYL ACETATE

2EE, mole %	Density d^{25}_4, g./ml.	Viscosity η/η_{H_2O}, 25°	Refractive index, $n^{25}D$
0	0.8764	0.7527	1.3918
8.26	.8786	.7779	1.3925
12.49	.8800	.7935	1.3929
14.54	.8808	.8037	1.3931
21.82	.8832	.8411	1.3938
39.51	.8905	.9558	1.3958
46.91	.8939	1.0238	1.3967
50.20	.8956	1.0564	1.3971
51.74	.8962	1.0714	1.3973
56.04	.8984	1.1186	1.3980
64.88	.9029	1.2327	1.3992
75.47	.9092	1.4082	1.4011
76.74	.9100	1.4286	1.4013
77.94	.9107	1.4509	1.4016
90.79	.9187	1.7517	1.4039
95.31	.9217	1.8761	1.4048
96.78	.9227	1.9261	1.4050
100	.9250	2.0316	1.4059

Viscosity of mixtures relative to water at 25°, listed in Table I, when plotted as a function of mole % show a curve bowed downward, below both the logarithmic[4,5] and linear[6] ideal type relations proposed for viscosity of solutions.

The boiling point–composition diagram, shown in Fig. 1, shows an azeotrope boiling at 125.7° at a composition of about 16 mole % 2-ethoxyethanol. The composition of this azeotrope was found to differ appreciably from that previously reported.[7]

(1) K. J. Miller, THIS JOURNAL, **61**, 932 (1957).

(2) D. F. Othmer, *Anal. Chem.*, **20**, 763 (1948).

(3) E. L. Piret and M. W. Hall, *Ind. Eng. Chem.*, **40**, 661 (1948).

(4) J. Kendall and A. H. Wright, *J. Am. Chem. Soc.*, **42**, 1776 (1920).

(5) R. E. Powell, W. E. Roseveare and H. Eyring, *Ind. Eng. Chem.*, **33**, 430 (1941).

(6) E. C. Bingham, *Am. Chem. J.*, **35**, 195 (1906).

(7) An azeotrope containing 35.7 weight % 2-ethoxyethanol has been reported; Carbide and Carbon Chemicals Co., "Cellosolve and Carbitol Solvents," 1956.

NOMENCLATURE AND RELATED PAMPHLETS

New Titles

Reports of the 1955 IUPAC Meeting at Zurich

Commission de Nomenclature de Chimie Organique. This includes tentative rules for the nomenclature of acyclic and cyclic hydrocarbons and heterocyclic compounds. (In English) $1.00

Commission de Nomenclature de Chimie Biologique. This includes rules (part of them tentative) for the nomenclature of vitamins and tentative rules for steroid nomenclature. (In English) .. $0.75

Commission des symbols et de Terminologie Physico-chimique. This includes many standardized symbols for units or quantities. (In English) $0.75

ACS Committee Reports

Definitive Report of the IUPAC Commission on the Reform of the Nomenclature of Organic Chemistry. Translation with comment and index by Austin M. Patterson ..... .20

The Pronunciation of Chemical Words. A committee report ..... .05

Nomenclature of the Hydrogen Isotopes and Their Compounds. A committee report ..... No charge

The Nomenclature of the Carotenoid Pigments. Report of the Committee on Biochemical Nomenclature of the National Research Council, accepted by the Committee on Nomenclature, Spelling, and Pronunciation of the American Chemical Society ... No charge

The Naming of Cis and Trans Isomers of Hydrocarbons Containing Olefin Double Bonds. A committee report ..... No charge

The Designation of "Extra" Hydrogen in Naming Cyclic Compounds. A committee report ..... No charge

Avogram. A committee report ..... No charge

The Naming of Geometric Isomers of Polyalkyl Monocycloalkanes. A committee report ..... No charge

IUPAC Commission de nomenclature de chimie inorganique. Report on 1949 meeting at Amsterdam (in English). This relates to the names of new elements or others concerning which there has been controversy as to names ..... .10

IUPAC Commission de nomenclature de chimie organique. Report on 1949 meeting at Amsterdam (in English). This includes rules on the nomenclature of organosilicon compounds (now covered by "Organosilicon Compounds" below), changes and additions to the Definitive Report, extended examples of radical names, and an extensive list of radical names ..... .30

Arene and Arylene. A committee report ..... No charge

Halogenated Derivatives of Hydrocarbons. A committee report ..... .10

Use of "Per" in Naming Halogenated Organic Compounds. A committee report ..... .10

Use of "H" to Designate Position of Hydrogens in Almost Completely Fluorinated Organic Compounds. A committee report ..... .10

Organic Compounds Containing Phosphorus. A committee report ..... .25

Organosilicon Compounds. A committee report ..... .10

Nomenclature of Natural Amino Acids and Related Substances. A committee report ..... .25

Carbohydrate Nomenclature. A committee report ..... .25

A New General System for the Naming of Stereoisomers. Rules proposed by G. E. McCasland and considered promising by the Advisory Committee on Configurational Nomenclature, but not official now. The advisory committee's first report is also included ..... .30

Introduction to the 1952 Subject Index. This includes an extensive list of organic groups and radicals (see "The Naming and Indexing of Chemical Compounds by Chemical Abstracts" as noted below) ..... .25

Nomenclature for Terpene Hydrocarbons. A committee report ..... .25

"Petrochemistry" and Its Variants. A committee report ..... .05

Miscellaneous

Directions for Abstractors and Section Editors of Chemical Abstracts. Much concentrated information on nomenclature, symbols, forms, and abbreviations is assembled in this 46-page booklet in form convenient for use ..... .25

The Standardization of Chemical Nomenclature. This reprint of an article by the committee chairman contains a list of references to sources of information on chemical literature ..... No charge

The Naming and Indexing of Chemical Compounds by Chemical Abstracts. Introduction to the 1945 Subject Index. A comprehensive, 109-page discussion of chemical nomenclature as applied to inorganic as well as organic compounds for systematic indexing, with a classified bibliography, an index, and the following appendixes (lists): (I) Miscellaneous chemical prefixes, (II) Inorganic groups and radicals, (III) Anions, (IV) Organic groups and radicals, (V) Organic suffixes, and (VI) 1945 ring index. Included is an insert of the 12-page 1952 Subject Index Introduction to show changes and additions. 75 cents. With Introduction to the 1952 Subject Index $1.00

Address all orders to

The CHEMICAL ABSTRACTS SERVICE

The Ohio State University, Columbus 10, Ohio